AD-777 988

NUTATING MECHANICAL TRANSMISSION (MAROTH DRIVE PRINCIPLE)

BOEING VERTOL COMPANY

PREPARED FOR
OFFICE OF NAVAL RESEARCH

JANUARY 1974

Unclassified
Security Classification

AD 777788

DOCUMENT CONTROL DATA - R & D

(Security classification of title, body of abstract and indexing annotation must be entered when the overall report is classified)

1 ORIGINATING ACTIVITY *(Corporate author)*
The Boeing Vertol Company
P.O. Box 16858
Philadelphia, Pa. 19142

2a. REPORT SECURITY CLASSIFICATION
Unclassified

2b. GROUP

3 REPORT TITLE
NUTATING MECHANICAL TRANSMISSION
(Maroth Drive Principle)

4 DESCRIPTIVE NOTES *(Type of report and inclusive dates)*
Final Report (30 June 1972 - 31 January 1974)

5 AUTHOR(S) *(First name, middle initial, last name)*
Raymond J. Drago and A. J. Lemanski

6 REPORT DATE	7a. TOTAL NO. OF PAGES	7b. NO. OF REFS
January 1974	xxiii + 226	

8a. CONTRACT OR GRANT NO.	9a. ORIGINATOR'S REPORT NUMBER(S)
N00014-72-C-0272	
b. PROJECT NO.	
c.	9b. OTHER REPORT NO(S) *(Any other numbers that may be assigned this report)*
d.	D210-10747-1

10 DISTRIBUTION STATEMENT
Reproduction in whole or in part is permitted for any purpose of the United States Government.

11 SUPPLEMENTARY NOTES	12. SPONSORING MILITARY ACTIVITY
	Department of the Navy Office of Naval Research Arlington, Virginia 22217

13 ABSTRACT

This final report presents an analysis defining the operational characteristics and potential load capacity of the nutating mechanical transmission (NMT) concept. Since a fully operational NMT capable of any substantial loading has not been constructed, the scope of this program has been largely analytical. Substantial technology has been borrowed from the gear and bearing fields to provide a sound basis for the derivation of some aspects of the analysis.

The geometry and general kinematic characteristics of the NMT have been thoroughly investigated. Its dynamic characteristics (unbalance) and load capacity have also been analyzed. Utilizing this analysis, the suitability of the mechanism for high-speed/high-power systems is investigated through the use of design examples.

To provide a cl , concise description of the NMT and its applications, limitations, and benefits, the main body of this report presents equations derived as required. For completeness, the full analysis including applicable equations, figures, etc.) is presented as an ppendix. Capsule summaries in the form of narrative figures are utilized throughout the main body of the report to highlight key ~~topics~~ topics.

DD FORM 1 NOV 68 1473

Unclassified
Security Classification

14 KEY WORDS	LINK A		LINK B		LINK C	
	ROLE	WT	ROLE	WT	ROLE	WT
Nutating Mechanical Transmission						
Gears						
Speed Reducer						
Cam Tooth						
Nutator						
Rotor Cam						
Stator Cam						

Contract N0001 4-72-C-0272
NR 259-102
Final Report/D210-10747-1
January 1974

NUTATING MECHANICAL TRANSMISSION (MAROTH DRIVE PRINCIPLE)

by

Raymond J. Drago and A. J. Lemanski

THE BOEING VERTOL COMPANY
(a division of The Boeing Company)
Philadelphia, Pennsylvania 19142

NOTES

U.S. Air Force Aero Propulsion Laboratory Director Funds (Fiscal Year 1972) Contributed to the Funding of the Study of the Maroth Transmission Concept.

Department of the Navy, Naval Air Propulsion Test Center Funds (Fiscal Year 1972) Contributed to the Funding of the Study of the Maroth Transmission Concept.

DEPARTMENT OF THE NAVY
Office of Naval Research
Arlington, Virginia 22217

FOREWORD

This is the Boeing Vertol Company's Draft Final Report covering the project entitled, "Nutating Mechanical Transmission (Maroth Drive Principle)". This report covers the work accomplished during the 18 month period from 30 June 1972 through 31 December 1973 for the Office of Naval Research, Department of the Navy under Contract N00014-72-C-0272.

Office of Naval Research Technical Direction has been provided by the Contracting Officer's Technical Representative, Lt. Richard Miller.

This program has been conducted at the Boeing Vertol Company under the technical direction of Mr. A. J. Lemanski (Program Manager), Chief of the Advanced Drive System Technology Department. Principal Investigator for the program is Mr. Raymond J. Drago (Project Engineer).

The "Nutating Mechanical Transmission (Maroth Drive Principle)" is the invention of Mr. Arthur M. Maroth, President of Maroth Engineering Company, Wilton, Connecticut. The U.S. patents covering the Maroth concept are: 3094880, 3139771, 3139772 and 3590659. Acknowledgement is also made to Mr. Maroth for the use of a concept model, related background data, and several photographs of a conceptual model.

Acknowledgement is also made to Mr. Robert Howells of the Advanced Drive Systems Technology Department for his efforts in the tedious task of checking and verifying much of the theoretical analysis as well as performing most of the calculations required for the design case studies.

TABLE OF CONTENTS

LIST OF ILLUSTRATIONS

LIST OF TABLES

LIST OF SYMBOLS

A^{1}_{35}	Rotation of the X_A, Y_A, Z_A system about the X_A axis in the Y_A, Z_A plane
AF	Distance defined in calculation of cam tooth root tensile stress (Figure A18)
A_{ijCA}	The angle between points i and j, where i and j may be an integer from 1 through 9, with the apex at the mechanism focus
a_{CAi}	The distance from load line to the intersection point of a tooth centerline with its critical section, measured perpendicular to the load line in the tooth mean plane
a_{OCA}	A nutator roller dimension (defined in Figures A19 and A20)
BKL_{CA}	Backlash of cam teeth
b_{CAi}	Contact bandwidth between tooth and roller
b_{OCA}	A nutator roller dimension (defined in Figures A19 and A20)
C	Rated dynamic capacity of a rolling element bearing
C_{OCA}	A nutator roller dimension (defined in Figures A19 and A20)
C_{PCA}	Angular pitch of the nutator rollers
C_{TCA}	Contact duration
c	Minimum axial clearance required between nutators in a double nutator unit
D	Total distance normal to nutator centerline required for each center support bearing
D_A	Total axial distance along the NMT centerline required for each center support bearing
D_{BM}	Maximum center support bearing mean diameter

D_{maxCA}	Total axial distance along NMT centerline inherently available on cam side of nutator for spreading center support bearings
DN	A factor which measures bearing operating speed
D_{SACT}	Actual shaft diameter
D_{SMAX}	Maximum shaft diameter possible for a specified support bearing ID
d	Diameter of rolling element of a cylindrical roller bearing
d_{CA}	Diameter of the rolling elements used to support a nutator roller on either the rotor or stator side of the nutator
d_{CAi}	Distance between the point of load application and the critical section of a cam tooth, measured parallel to tooth centerline
dc_{CA}	Axial clearance available within the center region of a cam
d_{OCA}	A nutator roller dimension (defined in Figures A19 and A20)
ds_{CA}	Axial clearance on either rotor or stator side of nutator required for the nutator structure and rollers as they sweep through angles σ and ν
E_{CA}, E_{RCA}	Elastic moduli for cam tooth and roller, respectively
e_{CAi}	One half the tooth thickness at its critical section
F_{ast}	Torsional shear stress allowable
FE	Distance defined in calculation of tooth root tensile stress (Figure A18)
F_e	Bending stress endurance limit
F_{FRCA}	Friction force required to prevent skidding of nutator roller
F_{MAXCA}	Maximum instantaneous load in the assumed roller load distribution

F_{mc}	Dynamic balancing force generated by a rotating nutator balance weight
F_{NCAi}	Normal load acting on the i^{th} cam tooth, or normal load on a roller at i^{th} contact point
F_{NFRCA}	Normal roller load required to prevent skidding of nutator roller
F_{RCAi}	The radial component of the normal load F_{NCAi} acting on the i^{th} cam tooth
F_{su}	Ultimate torsional shear stress limit
F_{TCAi}	The thrust component of the normal load F_{NCAi} acting on the i^{th} cam tooth
F_{TNXCA}, F_{TNYCA}, F_{TNZCA}	Net forces on the nutator
F_{TXCA}, F_{TYCA}, F_{TZCA}	Net loads on a cam due to the summation of the loads on all the cam teeth
F_X	Radial load at nutator center support bearing required to react the nutator driving loads
F_{XCAi}, F_{YCAi}, F_{ZCAi}	The X, Y, Z components, respectively, of the normal load F_{NCAi} acting on the i^{th} cam tooth
f	Coefficient of friction between nutator roller and cam tooth
f_b	Bending stress
fc_{CA}	Minimum radial clearance between nutator center support bearing and cam support structure
f_{st}	Torsional stress
g	Acceleration due to gravity
h_{CA}	Radial distance from mechanism centerline to point of intersection of cam tooth and cam support structure
ID	Inner diameter
IL_{ACA}	Integer component of L_{ACA}

I_S	Moment of inertia of nutator support shaft
I_{XA}, I_{YA}, I_{ZA}	Elements of nutator moment of inertia matrix $[I_N]$
I_{XN}, I_{YN}, I_{ZN}	Elements of nutator moment of inertia matrix $[I]_{XYZ}$
$[I_N]$	Moment of inertia matrix of the nutator in the X_A, Y_A, Z_A coordinate system
$[I]_{XYZ}$	Moment of inertia of the nutator as a function of time in the X, Y, Z coordinate system
J_{RCA}	Polar moment of inertia of nutator roller
J_{XYA}, J_{XZA}, J_{YXA}, J_{YZA}, J_{ZXA}, J_{ZYA}	Elements of nutator moment of inertia $[I_N]$
J_{XYN}, J_{XZN}, J_{YXN}, J_{YZN}, J_{ZX}, J_{ZY}	Elements of nutator moment of inertia $[I]_{XYZ}$
K'	A factor, based on the tooth/roller contact duration, used to adjust the frequency of the sinusoidal load function for the nutator roller
K_b, K_{st}	Stress concentration factors for shaft bending and torsion, respectively
L	Life (B-10) of a cylindrical roller bearing
L_{ACA}	Contact ratio
L_m	Distance from mechanism focus to center of mass of a nutator balancing weight measured along the mechanism axis
ℓ	Length of the rolling element of a cylindrical roller bearing
ℓ_{CA}	Length of a nutator roller on either the rotor or stator side of the nutator
ℓ'_{CA}	Length of roller/tooth contact
M	Overturning moment applied to nutator center support bearing and shaft

M_C	Mass of cylindrical hole through center of nutator roller
M_c	Mass of a nutator balance weight
MF	Material factor for cylindrical roller bearing
M_F	Mass of solid frustum of a cone
M_G	Reduction ratio
M_{GF}	Fixed reduction ratio
M_{GV}	Variable reduction ratio
M_{mc}	Moment generated by a rotating nutator balance weight
M_{mcX}, M_{mcY}, M_{mcZ}	Components of the moment M_{mc} generated by the synchronous nutator balance weight system
M_{TNXCA}, M_{TNYCA}	Net overturning moments about X_o and Y_o axes, respectively, acting on the nutator
M_{TXCA}, M_{TYCA}	Net overturning moments about the X_o and Y_o axes, respectively, acting on a cam
M_{XN}, M_{YN}, M_{ZN}	Moments due to nutator unbalance
M_{1CAi}, M_{2CAi}	Reaction moments which must be exerted by the nutator structure to restrain the roller at its outer and inner ends, respectively
M_{OCAi}	Maximum moment exerted on loaded portion of nutator roller shaft
N_{CA}	Number of teeth on cam
N'_{CA}	Number of teeth on cam not under consideration (e.g., if considering rotor $N'_{CA} = N_S$ and if considering stator $N'_{CA} = N_R$)
N_{NCA}	Number of rollers on cam side of nutator
n_{NCA}	Angular velocity of nutator
n_1	Input speed
OD	Outer diameter

P	Angular velocity of stator expressed as a fraction of input speed
P_m	Cubic mean radial load applied to a bearing
R'	Radial load at nutator center support bearing required to react the overturning moments
R_b	Ratio of actual to allowable bending stress
R_{BCCA}	Basic spherical radius on rotor or stator side
R'_{BCCA}	Radius perpendicular to mechanism axis
R_{BO}	Outer radius of nutator center support bearing
R_{CAi}	Radius to the load point, measured perpendicular to the shaft centerline
R_{FCA}	Cam tooth fillet radius
R_m	Radius from mechanism axis to center of mass of nutator balancing weight
RPM_{Rel}	Rotational speed of bearing outer race relative to inner race
R_{so}	Outside radius of nutator support shaft
R_{si}	Inside radius of nutator support shaft
R_{st}	Ratio of actual to allowable torsional stress
R_T	Total radial load on nutator center support bearing
R_{1CAi}, R_{2CAi}	Reaction forces which must be exerted by the nutator structure to restrain the roller at its outer and inner ends, respectively
r_{CA}	Nutator roller mean outside radius at R_{BCCA}
r'_{CA}	Nutator roller effective radius of curvature
r_{ICA}	Outside radius of nutator roller at end nearest mechanism outer diameter
r_{OCA}	Outside radius of nutator roller at end nearest mechanism centerline
r_{IN}	Radius of hole through center of nutator roller

r_{SCA}	Radius of nutator roller support shaft (cam follower mounting only)
S_{bCAi}	Stress in nutator roller at point at which maximum moment (M_{OCAi}) is exerted
S_{CCAi}	Maximum compressive stress between tooth and roller at i^{th} point
S_{FF}	Nutator roller skidding force factor
SO_{CA}	Amount by which nutator roller support structure extends outward past the greatest diameter of the roller
S_{TCAi}	Maximum bending stress at the fillet of a cam tooth
T_{CA}	Total torque on a cam
T_{FRCA}	Friction torque required to prevent skidding of a nutator roller
T_{TCA}	Theoretical cam tooth tip thickness
V_C	Volume of cylindrical hole through center of nutator roller
V_F	Volume of solid frustum of a cone
$V_{PCA/CA}$	Linear velocity of a point on the centerline of a nutator roller with respect to a cam
$V_{XPCA/CA}$, $V_{YPCA/CA}$, $V_{ZPCA/CA}$	Components of $V_{PCA/CA}$
W	Width of a nutator center support bearing
w	Spread distance between centerline of the nutator and the mid-width plane of a nutator center support bearing
X, Y, Z	Rectangular coordinate system fixed to nutator and with origin at mechanism focus
X_{HPCCA}, Z_{HPCCA}	Coordinates of mean tooth profile at initial point of tooth/roller contact (i.e., start of active profile)

X_{LPCCA}, Z_{LPCCA}	Coordinates of mean tooth profile at final point of tooth/roller contact (i.e., end of active profile)
X_O, Y_O, Z_O	Coordinate system with Z_O axis lying along mechanism axis, X_O axis horizontal, and Y_O axis vertical (Figure A16)
X_{PCA}, Y_{PCA}, Z_{PCA}	Coordinates of a point on the centerline of a nutator roller with respect to nutator null plane
$X_{PCA/CA}$, $Y_{PCA/CA}$, $Z_{PCA/CA}$	Coordinates of a point on the centerline of nutator roller relative to cam (i.e., pitch path)
$X_{PF/CAi}$, $Y_{PF/CAi}$, $Z_{PF/CAi}$	Coordinates of i^{th} point on a cam tooth profile
X_{TCA}, Y_{TCA}, Z_{TCA}	Coordinates of the tangent line to the pitch path
Y	Minimum installation clearance required between shaft outer radius and bearing bore radius
Y_{SCAi}	Nutator roller deflection at point at which maximum moment is exerted
Z_{SCAi}	Depth of maximum subsurface shear stress
α_{CA}	Angular pitch of cam teeth
α_{BKL}	Angular backlash
α_{PFCAi}	Angle between line a_{CAi} and the cam tooth centerline
α_{ROL}	Included roller half-angle
$\alpha_{RCA/CL}$	Angular acceleration of nutator roller about its own centerline
α_{TCA}	Angular cam tooth tip thickness
$\cos(\alpha_{CLCA})$, $\cos(\beta_{CLCA})$, $\cos(\gamma_{CLCA})$	Direction cosines of a line from the mechanism focus to a point on the centerline of a nutator roller

$\cos(\alpha_{PCA/CA})$, $\cos(\beta_{PCA/CA})$, $\cos(\gamma_{PCA/CA})$	Direction cosines of a line tangent to the pitch path
$\alpha'_{PCA/CA}$, $\beta'_{PCA/CA}$, $\gamma'_{PCA/CA}$	Derivatives of the coordinates of the pitch path
$\cos(\alpha_{PFCA})$, $\cos(\beta_{PFCA})$, $\cos(\gamma_{PFCA})$	Direction cosines of a line joining a point on a cam tooth profile and the pitch path (i.e., the direction cosines of the normal tooth load vector)
β_{CAi}	Angle between cam tooth fillet tangent line and the load line
γ_{CA}	Angle between path of nutator roller centerline and the plane of the nutator
$\gamma_{ROL/CA}$	Nutator roller taper angle
$[\gamma]$	Matrix of direction cosines of rotated position
$[\gamma]'$	Transpose of $[\gamma]$
$[\gamma_A]$	Matrix of direction cosines of the X, Y, Z coordinate system with respect to the X_A, Y_B, Z_B coordinate system, after rotation through angle A'_{35} about the X axis
$[\gamma_A]'$	Transpose of $[\gamma_A]$
$[\gamma_B]$	Matrix of direction cosines of the X, Y, Z coordinate system with respect to the X_A, Y_B, Z_B system, after rotation through angle τ_{CA} about the Y axis
$[\gamma_B]'$	Transpose of $[\gamma_B]$
$[\gamma]_C$	Equal to $[\gamma_B]$ $[\gamma_A]$, matrix of direction cosines after rotation thru A'_{35} and τ_{CA}
$[\gamma]'_C$	Transpose of $[\gamma]_C$, equal to $[\gamma_A]'$ $[\gamma_B]'$
Δ_{CA}	Cam tooth undercut
ζ_{SCAi}	Maximum subsurface shear stress of tooth/roller

$\theta_{CA/N}$	Relative angle of rotation between cam and nutator
θ_{FCA}	Angle between tooth centerline and tangent line to tooth fillet
$\theta_{PF/PPCA}$	The angle between the line defined by a point on the pitch path and the corresponding point on the tooth profile, and the tangent line to the pitch path at the point of interest.
$\theta_{PF/RVCA}$	The angle between the line defined by a point on the pitch path and the corresponding point on the tooth profile, and the radius vector from the mechanism focus to the point on the pitch path
θ_S	Angular rotation of the stator cam
θ_{1CAi}, θ_{2CAi}	Slope of nutator roller across its support bearings
μ_{CA}, μ_{RCA}	Poission's ratio for cam tooth and roller, respectively
ν	Nutation half-angle
ρ_{CAi}	Cam tooth profile curvature radius at i^{th} point
σ_{CA}	Nutator roller centerline coning angle on either rotor or stator side
τ_C	Output torque of mechanism
τ_{CA}	Rotation in the XZ plane of the X_A, Y_B, Z_B coordinate system about the Y axis
ω_C, $\omega_{C/G}$	Angular velocity of input (relative to ground)
ω_{CA}, $\omega_{CA/G}$	Angular velocity of cam (relative to ground)
$\omega_{C/CA}$	Angular velocity of input relative to cam
$\omega_{CA/C}$	Angular velocity of cam relative to input
$\omega_{CA/N}$	Angular velocity of cam relative to nutator
$\omega_{N/C}$	Angular velocity of nutator relative to input

$\omega_{N/CA}$	Angular velocity of nutator relative to cam
$\omega_{N/G}$	Angular velocity of nutator relative to ground
ω_{NCA}	Input angle at which roller/tooth contact begins
ω_{O}	Input shaft turning angle
ω_{Oi}	The i^{th} point in the sinusoidal load distribution cycle applied to the nutator roller
ω'_{Oi}	The angular distance form the start of tooth/roller contact to the i^{th} point in the load cycle
$\omega_{RCA/CL}$	Angular velocity of nutator roller about its own centerline
ω_{XCA}	Input angle at which tooth/roller contact ends
ω_{XN}, ω_{YN}, ω_{ZN}	Components of the nutator angular velocity
$\omega_{XN/S}$, $\omega_{YN/S}$, $\omega_{ZN/S}$	Components of the nutator angular velocity with respect to the stator

Subscripts

CA	General term referring to cam, where the cam may be either rotor (CA = R) or stator (CA = S)
N	Refers to nutator
R	Refers to rotor
S	Refers to stator

1. INTRODUCTION

A continuing need exists to design and develop advanced power train systems in order to keep pace with the advancing technology of prime movers (such as gas turbine engines) and vehicle design requirements including helicopter, surface effects ships, hydrofoils, etc.

For the past decade, power transfer systems have primarily dictated improvements in the power-to-weight ratio, reliability/maintainability, vibration/noise levels and system life. To achieve these improvement goals, past studies indicated a strong need to investigate advanced-concept-type mechanical power train systems such as the Maroth Nutating Drive, Harmonic Drive, Cyclo drive, Planocentric drive, etc. Recent Boeing Vertol studies indicated that the Maroth Nutating transmission had the most promise of achieving the improvement goals as compared to other advanced concepts. This drive, referred to as the nutating mechanical transmission (NMT), has unique features when compared to conventional gear arrangements which include very high profile contact ratio, high reduction ratio in one stage, the potential for low vibration/noise levels, high efficiency and design flexibility.

Current power train system designs utilize gear teeth as the critical connecting links in the continuity of the drive train. Standard gear designs have one pair of teeth carrying the major percentage of load in a given mesh. Failure of one tooth will result in relatively rapid loss of torque and possible system failure. By comparison however, the NMT concept provides for multiple load sharing between input and output by virtue of the numerous action and reaction cams and planes coupled by a nutating ring containing tapered pins. For this reason, failure of one or more cams, planes or pins would only increase load on those remaining, thereby reducing their B-10 lives. Since the pins are actually bearings, torque and phasing will be maintained, thereby immediate catastrophic failure would be precluded.

In addition, since the contact is theoretically pure rolling in the NMT (while that of gear teeth is theoretically rolling and sliding) the heat generated should be lower and the efficiency higher. Due to its general arrangement and number of load sharing elements, a decrease in relative vulnerability is to be expected.

This report presents the results of an analytical program undertaken to define the operational characteristics and potential load capacity of the nutating mechanical transmission (NMT) concept. Since a fully operational NMT capable of any substantial loading has not been constructed, the scope of this analysis has been largely analytical. Substantial technology has, however, been borrowed from the gear and bearing fields to provide a sound basis for the derivation of some aspects of the analysis.

The basic geometry of the mechanism and its general kinematic characteristics have been thoroughly investigated. The dynamic characteristics (unbalance) and load capacity of the NMT have also been analyzed during this program. Utilizing this analysis, the suitability of the mechanism for high speed/high power systems through the use of design examples is investigated.

In order to provide a clear, concise description of the NMT and its applications, limitations, and benefits, the main body of this report presents derived equations as required. For the sake of completeness, however, the full analysis including applicable equations, figures, etc. is presented as an appendix. In addition, in a format similar to that used in the annual report, capsule summaries in the form of narrative figures are utilized throughout the main body of the report to highlight key topics.

2. GENERAL DESCRIPTION AND OPERATION

The Nutating Mechanical Transmission (NMT) consists of three basic components: the rotor (output), the stator (fixed reaction), and the nutator. The general configuration of the mechanism is shown schematically in Figures 2-1 and 2-2. The nutator is mounted on the input shaft at some angle ν defined as the nutation half-angle. Rotation of the input shaft causes the nutator to nutate or wobble with respect to the shaft. The rollers, which are mounted on the nutator (see Figure 2-2), engage the teeth on the rotor and stator cams. Rotation of the input while one member (generally the stator) is held stationary causes a differential motion of the other member. This motion is proportional to the relative numbers of teeth and rollers on the component parts.

The rotor and stator cams are similar, in that they each contain tapered teeth which vanish (theoretically) at the mechanism focus; however, the parts do not have the same number of teeth. Figure 2-3 shows an assembled, motor-driven, kinematic demonstration model; the model is shown in a disassembled condition in Figure 2-4 so that the component parts may be observed. Since this model is a single nutator design, the balance weights shown in the figure must be utilized to maintain vibration-free action.

The shape and size of the teeth on each cam are strong functions of the nutation half angle, the nutator roller size, and the relative number of elements on the cam and nutator. In general the height of the cam tooth increases with increasing nutation half angle, and the thickness of the teeth decrease with increasing ratio and/or increasing roller size. The stator cam is the fixed reaction member and performs much the same function as the stationary internal ring gear of a simple planetary system. The contact conditions are, of course, quite different.

The rotor cam is the rotating output member, and performs about the same function as the carrier in a simple planetary system. In terms of the number of separate interrelated parts, the nutator is the most complicated part of the NMT.

The nutator may be supported at its inner or outer diameter, depending on the method of input and output. Whatever the support bearing arrangement, the configuration of the roller support area of the nutator is similar. Basically, the nutator consists of six distinct components: the rotor and stator side rollers, their support bearings, the nutator

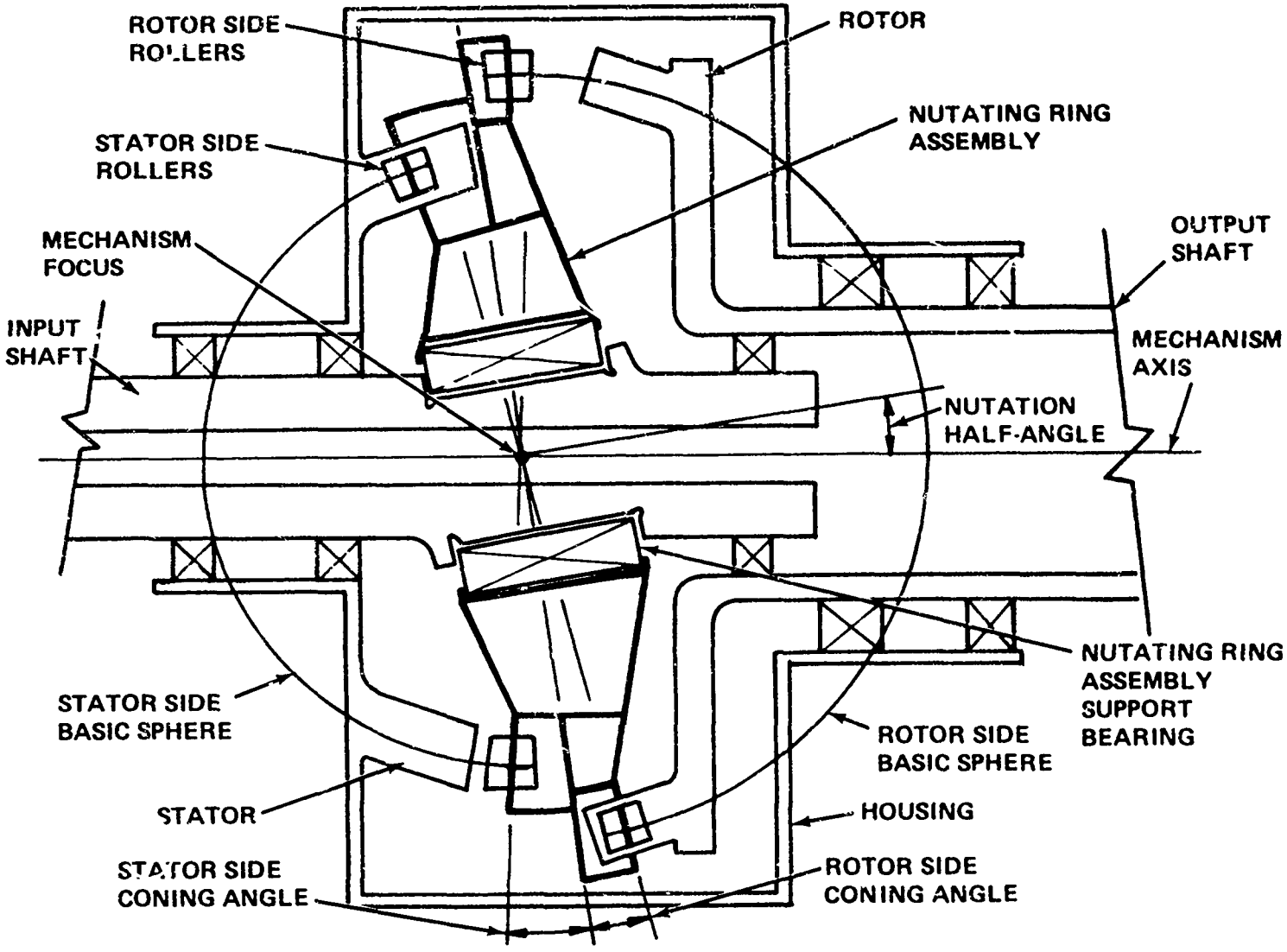

Figure 2-1. Nutating Mechanical Transmission Schematic.

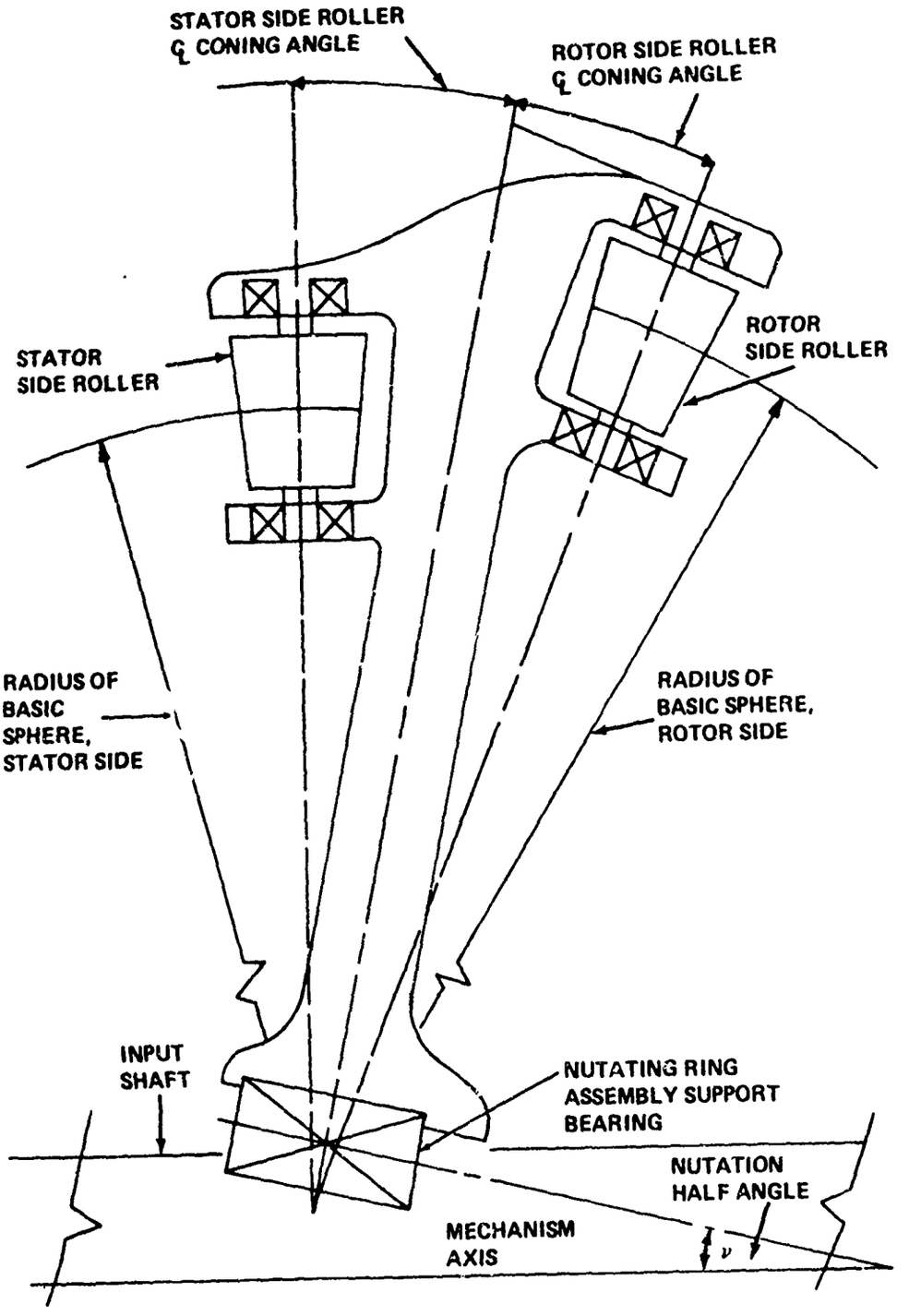

Figure 2-2. Nutator Schematic.

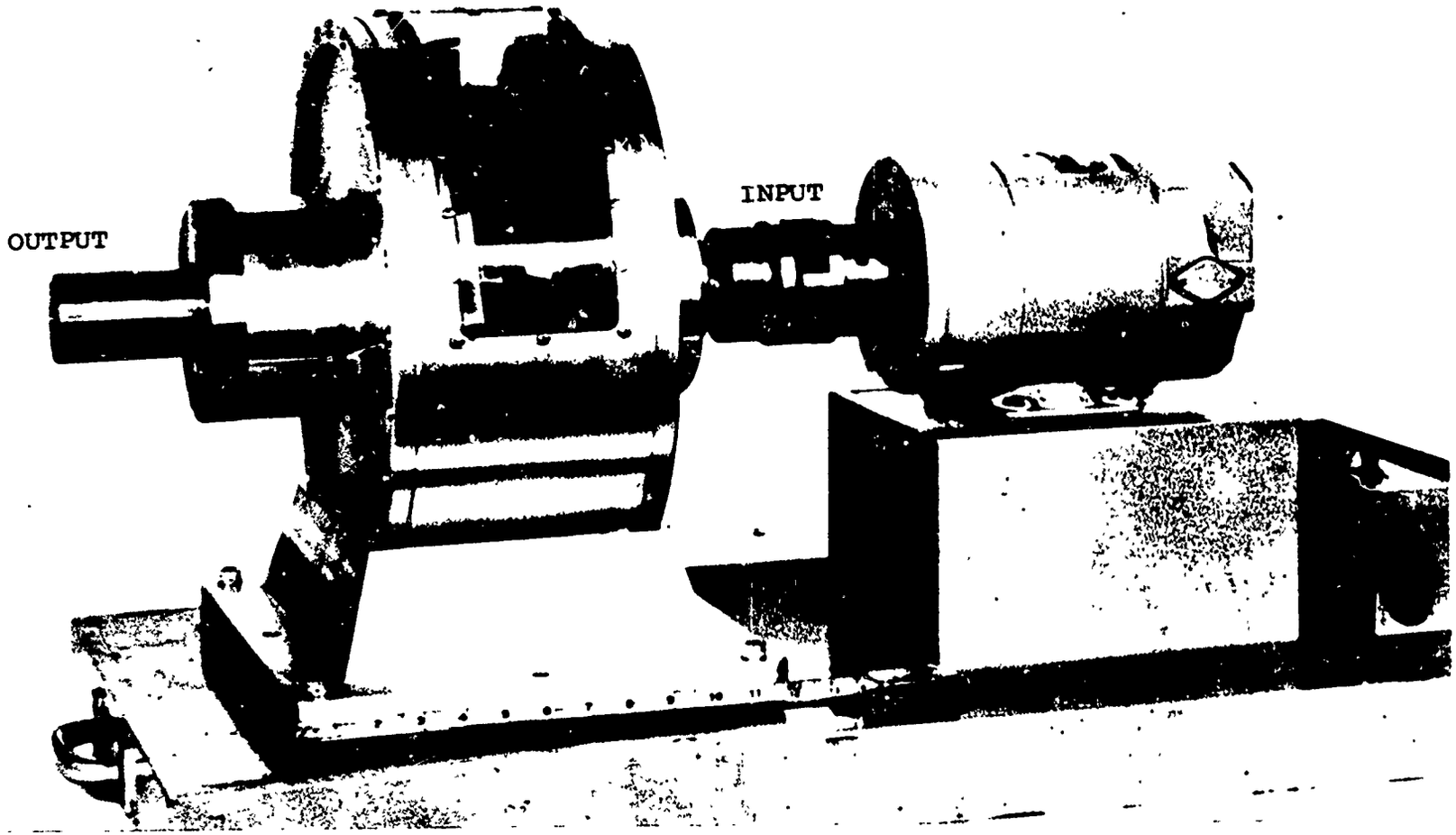

Figure 2-3. Nutating Mechanical Transmission Powered Model.

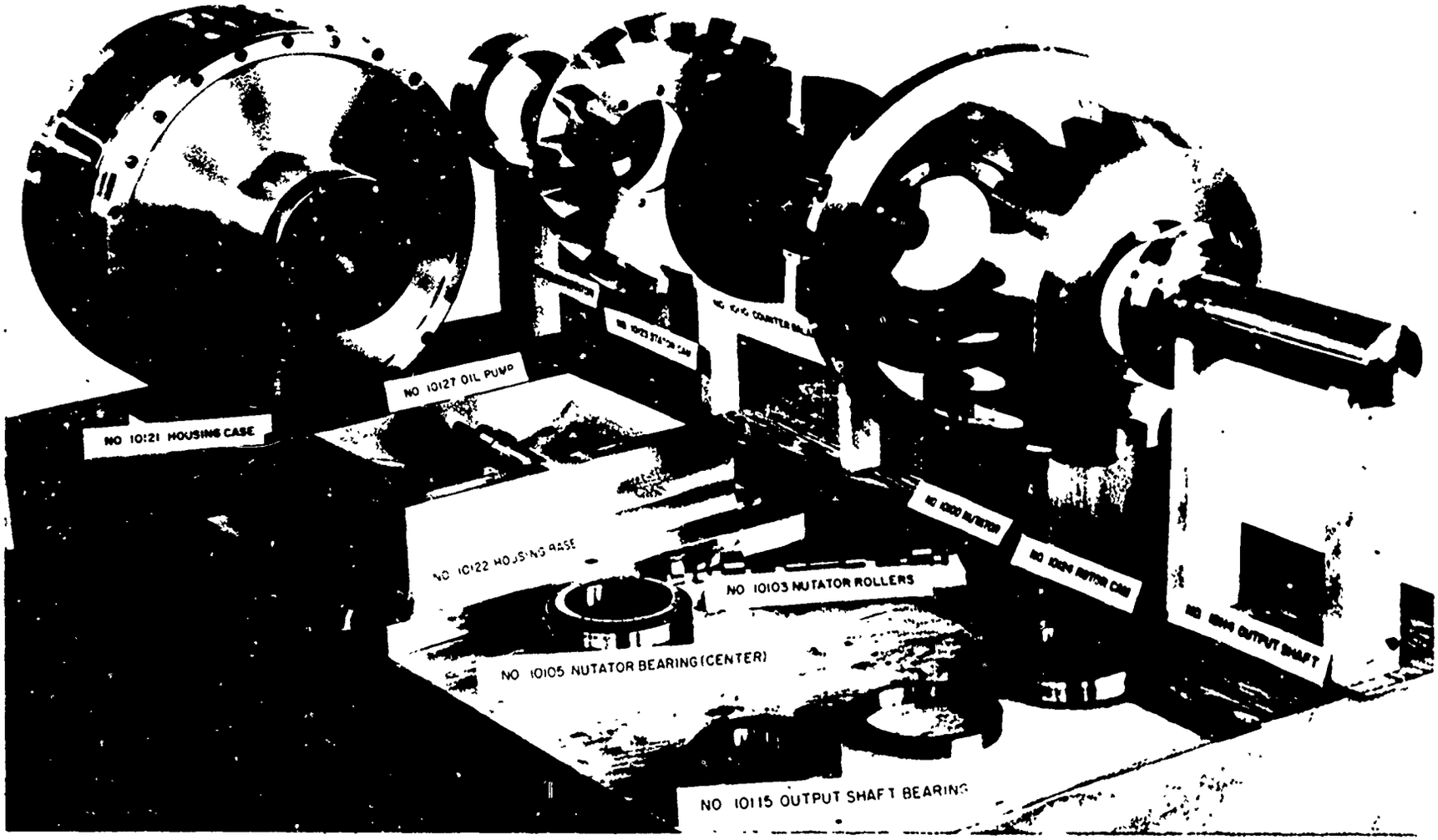

Figure 2-4. Exploded View of Conceptual Model.

structure, and the nutating ring assembly support bearing. Although the number of individual parts required to complete a single nutating ring assembly can be quite large (depending on the ratio), these parts are generally not individually critical, and the design may be configured to provide acceptable levels of reliability and maintainability while yielding excellent fail-safe capability. This very high fail-safe feature derives from the fact that, except for low speed ratios, the contact ratio (average number of rollers in contact with each cam) is quite high, thus the failure of a single element somewhere in the system will not cause a catastrophic system failure. Indeed, on some very high ratio designs the failure of a single element might cause only minimal disturbance.

It should also be noted that although the part count is generally high, the number of different part types is low; i.e., all the rollers and support bearings on each side of the nutator are identical. Consequently, the number of different parts is considerably reduced.

Each nutator roller must be supported on its own bearing system. Several methods of supporting the nutator rollers are available. If the roller is large enough, it may be made hollow so that a roller bearing may ride on the shaft between it and the roller, as is the case with a cam follower bearing (as shown in Figure 2-5). This configuration has the dual advantages of simplicity and light weight.

Minimizing the weight and inertia of the nutator rollers is an important design consideration since it may materially reduce their tendency to skid. However, if the roller diameter is relatively small, it must be supported by bearings at each end, as shown in Figure 2-6. Although this configuration requires more individual parts, it is the only practical way to support smaller rollers since it splits the load between two relatively large bearings, and thereby provides the required bearing life.

The rotor and stator cams are quite similar in both design and operation. The rotor cam is generally the output member while the stator cam serves as the reaction member. By releasing the stator and fixing the rotor to structure, the same cams will produce a mechanism with a different ratio. The new ratio would, in general, be both numerically and algebraically different (i.e., the output would change direction and speed). The basic similarity of the rotor and stator cams is thus obvious.

The teeth on each cam behave in much the same manner as gear teeth, with some very important differences. They must react both the bending and shear loads due to their contact with the nutator rollers, and they must support the surface loads also

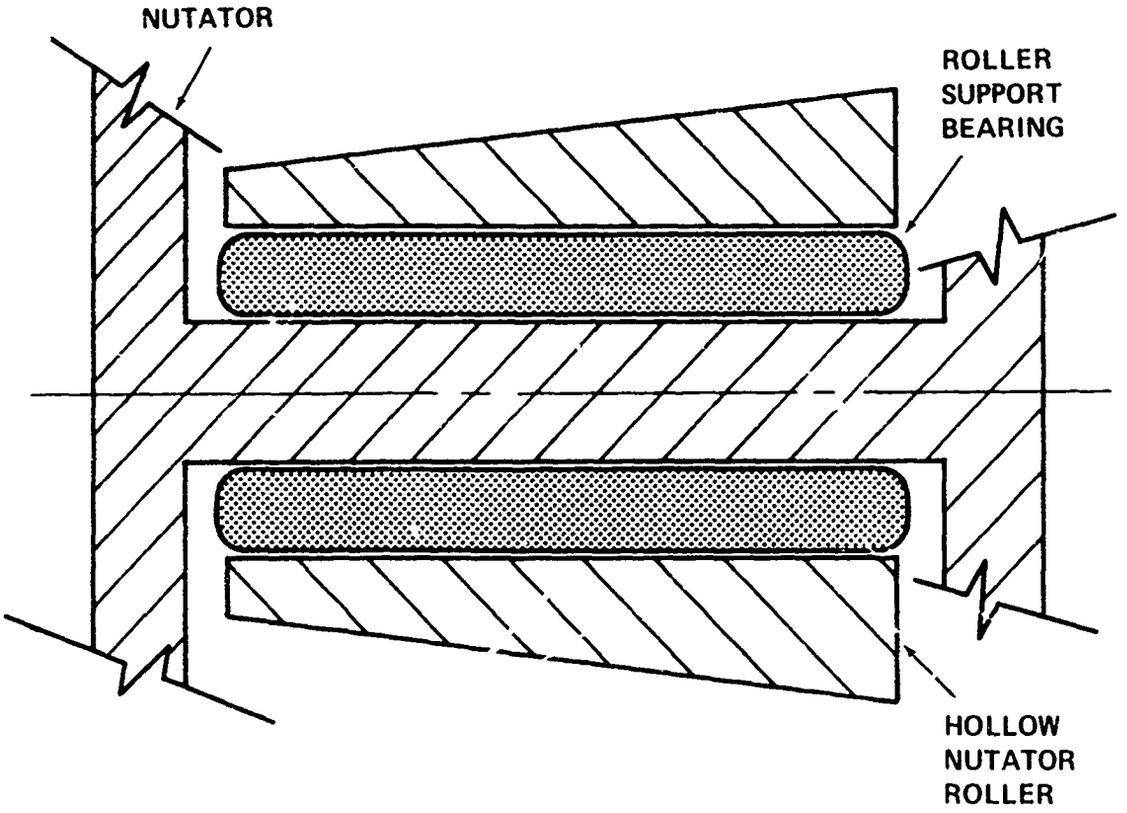

Figure 2-5. Typical Nutator Roller, Concentric Support Configuration.

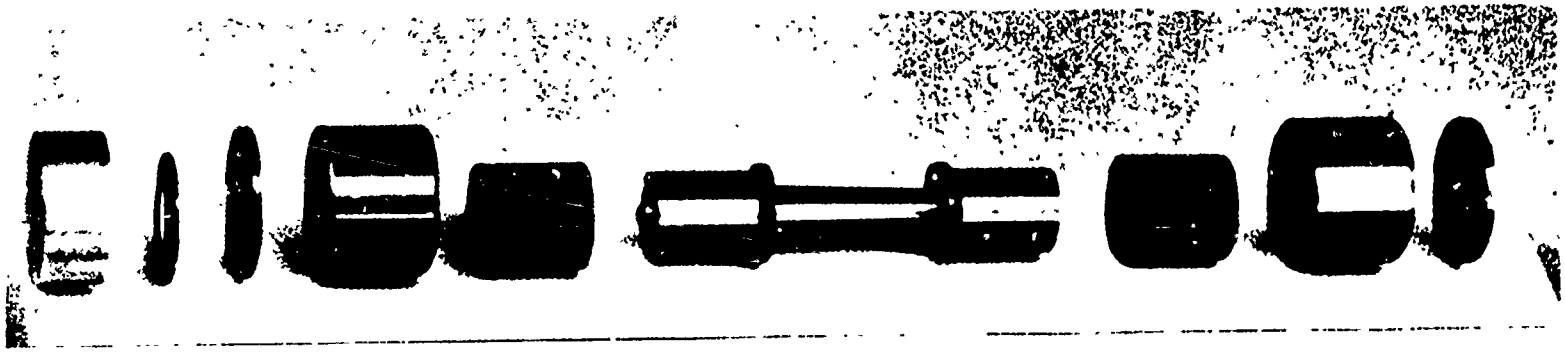

Figure 2-6. Typical Nutator Roller (End Support Configuration).

due to these rollers. For high-speed, high-load operation, the tips and flanks of the tooth profiles will probably be modified to avoid high, deflection-induced engagement and disengagement dynamic loads.

All of these properties are analogous to an involute gear system. One of the most important differences, however, is that, under ideal conditions, the cam tooth and the nutating roller mate with theoretically pure rolling contact. Even under perfect conditions, involute gears experience a significant amount of sliding throughout their mesh cycle. Although it is likely that under actual operating conditions the nutator rollers will skid slightly on engagement, this problem may be minimized by proper design.

The shape of the tooth profile within any theoretical sphere is determined by the motion of the component parts on the surface of that sphere. Since the radial form of the teeth at any section is a straight line, a basic spherical radius will be used in the ensuing analysis, for simplicity. Any other section may be obtained by linear ratio. Similarly, in manufacture, if a roller-shaped tool is used, it will only be necessary to specify mean section data. It may also be possible to use the finished stator cam to generate the rotor cam (or vice versa) to minimize errors or problems in matching the profile. This may be accomplished by using the stator as a master template to serve as the cam by which the rotor teeth are generated.

The basic operation of the mechanism is as follows. Turning the input shaft, in Figure 2-1, causes the nutator to wobble about its centerline in much the same way as a coin dropped on a table will wobble, except that the motion does not damp out. Since the stator is fixed to structure, the rotational motion of the nutator is restricted, resulting in the wobble. Depending on the relative tooth numbers involved, the nutator may or may not have a net rotational motion. Again, depending on the relative tooth numbers, the rotor will rotate either in a clockwise or counterclockwise motion.

It should be obvious that this motion results in some unbalanced oscillating loads due to the nutator wobble; however, at those speeds and sizes at which they are significant, various avenues are available to counteract their effects. The input may either be provided through the center (as shown in Figure 2-1) or by an external shell type input arrangement (as shown in Figure 2-7).

This configuration has the added advantages of providing a relatively large clear opening through the center of the drive (through which controls, instrumentation, etc. may be inserted) and a larger nutator support bearing diameter. Disadvantages

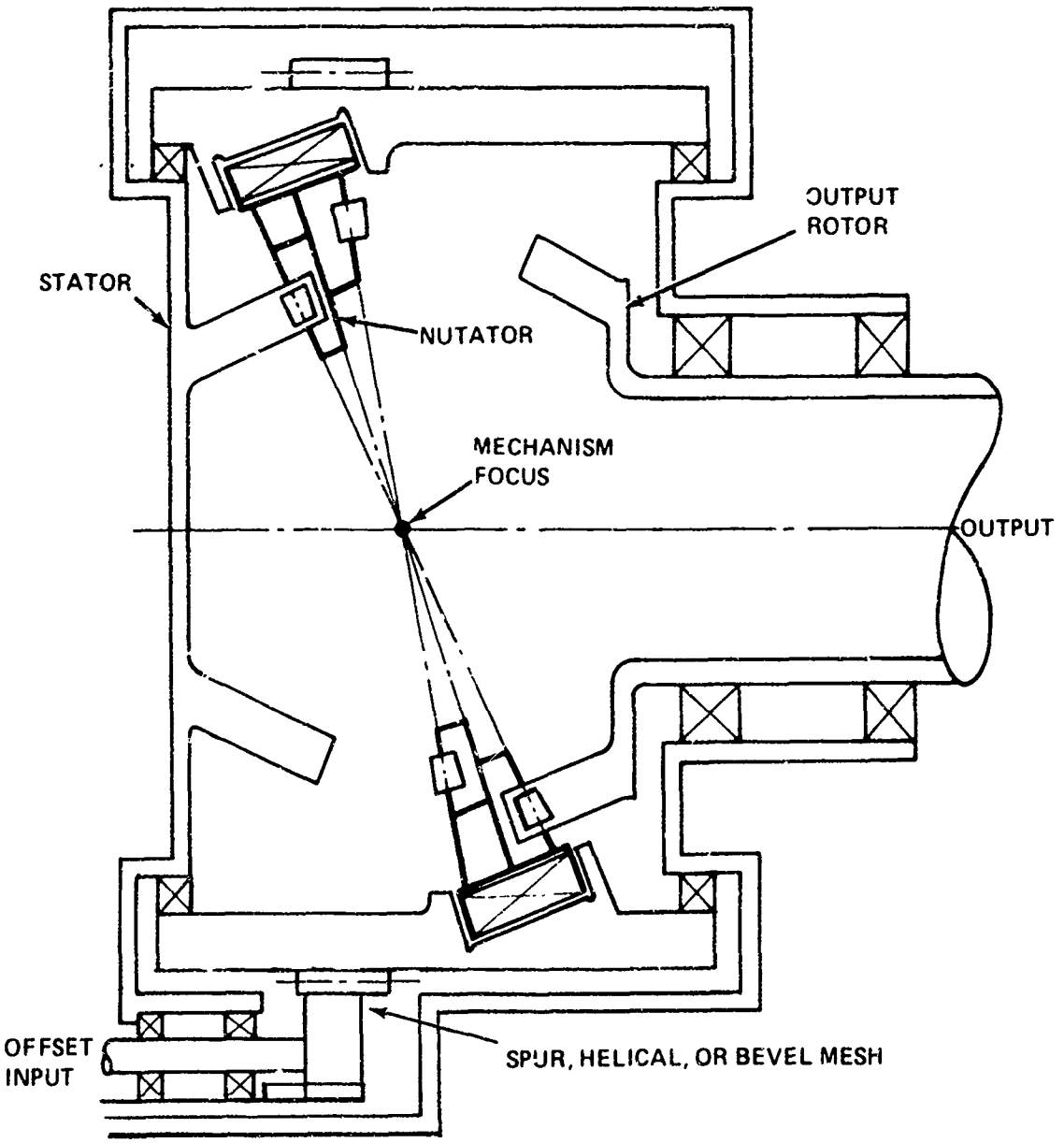

Figure 2-7. Nutating Mechanical Transmission Outer Bearing Concept.

include higher support bearing DN values and increased overall unit case size.

Many configurations and variations of the basic concept are possible; e.g., (1) the rollers on the nutator may be mounted in at least two different ways as shown in Figures 2-5 and 2-6, (2) the nutating ring assembly support bearing may be mounted either on the ID or the OD of the ring assembly as shown in Figures 2-1 and 2-7, respectively, (3) series or parallel nutators may be used to yield higher ratios or split power paths, or (4) the output may be made to rotate either in the same or opposite direction as the input.

The flexibility of application and configuration of the mechanism are readily apparent. This is not to say that each possible configuration is optimum for every application, nor that every application is even suitable for the nutating mechanical transmission concept. Each design situation requires the evaluation of many alternatives and a considerable design tradeoff study. Several detailed case studies are presented later in this document.

3. MECHANISM GEOMETRY

REDUCTION RATIO AND COMPONENT SPEEDS

The mechanism speed ratio is dependent on only four parameters: the number of teeth on the rotor and stator cams and the number of rollers on each side of the nutator. The ratio is independent of the size of the rollers and the cam teeth, as well as the nutation half-angle and the basic spherical radius. This is not to say that these parameters do not influence the selection of the mechanism ratio. The maximum, minimum, and optimum ratio for any specific application are all substantially influenced by the four parameters. For a constant ratio, the diameter of the rollers and the cam tooth thicknesses (pitch) increases with increasing basic spherical radius; that is generally, increasing the ratio on a constant basic sphere requires a progressively finer pitch. Unlike gears, the mating parts do not have a common pitch, since this pitch difference is the prime parameter upon which the ratio is dependent.

The relative numbers of teeth and rollers at the cam-nutator interface are limited by the practical restraints of roller size and cam tooth thickness. That is, if there are too many rollers and cam teeth (fine pitch) at a given diameter, the teeth and rollers become so small that mounting becomes very difficult and load capacity is impractically small. Too few rollers and cam teeth may result in an unsatisfactorily low contact ratio. If the difference between the number of rollers and the number of teeth on the mating cam is greater than about one or two, the cam teeth will become impractical in size. To yield a given ratio, two separate factors are present in the choice of a configuration: absolute and relative tooth numbers. Many other parameters will be discussed as they occur later in this report.

The kinematic model, shown in Figure 3-1, may be utilized to derive the ratio equation shown in Figure 3-2. The detailed derivation of this equation (as for all other equations used in the main body of this report) is shown in the appendix. It may be seen that this equation is identical to the ratio equation for a compound epicyclic gear train of a specific type. This similarity between the NMT and specific classical gearing systems will repeatedly manifest itself elsewhere in this analysis. The general ratio equation may be restricted to the special case shown in Equation (3.1) in which the numbers of rollers on both sides of the nutator are identical.

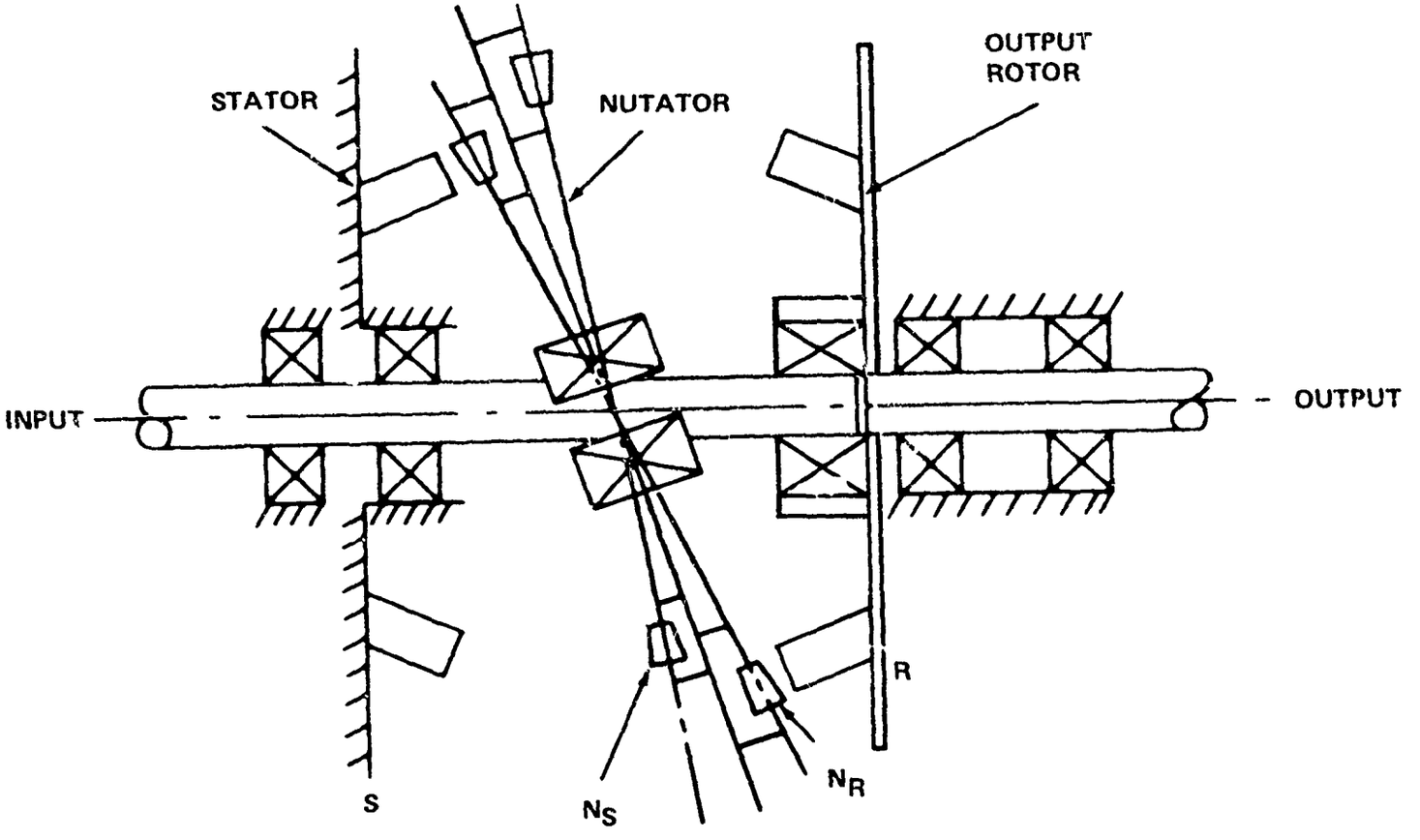

Figure 3-1. Nutating Mechanical Transmission Kinematic Model.

- RATIO IS A FUNCTION OF ONLY:
  - NUMBER OF TEETH ON ROTOR CAM
  - NUMBER OF ROLLERS ON ROTOR SIDE OF NUTATOR
  - NUMBER OF ROLLERS ON STATOR SIDE OF NUTATOR
  - NUMBER OF TEETH ON STATOR CAM
- RATIO IS INDEPENDENT OF:
  - NUTATION HALF-ANGLE
  - NUTATOR ROLLER CONING ANGLES
  - RADIUS OF BASIC SPHERE
  - SIZE OF ROLLERS
- RATIO EQUATION: (GENERAL CASE)

$$M_G = \frac{N_R N_{N_S}}{N_R N_{N_S} - N_{N_R} N_S} = \frac{1}{1 - \frac{N_{N_R}}{N_R} \cdot \frac{N_S}{N_{N_S}}}$$

WHERE:

M_G	=	RATIO
N_R	=	NUMBER OF TEETH ON ROTOR
N_{N_R}	=	NUMBER OF ROLLERS ON ROTOR SIDE OF NUTATOR
N_{N_S}	=	NUMBER OF ROLLERS ON STATOR SIDE OF NUTATOR
N_S	=	NUMBER OF TEETH ON STATOR

Figure 3-2. Mechanism Input/Output Speed Ratio Summary.

$$M_C = \frac{1}{1-\frac{N_S}{N_R}} \qquad (N_{NR} = N_{NS}) \qquad (3.1)$$

Equation (3.1) is identical to the ratio equation for a simple planetary. The apparent similarity to a planetary gear system is, however, just that - apparent. In a planetary, the numbers of teeth on the sun gear (N_R) and the ring gear (N_S) are generally quite different. They differ because reasonable sized planet gears (N_{NS} and N_{NR}) may fit in the annulus between them. Therefore, simple planetaries are generally limited to ratios in the range of 2.5:1 to 6:1, while compounds are similarly limited to a maximum of about 16:1 (higher or lower in some cases, depending on specific configuration).

The very advantage of the NMT over a planetary, however, lies in one of its limitations; that is, the numbers of teeth on its mating parts must be similar. For instance, if N_R were only slightly larger than N_S, it may be seen from Equation (3.1) that the denominator will be very small, yielding a very large quotient (ratio). This is clearly not possible with a planetary, but is a necessity in the design of an NMT. Therefore, the NMT is basically a high-ratio device. In spite of this, and with proper restraints, the NMT can be designed for low ratios, although these configurations will seldom be optimum.

With these restrictions in mind, ratios from as low as about 5:1 to several hundred (and higher in some cases) are possible. By varying the numbers of teeth on the component parts, virtually any ratio within the practical limitations noted earlier, including non-integer values, may be obtained. The simplest case occurs when the number of teeth on the stator and the number of rollers on both sides of the nutator are identical. In this case, the output may either rotate in the same direction as the input, Figure 3-3, or in the opposite direction, Figure 3-4. Also shown on these figures are the next simplest case; that is, the number of teeth on each cam is one more and one less than the number of rollers on the nutator, respectively. Almost an infinite number of similar plots may be made for various other groups of tooth-roller combinations. Figure 3-5 points out another advantage of the NMT. The direction or rotation of the output shaft may either be the same as, or opposite to, that of the input--a flexibility not provided by a planetary gearing system.

The nutator will always oscillate, depending on the nutation angle; however, it may or may not rotate with respect to the housing. That is, for one complete input rotation, the nutator may or may not return to its original angular orientation with respect to the stator. If the number of teeth on the stator and the number of rollers on the stator side of the nutator are identical, the nutator will oscillate with

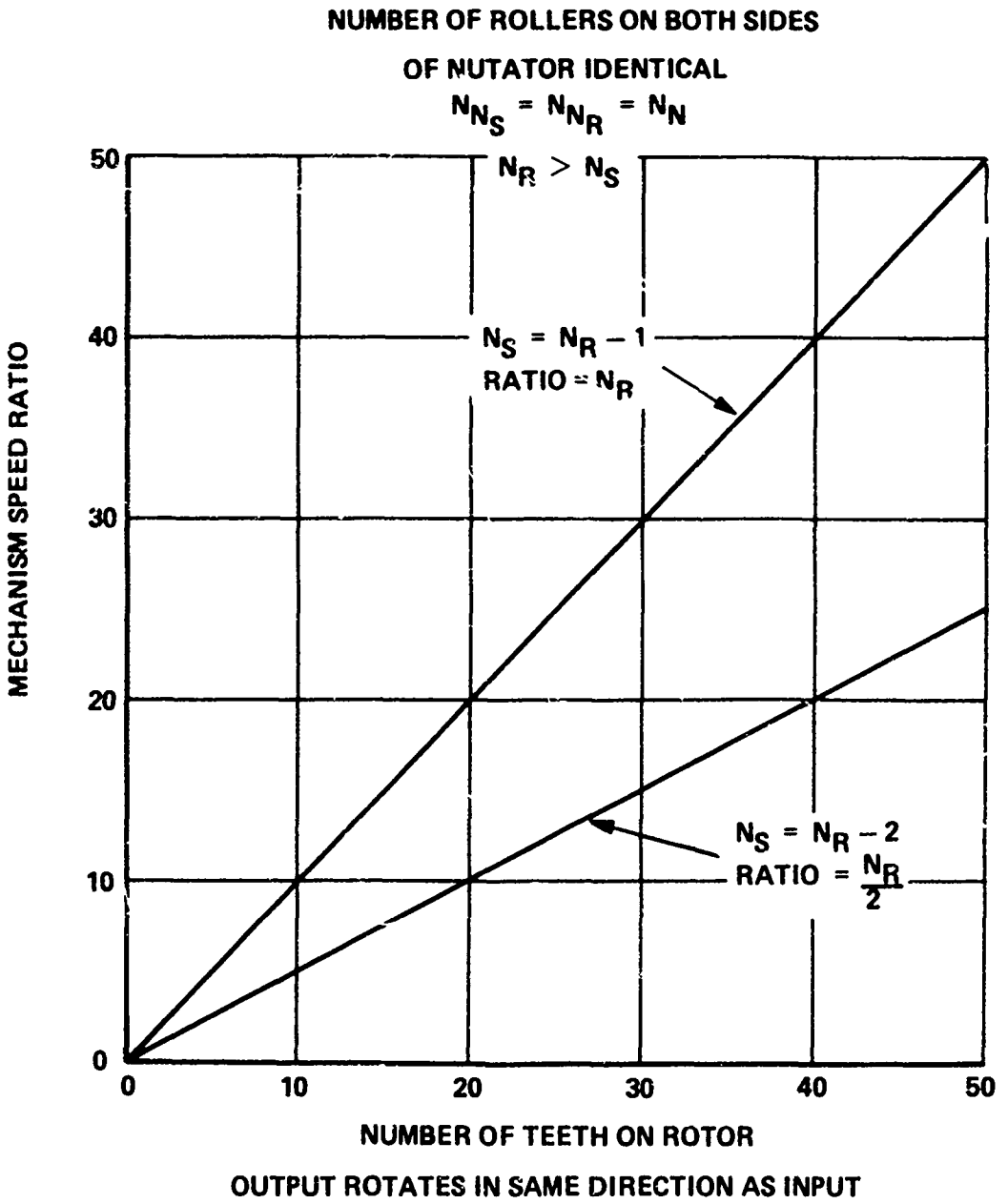

Figure 3-3. Mechanism Input/Output Speed Ratio With No Direction Change.

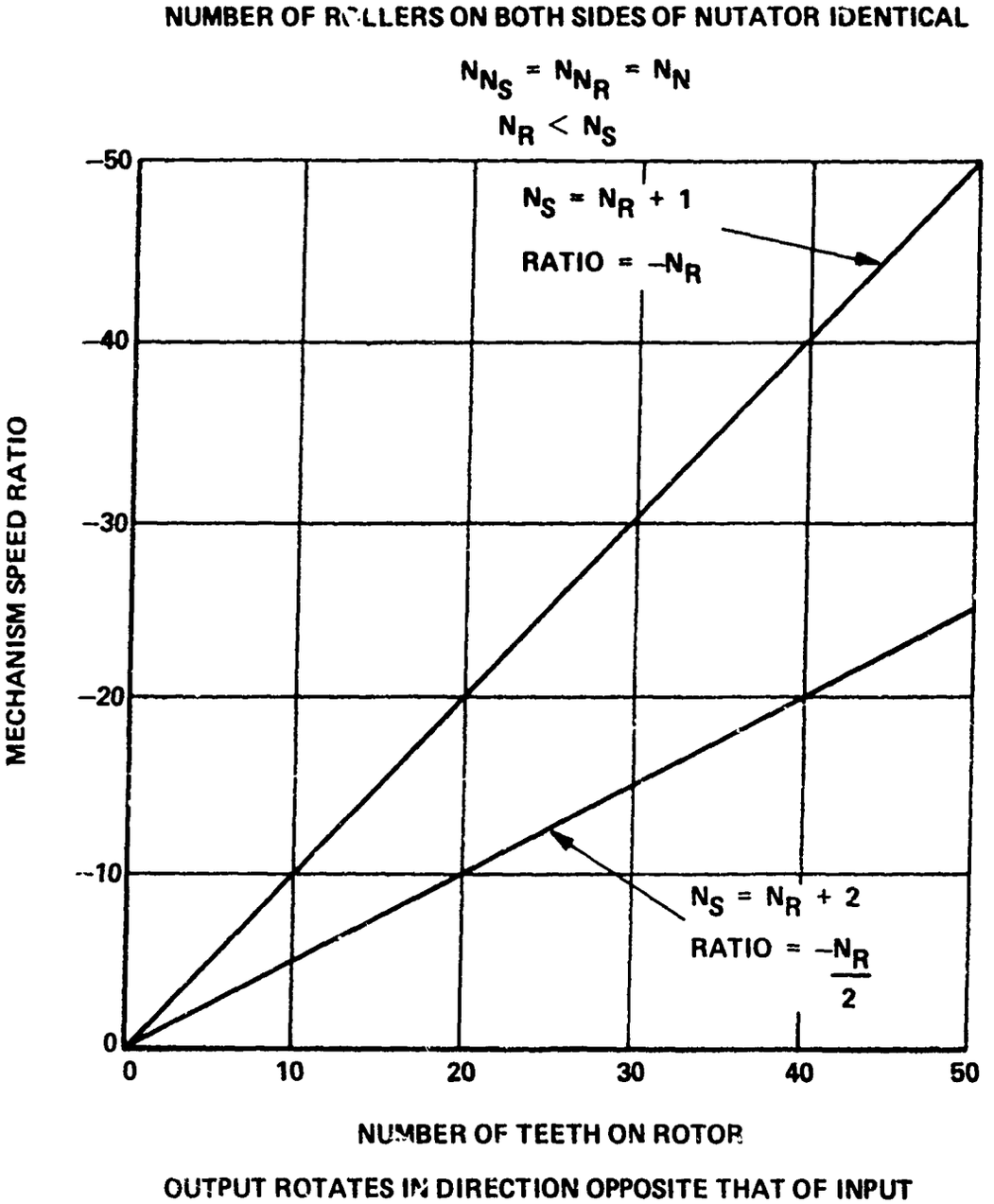

Figure 3-4. Mechanism Input/Output Speed Ratio with Direction Change.

- IS A FUNCTION OF ONLY:
  - NUMBER OF TEETH ON STATOR, N_S
  - NUMBER OF ROLLERS ON STATOR SIDE OF NUTATOR, N_{N_S}
- IF $N_{N_S} > N_S$
  - NUTATOR ROTATES IN SAME DIRECTION AS INPUT
- IF $N_{N_S} = N_S$
  - NUTATOR DOES NOT ROTATE
- IF $N_{N_S} < N_S$
  - NUTATOR ROTATES IN DIRECTION OPPOSITE THAT OF INPUT
- EQUATION:

$$n_N = \left[\frac{N_{N_S} - N_S}{N_{N_S}} \right] n_I$$

WHERE:

n_N = NUTATOR SPEED

n_I = INPUT SPEED

N_{N_S} = NUMBER OF ROLLERS ON STATOR SIDE OF NUTATOR

N_S = NUMBER OF TEETH ON STATOR

Figure 3-5. Angular Velocity of Nutator.

respect to the stator, but will not undergo any net nutation. For any other condition, the nutator will index with each input rotation.

A knowledge of the magnitude and direction of this rotation will be required to evaluate the life of the nutating ring assembly support bearing. The angular velocity of this member with respect to the housing is dependent only on the number of teeth on the fixed (to the housing) stator cam and the number of rollers on the stator side of the nutator. The relationship between nutator and rotor does not effect the conditions. The equation defining this speed relationship and some observations as to its variation are shown in Figure 3-4. Under most practical situations, the nutator speed will generally be quite slow with respect to the input speed. In fact for most practical tooth-roller combinations, the ratio of nutator speed to input speed, Figure 3-6, is close to zero and seldom greater than 0.05.

Although our attention has been restricted to the special case of the nutator relative to stator, the more general case of nutator with respect to cam (cam being a general term for either rotor or stator) is also important. The path of the rollers within each cam is directly dependent on the angular velocity of the nutator with respect to that cam. This path, in turn, is a determining factor in the development of the cam tooth forms. Obviously then, the equation detailing this parameter is important in defining the operational characteristics of the mechanism. This equation as well as those factors influencing it are shown in Figure 3-7. As was the case with ratio, the many possible combinations of tooth numbers produce an equal number of variation curves. A typical set for the relative angular velocity of the nutator with respect to the stator and rotor are shown in Figures 3-8 and 3-9, respectively. In both cases, the relative nutator speed is highest at the lower tooth numbers and asymptotically approaches zero at the higher tooth numbers. The high degree of differential motion within the mechanism is demonstrated by observing the relatively low relative nutator speed at all tooth numbers.

It should be noted that the shape of the curves shown in Figures 3-8 and 3-9 at the lower tooth number,; i.e., rapidly increasing relative nutator speed, is a significant factor which limits the NMT to tooth numbers appreciably above ten, especially for the cases shown. This high relative rotation produces a sweeping motion of the nutator within the cam which tends to reduce the available tooth thickness below practical levels. Also, the roller speeds and accelerations may be adversely affected.

It should be noted that much of the information to be

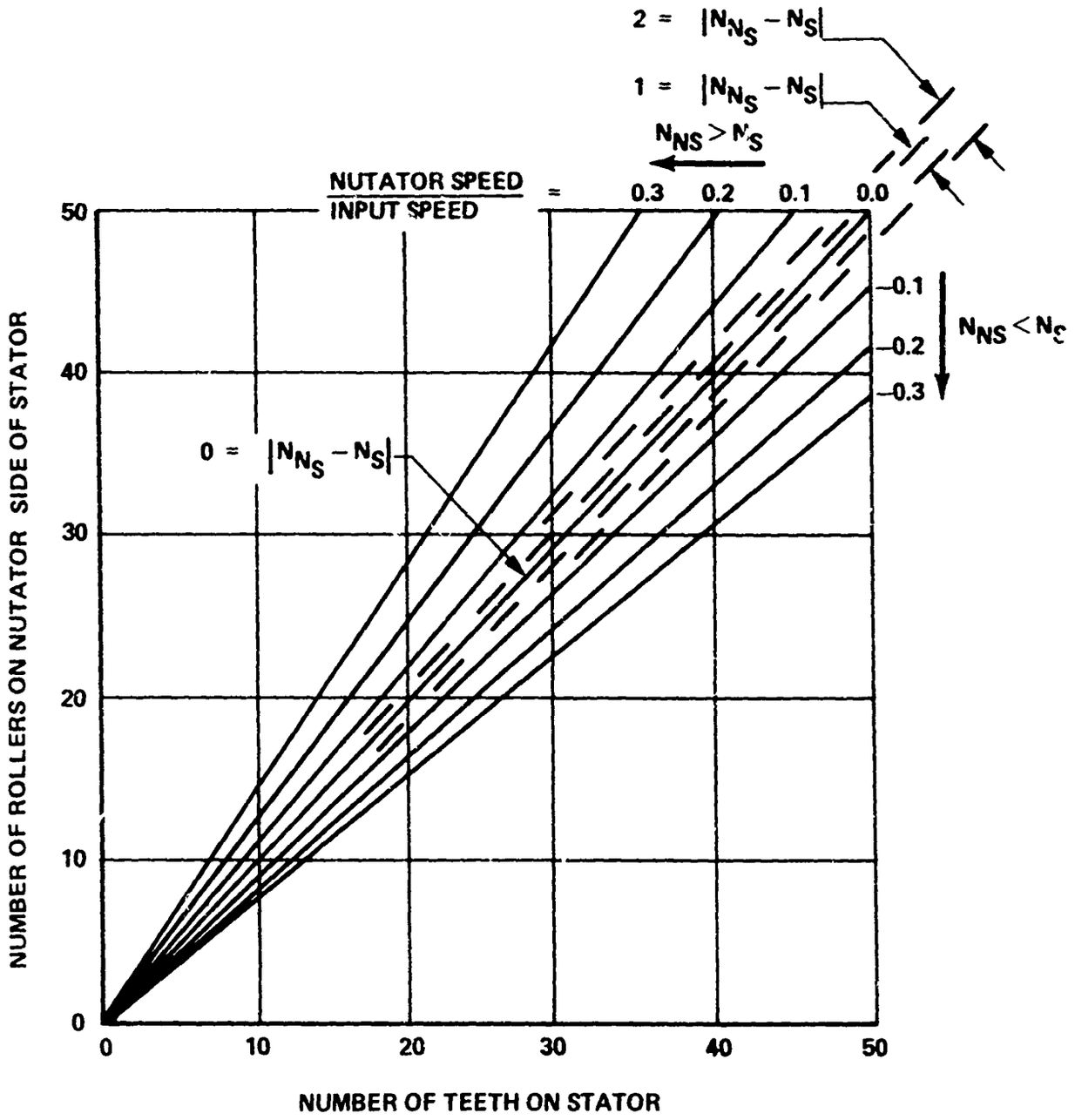

Figure 3-6. Nutator Speed Chart.

- IS A FUNCTION OF:
  - NUMBER OF TEETH ON ROTOR AND STATOR
  - NUMBER OF ROLLERS ON ROTOR AND STATOR SIDES OF NUTATOR
- EQUATION

$$n_{NCA} = \left[\frac{N_{NCA}\, N'_{CA} - N_S\, N_R}{N_R\, N_{N_S}} \right] n_I$$

WHERE:

n_{NCA}	=	RELATIVE ANGULAR VELOCITY OF NUTATOR
n_I	=	INPUT SPEED
N_{NCA}	=	NUMBER OF ROLLERS ON SIDE OF NUTATOR UNDER CONSIDERATION
N'_{CA}	=	NUMBER OF TEETH ON CAM NOT UNDER CONSIDERATION
N_S	=	NUMBER OF STATOR TEETH
N_R	=	NUMBER OF ROTOR TEETH
N_{N_S}	=	NUMBER OF ROLLERS ON THE STATOR SIDE OF THE NUTATOR

Figure 3-7. Relative Angular Velocity of Nutator.

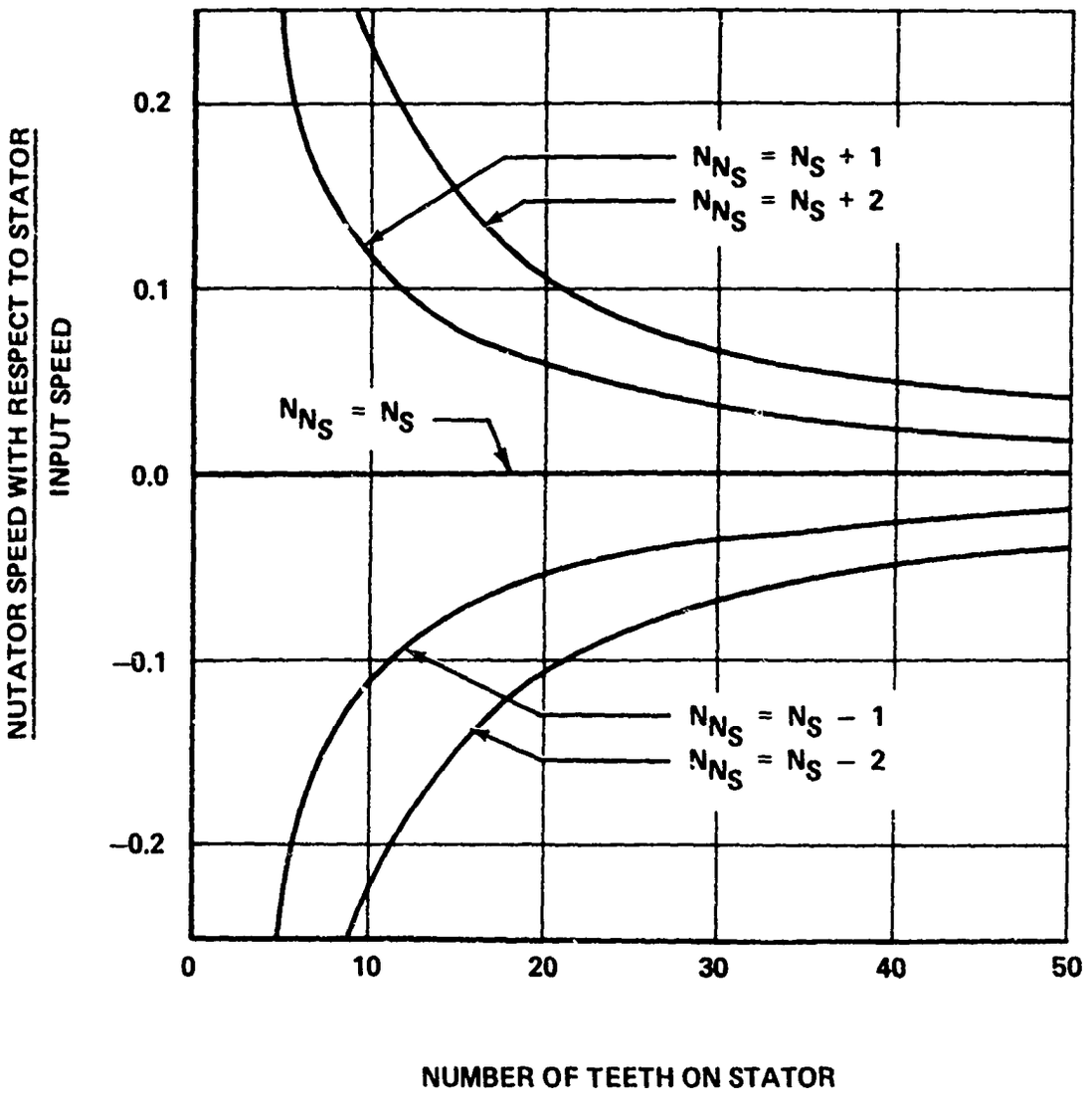

Figure 3-8. Angular Velocity of Nutator with Respect to Stator.

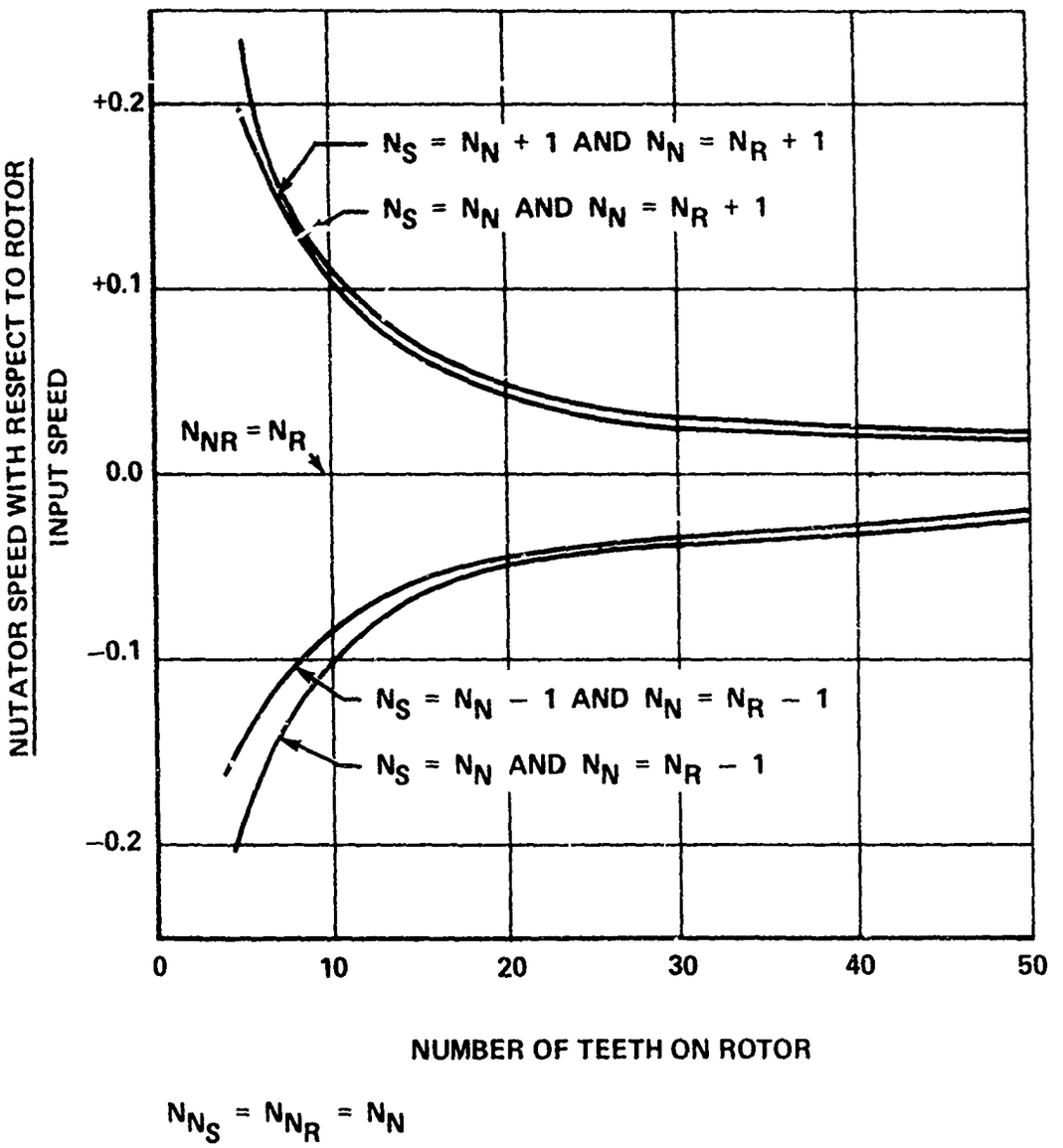

Figure 3-9. Angular Velocity of Nutator With Respect to Rotor.

presented, regarding the components of the NMT, is common to both the rotor/nutator and stator/nutator interfaces, excluding the differences in tooth numbers. Whenever this phenomena exists, the term cam will be used along with the subscript CA. This convention will reduce the volume of material which would otherwise be required and also avoid needless repetition of equations, figures, etc.

PATH OF NUTATOR ROLLERS

The path which a point follows on the centerline of a nutator roller within the cam will determine the profile required on the teeth of that cam to yield uniform output motion. Since the nutator itself, in the most general case, undergoes oscillatory and rotary motion, we may consider the path of a point on the centerline of a nutator roller within a cam as the vector sum of the distances traveled as a result of these individual motions. Consider an imaginary reference plane attached to and rotating with the nutator. This plane, which may be referred to as the nutator null plane, is perpendicular to the mechanism axis and contains the mechanism focus. The oscillatory component of the nutator may be referred to this plane. The rotary motion of the nutator is simply the rotation of the null plane with respect to the cam.

The path of a point on the centerline of a nutator roller, with respect to the nutator null plane, may then be defined with the aid of Figure 3-10. The point of interest on the centerline of a nutator roller is shown as point 2 on the figure. Initially, this point will be coincident with point 9, or point 1 if no roller coning is present. After 90 degrees of rotation, it will be coincident with point 8, or point 7 if no roller coning is present. Spherical trigonometry may be utilized to find the coordinate location of point 2 at any angular orientation, ω_O, of the axis system fixed to and rotating with the nutator null plane. From Figure 3-10, it can be observed that the position of point 2 relative to the coordinate system will initially lag behind that of point 4 and subsequently "catch up"; i.e., the angle A54 is initially zero (at ω_O = 0 degrees) then builds to a maximum value and finally reduces to zero again (at ω_O = 90 degrees). This motion produces an octoidal or lemniscate-like path with respect to the nutator null plane.

Figure 3-11 is an elaboration of Figure 3-10, looking along the mechanism axis. The lead-lag relationship of point 2 with respect to the axis system is clearly apparent. The equations shown in Figure 3-12 have been developed to define the path of a point on the centerline of a nutator roller with respect to the nutator null plane (see the appendix). Examination of these equations will reveal some interesting characteristics.

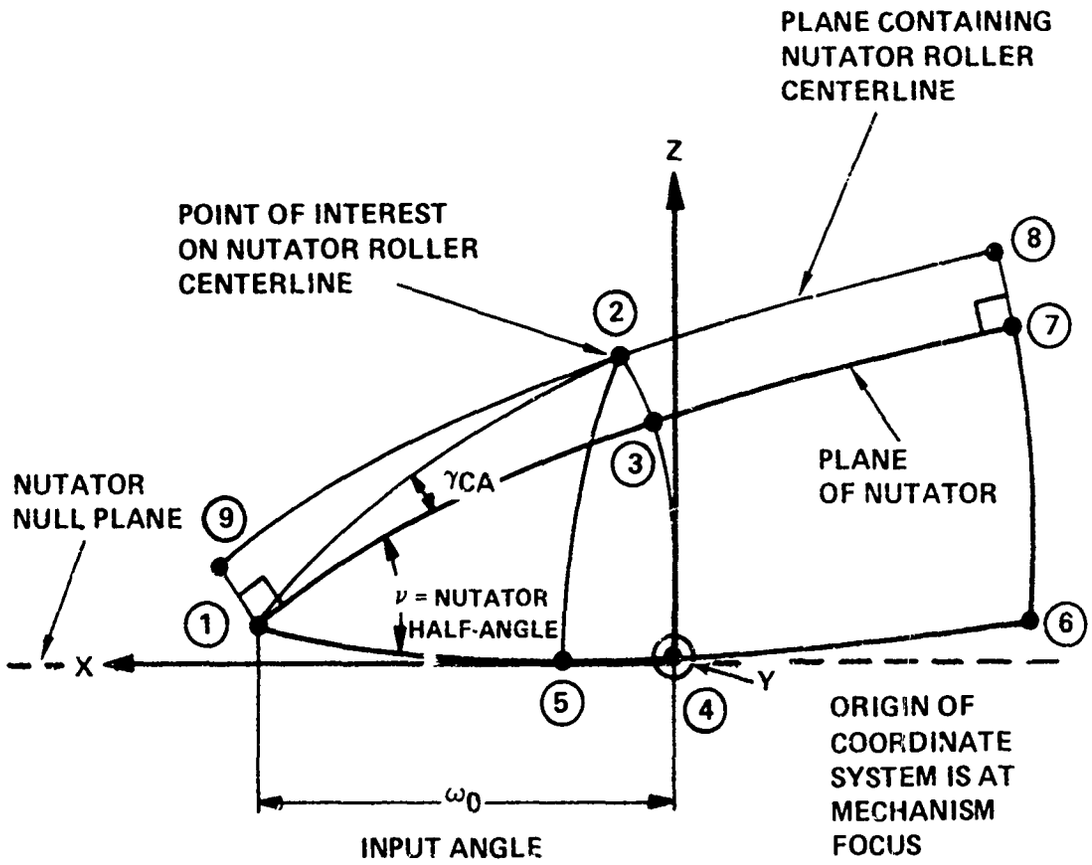

NOTE: A_{25} IS THE ANGLE BETWEEN POINTS 2 AND 5, WITH THE APEX AT THE MECHANISM FOCUS, ALL OTHER "A" ANGLES ARE SIMILARLY DEFINED

Figure 3-10. Spherical Projection of Instantaneous Nutator Position With Respect to Nutator Null Plane (No Relative Motion of Cam).

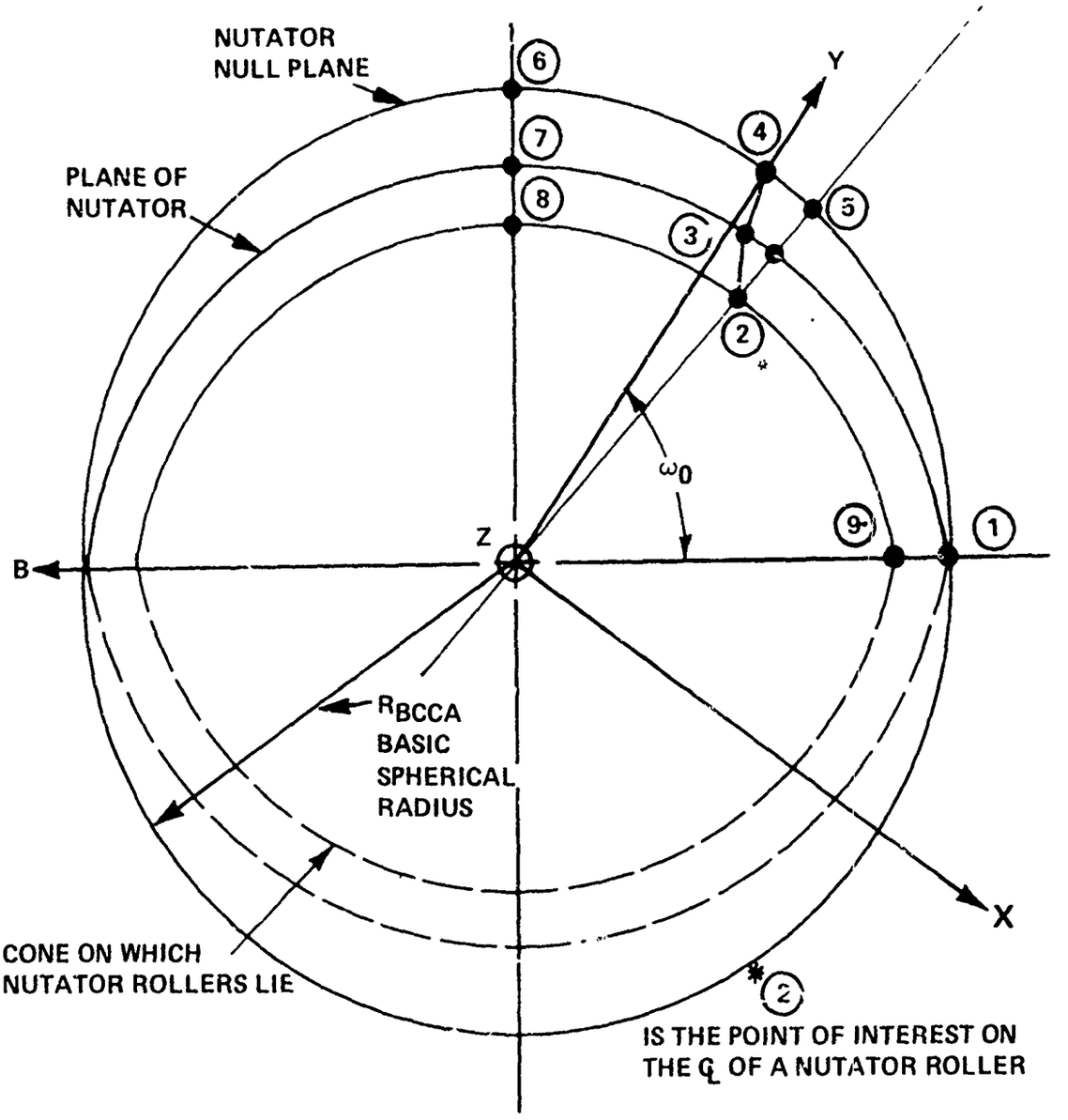

Figure 3-11. Schematic of Basic Sphere

$$X_{PCA} = R_{BCCA} \cos(A_{25CA}) \sin(A_{54CA})$$

$$Y_{PCA} = R_{BCCA} \cos(A_{25CA}) \cos(A_{54CA})$$

$$Z_{PCA} = R_{BCCA} \sin(A_{25CA})$$

WHERE: $$A_{54CA} = \omega_o - \sin^{-1}\left[\frac{\tan(A_{25CA})}{\tan(\gamma_{CA} + \nu)}\right]$$

$$\gamma_{CA} = \sin^{-1}\left[\frac{\sin(\sigma_{CA})}{\sin[\cos^{-1}[\cos(\sigma_{CA})\cos(\omega_0)]]}\right]$$

$$\alpha_{CA} = 0.0 \ (\sigma_{CA} = 0.0)$$

$$A_{25CA} = \sin^{-1}\left[\frac{\sin(\gamma_{CA} + \nu)}{\csc[\cos^{-1}[\cos(\sigma_{CA})\cos(\omega_o)]]}\right]$$

ω_o = INPUT TURNING ANGLE
ν = NUTATION HALF ANGLE
σ_{CA} = ROLLER ℓ CONING ANGLE

R_{BCCA} = BASIC SPHERICAL RADIUS

Figure 3-12. Equations of the Path of a Point on the Centerline of a Nutator Roller with Respect to the Nutator Null Plane.

The coordinates of the path are all linear functions of the basic spherical radius; therefore, the entire surface may be defined by solving these equations at the basic spherical radius and ratioing to obtain the values at any other point. More simply, this can be defined by solving in terms of the non-dimensional quantities X_{PCA}/R_{BCCA}, Y_{PCA}/R_{BCCA}, and Z_{PCA}/R_{BCCA} which may then be used to obtain dimensions at any radius. In addition, the same equations are valid for both the rotor and stator cam sides. The only restriction is that the appropriate values be utilized for the variables with a CA subscript. This notation, as specified earlier, will be utilized throughout the ensuing analysis to provide commonality among the equations developed involving both cams. Some feeling for the effects on the path shape and size of varying some of the basic parameters may be obtained by plotting the equations shown in Figure 3-12 over reasonable ranges. The only parameters which influence these equations are the basic spherical radius, the nutation half angle, and the coning angle. The basic spherical radius acts much like a scaling factor, thus its effect is linear. The effects of nutation half angle and roller coning are shown in Figures 3-13 and 3-14, respectively. From Figure 3-13, it is obvious that by increasing the nutation angle the path length is increased. Since at a constant input speed, a roller must cover the full path in the same time, regardless of nutation angle, it should be obvious that higher nutation angles also imply higher roller speeds. This phenomena will be covered in more detail in a later section of this report. A similar effect occurs with coning, but to a much lesser degree. Figure 3-15 summarizes some basic information about the path with respect to the null plane.

Having defined the path of the rollers with respect to the null plane, this information may be combined (Figure 3-16) with the relative motion between the nutator and each cam to yield the path of the rollers within each cam. This, in turn, will be used to define the cam tooth profiles.

At this point, it may be noted that, qualitatively, the net path of a point on the centerline of a nutator roller within a cam will resemble either a sine wave or a lemniscate wrapped on a sphere, as shown in Figure 3-17. If the nutator does not undergo any net rotation with respect to the cam, the path will be lemniscular; that is, the same nutator roller will oscilate in and out of the same cam tooth space during every cycle.

Conversely, if the nutator rotates relative to the cam, the path will resemble a sine type wave whose frequency is inversely proportional to the speed of the nutator with respect to the cam. A nutator roller, therefore, rolls in and out of successive tooth spaces during each cycle.

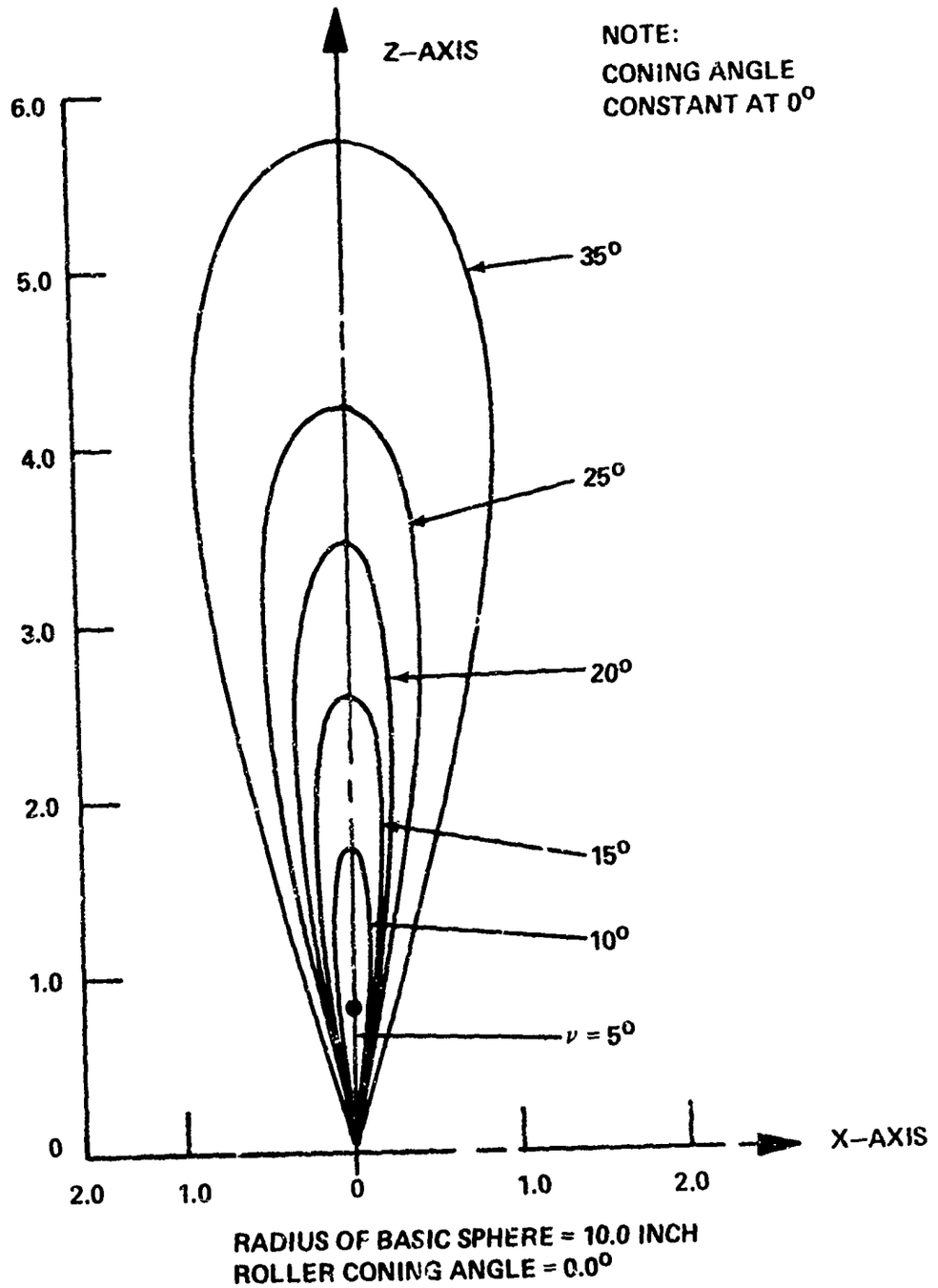

Figure 3-13. Path (on X-Z Plane) of a Point on the Centerline of a Nutator Roller With Respect to the Nutator Null Plane.

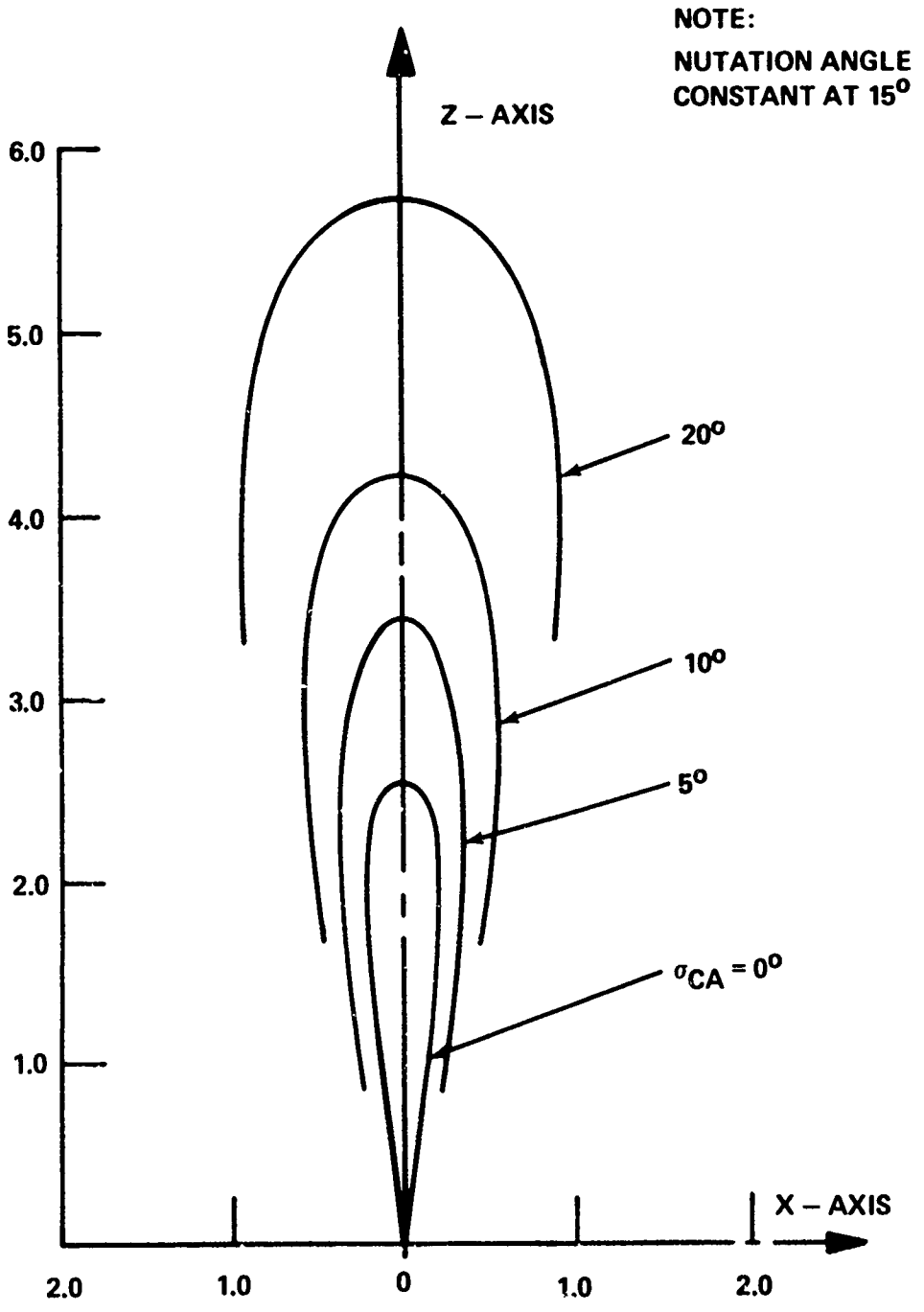

Figure 3-14. Effective Active (X-Z Plane) Path of a Point on the Centerline of a Nutator Roller With Respect to the Nutator Null Plane.

- RESEMBLES ELONGATED LEMNISCATE WRAPPED ON SURFACE OF SPHERE
- INDEPENDENT OF:
  - RATIO
  - SPEED
  - NUMBERS OF TEETH
- IS A FUNCTION ONLY OF:
  - NUTATION HALF-ANGLE
  - RADIUS OF BASIC SPHERE
  - CONING ANGLE OF ROLLERS ON NUTATOR
- INFLUENCES:
  - SHAPE OF ROTOR CAM TEETH
  - SHAPE OF STATOR CAM TEETH
- HAS NO EFFECT ON OUTPUT SPEED

Figure 3-15. Nutator Roller Path With Respect to Nutator Null Plane.

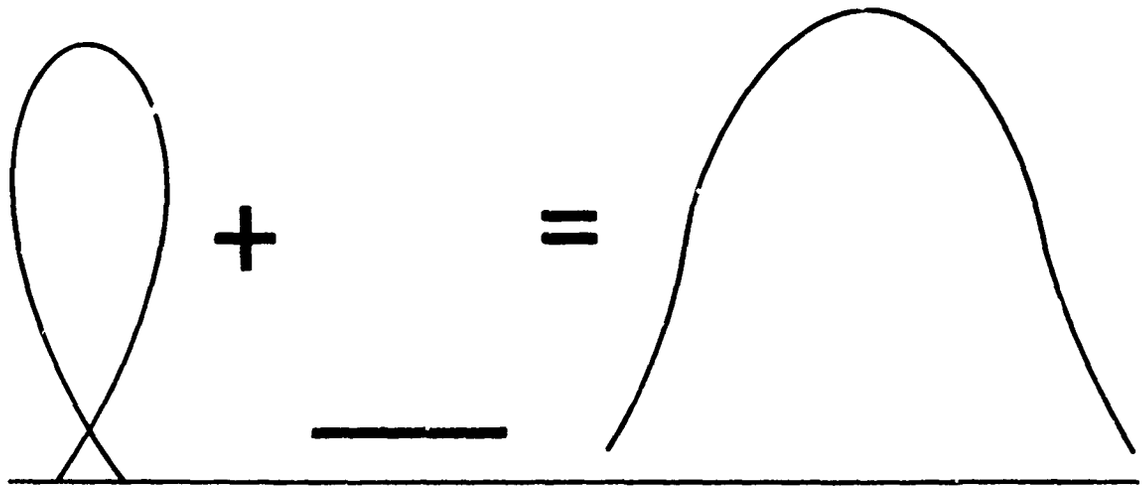

LEMNISCULAR MOTION OF POINT ON NUTATOR ROLLER ℓ WITH RESPECT TO NUTATOR NULL PLANE

+

MOTION OF NUTATOR NULL PLANE DUE TO ANGULAR VELOCITY OF NUTATOR WITH RESPECT TO CAM

=

PATH OF POINT ON NUTATOR ROLLER ℓ WITH RESPECT TO CAM

Figure 3-16. Development of the Path of a Point on the Centerline of a Nutator Roller With Respect to Rotor and Stator Cams.

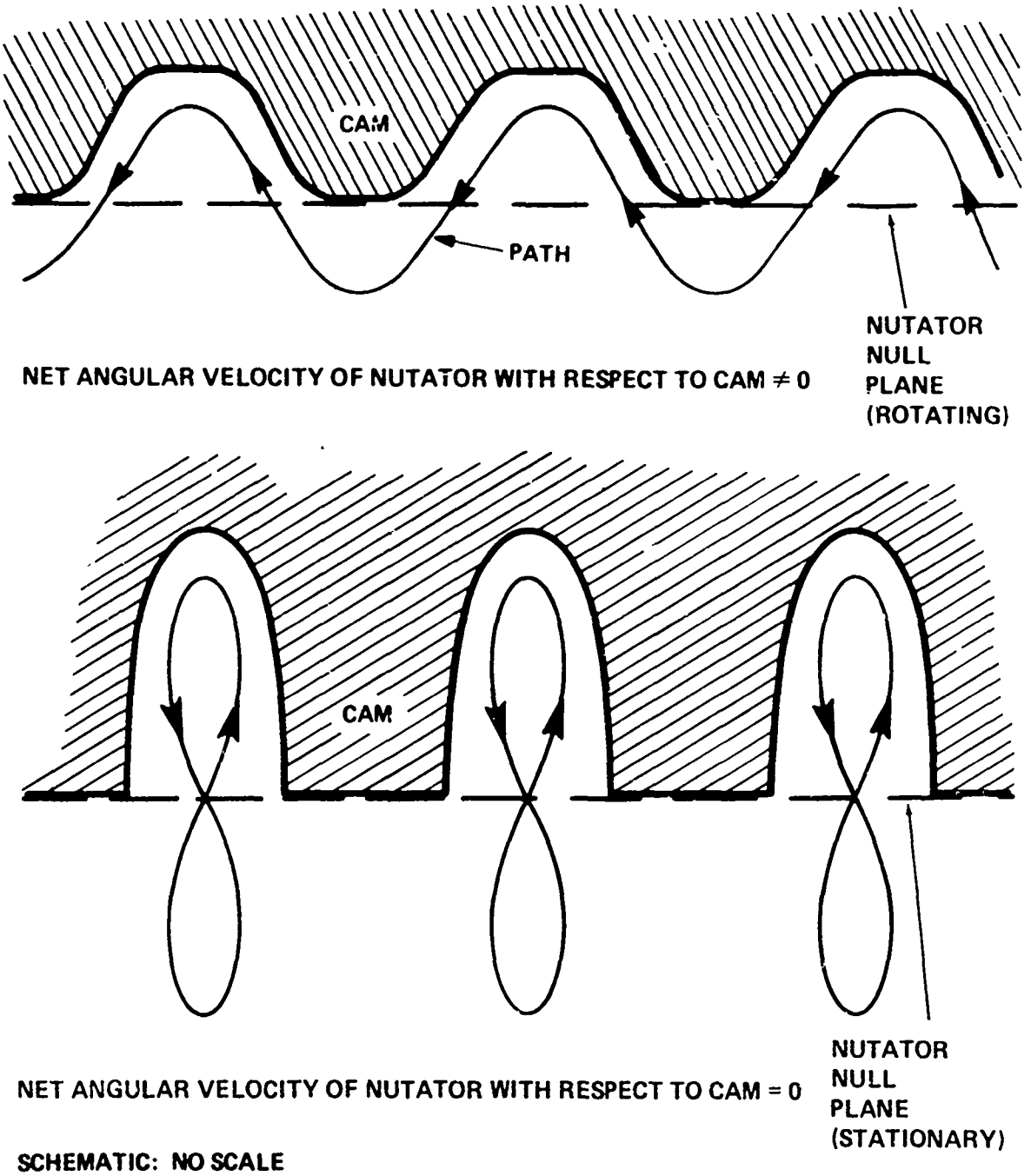

Figure 3-17. Schematic of the Path of a Point on the Centerline of a Nutator Roller with Respect to Rotor and Stator Cams.

The coordinates of the net path may be developed in a manner similar to that used for the path equations with respect to the null plane. Figure 3-18 is simply Figure 3-10 elaborated to include the relative motion of the null plane with respect to the cam. Keeping in mind the fact that the net motion is composed of two separate motions, a set of equations similar to those shown in Figure 3-12 may be developed to define the net path. If the relative angle of rotation between the cam and nutator is denoted by $\theta_{CA/N}$, then the equations shown in Figure 3-19 may be developed to define the net path of a point on the centerline of a nutator roller within the cam.

Although considerable design latitude is permitted in the choice of the basic geometric parameters such as nutation half angle, basic spherical radius, numbers of teeth/rollers, etc., certain restrictions must be traded off and adjusted to achieve an optimum design. These tradeoffs will be discussed in a later section of this report. Improper choice of nutation angle, ratio, and coning angle will result in an unsatisfactory path, either re-entrant or sharp-bottomed which, of course, will result in undesirable tooth profile shapes.

Parallels may be drawn to involute gear design to better illustrate the point. For example, although it is theoretically possible to design gears with extremely long addendums to increase the contact ratio, the practical restraints of pointed teeth limit the effective addendum proportions. Similarly, any number of teeth may theoretically be cut on an involute gear; however, as the tooth numbers become small, practical problems associated with undercutting affect the design. Similar limitations exist in the NIIT and will become apparent from the ensuing series of charts.

In order to provide some insight into the shape and variation of the path within each cam, several representative cases have been plotted as X-Z projections. The simplest case occurs when the number of teeth on the stator cam is equal to the number of rollers on both sides of the nutator and, further, that this number is one less than the number of teeth on the rotor cam. The effect of ratio on this particular configuration is shown in Figure 3-20. Since there is no relative motion between the nutator and the stator, the path within the stator remains invariant. Predictably, the rotor cam path reduces in width as the ratio increases, but at a reducing rate. At a ratio of ∞, the cam path would look exactly like the stator cam path, and the output shaft would be stationary.

Although this configuration would appear to be the simplest, it has several limitations which must be considered in a design tradeoff. The primary limitation is that the direction of nutator roller rotation is opposite on each cam, necessitating some form of dual roller configuration to prevent

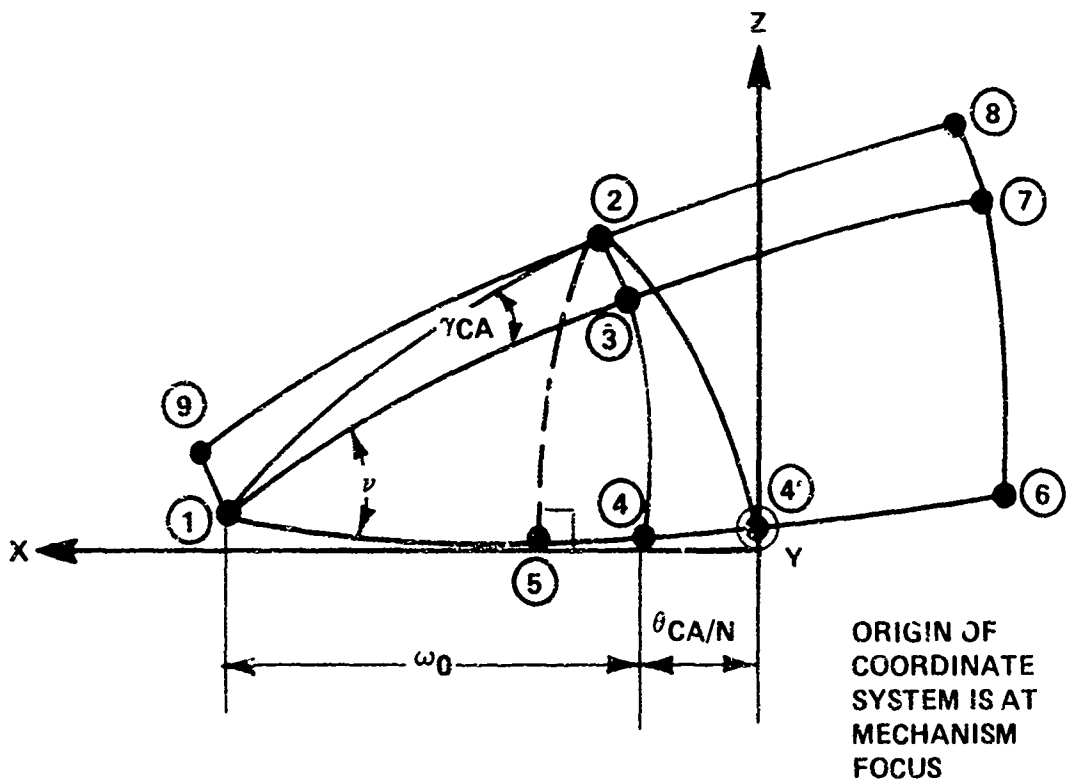

Figure 3-18. Spherical Projection of Instantaneous Nutator Position With Relative Cam Motion.

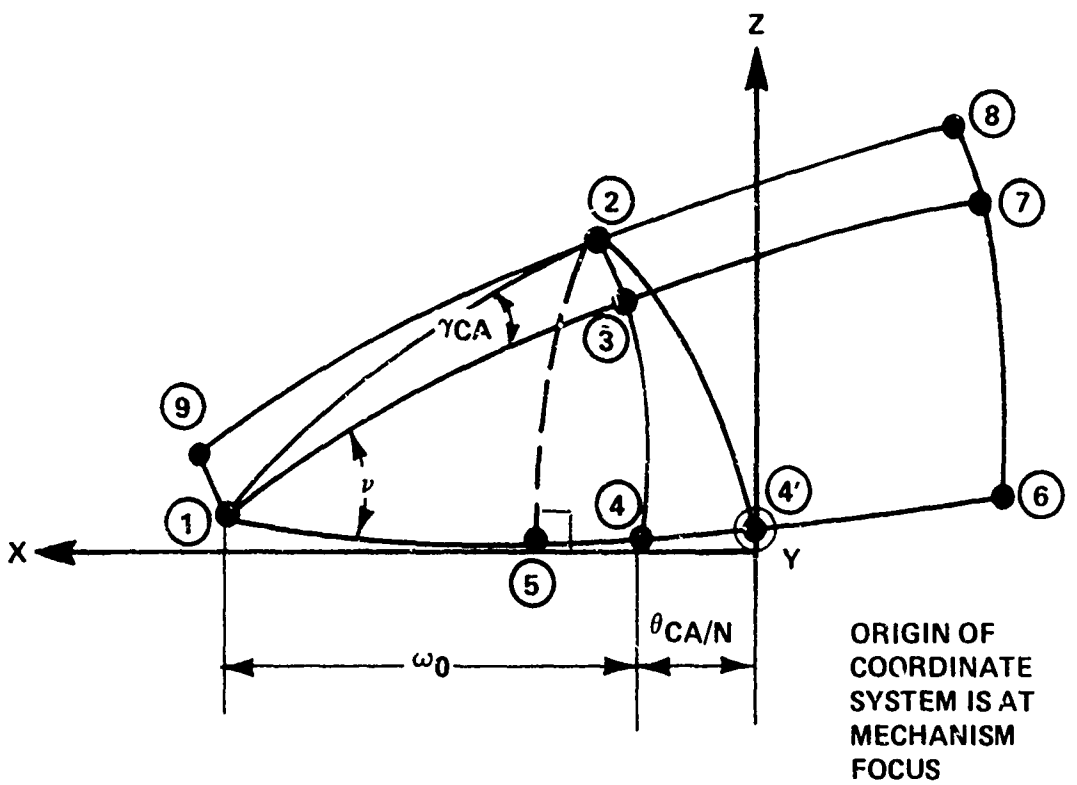

Figure 3-18. Spherical Projection of Instantaneous Nutator Position With Relative Cam Motion.

$$X_{PCA/CA} = R_{BCCA} \cos(A_{25CA}) \sin(A'_{54CA})$$

$$Y_{PCA/CA} = R_{BCCA} \cos(A_{25CA}) \cos(A'_{54CA})$$

$$Z_{PCA/CA} = Z_{PCA}$$

WHERE

$$A'_{54CA} = \omega_0 - \sin^{-1}[\tan(A_{25CA})/\tan(\gamma_{CA} + \nu)] + \theta_{CA/N}$$

$\theta_{CA/N}$ = ANGULAR MOTION OF CAM WITH RESPECT TO NUTATOR

Figure 3-19. Equations of the Path of a Point on the Centerline of a Nutator Roller Within a Cam.

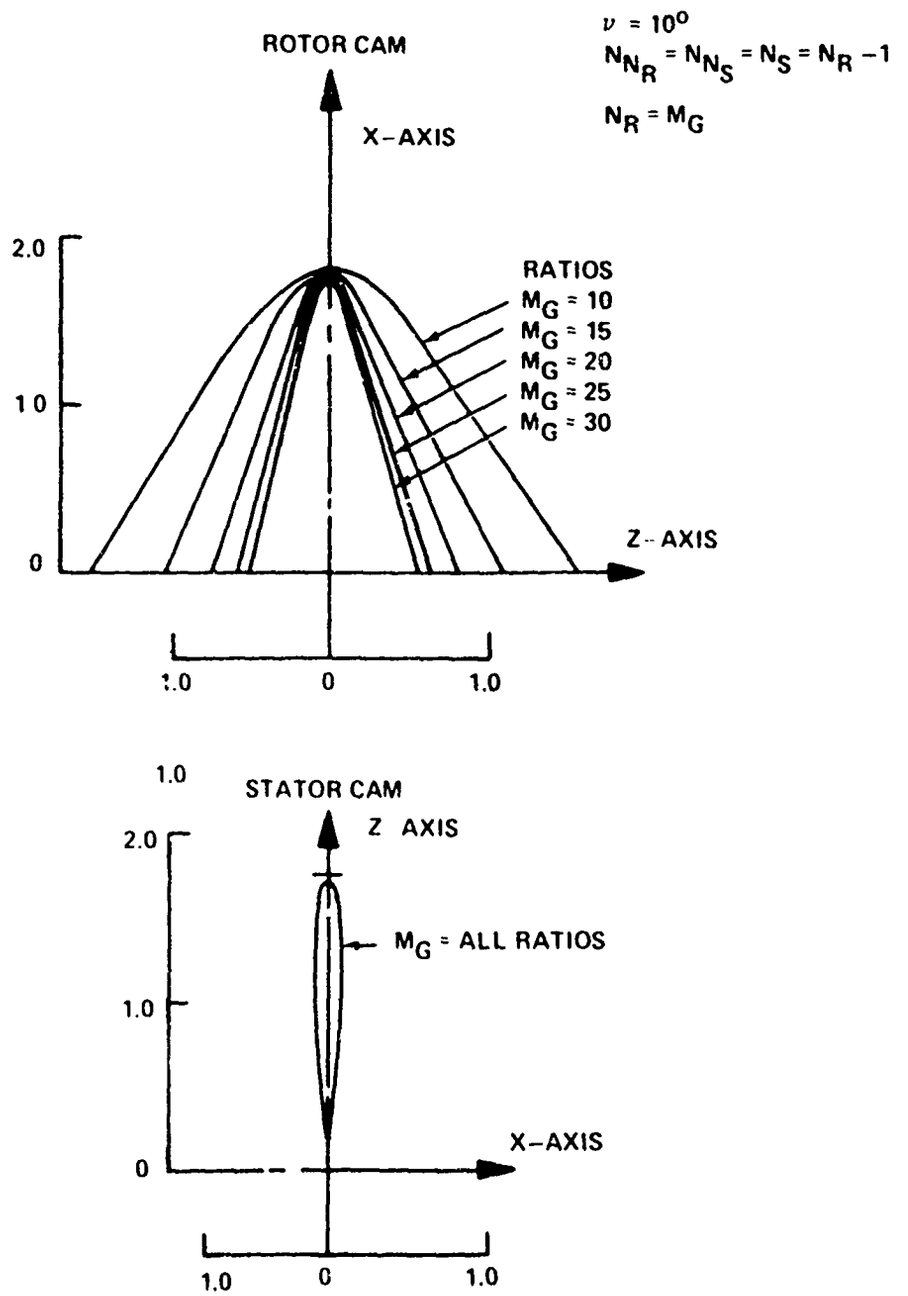

Figure 3-20. Effective Active (X-Z Plane) Path of a Point on the Centerline of a Nutator Roller Within Rotor and Stator Cams as a Function of Ratio.

severe roller skidding on all but the slowest speed units. This configuration also does not allow the nutator to undergo any net rotation. Next in order of complication is the configuration in which the number of teeth on the stator is one less than the number of rollers on the nutator which is, in turn, one less than the number of teeth on the rotor cam. This configuration, though seemingly similar to that previously discussed, is quite different. Primarily, the reduction ratio for a given number of rotor teeth is half that of the early configuration; however, the nutator rollers rotate in the same direction within the rotor and stator cams. A comparison of the paths for each of these configurations within the rotor and stator cams is shown in Figures 3-21 and 3-22, respectively. The greater path length which must be covered as the nutation angle increases is apparent from an examination of this figure. Since the same time is required for a complete nutator cycle regardless of nutation angle, the roller speed should increase with nutation angle. Conversely, it should be noted that increasing the nutation angle decreases the effective pressure angle of the cam tooth; therefore, for a given transmitted torque, increasing the nutation angle tends to reduce the thrust load. This, in turn, reduces the net normal load on the nutator rollers. It should be obvious that the selection of nutation angles, as well as the other basic parameters, cannot be made at random. Rather, a definite series of design tradeoffs must be considered.

Roller coning is a valuable design feature, particularly for those configurations which involve roller rotation direction reversal between rotor and stator cams. Coning the rollers away from the plane of the nutator permits the use of separate sets of rollers to mate with the roller and stator cams, eliminating the reversal problem. It should be noted that this problem occurs with only one group of configurations. The effect of roller coning on the nutator roller path is shown in Figure 3-23. An additional advantage of roller coning is that it allows both ends of the nutator rollers to be supported by solid structure rather than by the spoke and wheel arrangement otherwise required (more details on this topic will be provided in the powerflow and load capacity section). Like all other variations, coning has limiting disadvantages such as increased weight, increased axial length of unit, and increased mass in the nutator which must be balanced. A brief summary of the factors affecting the nutator roller path is presented in Figure 3-24.

ROTOR AND STATOR CAM TOOTH FORMS

Once the path of a point on the centerline of a nutator roller has been defined, the problem of defining the equations of the rotor and stator tooth forms reduces to that of a three-dimensional cam. The cam tooth forms may conceptually be

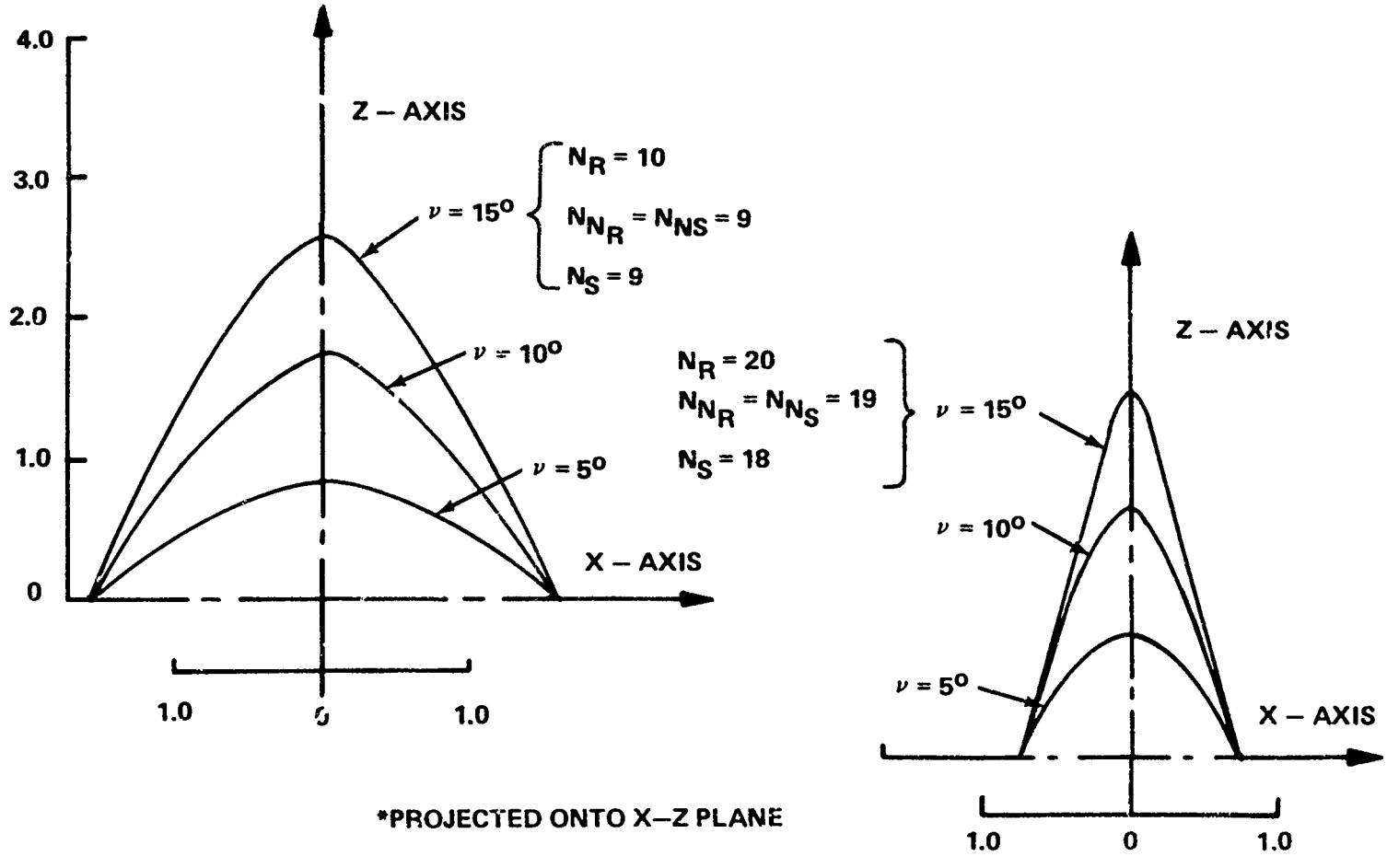

Figure 3-21. Effective Active (X-Z Plane) Path of a Point on the Centerline of a Nutator Roller Within the Rotor Cam.

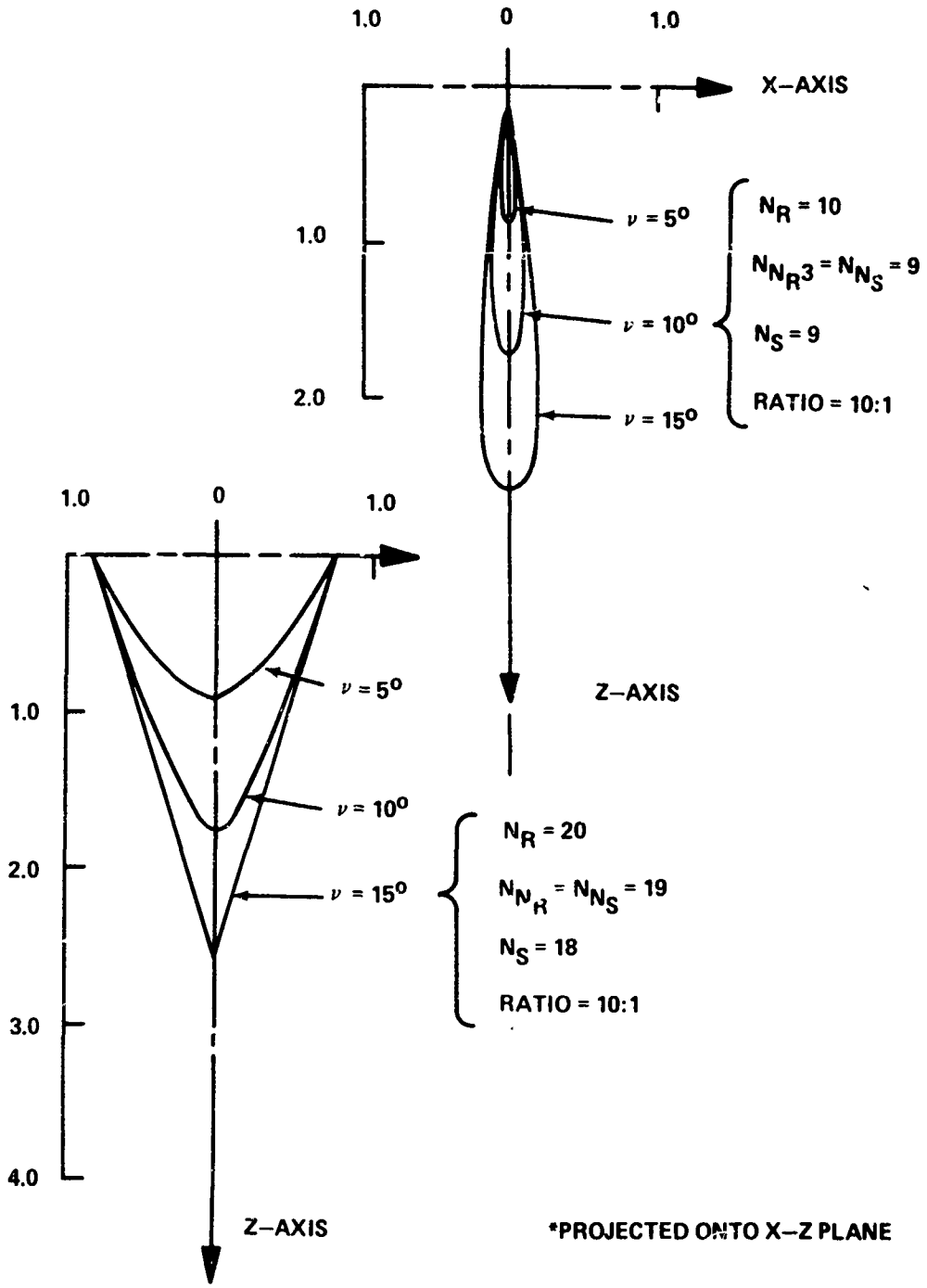

Figure 3-22. Effective Active (X-Z Plane) Path*of a Point on the Centerline of a Nutator Roller Within the Stator Cam.

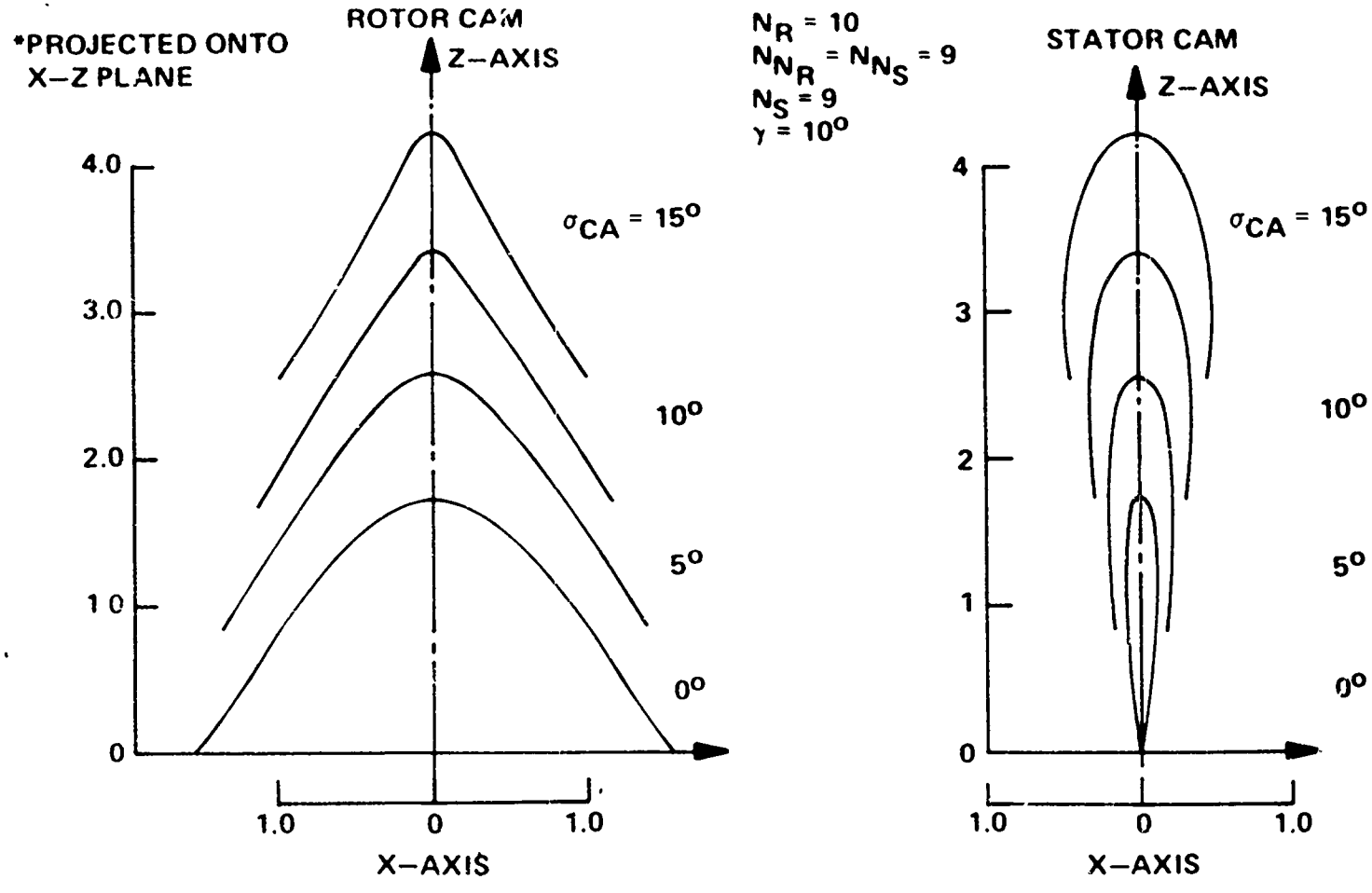

Figure 3-23. Effective Active (X-Z Plane) Path*of a Point on the Centerline of a Nutator Roller Within Rotor and Stator Cams With Roller Coning.

- IS A FUNCTION OF:
  - PATH OF POINT ON $\mathbb{Q}$ OF NUTATOR ROLLER WITH RESPECT TO NUTATOR NULL PLANE
  - ANGULAR ROTATION OF NUTATOR WITH RESPECT TO ROTOR AND STATOR CAM
  - NUTATION HALF-ANGLE
  - CONING ANGLE OF ROLLERS ON NUTATOR
  - RADIUS OF BASIC SPHERE
  - NUMBERS OF TEETH ON ROTOR AND STATOR CAMS
  - NUMBERS OF ROLLERS ON STATOR AND ROTOR SIDE OF NUTATOR
- INFLUENCES:
  - TOOTH FORM OF ROTOR AND STATOR TEETH
  - UNIFORMITY OF OUTPUT SPEED
  - ANGULAR VELOCITY OF NUTATOR ROLLERS
  - ANGULAR ACCELERATION OF NUTATOR ROLLERS

Figure 3-24. Path of a Point on the Centerline of a Nutator Roller Within the Rotor and Stator Cams.

defined as shown in Figure 3-25. The cam tooth profiles are determined solely by the path of a point on the centerline of a nutator roller within the cam and the roller radius. Like the path itself, the cam tooth profile is a linear function of the spherical radius; therefore, the equations need only be solved at the basic spherical radius and all other points found by linear ratio. As with any other cam, the choice of roller (or follower) radius is quite important, both from a stress and kinematic viewpoint. A roller radius which is too small may result in very high speeds and surface stress levels, while one which is too large may well result in interference. The proper definition of the cam tooth profiles will influence many, if not all, of the mechanisms operational characteristics such as the uniformity of the output speed, operational smoothness, and noise levels.

The tooth profile is, of course, simply the locus of all instantaneous roller tangency points. The equations defining the coordinates of the tooth profile may be determined by defining a series of direction cosines and ultimately solving a series of three simultaneous equations in three unknowns. First, the direction cosines of a line tangent to the path of a point on the centerline of a nutator roller must be defined. Next, the direction cosines of a line joining this point and the corresponding point on the tooth profile (actually a directed roller radius) should be defined. Finally, the direction cosines of a vector from the focus of the mechanism to the point on the cam tooth profile may be defined. Using these direction cosines, the actual tooth profile coordinates may be determined. In standard cam terminology, the path of a point on the centerline of a nutator roller within the cam may be considered as the pitch path. This procedure and some of the pertinent angles are shown in Figure 3-26. The developed equations are shown in Figure 3-27.

Many methods are available to manufacture the cams. Since, if properly designed, the cams will have no undercut and no reentrant points, they are ideally suited to precision forging or sintering techniques (depending, of course, on size, mass, etc.). In addition, since the profile shape is defined by a system of coordinates, the profiles are readily adaptable to numerically controlled machining. If the profiles are to be cut by numerically controlled methods, a knowledge of the actual tooth forms is superfluous, since a roller-shaped cutter when driven through the pitch path will generate the desired tooth shape. Again, drawing on gearing technology, master cams can be used either for checking production cams or for use as templates in the generation of additional cams.

In the MECHANISM KINEMATICS section, the variation of nutator roller velocity will be examined. Briefly, the angular velocity of the nutator roller may vary substantially during

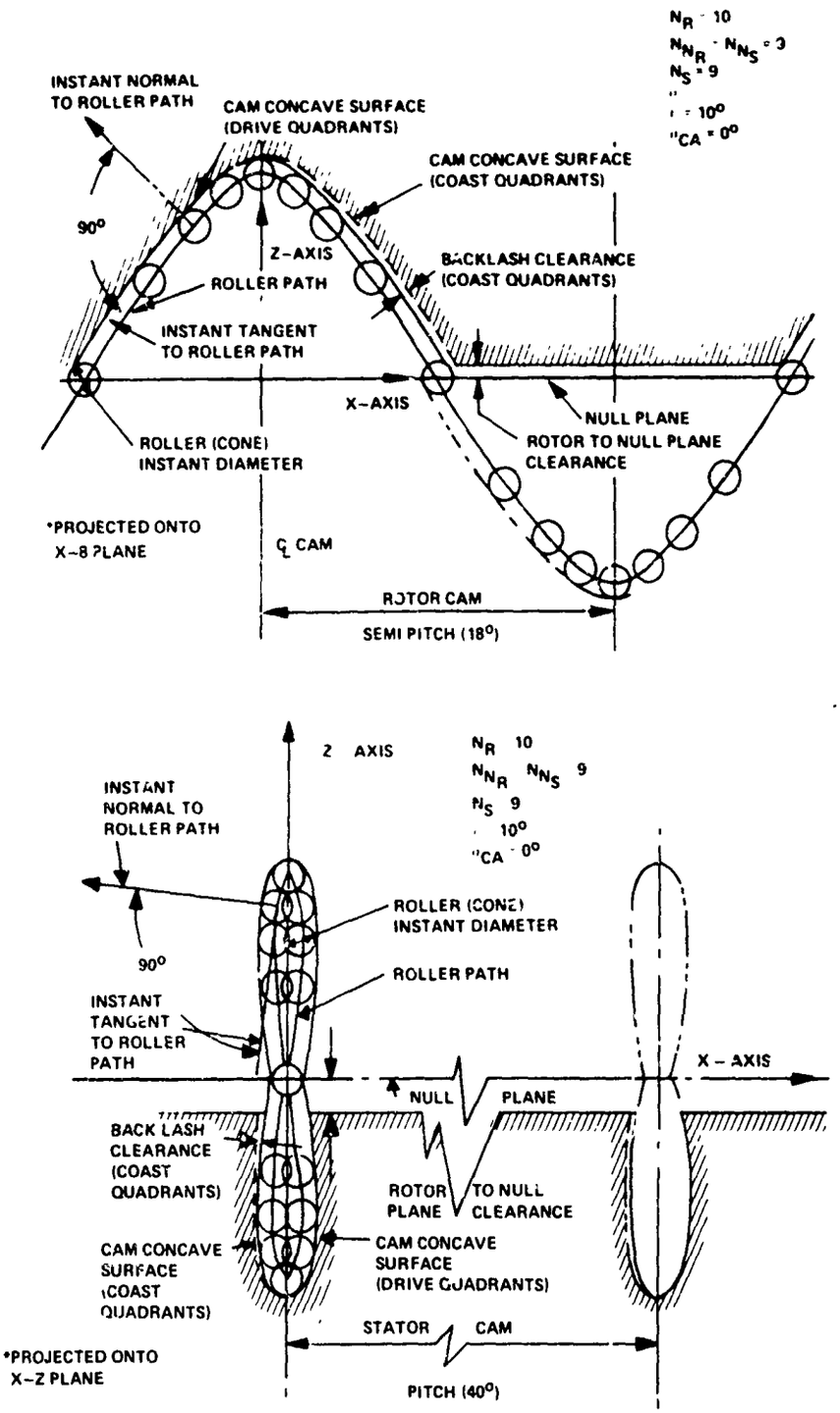

Figure 3-25. Development of Cam Surface (Projected onto X-Z Plane) From Effective Active Roller Path and Diameter.

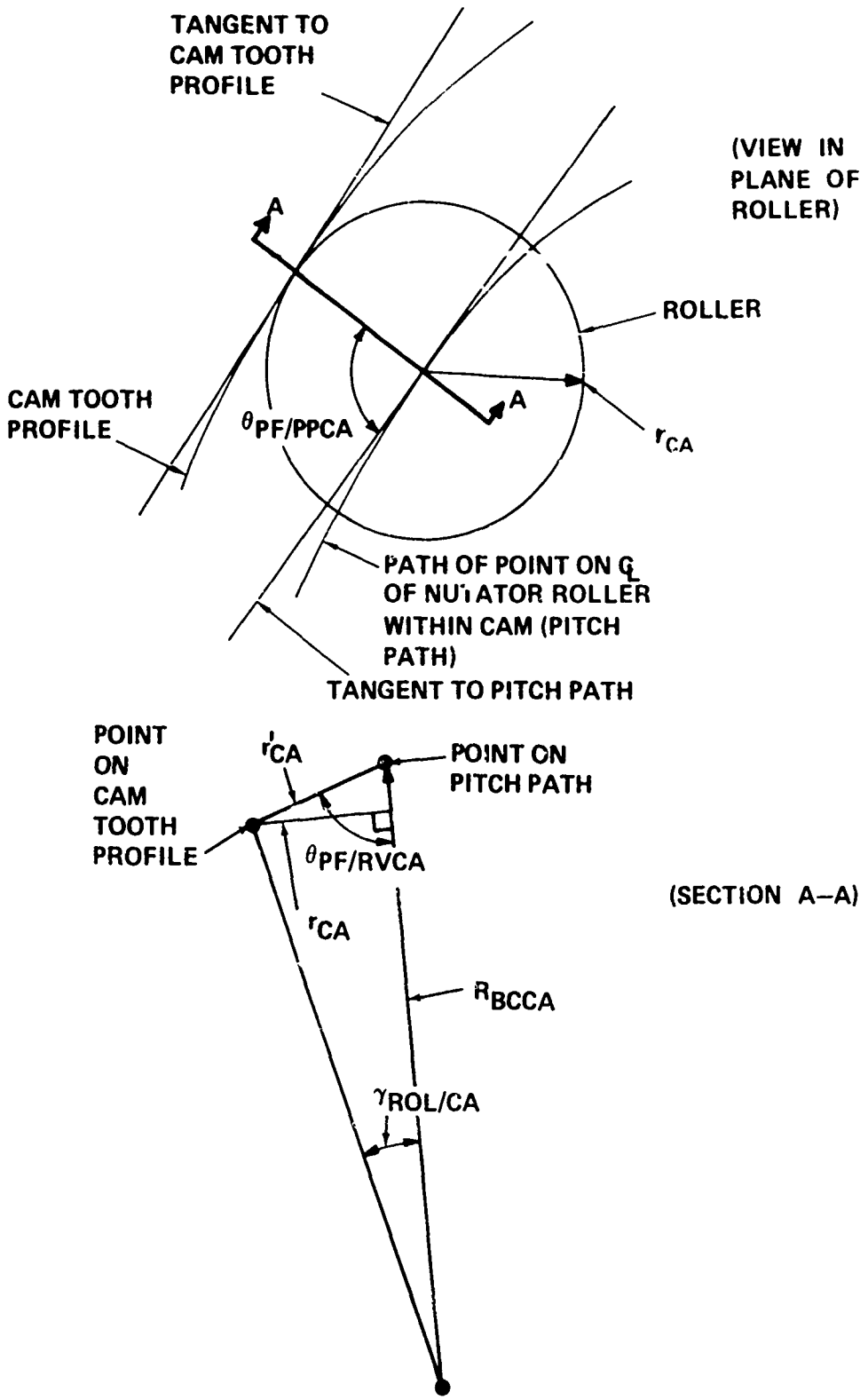

Figure 3-26. Schematic of Tooth Form Development.

$$X_{PF/CA} = r'_{CA} \cos(\alpha_{PFCA}) + X_{PCA/CA}$$

$$X_{PF/CA} = r'_{CA} \cos(\beta_{PFCA}) + Y_{PCA/CA}$$

$$Z_{PF/CA} = r'_{CA} \cos(\gamma_{PFCA}) + Z_{PCA/CA}$$

WHERE r'CA IS ADJUSTED ROLLER RADIUS COS (α_{PFCA}), COS (β_{PFCA}), AND COS (γ_{PFCA}) ARE THE DIRECTION COSINES OF A LINE BETWEEN THE POINT OF INTEREST ON CAM TOOTH PROFILE AND THE PITCH PATH.

Figure 3-27. Cam Tooth Form Equations.

its contact with the cam tooth. Since this variation may be greater than two to one, it may be necessary to modify the cam tooth profiles such that the roller accelerations will remain within reasonable ranges. This may be accomplished simply by relieving the contact at either the root or tip end or both. This modification must necessarily be accomplished with care to ensure that the created side effects are not more serious than the original problem. One immediate problem is an undercut fillet; because in order to relieve the contact in the root area, it may be necessary to undercut the tooth root to provide run-out space for the roller.

Depending on cam tooth thickness, this may possibly have an adverse affect on tooth-bending strength. Generally however, this factor is of little concern, since the cam teeth have not been found to be critical in bending. The real problem with undercutting is that, if it is severe enough, precision forging or sintering is eliminated as possible manufacturing methods. This is of concern only for the smaller sizes, since these methods are not practical for very large parts anyway.

The contact between the rollers and the cam teeth is essentially rolling and shares the problems of a traction drive (refer to the KINEMATICS section). With this in mind, it may be necessary to harden and grind the cam teeth even in moderate-size units so that reasonable cam tooth life may be obtained. This can be accomplished by means similar to numerically controlled cutting. The materials and processes utilized in the manufacture of the cam teeth will, due to the contact conditions, be the same as those used in conventional gearing of similar quality and load capacity. Since much of the mechanisms load capacity is dependent upon the multiple load sharing which occurs among the rotor and stator tooth/roller sets, the index accuracy, the cam tooth thicknesses, and the roller diameters become critical dimensions. Excessive errors in any of these parameters will result in overloading of one or more of the nutator rollers which will, in turn, increase the operating noise level and reduce life. The need for accuracy is, therefore, neither less nor greater than that in a precision gear system.

CONTACT RATIO AND ROLLER-SIZE/TOOTH-THICKNESS RELATIONSHIP

By virtue of the nature of the contact, the NMT has a high degree of load sharing among the component parts. A common measure of the degree of load sharing widely used in gearing technology is the contact ratio. The contact ratio as applied to gears may be thought of as the average number of teeth which share the load during the meshing cycle. Therefore broadly interpreted, a contact ratio of 1.3 would indicate that at least one pair of teeth carry load during 100 percent of the mesh cycle while for approximately 30 percent of the cycle, the load

is shared between two tooth pairs. Typical values of the contact ratio for spur gears are in the range of 1.2 to 2.1. Helical gears would have higher contact ratios and in some cases, particularly marine drives, the helical contact ratio may approach 20 or more. This is somewhat deceiving, however, because with helical gears only a small portion of the width of a tooth carries load at any time. Therefore, although noise levels are lower than an equivalent spur set, the load capacity may only be improved by 10 to 20 percent. In the case of the NMT, the entire length of each tooth which is in contact carries load; therefore, the load capacity of the mechanism will generally improve with increasing contact ratio. Since the contacts on the rotor and stator sides of the nutator are essentially independent, the contact ratio for each cam will be different, although quite similar in most cases. Theoretically, the nutator rollers may be in contact with each cam during a full 90-degree quadrant.

However, in order to minimize roller velocity variation and to provide tip and root relief to account for tooth deflections, most high-capacity, high-speed designs will have some active profile removed from both the tip and root areas of the cam teeth. Although this profile modification is quite beneficial, especially in minimizing the possibility of roller skidding on engagement, a contact ratio penalty must be paid to achieve these other benefits (see Figure 3-28).

Unlike gearing in which the contact ratio is only very slightly sensitive to the speed ratio, the NMT contact ratio shows a very strong dependence on ratio (see Figure 3-29). This figure also details the strong dependence of contact ratio on the specific configuration chosen. This factor must, however, be examined further in terms of other parameters. For example, for Configuration A at any given ratio, although the contact ratio is much higher than that for Configuration B, the pitch is much finer, forcing the use of thinner cam teeth and smaller nutator rollers. This is another tradeoff area which must be considered in the design optimization of an NMT.

The amount of profile modification applied also affects contact ratio as shown in Figure 3-30. Care must be exercised in modifying the tooth profiles to insure that the benefits gained are not obviated by the deleterious effects of contact ratio reduction. It should also be noted that at the lower ratios, the effects of profile modifications are much less severe than at high ratios. Although not shown in Figure 3-30 for some configurations, it may be more advantageous to remove more material from the root than from the tip. Examination of any of the figures in the NUTATOR ROLLER VELOCITIES section will reveal a very high slope to the roller speed line as the roller approaches the root. A proportionately greater reduction in roller velocity variation may then be realized by

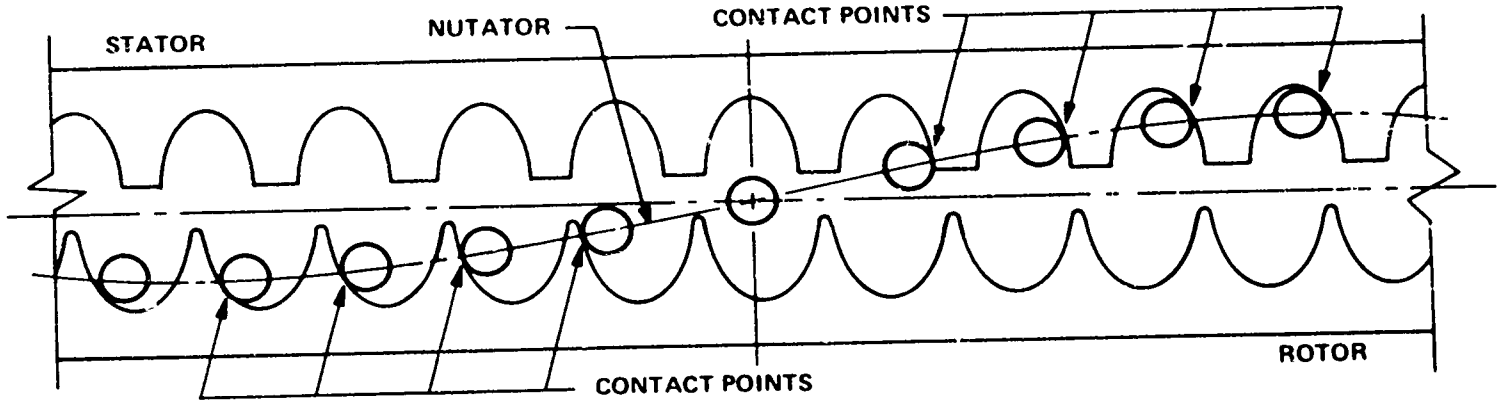

FULL PROFILE ROTOR AND STATOR

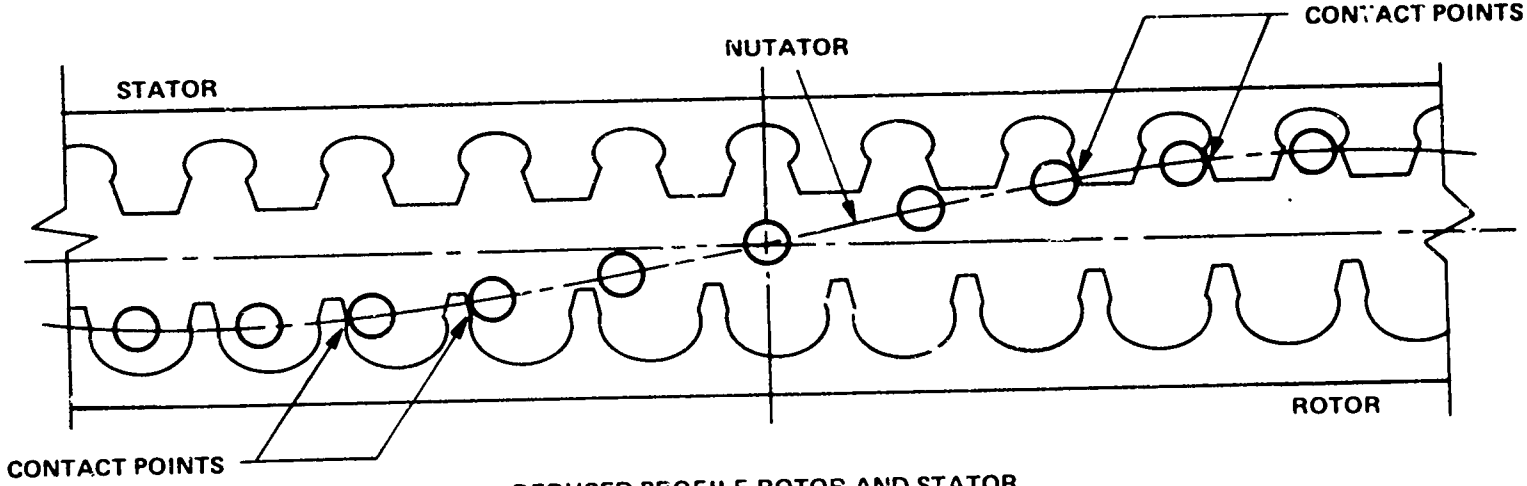

REDUCED PROFILE ROTOR AND STATOR

Figure 3-28. Schematic Showing the Effect of Reducing Active Profile To Decrease Variation of Nutator Roller Speed.

A: $N_{NS} = N_{NR} = N_R - 1$
$N_S = N_R - 2$

B: $N_S = N_{N_S} = N_{N_R} = N_R - 1$

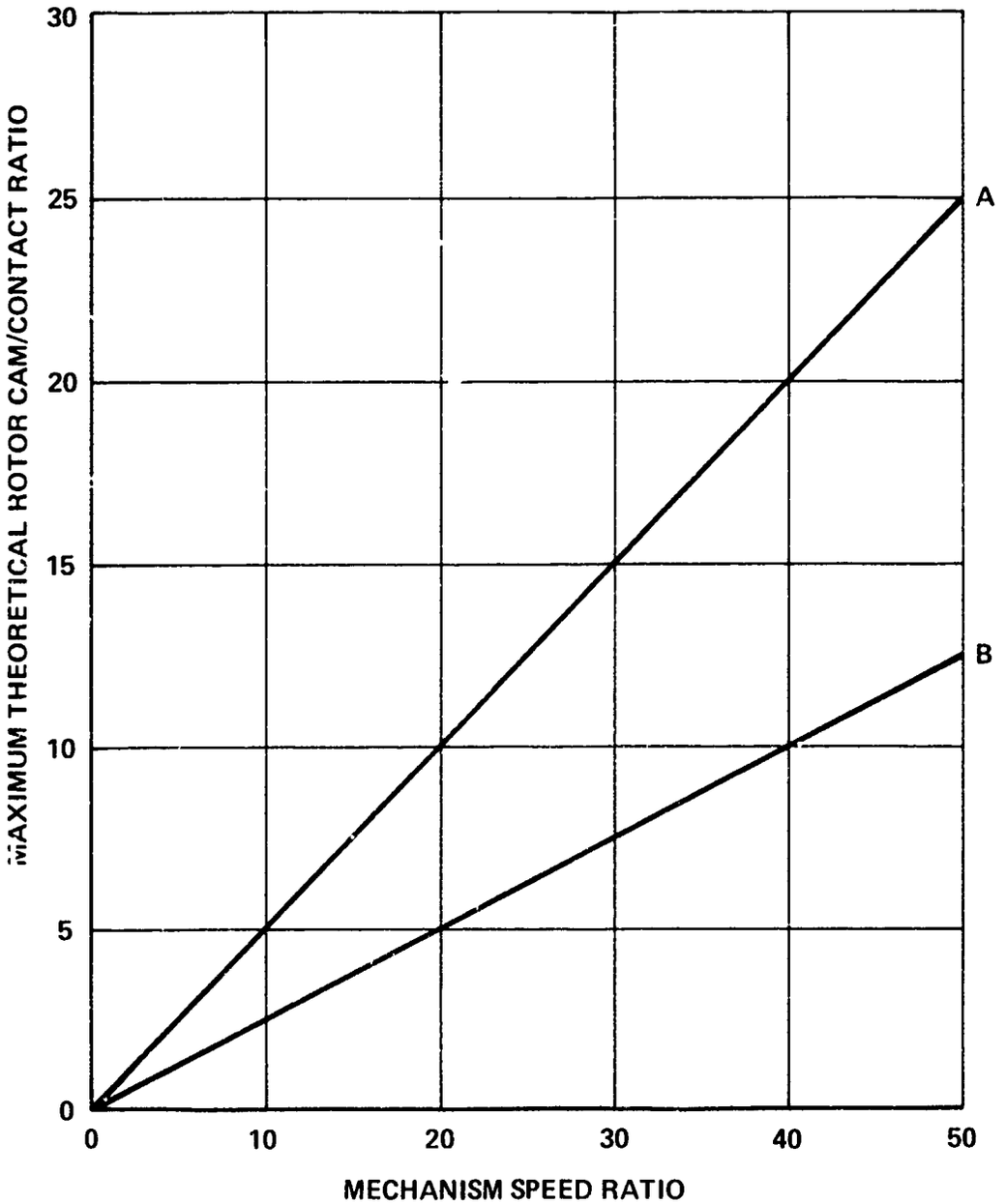

Figure 3-29. Maximum Theoretical Rotor Cam Contact Ratio as a Function of Mechanism Speed Ratio

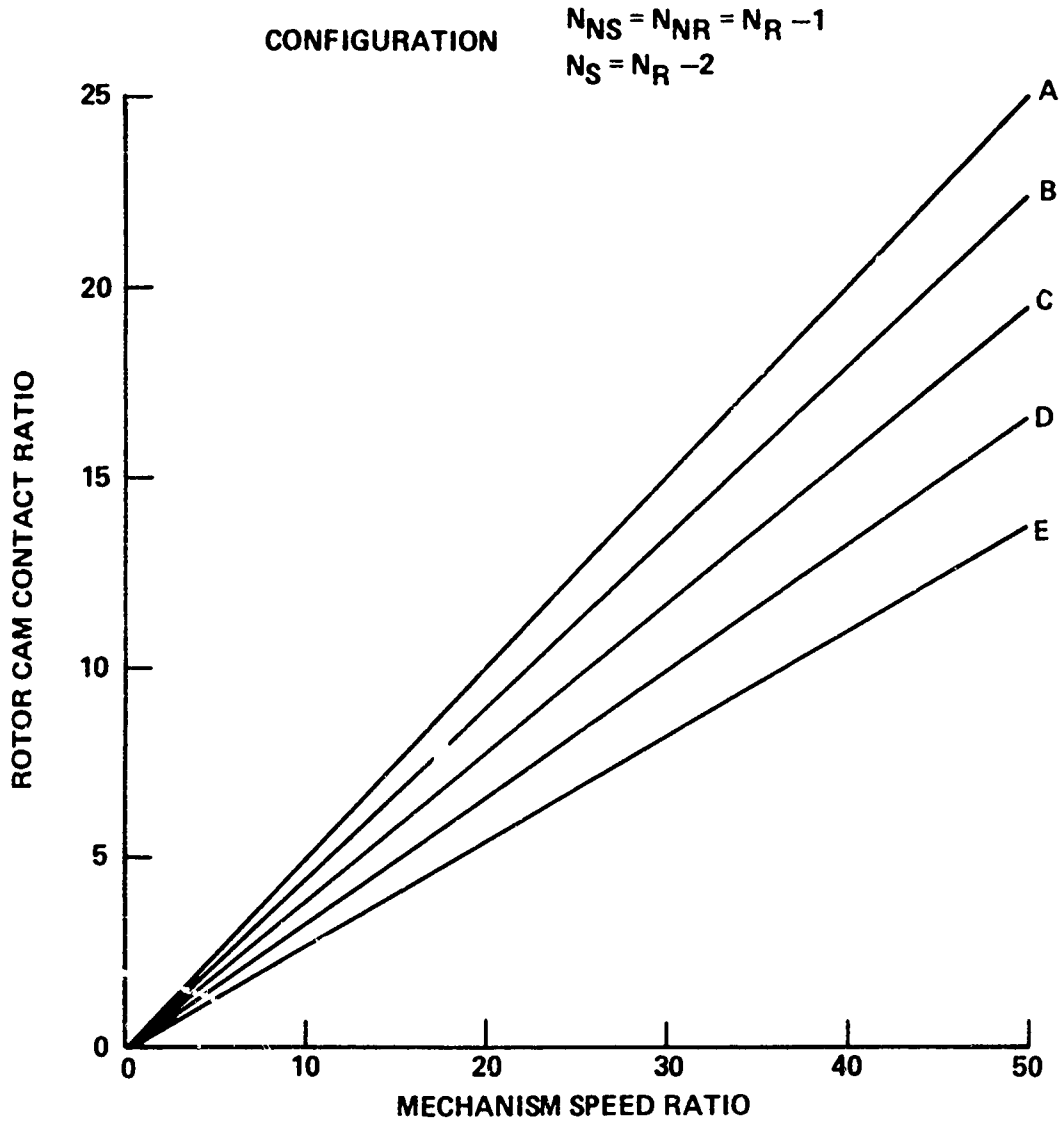

A: MAXIMUM THEORETICAL (NO RELIEF)
B: TIP AND ROOT RELIEVED 5^o EACH
C: TIP AND ROOT RELIEVED 10^o EACH
D: TIP AND ROOT RELIEVED 15^o EACH
E: TIP AND ROOT RELIEVED 20^o EACH

NOTE: TIP AND ROOT RELIEF BASED ON A MAXIMUM 90^o QUADRANT OF CONTACT.

Figure 3-30. Effect of Cam Tooth Tip and Root Modifications on Rotor Cam Contact Ratio

modifying the root area. Conversely, the tip is generally the area of maximum roller speed; therefore, if nutator roller bearing DN is critical, tip modification is most desirable. In general, some combination of tip and root modification will be used, and in many cases, the amount at each location will be quite similar.

The thickness of the cam teeth and the diameter of the nutator rollers are closely related. As shown in Figure 3-31, the space between the centerlines of two adjacent cam teeth is completely utilized by some combination of cam tooth thickness, nutator roller diameter, backlash allowance, and relative motion of the nutator within the cam. Clearly for any configuration, an increase in the cam tooth thickness must be traded off against a decrease in allowable nutator roller size. Also, the rotation of the nutator as a unit within the cam is obvious.

As this quantity increases, both the cam tooth thickness and the roller diameter decrease. It was noted earlier that differences of greater than one or two between the number of teeth on a cam and the number of nutator rollers which mate with it are seldom practical. Referring to the earlier discussion of nutator rotation with respect to the cam, it can be seen that this motion increases as the tooth-roller difference increases. High differential motion, therefore, reduces the practical load-carrying limits of the cam tooth thickness and the roller diameter. In the opposite sense, a limiting case occurs when the nutator undergoes no net rotation relative to the cam as is the case for the stator when $N_S = N_{NS}$. In this case, the nutator roller and the cam tooth thickness are mutually maximum. The relationship between cam tooth thickness and nutator roller size is shown, for this special case, in Figure 3-32. At the lower tooth numbers, the choices of basic spherical radius and the proportional split between cam tooth thickness and nutator roller diameter are many. However as the number of teeth on the stator increases, implying a corresponding increase in ratio, the basic spherical radius is limited to increasing sizes to simply allow a reasonable amount of material for the cam teeth and nutator rollers. Although conventional gearing systems also exhibit a similar relationship between size and ratio, it is not quite as strong as with the NMT. An advantage of the NMT, readily apparent from Figure 3-32, is the relatively large size of the cam teeth. The bending stresses which so often limit conventional gear systems are minimized.

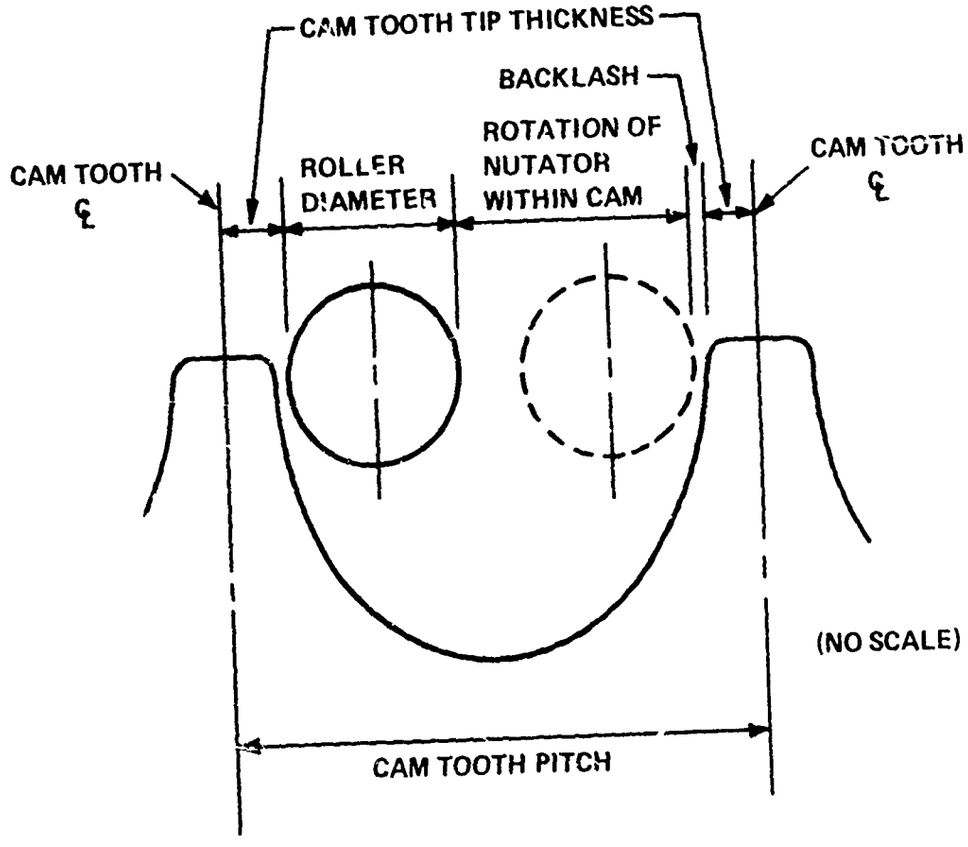

Figure 3-31. Schematic of Cam Tooth Pitch Utilization

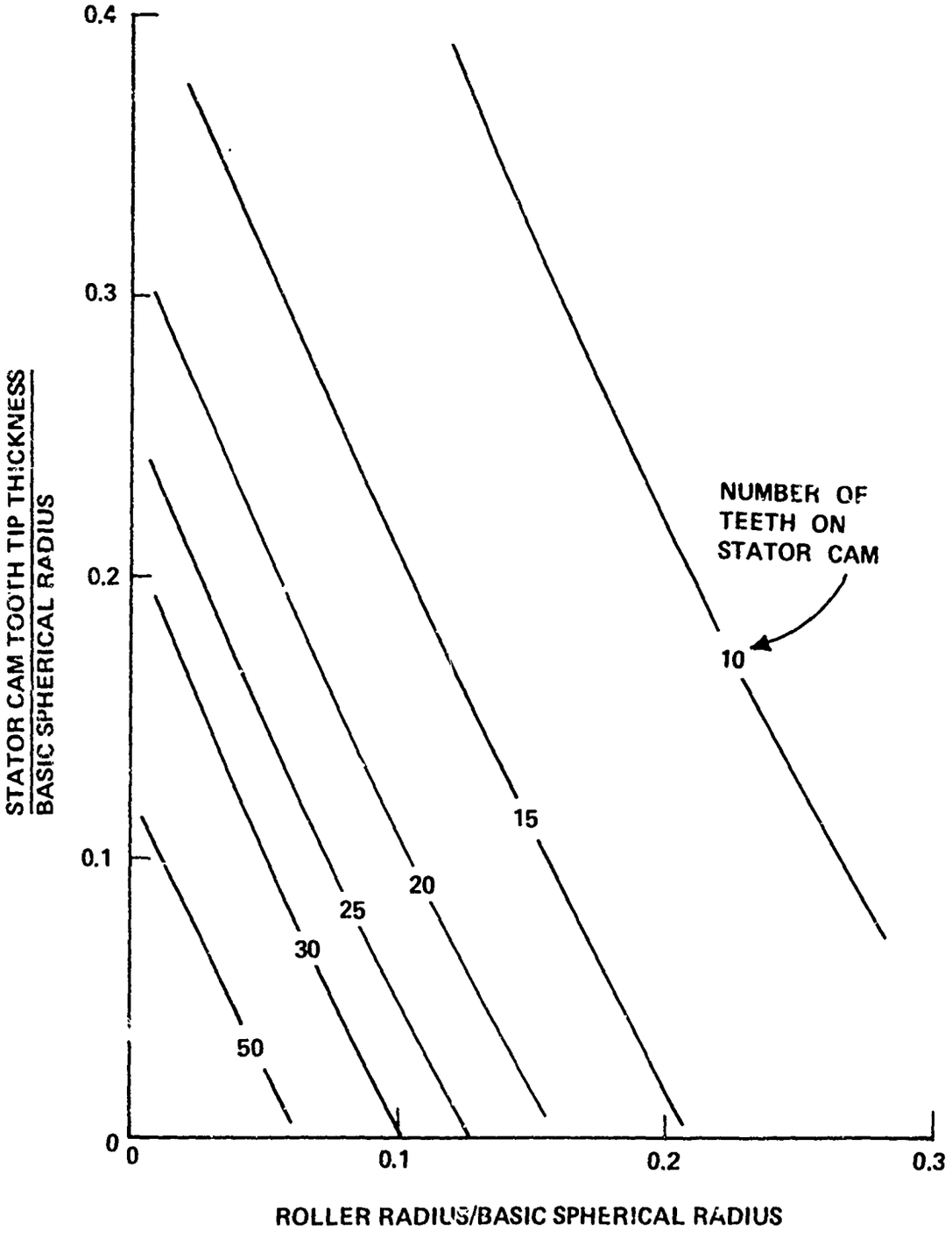

Figure 3-32. Relationship Between Cam Tooth Tip Thickness and Roller Radius.

4. MECHANISM KINEMATICS

NUTATOR ROLLER VELOCITIES

As the nutator rollers traverse the cam tooth profiles, assuming sufficient tractive forces exist to prevent slippage, their angular velocity varies in proportion to the linear velocity of a point on the roller centerline. The magnitude and variation of this velocity is critical to the proper design of the mechanism. The maximum value of this speed must be kept within the allowable speed for the particular type bearing being used. Since the lives of the roller support bearings are directly proportional to their speeds, it is quite important to minimize these speeds. The speed of the rollers is a function of many parameters including input speed, ratio, number of teeth and rollers, roller radius, basic spherical radius, coning angle and, particularly, the nutation angle.

The equations defining the angular velocity of the rollers may be defined by first considering the linear velocity of a point on the centerline of a nutator roller as it traverses the pitch path within the cam. The linear velocity is simply the first derivative of the position equations shown in Figure 4-1 with respect to time. The component velocities may then be summed vectorially to yield the net linear velocity. This net velocity may then be combined with the roller radius to finally yield the required angular velocity, as shown in Figure 3-28.

Having defined the roller velocity equations, the effects of the various parameters may be evaluated. The input speed has a purely linear effect on the roller velocity. The most significant influence on roller velocity is exercised by the nutation angle. Varying the nutation angle from 5 to 20 degrees produces a better than 2:1 variation in roller speed, as shown in Figures 4-2 and 4-3. This severe dependence is explained as follows. As the nutation angle increases, the length of the path which the roller must traverse increases; however, the time required for one cycle remains constant. In order to cover this greater distance, the velocity must increase. It is obvious then that in order to minimize the roller speed, the nutation angle must be minimized. Of course, it must be remembered that the thrust loading on the cams and the normal roller loads increase with decreasing nutation angle.

To further complicate the tradeoff, it should be noted that

$$\omega_{RCA/CL} = \frac{V_{PCA/CA}}{Y_{CA}}$$

$$V_{PCA/CA} = \left(V^2_{XPCA/CA} + V^2_{YPCA/CA} + V^2_{ZPCA/CA}\right)^{1/2}$$

$$V_{XPCA/CA} = \frac{dX_{PCA/CA}}{dA}$$

$$V_{YPCA/CA} = \frac{dYPCA/_{CA}}{dt}$$

$$V_{ZPA/CA} = \frac{d\,t_{PCA/CA}}{dt}$$

WHERE: $\omega_{RCA/CL}$ IS THE ANGULAR VELOCITY OF THE NUTATOR ROLLER ABOUT ITS OWN ℄

$V_{PCA/CA}$ IS THE LINEAR VELOCITY OF APOINT ON THE ℄ OF A NUTATOR ROLLER WITH RESPECT TO THE CAM

Figure 4-1. Equations of Angular Velocity of Nutator Rollers About Their Own Centerline.

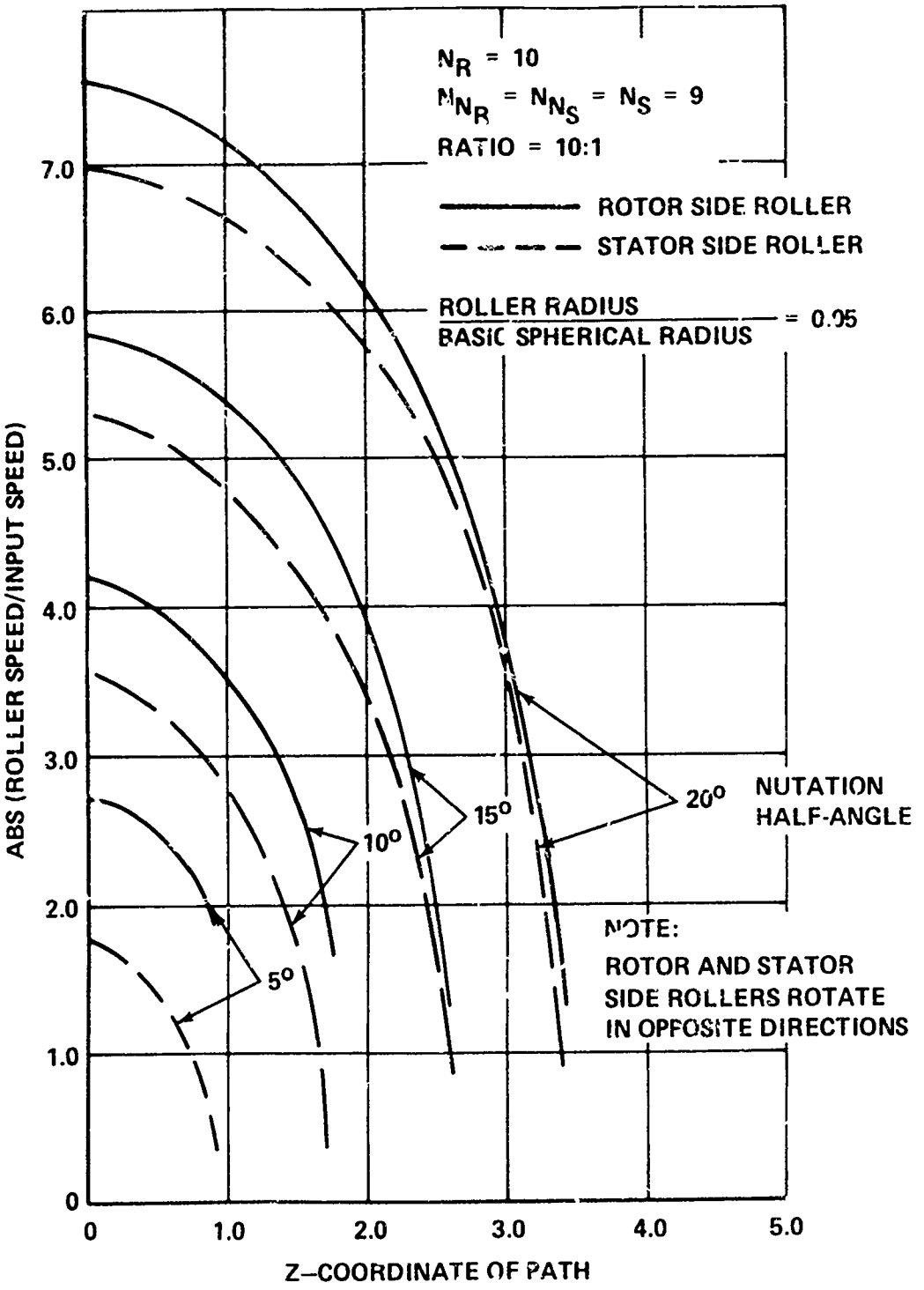

Figure 4-2. Angular Velocity of Nutator Rollers as a Function of Nutation Half Angle (10, 9, 9, 9).

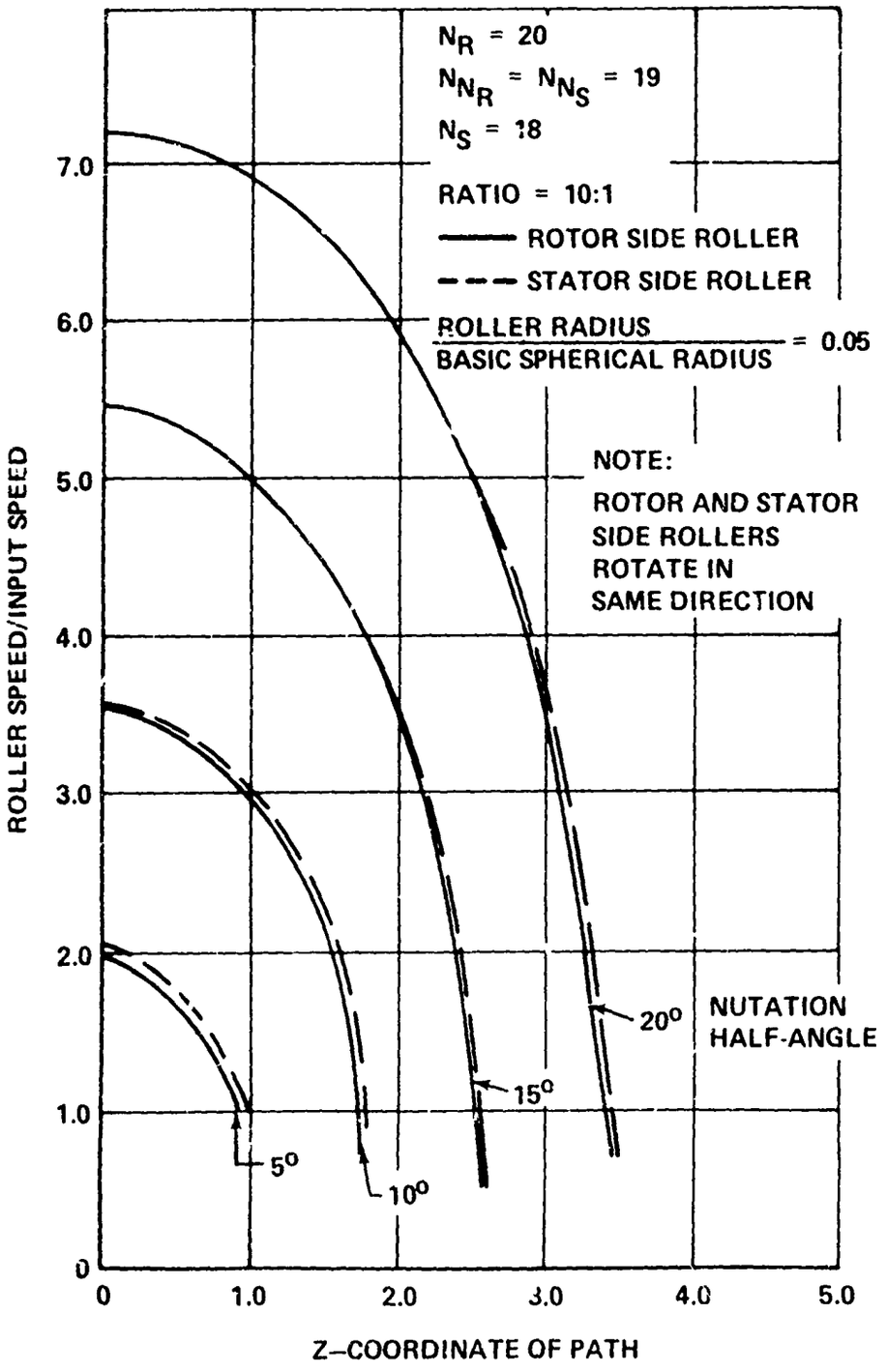

Figure 4-3. Angular Velocity of Nutator Rollers as a Function of Nutation Half Angle (20, 19, 19, 18).

sufficient normal loading must be maintained on the nutator rollers to prevent them from slipping. Examination of Figures 4-2 and 4-3 reveals a rather large variation in the angular velocity of a roller along the tooth profile at any value of nutation angle. This variation gives rise to high angular accelerations. Therefore, in order to accelerate the rollers without slippage, a certain normal load is required, depending of course, on roller inertia. Clearly then, the optimum choice of nutation angle, from a roller velocity viewpoint, is neither very low nor in the moderate to high range; it should be in the low range.

The relationship between the roller radius and the basic spherical radius is second only to the nutation angle in its influence on both the magnitude of the maximum roller velocity and the variation of the roller velocity along the profile. Figure 4-4 shows the variation of roller velocity as a function of both roller radius and spherical radius. Varying the ratio of the roller radius to the basic spherical radius over a range of 3:1 yields a corresponding 3:1 change in roller velocity. Of equal importance is the fact that variation between the maximum and minimum roller speeds increases rapidly as this ratio decreases. From the chart, it would appear that a small further increase in the roller radius (or a corresponding decrease in spherical radius) might reduce the speed variation to a minimum.

As is the case with any other tradeoff parameter, the maximum and minimum values which may be assigned to the roller radius at any given spherical radius are limited by the physical restraints of the system, such as keeping the rollers small enough to allow adequate cam tooth thickness, yet large enough to keep the stresses and deflections within the design allowables. A further complication is that the type of roller support bearing used (i.e., end support or cam follower type) is also influenced by the roller size and speed. The roller support bearing life is, of course, also significantly affected by the nutator roller speed.

For a constant input speed, the mechanism speed ratio has relatively little effect on either the maximum speed or the speed variation, as shown in Figure 4-5. The obvious explanation for this insensitivity is as follows. Holding all other parameters constant and varying only the ratio (which, of course, also implies a change in the number of teeth) does not change the cycle time for the nutator, which is primarily dependent upon input speed. The path length which the roller must traverse decreases very slightly with increasing ratio (due to the finer cam tooth pitch), thus the speed also decreases slightly.

The final parameter which may affect the nutator roller

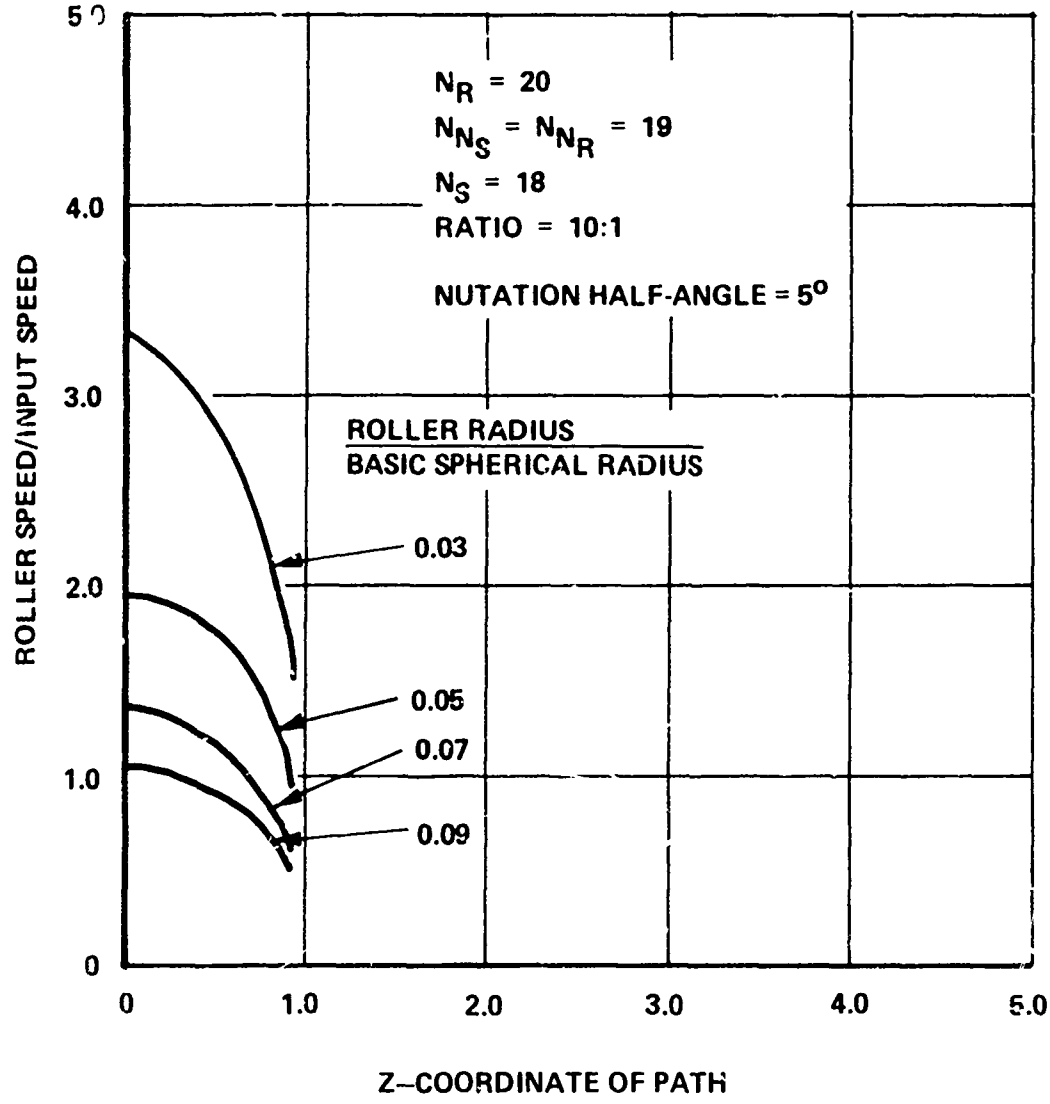

Figure 4-4. Angular Velocity of Nutator Rollers as a Function of Roller and Basic Spherical Radii

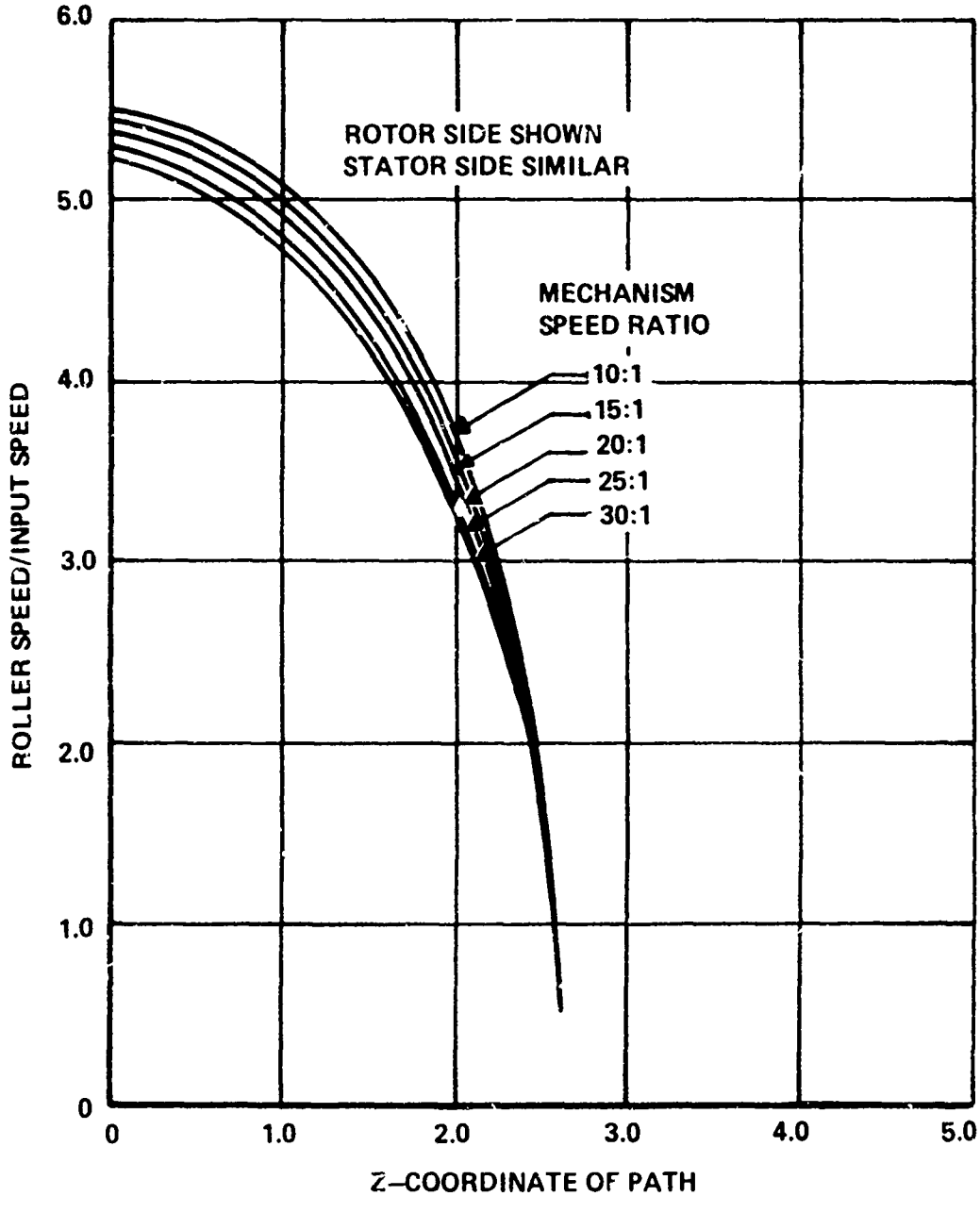

$N_{N_S} = N_{N_R} = N_R - 1$

$N_S = N_R - 2$

$\frac{\text{ROLLER RADIUS}}{\text{BASIC SPHERICAL RADIUS}} = 0.05$

NUTATION HALF-ANGLE = 15^{o}

Figure 4-5. Angular Velocity of Nutator Rollers as a Function of Speed Ratio.

velocity is the coning angle. The simplest case, of course, is a zero coning angle; however, it may be necessary to employ coning, for a variety of reasons. From Figure 4-6, it may be seen that a slight decrease in roller maximum speed and speed variation is possible through the use of roller coning; however, this change alone is not sufficient to warrant the extra weight and complexity involved in roller coning. It should be noted that for certain configurations (e.g., $N_S = N_{NS} = N_R - 1$) the nutator roller reverses direction when meshing with the rotor and stator cam teeth. Considering the high rotational speeds of the roller, this configuration would clearly lead to appreciable skidding at the roller-cam interface. One solution to this problem is to provide separate rollers to mesh with the rotor and stator cams by some method such as coning, to keep the roller velocities unidirectional.

Some general observations may be made with respect to the roller speeds and their relationship to overall system design. Since their magnitudes may become quite large with respect to the input speed, care must be exercised in the choice of the specific bearing configuration to be used. A "low" speed (input) unit could easily have "high" speed nutator rollers requiring accurate races and roller guidance. Similarly, higher speed bearings are more sensitive to deflections across the bearings (because of the increased possibility of skewing and skidding). The constantly changing angular velocity of the rollers must be carefully examined and minimized. As the bearings accelerate and decelerate, if the loads are not high enough, skidding and premature bearing failure could occur. A balance must be kept between minimizing load to insure adequate life and providing sufficient load to prevent skidding.

NUTATOR ROLLER ACCELERATION AND SKIDDING CHARACTERISTICS

From the previous discussion, it is apparent that the rollers on the nutator undergo significant accelerations. By themselves, these accelerations do not present an appreciable problem; however, when they are examined to determine the tractive forces required to prevent roller skidding they assume greater significance. If the accelerations become large enough, the tractive forces at the roller-tooth interface may not be sufficiently large to prevent skidding at some point along the profile. In addition, a balance must be struck between sufficient load at engagement to prevent excessive skidding and sufficient load limitation to minimize noise generation.

The acceleration of the rollers is a function of many parameters such as ratio, nutation angle, roller radius, basic spherical radius, coning angle, roller speed, and particularly, input speed. Surprisingly, the roller acceleration does not vary as drastically along the tooth profile as does the roller

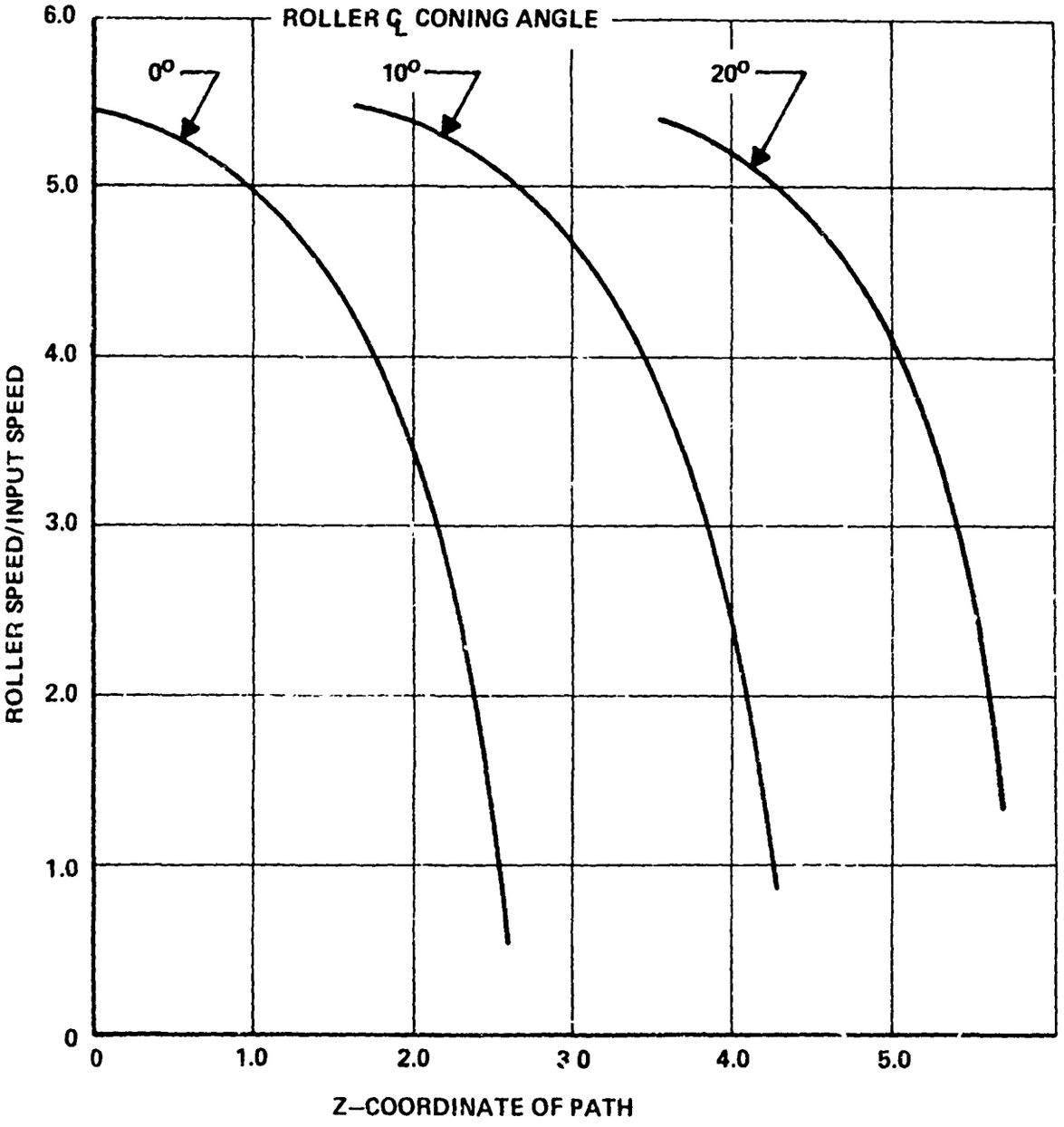

Figure 4-6. Angular Velocity of Nutator Rollers as Function of Roller Coning Angle.

velocity. Although the roller acceleration is a direct indication of its tendency to skid, specific conclusions must be coupled with the type and size of nutator roller under consideration. It should also be noted that the roller acceleration is an exponential function of the input speed. The determination of whether or not skidding will occur is actually dependent on three specific factors: roller acceleration, roller inertia, and the coefficient of friction between the roller and the cam tooth.

The coefficient of friction for many material and lubricant combinations is readily available from many standard texts. Data from rolling element testing and traction drive devices will prove particularly applicable due to the similarity of the contact conditions. Ideally, of course, the friction coefficient should be determined from specimen testing; consequently, wherever possible, the data in the charts of this section will be shown with the friction coefficient as a variable. Typically, the friction coefficient may vary from about 0.001 to 0.01 or greater; however, with the materials and lubricants currently employed in more conventional drives, it is likely to lie in the low end of this range.

The roller moment of inertia is purely a function of the geometry and mass of the roller. These factors are, in turn, influenced by both roller type and mounting method. The shell type cam follower roller generally provides the lowest rotating mass and inertia configuration, while the end-mounted shaft type roller generally provides a stiffer system.

The angular acceleration of the nutator rollers may be obtained by differentiating the angular velocity equations with respect to time. The product of this angular acceleration and the roller moment of inertia will yield the torque which must be applied to the roller in order to maintain the stated acceleration. The only force which may apply this torque is the frictional force acting at the roller/cam-tooth interface. Having defined these parameters, the normal force which must be applied to the roller to prevent skidding may be determined, as shown by Figure 4-7. Since the friction coefficient is a variable which is generally not affected by the NMT configuration or properties, it will be advantageous to examine the variation of the product of the normal force and the friction coefficient rather than to try to separate their effects. In addition, the friction coefficient may be varied by many methods including surface treatments and the use of tractive lubricants such as used in traction drives.

With this in mind, it will be useful to define a "skidding force factor" (Figure 4-7) to be used in the investigation of the effects of various geometric parameters on the skidding tendencies of the NMT. From Figure 4-8, which shows the

$$\alpha_{RCA/CL} = \frac{d\omega_{RCA/CL}}{dt}$$

$$T_{FRCA} = J_{RCA}\,\alpha_{RCA/CL}$$

$$F_{N_{FRCA}} \simeq \frac{T_{FRCA}}{r_{CA}\,f}$$

OR

WHERE $F_{N_{FRCA}}$ IS THE MEAN NORMAL TOOTH LOAD REQUIRED TO PREVENT ROLLER SKIDDING

f IS THE COEFFICIENT OF FRICTION

$\alpha_{RCA/CL}$ IS THE ROLLER ANGULAR ACCELERATION

J_{RCA} IS ROLLER POLAR MOMENT OF INERTIA

S_{FF} = SKIDDING FORCE FACTOR

MINIMUM NORMAL LOAD REQUIRED TO PREVENT SKIDDING = SKIDDING FORCE FACTOR / FRICTION COEFFICIENT

$$F_{NSCA} = \frac{S_{FF}}{f}$$

- THE NORMAL FORCE REQUIRED TO PREVENT SKIDDING INCREASES MORE THAN LINEARLY WITH INCREASING INPUT SPEED

Figure 4-7. Relationship Between Normal Tooth Load and Skidding Torque.

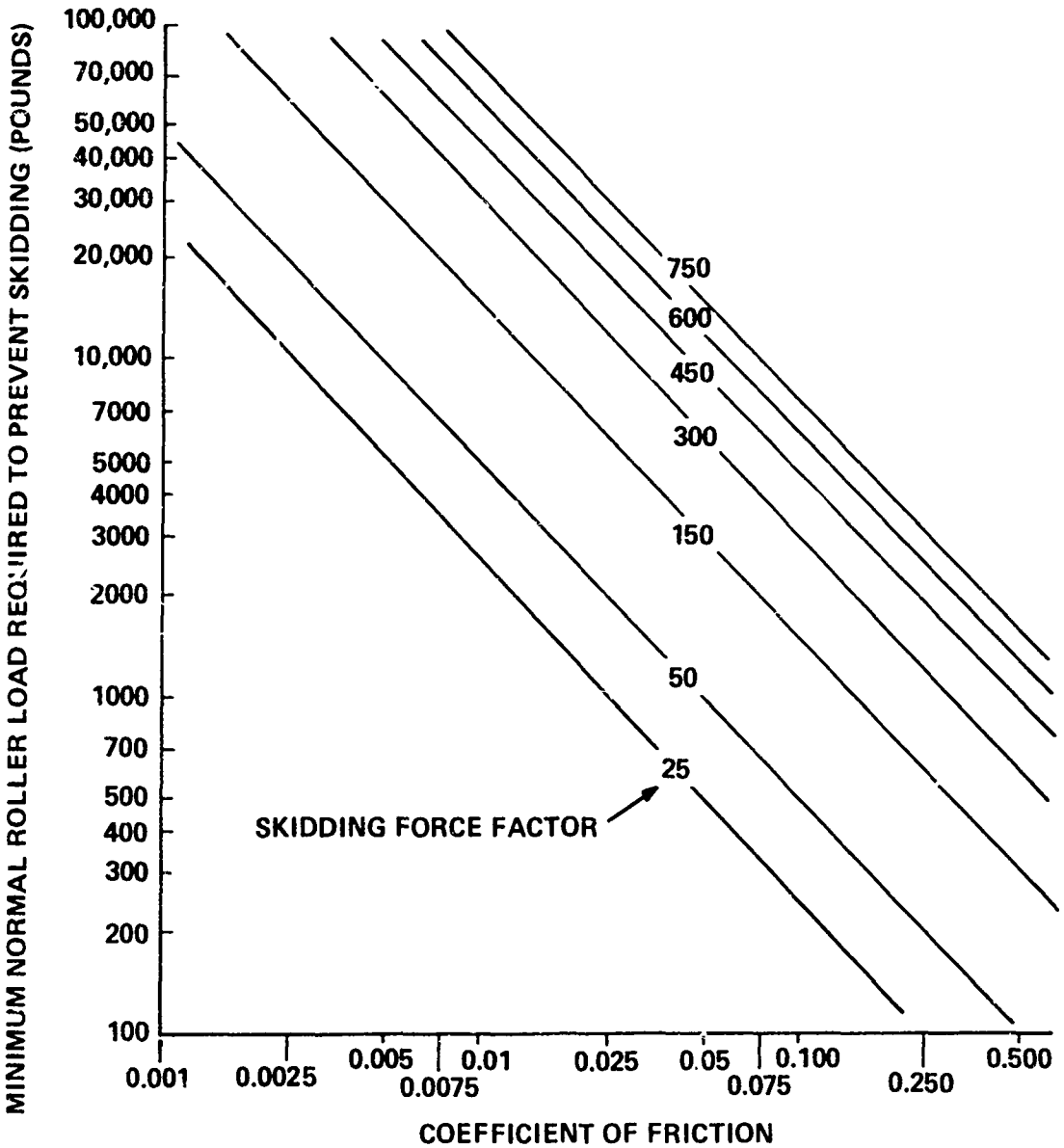

Figure 4-8. Minimum Roller Load Required to Prevent Skidding as a Function of the Skidding Force Factor and Friction Coefficient.

relationship between the skidding force factor and the friction coefficient, it may readily be seen that even at low values of the skidding force factor, the minimum normal load required to prevent skidding may be substantial. For example, with a friction coefficient of 0.01 and a skidding force factor of 50 pounds, the minimum normal roller load required to prevent skidding is about 5000 pounds.

Typical friction-coefficient values for well-lubricated, hardened steel contacts may vary from about 0.005 to 0.15. High capacity gears generally exhibit friction coefficients in the range of 0.01 to 0.07, while the range for rolling element bearings may begin as low as 0.0015. Obviously, this parameter is of critical importance in the design of an NMT, particularly at high input speeds.

The skidding force factor varies with several NMT geometric design parameters and, of course, input speed. The plots on Figures 4-9 through 4-12 investigate the more significant of these interactions.

The relationship between the basic spherical radius and roller mean radius is the single most influential parameter. Figure 4-9 shows the variation of minimum skidding load as a function of the ratio of roller radius to the basic spherical radius. As the roller radius increases or the basic spherical radius decreases, the required load increases rapidly. This result is readily apparent if one considers that the angular velocity itself as well as the net variation of this velocity (and thus its acceleration) increases with increasing spherical radius. This effect is further compounded by the fact that as the roller increases in diameter, its inertia increases as the square of its diameter (although its rotational velocity decreases linearly). The net effect is therefore an increase in the normal load required to prevent the roller from losing traction and skidding.

These curves may be modified somewhat by fine adjustments to specific roller configurations to make the effect either more or less severe than that shown; however, the relative trend - which is of prime interest - generally holds true. At the larger diameters, the unit loading may well be less than that at the smaller diameters (even though the net loading may be the same or even higher); therefore, the proportional wall thickness and/or roller length may be reduced, which will tend to lessen the required load increase. It should be noted that the increase with the roller/sphere ratio is quite nonlinear, as is obvious when the rapidly increasing spans between curves in the vertical direction are examined.

Increasing the nutation angle, in effect, lengthens the path which the rollers must traverse within a single cycle. As

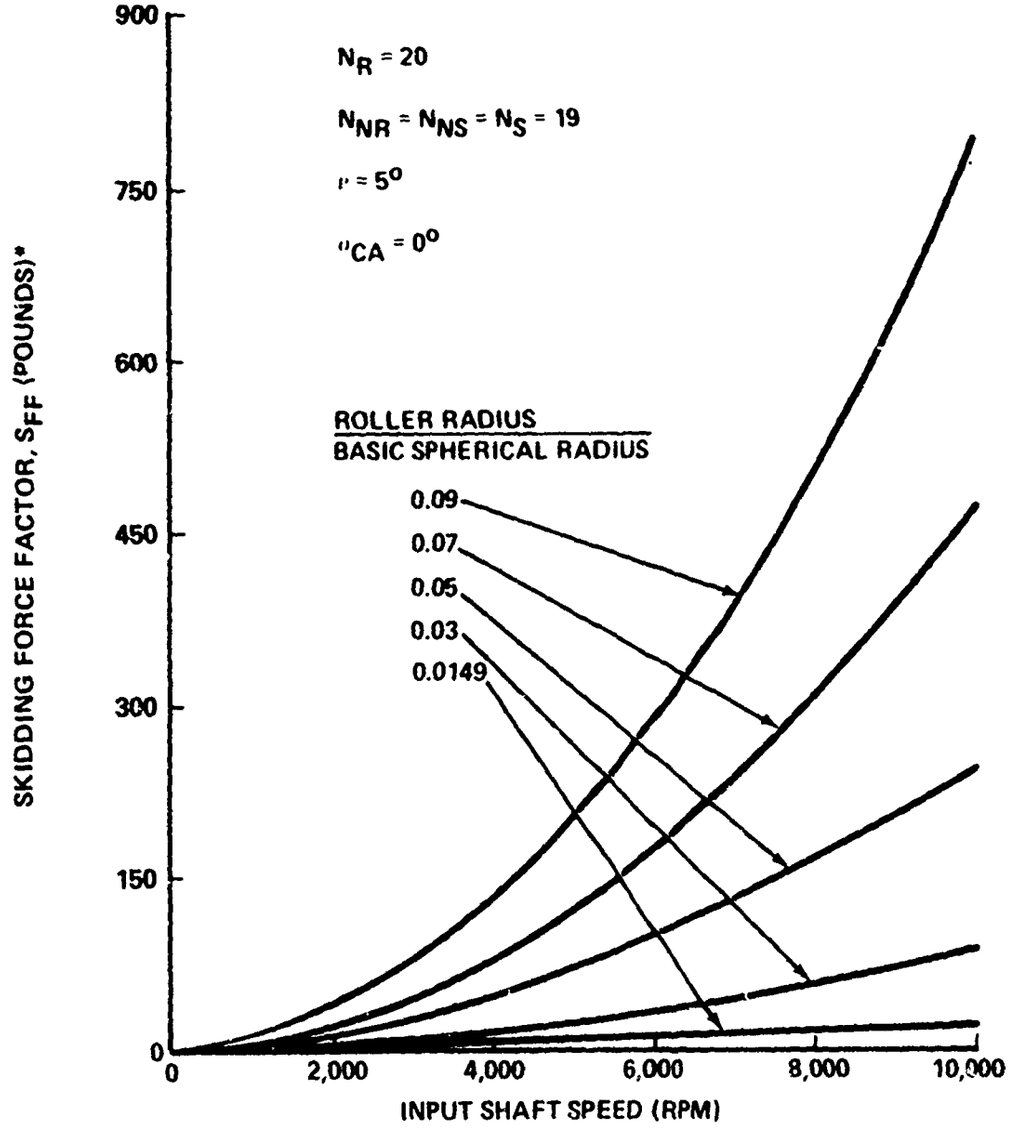

*NOTE

MINIMUM NORMAL LOAD REQUIRED TO PREVENT SKIDDING = SKIDDING FORCE FACTOR / FRICTION COEFFICIENT

Figure 4-9. Anti-Skid Roller Normal Load Required Vs. RPM and Roller/Sphere Ratio.

noted earlier, however, the time required for a single cycle remains invariant, which, in turn, implies both higher roller speeds and accelerations. Therefore, the normal load required to prevent skidding also increases. This effect is compounded by a change in roller and/or basic spherical radius, as shown in Figure 4-10. The spread caused by increasing nutation angle also increases as the roller/sphere ratio increases. A lower nutation angle generally increases the proportion of thrust to tangential (driving) force on the cams; therefore, the net normal load on the cams decreases with increasing nutation angle. If a specific configuration were close to the critical skidding load, an increase in nutation angle may push the operation into the skidding range, an interaction which is the basis for yet another tradeoff decision. The benefits of lower cam thrust and normal roller loads obtainable with higher nutation angles must be balanced against the higher anti-skidding loads required and several other parameters.

The coning angle (Figure 4-11) has very little effect on the load required to prevent skidding, a result to be expected from the previous discussion in this section.

The plot in Figure 4-12 is an interesting conglomerate representation of several individual parameters and combinations thereof. The ratio does not play a significant role in determining the load required to prevent skidding, a not unexpected result when the effect of ratio on roller velocity, and, in particular the variation of roller velocity is considered, as discussed earlier in this section.

A more significant parameter is the relationship between the relative numbers of teeth required to yield a given ratio for two different NMT configurations. The compounding effect of multiple changes is also apparent. The difference between the two configurations at the lower roller/sphere ratio (r_{CA}/R_{BCCA}) is much less severe than at the higher ratio shown. The essential difference between the two configurations shown is their effective pitch; i.e., the $N_R = N_S + 2$ configuration has a much finer pitch than the $N_R = N_S + 1$ configuration at any given ratio.

General examination of all the graphs in this section, reveals several overall interreactions among the significant parameters. The influence of input speed as a compounding factor is evident on every chart; that is, the change in anti-skidding load due to any single parameter becomes more significant as the speed increases. For example, in Figure 4-9 it can be seen that at 2000 rpm input speed a threefold increase in the roller/sphere ratio yields only a triple increase in the skidding force factor. However, at 6000 rpm, the same roller/sphere ratio increase produces approximately an eightfold increase in the skidding force factor. The compounding

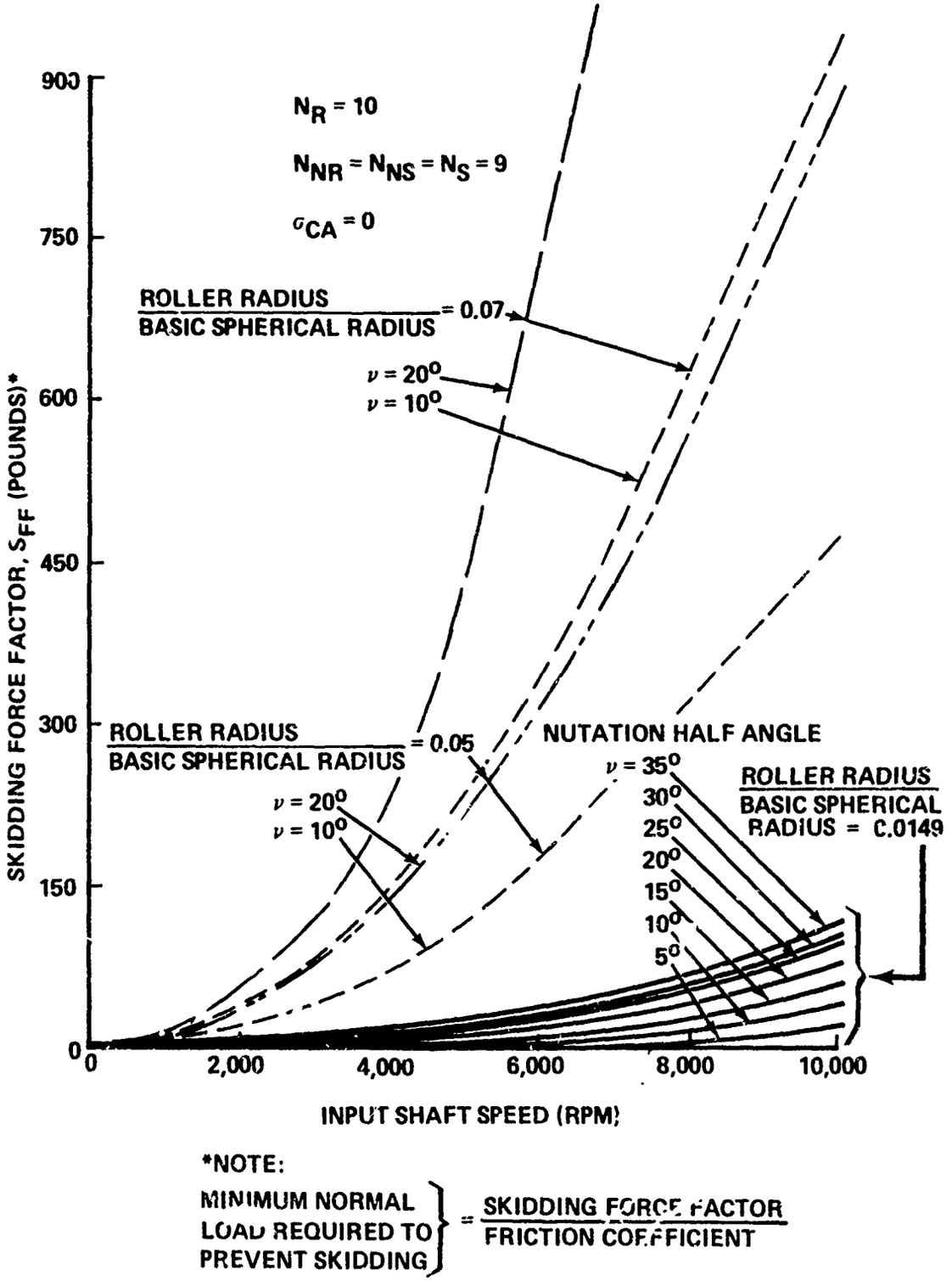

*NOTE:

MINIMUM NORMAL LOAD REQUIRED TO PREVENT SKIDDING } = SKIDDING FORCE FACTOR / FRICTION COEFFICIENT

Figure 4-10. Anti-Skid Roller Normal Load Required Vs. RPM and Nutation Half Angle.

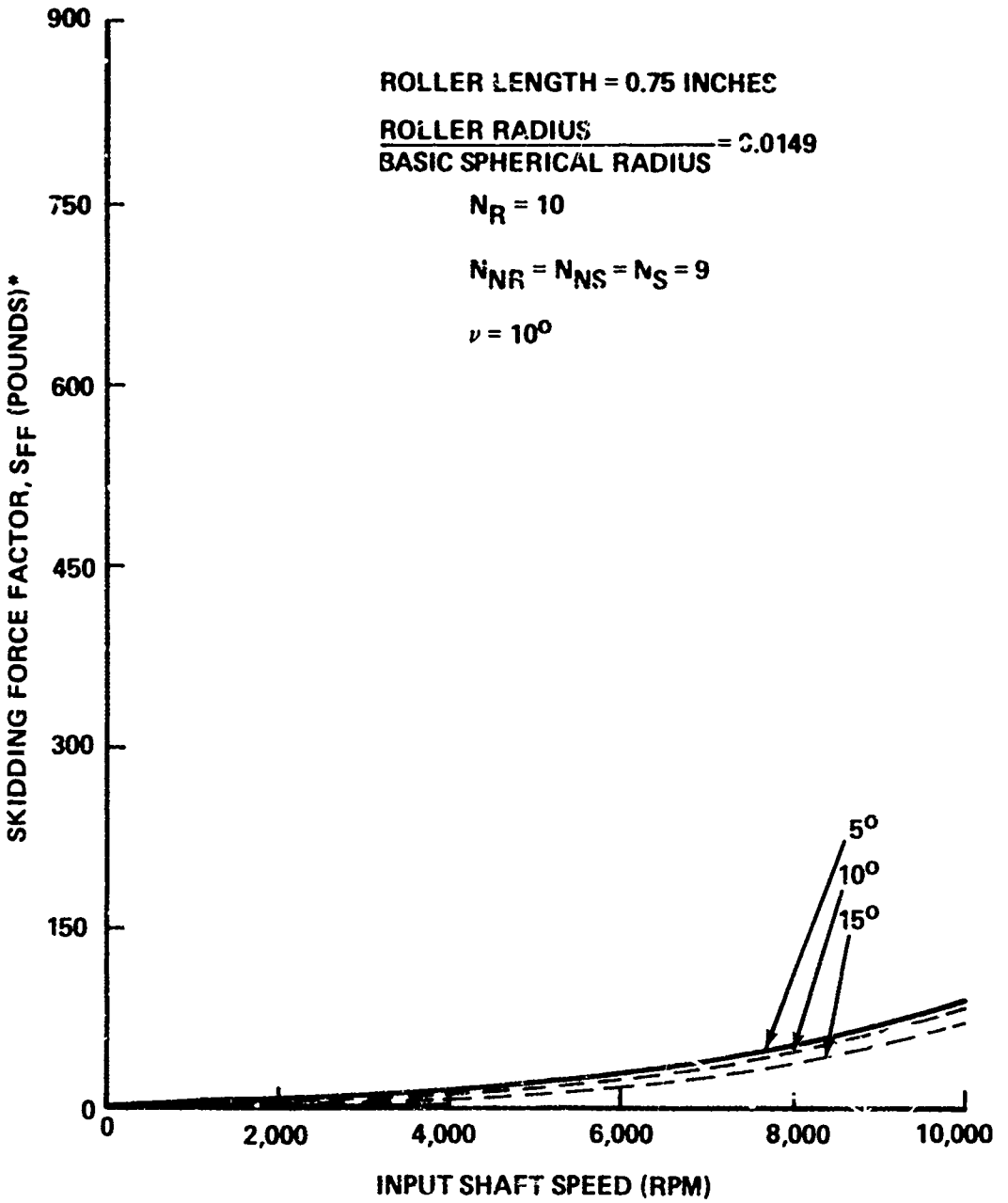

*NOTE:

MINIMUM NORMAL LOAD REQUIRED TO PREVENT SKIDDING = SKIDDING FORCE FACTOR / FRICTION COEFFICIENT

Figure 4-11. Anti-Skid Roller Normal Load Required Vs. RPM and Coning Angle.

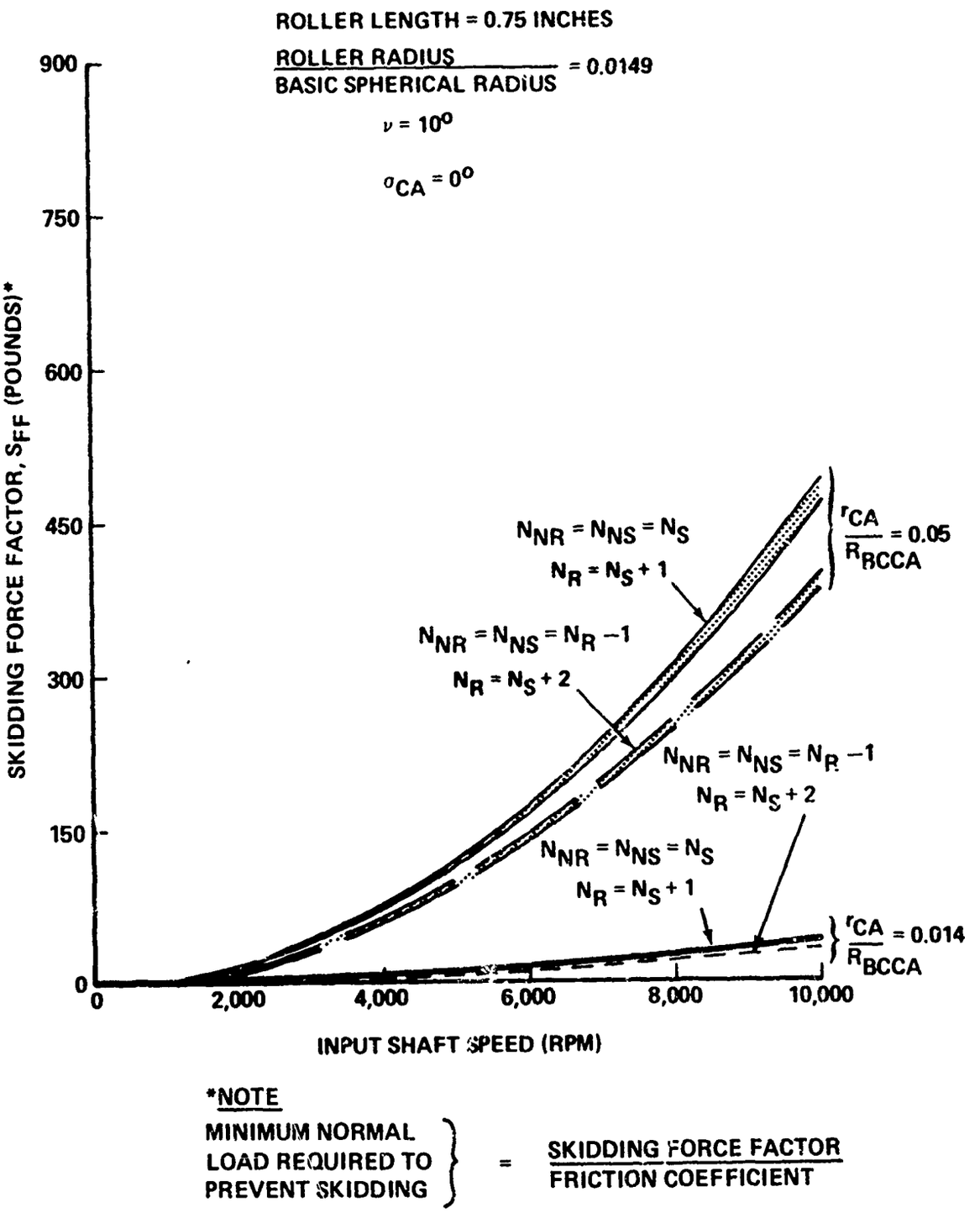

*NOTE

MINIMUM NORMAL LOAD REQUIRED TO PREVENT SKIDDING = SKIDDING FORCE FACTOR / FRICTION COEFFICIENT

Figure 4-12. Anti-Skid Roller Normal Load Required Vs. RPM and N_R: N_S ($10:1 \leq M_G \leq 30:1$).

effect of multiple parameter interactions is thus apparent. The results of any group of changes may not be simply superimposed on one another to yield the total effect.

For all parameters investigated, the skidding force factor is almost negligible below about 1800 rpm input speed. However, it becomes quite important at speeds above this value, at an increasing rate.

5. MECHANISM DYNAMICS

NUTATOR UNBALANCE MOMENTS

Due to the reciprocating motion of the nutator, significant unbalance moments may be developed during normal operation of the mechanism. The equations defining the moments applied to the system are quite complex and tedious to evaluate. In addition, they are quite sensitive to the geometry of the specific nutator being considered. Therefore, two systems--each having the same numbers of rollers and cam teeth, the same nutation angle, etc.--may vary quite substantially at higher input speeds in their dynamic characteristics due to the detailed design of the nutating ring assembly.

The overall configuration of this assembly is not dictated by any NMT design constraints, since many different nutator configurations will behave kinematically in an identical manner. A single nutator system is inherently unbalanced. This is not to say that this configuration is not practical; however, it is limited to very low input speeds and relatively small sizes. The magnitude of the unbalance moments is influenced to a great extent by input speed and nutation angle. The reasons for both interactions are obvious. Higher speeds imply higher accelerations which, of course, lead to higher forces (moments). Larger nutation angles also cause higher oscillatory speeds (at constant input speed), leading to higher accelerations and forces. The basic equations defining the unbalance moments are available in many basic texts; therefore, they only need to be rearranged into a form suitable for use in the NMT analysis.

The moment of inertia matrix for the nutator assembly which is the prime geometric parameter involved is, in general, a function of time. As shown in Figure 5-1, the nutator angular velocity matrix is also a function of time. Due to the strong influence of the nutator detail design on the results of these equations through the inertia matrix, it is not practical to develop a complete series of parameteric plots. A representative case was chosen, however, and the curve shown in Figure 5-2 was developed.

As would be expected, the magnitude of the unbalance moments is a strong function of input speed. At lower input speeds, the moment is relatively inconsequential; however, its importance in the design process increases exponentially with input speed. The strong influence of the moment of inertia matrix provides wide latitude in the choice of nutator

- IN THE MOST GENERAL CASE, BOTH THE NUTATOR ANGULAR VELOCITY MATRIX AND THE NUTATOR INERTIA MATRICIES ARE FUNCTIONS OF TIME

$$M_{XN} = \frac{d}{dt}\left(I_{XN}\omega_{XN} - J_{XYN}\omega_{YN} - J_{XZN}\omega_{ZN}\right)$$

$$M_{YN} = \frac{d}{dt}\left(I_{YN}\omega_{YN} - J_{YZN}\omega_{ZN} - J_{YXN}\omega_{XN}\right)$$

$$M_{ZN} = \frac{d}{dt}\left(I_{ZN}\omega_{ZN} - J_{ZX}\omega_{XN} - J_{ZY}\omega_{YN}\right)$$

- THE INSTANTANEOUS MOMENT OF INERTIA MATRIX MAY BE EXPRESSED BY USING A SIMILARITY TRANSFORMATION

$$[I]_{XYZ} = [\gamma]_C\,[I_N]\,[\gamma]_C'$$

WHERE $[\gamma]_C$ AND $[\gamma]_C'$

ARE RESPECTIVELY THE MATRIX OF DIRECTION COSINES OF THE ROTATED POSITION AND ITS TRANSPOSE.

Figure 5-1. Nutator Unbalance Equations.

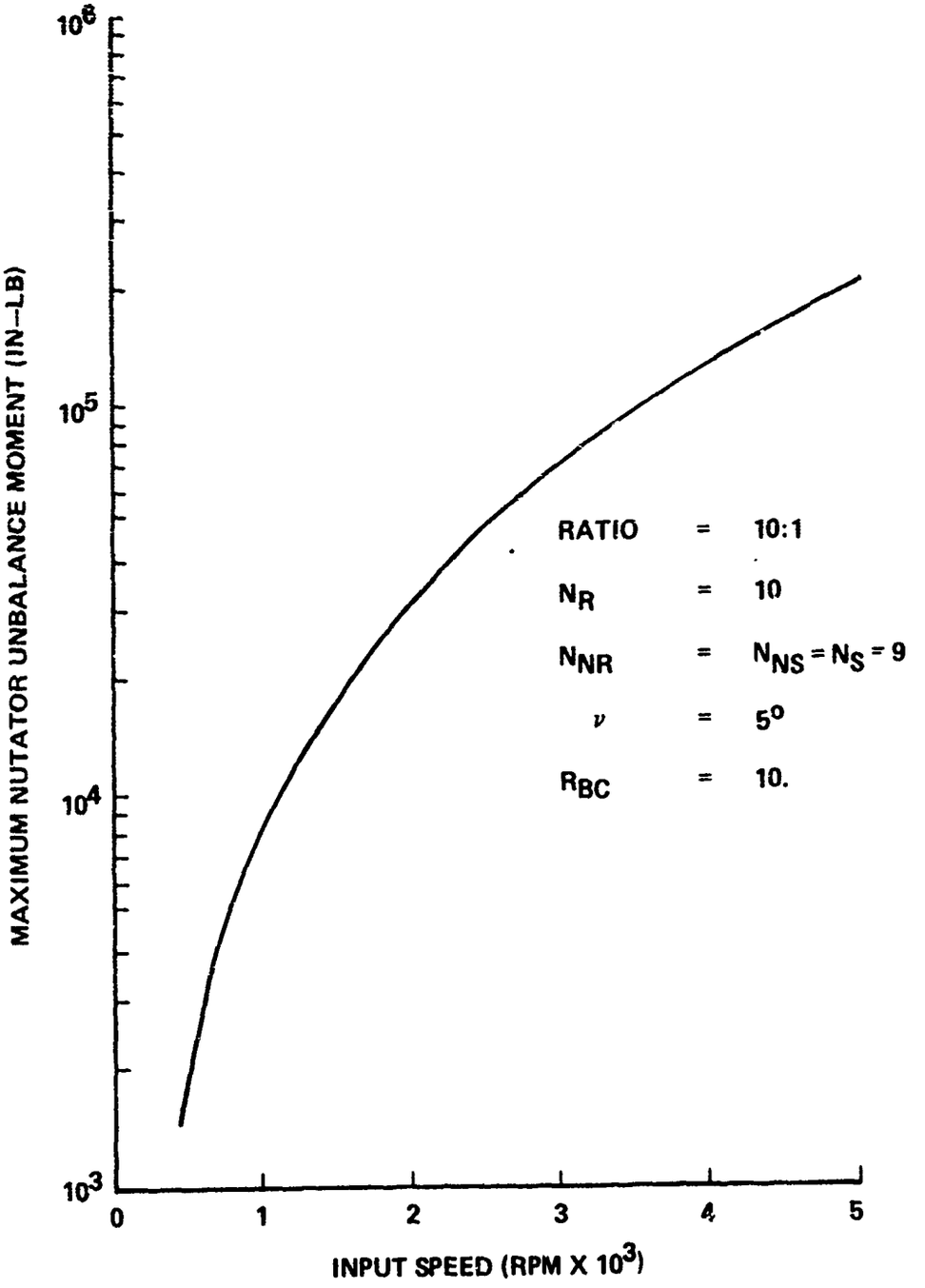

Figure 5-2. Nutator Unbalance Moments About X-Axis Versus Input Speed.

configuration. Conversely, the nutator must be designed to be as light as practical, particularly at high speeds and consistent with stress and life limitations.

Although Figure 5-2 refers to a representative case, it may certainly not be considered as typical. An in-depth investigation of the nutator construction, material selection, structural analysis, and detailed design drawings would be required for a series of such charts. An effort of this magnitude is beyond the scope of this analytical investigation.

NUTATOR BALANCING TECHNIQUES

Some type of balancing mechanism is required at all but relatively low input speeds to provide for acceptable vibration levels during operation of the NMT. In general, two methods are available to accomplish this balancing task. For a single nutator configuration or for multistaged single nutator configurations, a set of synchronous rotating weights may be mounted on the input shaft such that the couple created by their unbalanced rotation exactly matches that produced by the nutator, but with opposite sense. This mechanism will then effectively balance the total system so that no net vibratory loads are apparent. This concept is shown in Figure 5-3. A benefit of this system is that the unbalance which would ordinarily be present in any drive due simply to manufacturing and assembly tolerances may be tuned out at final assembly by proper choice and modification of a weight system. In order to utilize this balancing method in the design of an actual NMT, it has been necessary to develop a system of equations which define the moments caused by the weight system, as shown in Figure 5-4.

The use of this type of balance weight system may be eliminated by using a split-power, double-nutator configuration as shown in Figure 5-5. In this system, two identical nutators are mounted on the input shaft exactly out of phase (180^{o}), such that the moments generated by each nutator are equal in magnitude and opposite in direction; therefore, the vibratory unbalanced loads are completely cancelled. This arrangement, of course, involves a considerable increase in cost and complexity. Two stators, two complete nutating ring assemblies, and a double-faced rotor are required. Also, implied is the need for an offset input to allow for the doubly connected rotor and stator cam system. This configuration is, however, inherently self balancing, requires no ancillary equipment, and has a weight advantage in certain size ranges.

Clearly, some tradeoffs are necessary to make a decision regarding the choice of configuration for any specific design application. The power and speed requirements of the unit

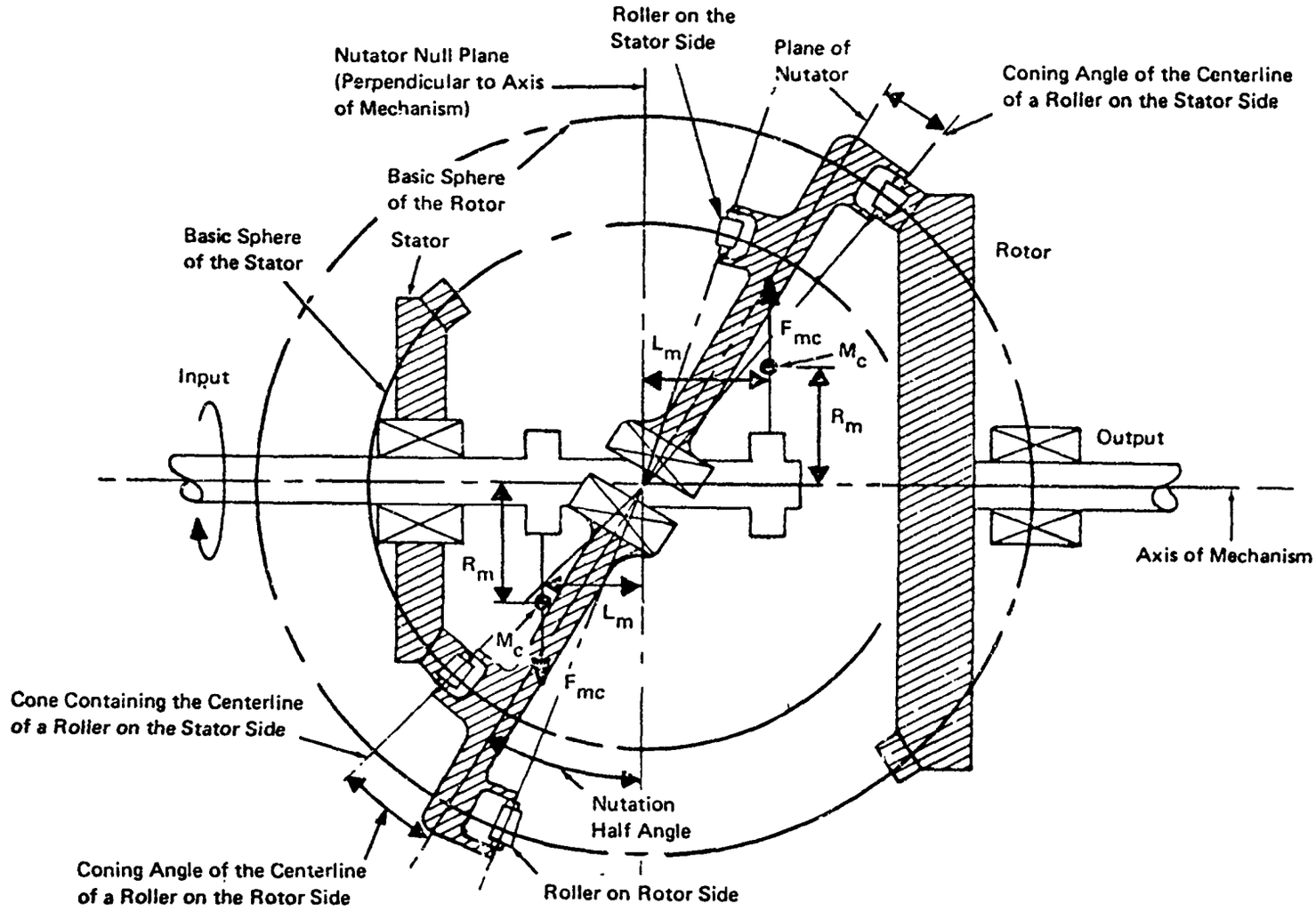

Figure 5-3. Nutating Mechanical Transmission Balance Weight Schematic.

- THE INSTANTANEOUS MOMENTS GENERATED BY THE SYNCHRONOUS WEIGHT SYSTEM ARE GIVEN BY

$$M_{mcX} = 2 M_c R_m \omega_C^2 L_m \cos(\omega_0)$$

$$M_{mcY} = 2 M_c R_m \omega_C^2 L_m \sin(\omega_0)$$

$$M_{mcZ} = 0.0$$

WHERE
- ω_C IS INPUT SPEED
- R_m IS RADIUS FROM MECHANISM AXIS TO BALANCING WEIGHT CENTER OF MASS
- L_m IS DISTANCE FROM MECHANISM FOCUS TO BALANCING WEIGHT CENTER OF MASS MEASURED ALONG MECHANISM AXIS
- M_c IS MASS OF BALANCE WEIGHT
- ω_0 IS INPUT SHAFT TURNING ANGLE

Figure 5-4. Nutator Balancing Equations.

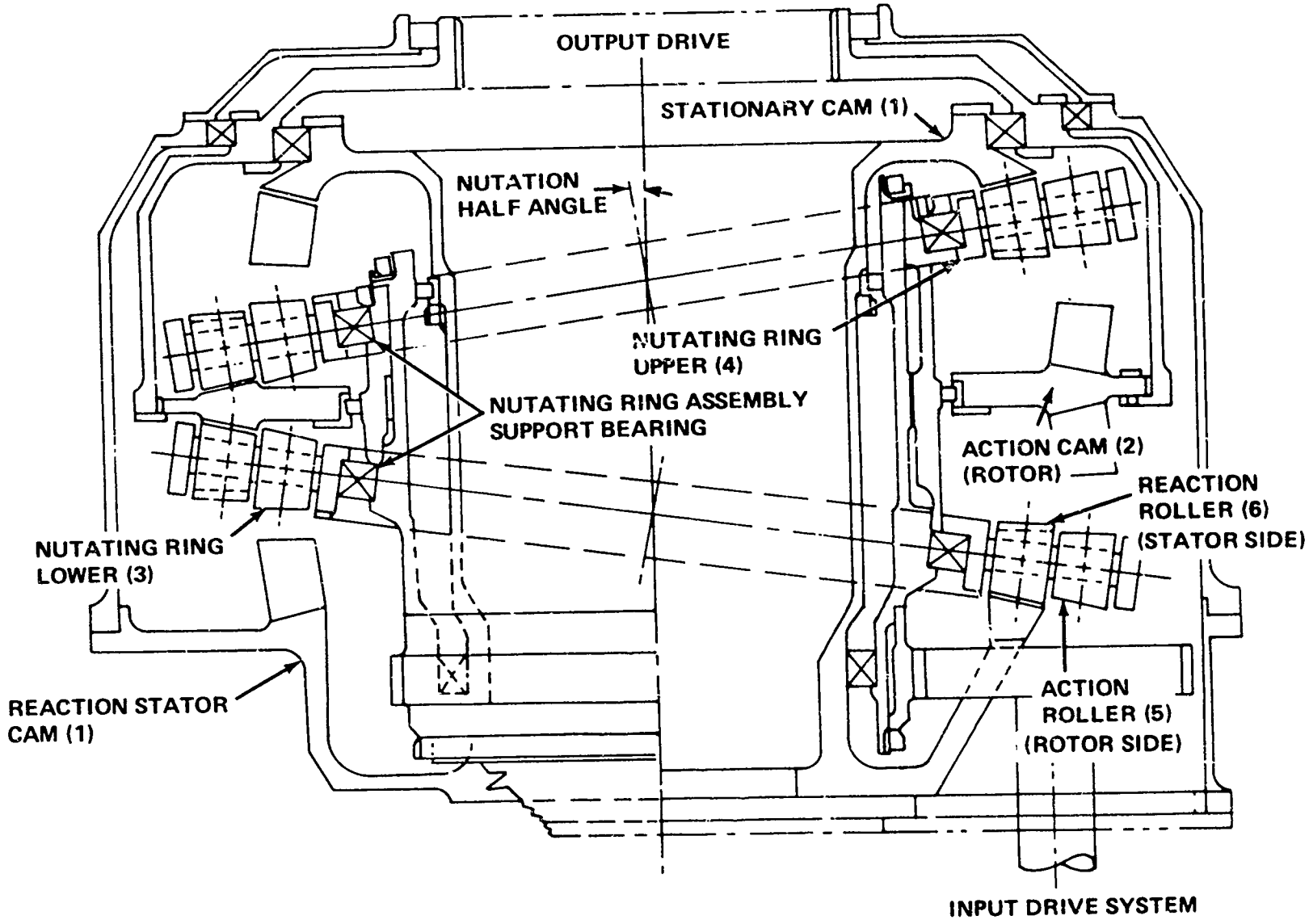

Figure 5-5. Schematic of Split Power Concept.

being considered will fix the basic spherical radius, the nutator roller size, etc. independent of any balancing considerations. Generally, therefore, the weight required for any balancing apparatus simply serves to increase the overall weight of the unit without contributing to the mechanism's load capacity. This could be undesirable in critical weight applications such as aircraft or shipboard units. The double-nutator, split-power configuration, however, utilizes all of its weight in the load carrying function with no waste through balance weights. The tradeoff between the two concepts, not including weight, comes through envelope size. The single-nutator type tends to be larger in diameter and shorter in length in somewhat of a pancake shape; while the split power type tends to be smaller in diameter and longer, giving more of a cylindrical shape.

In the course of conducting the design case studies, reported in a later section of this document, it became apparent that for the specific configurations considered, the single nutator with balance weight concept was impractical. In addition to the reasons cited above, the support bearing DN was beyond near term state-of-the-art values.

Some torsional oscillations are introduced into the system by the action of the nutator, and although the dynamic loading may be essentially completely eliminated, some residual torsional vibrations are likely to remain. The magnitude of these forces depends, of course, on the specific nature of the balancing system and the accuracy with which the unit is made. The total effect of this phenomena is likely to simulate the dynamic tooth forces of conventional gearing.

6. MECHANISM POWER FLOW AND LOAD CAPACITY

NUTATOR AND SUPPORT BEARINGS

The speed reduction and torque multiplication of the NMT occurs at the nutator/rotor and nutator/stator interfaces. The rotary motion of the input shaft is converted to an oscillatory motion of the nutator, and, in turn through differential motion, to rotor rotation. The nutating ring assembly must react output loads, while rotating at close to the input speed.

The nutator loads from these interactions may generally be resolved into components along the axis of a cartesian coordinate system fixed to the nutator as shown in Figure 6-1. These loads must, of course, ultimately be reacted by the nutating ring assembly support bearing system. The figure shows a center support bearing which is typical of the configurations discussed in the ensuing section; however, the conditions for an outer support bearing are similar. Basically, there are three load components: thrust, radial, and tangential. The tangential load is the driving force which causes the rotor to rotate and, therefore, is the only useful force. The thrust and radial loads are extraneous and dependent on many design factors such as nutation angle, roller diameter, etc. The tangential loads (F_{TNXR} and F_{TNXS}) will remain constant for any given torque at a constant basic spherical radius, while the radial (F_{TNYR} and F_{TNYS}) and particularly the thrust (F_{TNZR} and F_{TNZS}) loads may vary substantially with the previously noted design parameters. This relationship is analogous to that of a spiral bevel gear set in which the tangential load is invariant at a constant pitch diameter, but the thrust and separating forces vary with pressure angle, spiral angle, etc. Since the tangential load remains constant, the normal (or total) load will be increased or decreased with similar changes in the thrust and radial loads, it would seem that the optimum design would maximize the tangential driving force, while minimizing the radial and thrust forces. This simplified approach, however, is not valid since many other interactions must be accounted for. The radial loads, due to rotor and stator contacts, for most configurations will cancel each other either completely or in part; therefore, their effect on the nutator support bearing will be minimal when compared to the effects of the remaining loads. In addition, the magnitude of this radial load is relatively small in comparison with the other components. It should be obvious that this radial load is simply the thrust load applied to the nutator rollers. The magnitude of this load

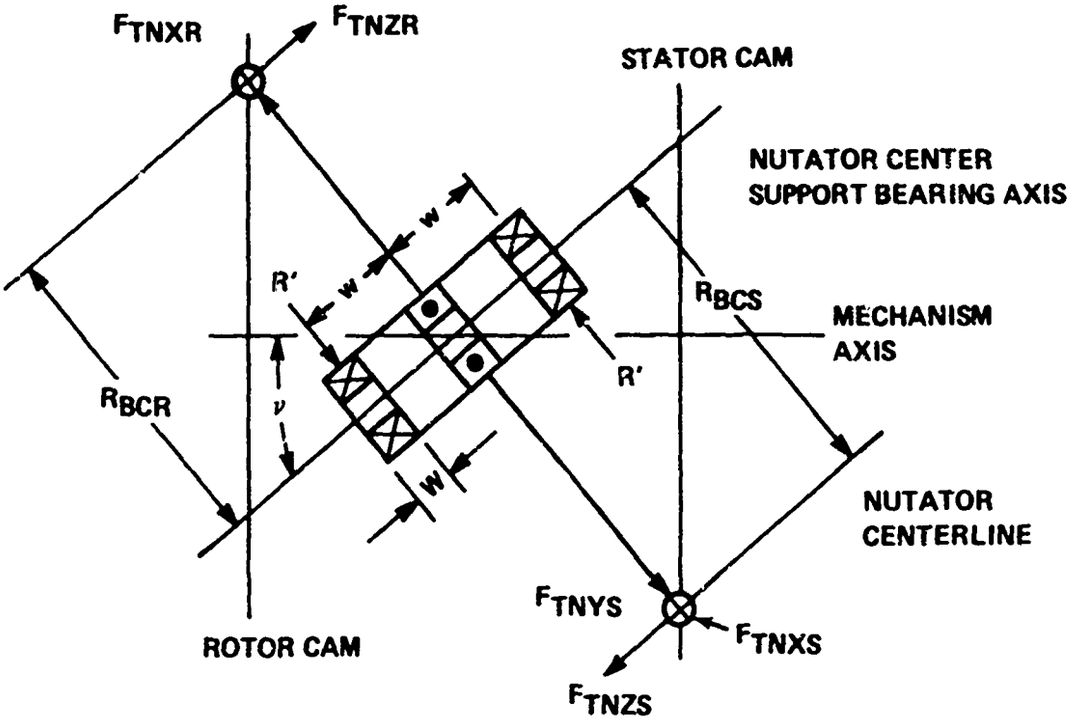

A. VIEW LOOKING INWARD ALONG A RADIAL LINE

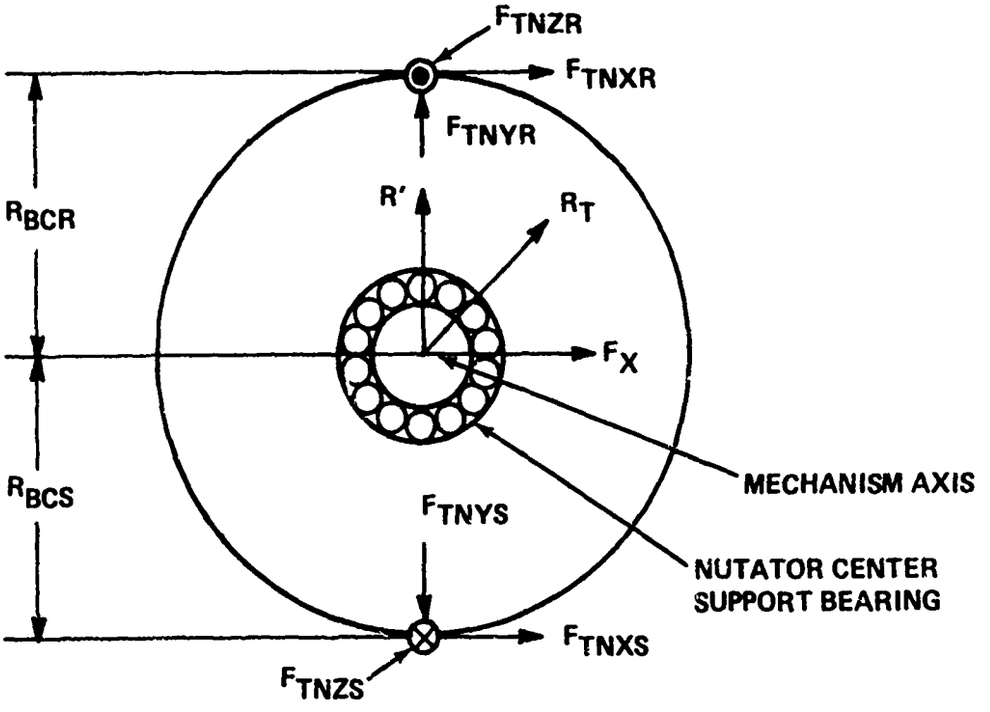

B. VIEW LOOKING ALONG MECHANISM AXIS TOWARD ROTOR

Figure 6-1. Nutator Center Support Bearing Loads.

relative to the normal roller load (the vector sum of the cam tooth loads) is shown in Figure 6-2. This radial nutator load (nutator roller thrust load) is chiefly a function of the ratio of the mean roller radius to the basic spherical radius, that is the roller's taper angle. Except in an indirect fashion through the affect these parameters have on the normal roller/cam tooth loads, this load is not affected by basic design parameters such as nutation angle.

The thrust loads (F_{TNZR} and F_{TNZS}) are principally affected by the nutation angle. The net thrust loading on the nutator is reacted by the nutating ring assembly support bearing set through the ball thrust bearing mounted between the two radial bearings. Due to each cam, the thrust loading is applied to the nutator in opposite directions. Since the configurations of each cam are quite similar, these thrust loads will be close in magnitude, though opposite in direction; therefore, they will largely cancel each other to yield a relatively low net thrust loading on the nutator. The thrust loads do, however, combine to produce a relatively large couple which must be reacted at the two radial roller bearings with an equal and opposite couple. The two principle loads which must be reacted by the nutator support bearing are this couple and the tangential loads. These loads may be converted to an equivalent radial load at each bearing and the bearing B_{10} life then calculated. Since the thrust induced couple must be reacted by a couple at the bearings and this bearing reaction couple is, in turn, a function of the spread between the bearings, considerable design latitude may be exercised by adjusting this spread. In addition to the bearing life aspects of these net loads, their affect on the shaft stresses must also be carefully considered.

ROTOR AND STATOR CAMS

The rotor and stator cams are subjected to very similar loading conditions. Each is acted on by a tangential, radial, and thrust load at each tooth contact. The tangential loads combine to produce the output and reaction torques on the rotor and stator cams, respectively, The thrust loads tend to cause plate bending and axial thrust on each cam. The tangential loads are the driving forces and, as such, constitute the only useful loads; i.e., they are the only loads which directly contribute to the output torque.

The radial loads which act to stress the cams outward in much the same way as centrifugal force will affect a spinning disk are low in comparison with the other loads so that their net effect is small. In addition, these radial loads tend to cancel each other to a greater or lesser degree, depending on the precise configuration under consideration. The cams

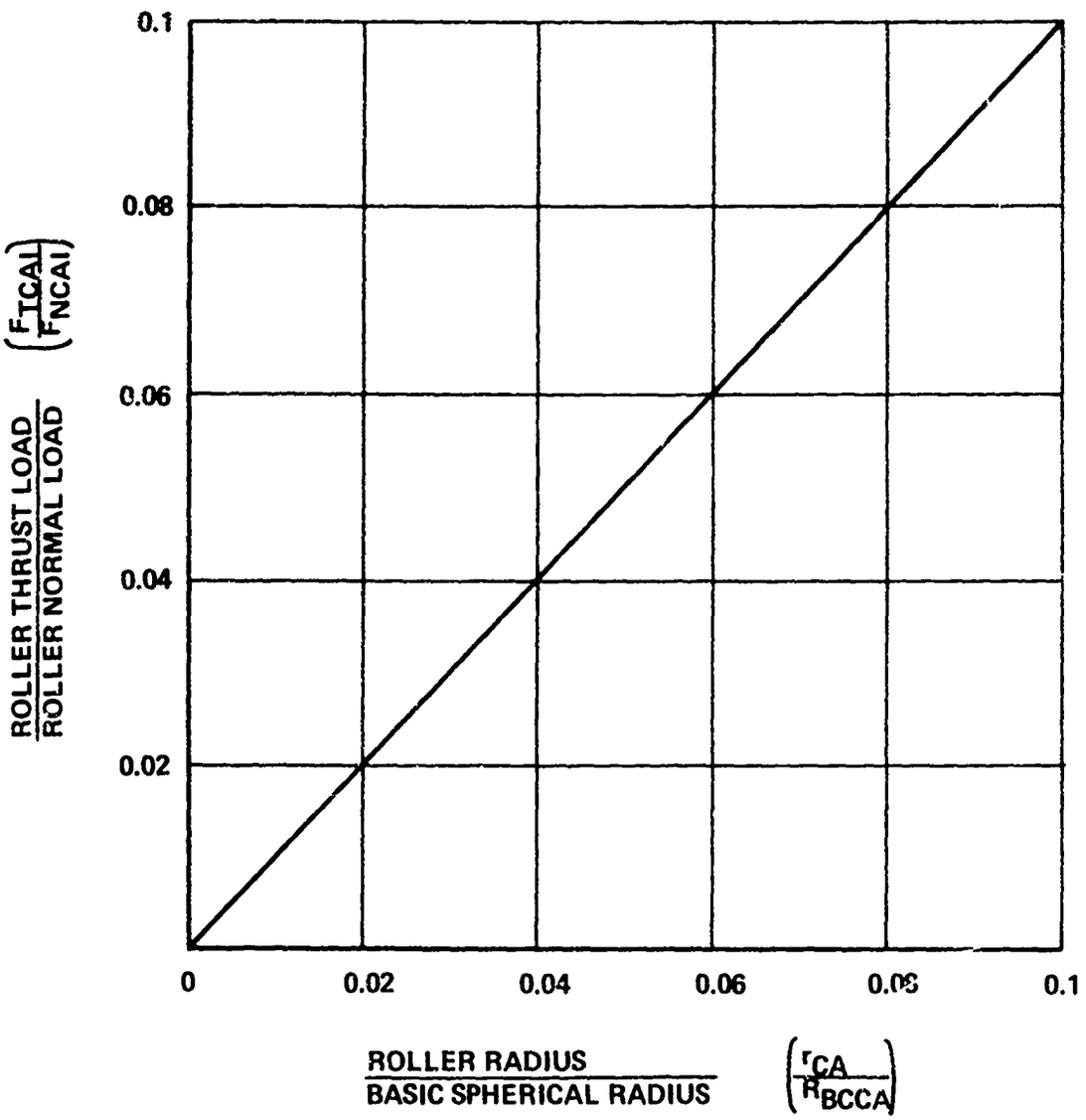

Figure 6-2. Variation of Nutator Roller Thrust Load.

themselves, as is the case with gear webs, are not generally the critical stress items, rather the root tensile stress of the cam teeth is generally the determining factor. The thrust on the cams and its reactions on the nutator, are of great importance in sizing the thrust bearings for acceptable lives. The cam thrust loading is primarily a function of the nutation angle, as shown in Figure 6-3. Although it appears that higher nutation angles are advantageous (due to the lower thrust loading) this is generally not the case. In fact, just the opposite is usually true due to the greatly increased roller velocities and accelerations. It has been noted that the cam tooth root tensile stress is the critical parameter in the design of the cams. The root stress is related to the thickness of the cam tooth at the critical bending section which is, in turn, related to the cam tooth tip thickness. The range over which the cam tooth thickness may vary is determined on the low side by the consideration of pointed teeth, while the maximum is limited by roller size restrictions. As the nutator roller diameter increases, the cam tooth thickness (and consequently, the cam tooth tip thickness) must decrease if all other conditions remain unchanged. Increasing the cam tooth tip thickness tends to reduce the root tensile stress in the cam tooth; while increasing the nutator roller diameter decreases the contact stress, increases its support bearing capacity, and reduces the slope across these bearings. Obviously, some compromise must be reached between roller size and cam tooth size.

The relationship between cam tooth bending (root) stress and cam tooth/nutator roller contact stress as a function of roller diameter and cam tooth tip thickness is shown in Figure 6-4. Over the range shown, the change in contact stress (37 percent) is considerably greater than the change in bending stress (21 percent). In many designs, it will, therefore, be desirable to use the largest roller size compatible with the maximum allowable tooth bending stress.

NUTATOR ROLLERS AND SUPPORT BEARINGS

In general, the design of the nutator rollers and their support bearings and structure will be more critically important than the cam tooth stress levels. The capacity of the nutator roller bearings is very much dependent on the size of the nutator rollers and the mounting configuration utilized shown in Figure 6-5.

In reviewing this Figure 6-5, it should be noted that bearing life is related to bearing dynamic capacity by the 10/3 power; therefore, a twofold increase in dynamic capacity will result in approximately a tenfold increase in the B_{10} life of the bearings.

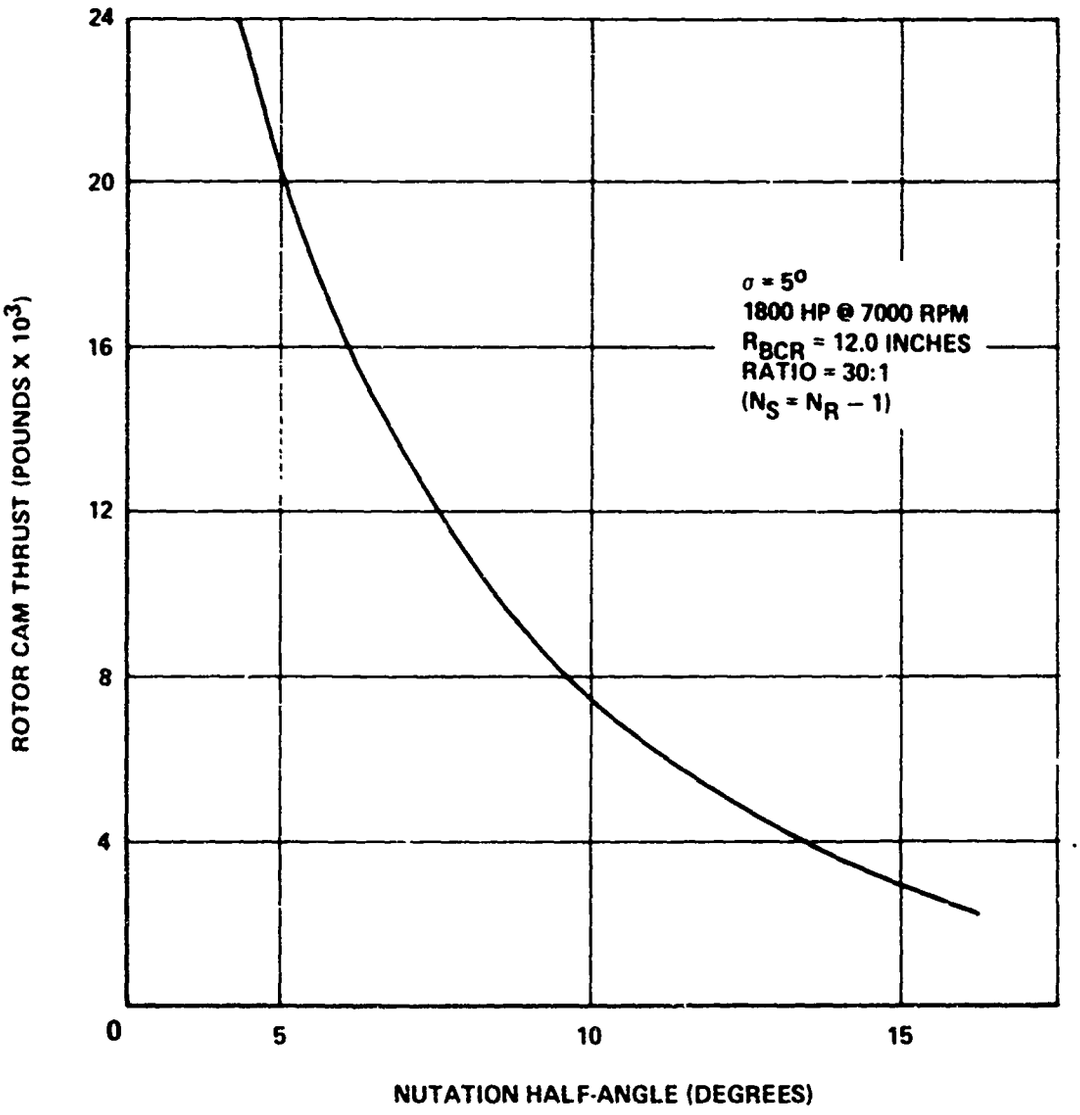

Figure 6-3. Variation of Cam Thrust Load with Nutation Half-Angle.

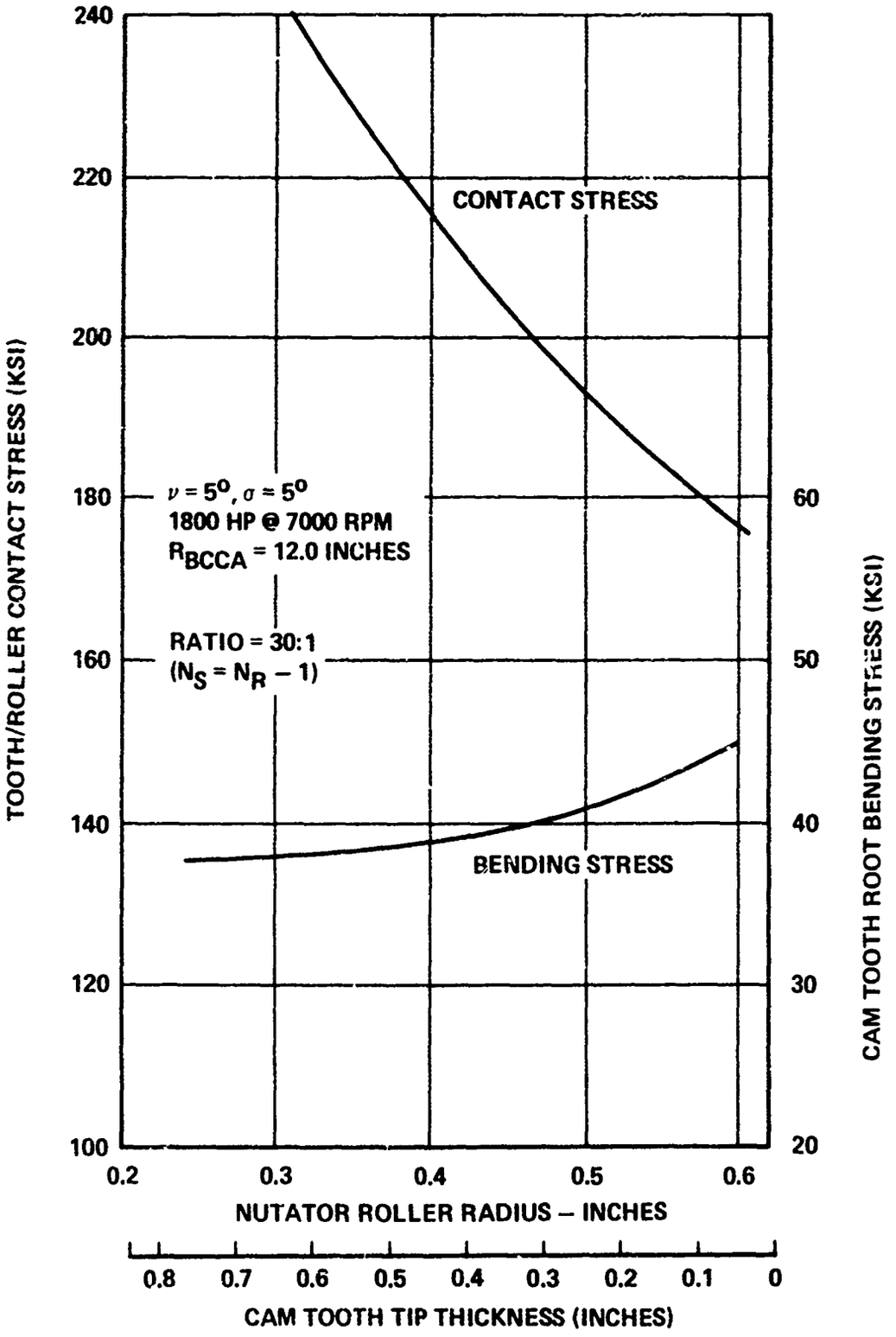

Figure 6-4. Effect of Cam Tooth and Nutator Roller Size on Stress Levels.

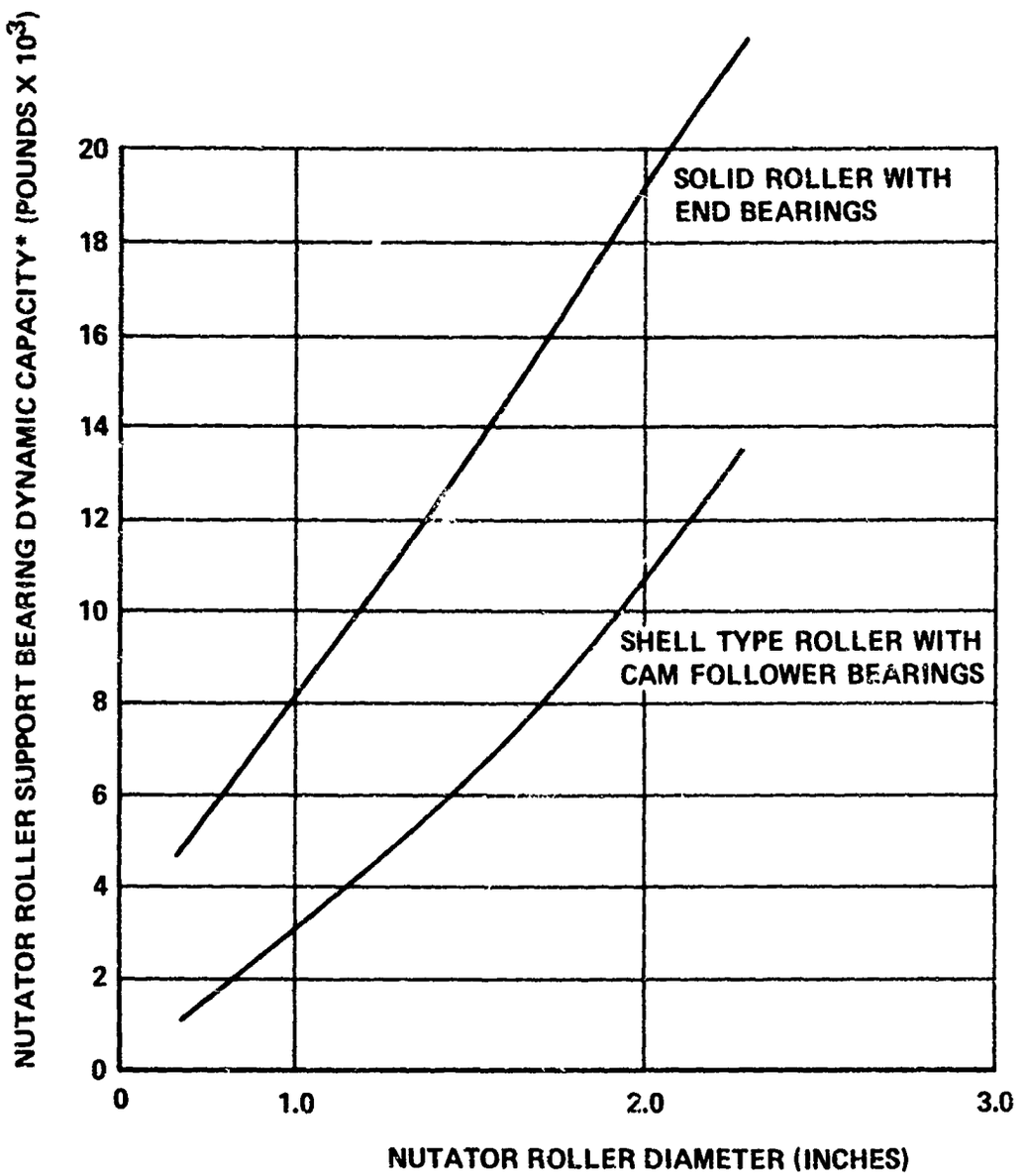

Figure 6-5. Variation of Nutator Roller Support Bearing Capacity with Roller Diameter.

Several general conclusions may be drawn regarding the overall design decisions affecting the nutator rollers and their support bearings. The solid roller configuration provides considerably greater bearing capacity and, therefore, longer life than the cam follower-type mounting. The cam follower type is, however, generally lighter and much shorter in overall length. In either case, increasing the roller diameter provides a sharp increase in bearing dynamic capacity. This increase in diameter must, of course, be coupled with a decrease in cam tooth thickness and the ensuing increase in cam tooth root (bending) tensile stress. Generally, for the configuration shown in the Figure 6-5, about a 0.50- to 0.75-inch increase in diameter is required to obtain the dynamic capacity of a solid roller configuration through the use of a cam follower (shell type) nutator roller.

Another parameter of great interest in the proper design and performance of the nutator rollers is the slope across their support bearings. In some cases this may be so severe a restriction as to be the sole basis for choosing one configuration over another.

For instance, the 30:1 ratio, 12-inch basic spherical radius configuration whose nutator roller slopes are plotted in Figure 6-6 is limited to rollers of less than 1.0 inch in radius. Since, for proper operation, the slope across a roller bearing should be limited to less than 0.0005 in/in, it should be obvious that a hollow cam, follower-type roller may not be used until the roller radius exceeds 0.85 inch, while the solid roller configuration may be used for any roller radius above 0.45 inch. Below 0.45 inch no roller configuration (at the stated length) is suitable for satisfactory operation. For the particular configuration shown on the graph, the maximum roller radius is in the vicinity of 0.60 inch which allows only the use of a solid roller configuration, without regard to life or stress considerations. Another observation may be made from Figure 6-6 that the slope across the shell-type roller is much more severely affected by a change in roller diameter than is the solid configuration. It may generally be concluded that the solid roller with end support bearings is superior in all respects except weight, compactness, and installation flexibility. An additional advantage of the solid roller configuration is that with all other conditions constant, the shaft stresses are lower. In a solid roller with end bearings, the roller itself is the bending nd shear carrying member. Because of the end support condition, the diameter at the critical stress section is the full roller diameter at that section. The hollow, shell-type cam follower configuration, however, utilizes a shaft much smaller then the roller diameter as the bending and shear carrying member. The size of the shaft is dictated by the thickness of the roller shell and the diameter of the rolling

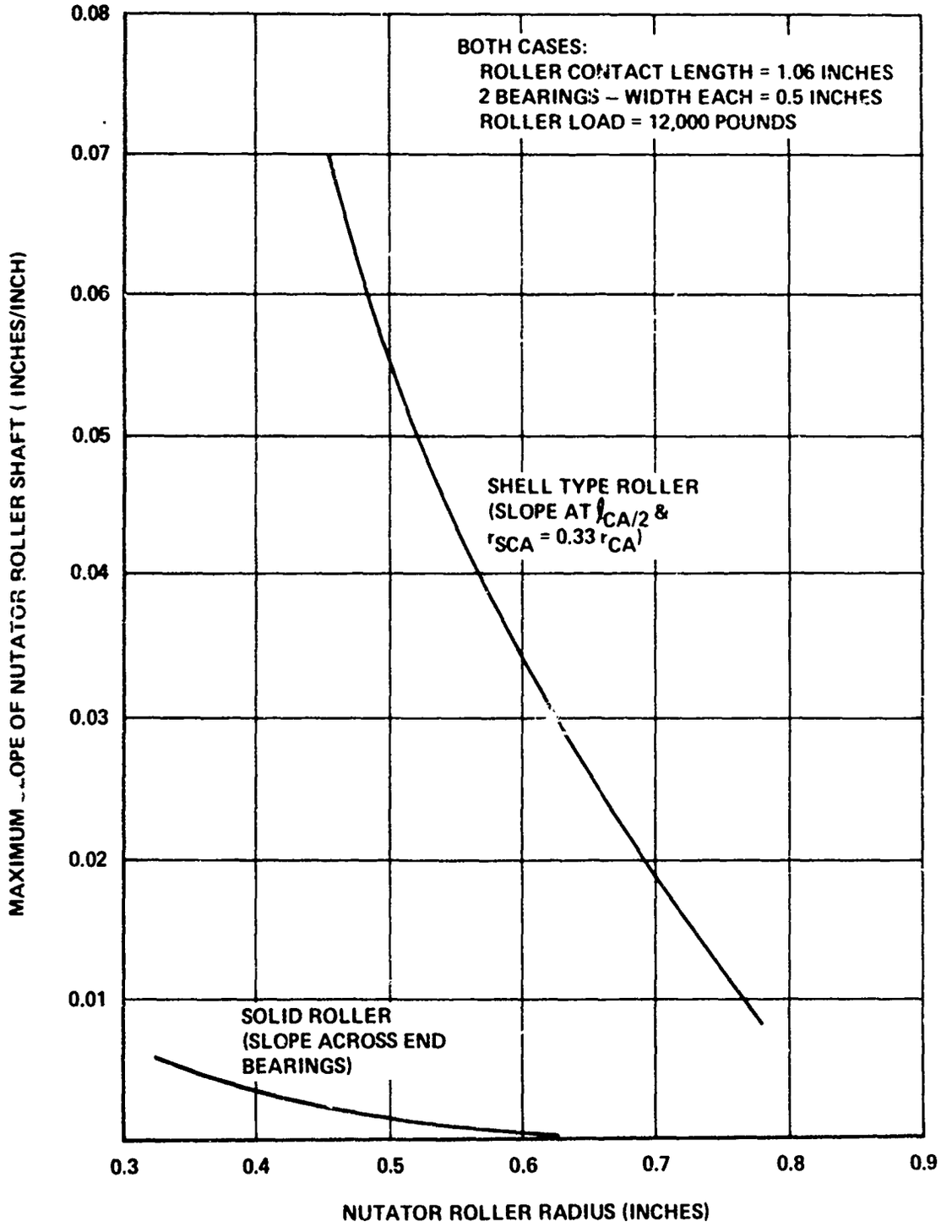

Figure 6-6. Nutator Roller Shaft Slope Variation with Roller Radius.

elements of the bearing which must fit between the shaft and the roller shell (for more information, refer to the MECHANISM GEOMETRY Section). Therefore, the diameter of the main load-carrying member is much smaller for the small configuration. Also, since the bending stress is approximately proportional to the cube of the shaft diameter, the stresses are much higher. This does not preclude any application of the cam follower configuration. In applications in which the cam follower configuration meets the minimum slope, life, and stress requirements, it is, in fact, superior to the solid design (because of lower weight space requirements).

The load and speed spectrum to which the nutator rollers are subjected during each mesh cycle is somewhat unusual and atypical of most conventional rolling element bearing applications. The main speed effects have been documented elsewhere in this report (see MECHANISM KINEMATICS Section) and will not be repeated here. However, during a typical mesh cycle, a nutator roller will be in contact with a cam tooth and under load for a maximum of 50 percent of the cycle. This loaded contact may, in the case of a coned nutator with relieved contact, be as short as 15 to 20 percent of the cycle time. If a single set of nutator rollers is utilized (no roller coning), the rollers will make contact with the rotor cam during 25 percent of the mesh cycle and with the stator cam during an additional 25 percent of the mesh cycle. During the remaining 50 percent of the mesh cycle, the roller will spin free (zero load), as shown in Figure 6-7. If roller coning is present, each roller set will contact only one cam during each cycle; therefore, loaded contact on each roller occurs during a maximum of 25 percent of the mesh cycle, while the rollers spin free and unloaded during the remaining 75 percent of the mesh cycle as shown in Figure 6-7.

The effects of this cyclical loaded and unloaded phases are significant in several areas. Since the roller spins free for a considerable period of time, it is possible that the roller will considerably slow down during this time so that skidding may occur during engagement. However, for a unit with a 6000 rpm input, the maximum time available for slowdown is approximately 8×10^{-3} seconds. For a rolling element bearing operating with good lubrication, only negligable slow down and the consequential skidding should occur during this period. The effective or cubic mean loading upon which the bearing life calculations are based must be carefully evaluated so that a realistic life may be defined. Consideration of these cyclical loading patterns and averaging out the varying speed conditions yields a life far in excess of that predicted by considering the maximum load and speed conditions which actually only occur for a very small fraction of the total time.

In addition to the cyclical loading effect, the amount of

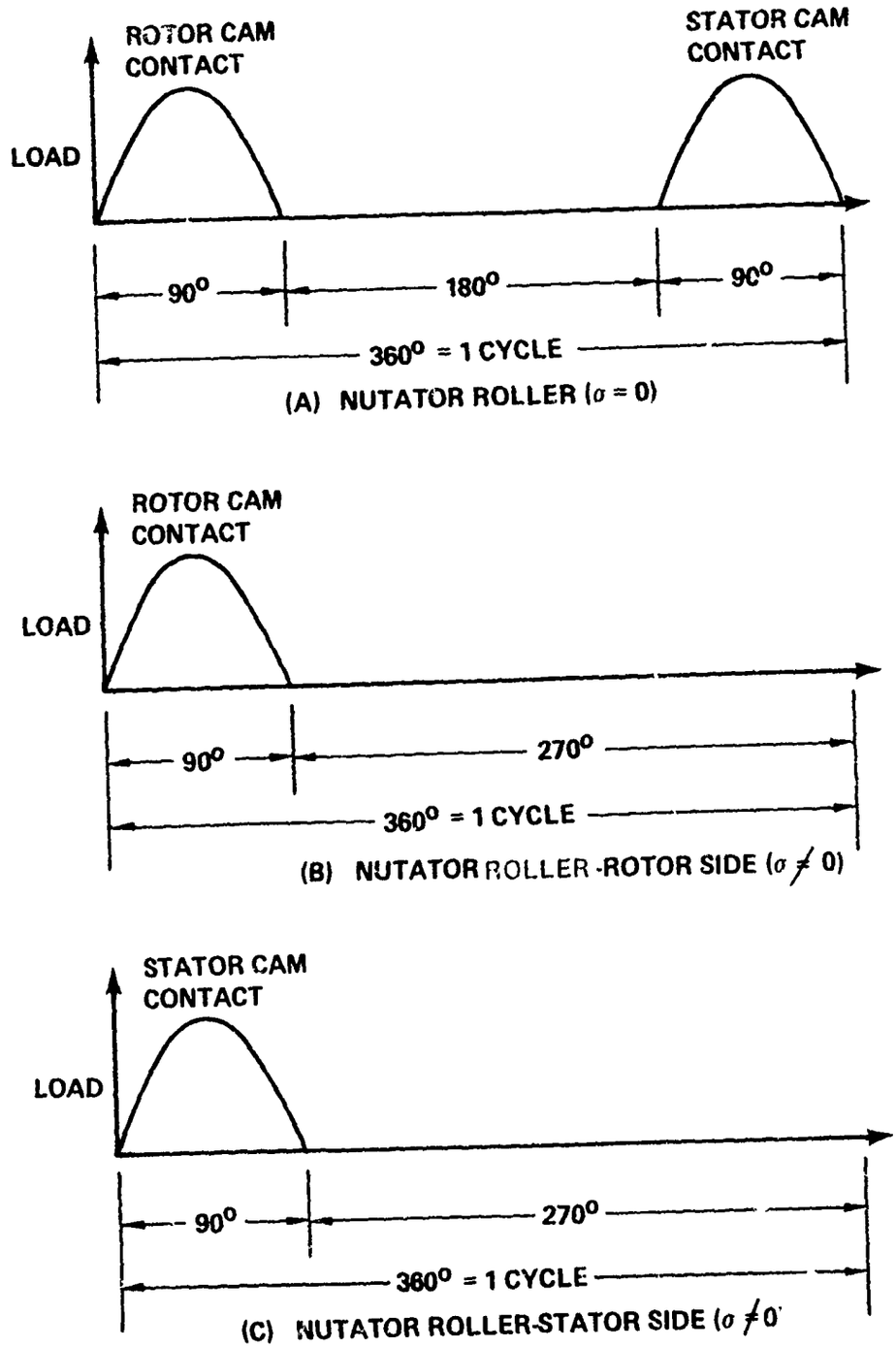

Figur 6-7. Typical Load Spectrums.

profile relief or more correctly, the contact ratio exerts considerable influence on the magnitude of the maximum load upon which the cubic mean load is based. As the contact ratio decreases, the ratio decreases, the loads carried by each cam tooth and roller combination are increased, as shown in Figure 6-8. The effect of reducing contact ratio is more severe at lower absolute values of this parameter than at high values. This may be easily understood if one considers the percentage of the total load carried by one or two tooth/roller combinations when considering large and small total number of contacts; for example, 2 is 50 percent of 4 but only 25 percent of 8.

INPUT SHAFT

The input shaft, because of the special configuration required to mount the nutating ring assembly support bearing, must be given special consideration when evaluating its load capacity. The stress concentration effect of the fillet at the bearing mounting point must be evaluated. The bearing bore and the basic spherical radius must be chosen such that the combined torsional and bending stresses in the shaft are within acceptable levels.

In summary, the primary areas of concern from a load and stress viewpoint in the design of an NMT are the nutator roller and ring support bearing lives, the input shaft, cam tooth and tooth-roller interface stress levels, and the nutator roller shaft stresses and slopes. The Appendix and particularly, the DESIGN CASE STUDIES sections of this report provide further definition and elaboration of the specific items discussed briefly in this section.

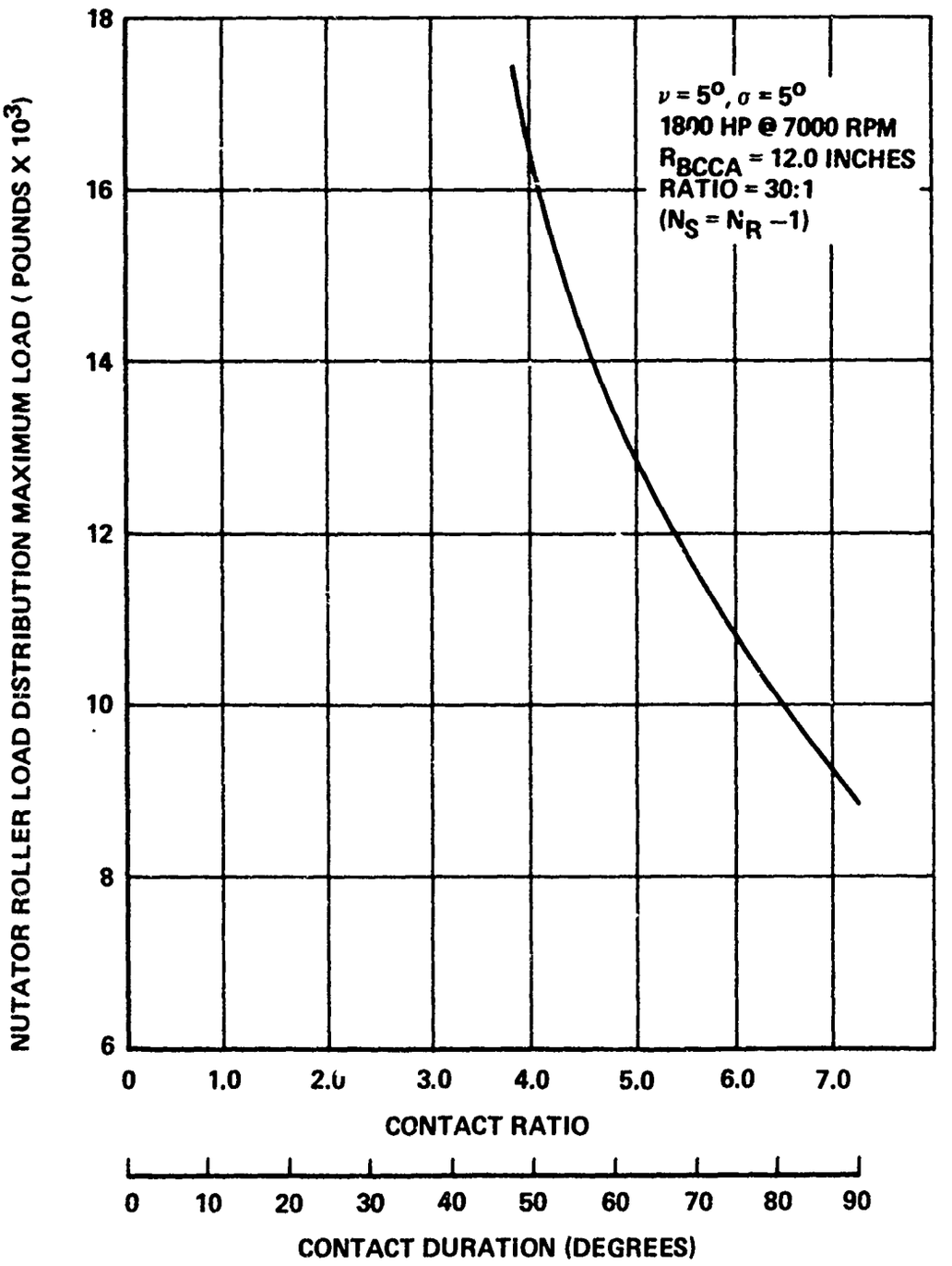

Figure 6-8. Effect of Contact Ratio on Nutator Roller Load.

7. DESIGN TRADEOFF SUMMARY

In the design of any mechanical system, a multitude of tradeoffs must be made to realize an optimum overall system configuration. Prior to accomplishing the required trade study, each basic design parameter must be identified and its relative effect on the system defined as it varies over its normal operational range. Figure 7-1 presents a brief summary of the basic design parameters for the nutating mechanical transmission. Some of these are secondary parameters, such as nutator mounting method or nutator roller support method, which may indeed be limiting factors in an actual design.

NUTATION HALF-ANGLE

The nutation half-angle is perhaps the most important single design parameter. A brief, but by no means all-inclusive, list of typical tradeoff points for nutation angle is shown in Figure 7-2. It appears that a nutation angle as low as possible consistent with the other system restraints provides the most nearly optimum system, especially at higher input speeds. One of the prime considerations is that of roller speed. Since one complete nutation cycle requires the same amount of time, regardless of the nutation angle, it is obvious that in order to traverse the longer path length defined by the larger nutation angle, higher roller speeds and accelerations are required.

At moderate to high input speeds, the nutator roller speeds become quite high, in some cases exceeding the allowable speed limit of their support bearings, thus making the design unfeasible. Since the life of a rolling element bearing is directly proportional to its speed, increasing the nutator roller speed by increasing nutation angle also has a detrimental effect on system life. Conversely, decreasing the nutation angle tends to increase the normal roller load for any given output torque, which of course, also tends to decrease the nutator bearing life.

Obviously, then, a balance must be sought in any given design configuration to obtain an optimum system. It should also be noted that the increased normal load due to a lower nutation angle may be beneficial in certain instances, such as occurs whenever the skidding force factor and the coefficient of friction combine to yield a load required to prevent skidding which is greater than the applied load. In this case, a reduction in nutation angle reduces the skidding force factor

- **BASIC PARAMETERS MUST BE VARIED SINGLY AND IN VARIOUS COMBINATIONS TO ACHIEVE OPTIMUM CONFIGURATION**
  - SINGLE OR DOUBLE NUTATOR
  - NUTATION HALF-ANGLE
  - DURATION OF TOOTH/ROLLER CONTACT
  - BASIC SPHERICAL RADIUS
  - NUTATOR ROLLER MOUNTING METHOD
  - NUTATOR ROLLER RADII/CAM TEETH THICKNESS
  - NUMBER OF ROLLERS ON NUTATOR/TEETH ON CAMS
  - NUTATOR SUPPORT BEARING CONFIGURATION
  - ROLLER CENTERLINE CONING ANGLE
  - ROLLER LENGTH
- **OPERATIONAL CONDITIONS MUST BE EVALUATED TO DETERMINE SUITABILITY OF OPTIMIZED NUTATING MECHANICAL TRANSMISSION CONFIGURATION**

Figure 7-1. Summary of Basic Design Parameters.

HIGHER VALUES	LOWER VALUES
– CAUSE RE-ENTRANT OR UNDER CUT CAM TOOTH FORMS (D)	– SMOOTH CONCAVE CAM TOOTH FORMS (A)
– INCREASED VARIATION IN ROLLER SPEED OVER TOOTH PROFILE (D)	– REDUCED VARIATION IN ROLLER SPEED OVER TOOTH (A)
– REDUCED THRUST LOADING ON CAM (A)	– INCREASED THRUST LOADING ON CAM (D)
– HIGHER UNBALANCE LOADS (D)	– LOWER UNBALANCE LOADS (A)
– HIGHER NORMAL TOOTH LOAD REQUIRED TO PREVENT SKIDDING (D)	– LOWER NORMAL TOOTH LOAD REQUIRED TO PREVENT SKIDDING (A)
– LOWER NORMAL LOAD FOR GIVEN TRANSMITTED TORQUE (A)	– HIGHER NORMAL LOAD FOR GIVEN TRANSMITTED TORQUE (D)
– INCREASED AXIAL LENGTH OF UNIT (D)	– DECREASED AXIAL LENGTH OF UNIT (A)
– LOWER NUTATOR ROLLER SUPPORT BEARING LIFE (D)	– INCREASED NUTATOR ROLLER SUPPORT BEARING LIFE (A)

(A)= ADVANTAGE
(D)= DISADVANTAGE

Figure 7-2. Geometry Tradeoff Factors - Nutation Half Angle.

and increases the normal load, both of which tend to decrease the probability that the roller will skid.

BASIC SPHERICAL RADIUS

A change in load intensity is the most direct effect of a change in basic spherical radius, however, this effect is compounded by the fact that a larger basic spherical radius also permits the use of larger rollers. This decreased loading applies only to the nutator rollers, since for a given spread between the nutator support bearings, the loading which they must react remains relatively constant. This is true because the loading is primarily moment, therefore, although the load decreases with increasing basic spherical radius, the moment arm also increases, yielding a relatively constant moment.

Consequently, the basic spherical radius mainly affects only the load and geometry conditions at the nutator rollers. However, the use of a larger basic spherical radius allows a larger diameter nutator support bearing to be used, thus indirectly improving the life and/or load capacity of this bearing. In fact, the only two options available for varying the capacity of the nutator support bearings are the use of larger bearings or an increase in the spread between the bearings.

In general, increasing the basic spherical radius also increases the nutator moment of inertia and thus the dynamic unbalance loading. This factor may be of only secondary importance in a double nutator, split power configuration, because of its inherent self-balancing characteristics. Increasing the spherical radius also improves the conformity of the contact between the rollers and the cam teeth. A brief tradeoff summary for this parameter is shown in Figure 7-3.

NUMBER OF CAM TEETH/NUTATOR ROLLERS

In general, the largest nutator roller size possible should be used to provide for minimum contact stress; the tradeoff occurs, of course, when roller skidding becomes a problem. The maximum and minimum roller sizes are both fixed by system constraints, and it is possible that the two may be incompatible for a given system. The size of the rollers is intimately related to both the number of cam teeth and the basic spherical radius. As defined in Figure 7-4 several specific tradeoff points may be established.

Although increased cam tooth thickness is desirable from a bending stress standpoint, the nutator roller support bearing life is generally a more critical factor than the cam tooth bending stress.

LARGER VALUES	SMALLER VALUES
– REDUCE UNIT TOOTH LOADING FOR GIVEN TORQUE (A)	– INCREASE UNIT TOOTH LOADING FOR GIVEN TORQUE (D)
– INCREASED VARIATION OF ROLLER SPEED OVER PROFILE (D)	– DECREASED VARIATION OF ROLLER SPEED OVER PROFILE (A)
– ALLOWS USE OF LARGER NUTATOR ROLLERS (A)	– SMALLER NUTATOR ROLLERS MUST BE USED (D)
– INCREASED NUTATOR ROLLER SPEED (D)	– DECREASED NUTATOR ROLLER SPEED (A)
– ALLOWS USE OF THICKER CAM TEETH (A)	– THINNER CAM TEETH MUST BE USED (D)
– CAM TOOTH PROFILES MORE CONFORMAL (A)	– CAM TOOTH PROFILES LESS CONFORMAL (D)
– INCREASED UNIT ENVELOPE (D)	– DECREASED UNIT ENVELOPE (A)
– RELATIVELY GREATER TENDENCY TO ROLLER SKIDDING (DUE TO REDUCED TOOTH LOADING) (D)	– RELATIVELY LOWER TENDENCY TO ROLLER SKIDDING (DUE TO INCREASED TOOTH LOADING) (A)
– GENERALLY HIGHER UNBALANCE MOMENTS (D)	– GENERALLY LOWER UNBALANCE MOMENTS (A)

(A)= ADVANTAGE (D)= DISADVANTAGE

Figure 7-3. Geometry Tradeoff Factors - Basic Spherical Radius.

LARGER VALUES	SMALLER VALUES
– REDUCED MAXIMUM ROLLER SPEED (A)	– INCREASED MAXIMUM ROLLER SPEED (D)
– REDUCED VARIATION OF ROLLER SPEED ALONG PROFILE (A)	– INCREASED VARIATION OF ROLLER SPEED ALONG PROFILE (D)
– REDUCED HERTZ CONTACT STRESS (A)	– INCREASED HERTZ CONTACT STRESS (D)
– ALLOWS LARGER SUPPORT BEARING SIZE (A)	– REQUIRES SMALLER SUPPORT BEARING SIZE (D)
– INCREASED POLAR MOMENT OF INERTIA (D)	– DECREASED POLAR MOMENT OF INERTIA (A)
– INCREASED THRUST LOAD ON ROLLER (D)	– DECREASED THRUST LOAD ON ROLLER (A)
– INCREASED NUTATOR UNBALANCE MASS (D)	– DECREASED NUTATOR UNBALANCE MASS (A)
– REDUCED CAM TOOTH THICKNESS (D)	– INCREASED CAM TOOTH THICKNESS (A)

- MAXIMUM ROLLER SIZE LIMITED BY SPECIFIC SYSTEM RESTRAINTS
  - PITCH OF CAM TEETH
  - RELATIVE TOOTH/ROLLER NUMBER

(A) = ADVANTAGE (D) = DISADVANTAGE

Figure 7-4. Geometry Tradeoff Factors - Nutator Roller Radii.

In choosing tooth/roller numbers for the components, the primary tradeoff is between ratio and diameter; i.e., the numbers of teeth/rollers chosen must yield the desired ratio, while the diameter chosen must provide the optimum combination of tooth load and pitch. Careful selection of tooth/roller numbers may also cause the nutator to precess in the same direction as the input shaft rotation, thus reducing the relative rotational speed experienced by the nutator support bearing and increasing the bearing life.

In order to obtain non-integer ratios, relative numbers of teeth must be carefully chosen and, in general, roller coning must be utilized. In addition, it may be necessary, or even desirable to use different basic spherical radii for both rotor and stator sides, depending on the relative tooth numbers. This procedure may result in a more nearly optimum, lighter system. A brief summary of some of the design tradeoff considerations involving the numbers of cam teeth and/or nutator rollers is shown in Figure 7-5.

CONING ANGLE

As noted earlier, roller centerline coning is not a basic design parameter but is rather a "means to an end." Roller coning is used to obtain some basic condition such as a variation in the number of teeth in contact with the rotor independently of those in contact with the stator. In some instances, it may be used simply to avoid roller reversal by providing a separate set of rollers to contact the rotor and stator. Some comments concerning the use of roller centerline coning are presented in Figure 7-6.

In general, the introduction of coning, all other conditions being equal, leads to some increase in system weight and inertia. It seems likely, however, that many high capacity designs will employ some coning so that the proper ratio-diameter-length combination may be obtained. Coning also allows both ends of the nutator rollers to be supported in structure rather than by the "spoke-and-wheel" method required in the absence of coning. Coning also causes an increase in axial unit length; however, this may also be advantageous if the nutator support bearing life may thereby be improved by the increase provided in bearing spread.

ROLLER LENGTH

The length of the rollers must be carefully chosen, as shown in Figure 7-7, so they are long enough to provide a reasonable unit loading and short enough to prevent serious misalignment and deflection problems. Consideration must also be given to

- **NUMBER OF TEETH ON CAMS**
- **NUMBER OF ROLLERS ON NUTATOR**
  - IF NUMBER OF ELEMENTS ON NUTATOR AND STATOR ARE IDENTICAL, ROLLERS MUST REVERSE DIRECTION BETWEEN ROTOR AND STATOR CAMS (NUTATOR DOES NOT ROTATE WITH RESPECT TO STATOR)
  - TO PREVENT ROLLER REVERSAL, NUTATOR AND STATOR MUST HAVE UNEQUAL ELEMENT NUMBERS (CAUSING RELATIVE ROTATION BETWEEN STATOR AND NUTATOR) OR NUTATOR MUST HAVE DUAL SET OF CONED ROLLERS, OR DUALIZED SYSTEM MUST BE USED
  - RELATIVE NUMBERS OF TEETH CHOSEN BASED ON RATIO AND SIZE REQUIREMENTS
  - THE DIFFERENCE BETWEEN THE NUMBER OF ELEMENTS ON THE NUTATOR AND EACH CAM ARE LIMITED TO ABOUT 1 OR 2 SO THAT SUFFICIENT TOOTH THICKNESS MAY BE OBTAINED TO TRANSMIT LOADS
  - SUBJECT ONLY TO THE RESTRAINTS IMPOSED BY PITCH, THE NUMBERS OF ELEMENTS ON THE ROTOR SIDE OF THE SYSTEM MAY BE CHOSEN INDEPENDENTLY OF THOSE ON THE STATOR SIDE IN ORDER TO OBTAIN THE DESIRED RATIO
  - NUTATOR MAY BE CAUSED TO PRECESS IN SAME DIRECTION AS INPUT SHAFT ROTATION LEADING TO BETTER NUTATOR SUPPORT BEARING LIFE

Figure 7-5. Geometry Tradeoff Factors - Element Numbers.

• ROLLER CENTERLINE CONING ANGLE

- CONING MUST BE UTILIZED WHEN THE RATIO REQUIREMENTS ARE SUCH THAT THE ROTOR AND STATOR CAMS MUST EACH MESH WITH A DIFFERENT NUMBER OF NUTATOR ROLLERS
- CONING IS ONE SOLUTION TO THE ROLLER REVERSAL PHENOMENA WHICH OCCURS IF $N_{NS} = N_S$
- IN GENERAL, CONING IS NOT A DESIGN PARAMETER OF ITSELF, BUT RATHER A MEANS BY WHICH OTHER PARAMETERS MAY BE UTILIZED

HIGHER VALUES	LOWER VALUES
– SLIGHT REDUCTION IN ROLLER SPEED VARIATION ALONG PROFILE (A)	– SLIGHT INCREASE IN ROLLER SPEED VARIATION ALONG PROFILE (D)
– INCREASED AXIAL LENGTH OF UNIT (D)	– DECREASED AXIAL LENGTH OF UNIT (A)
– INCREASED NUTATOR MOMENT OF INERTIA (D)	– DECREASED NUTATOR MOMENT OF INERTIA (A)
– ALLOWS USE OF LARGER ROLLERS (A)	– SMALLER ROLLERS MUST BE USED (D)

(A) = ADVANTAGE

(D) = DISADVANTAGE

Figure 7-6. Geometry Tradeoff Factors - Roller Centerline Coning Angle.

- ROLLER LENGTH

LONGER	SHORTER
– GREATER CHANCE OF MISALIGNMENT (D)	– LESSER CHANCE OF MISALIGNMENT (A)
– DECREASED SURFACE LOADING (A)	– INCREASED SURFACE LOADING (D)
– ALLOWS USE OF LONGER SUPPORT BEARING (A)	– REQUIRES USE OF SHORTER SUPPORT BEARING (D)
– INCREASES ROLLER SUPPORT BENDING MOMENT (D)	– REDUCES ROLLER SUPPORT BENDING MOMENT (A)
– INCREASES NUTATOR MOMENT OF INERTIA (D)	– REDUCES NUTATOR MOMENT OF INERTIA (A)
– INCREASED UNIT DIAMETER (D)	– REDUCED UNIT DIAMETER (A)

- IN GENERAL, FOR ANY SYSTEM, AN OPTIMUM COMBINATION OF ROLLER LENGTH AND BASIC SPHERICAL RADIUS EXISTS

(A) = ADVANTAGE

(D) = DISADVANTAGE

Figure 7-7. Geometry Tradeoff Factors - Roller Length.

the effect of length on roller skidding tendencies and the mounting method within the nutating ring assembly. For an NMT using the cam follower type of nutator roller support, the roller must be sufficiently long that a bearing(s) of adequate capacity may be installed under it.

Greater latitude in the choice of roller length is provided if roller coning is utilized, since, as noted earlier, the spoke and wheel effect is eliminated. The roller length must also be balanced against both basic spherical radius and roller diameter to yield an optimum system.

SELECTION OF BEARINGS

Since the NMT uses many bearings which generally operate at high speeds and loads, special consideration must be given to designing for bearings with maximum size (load capacity) in order to obtain satisfactory operating life. After establishing the minimum tooth/roller sizes based on the maximum allowable stress levels, the design must be adapted to nutator roller and center support bearings of adequate capacity. The relationship must be optimized between the bearing capacity, maximum and minimum allowable shaft diameter that the bearing will accept, and the maximum bearing OD, which is fixed by the basic spherical radius and reduction ratio constraints.

NUTATOR ROLLER SUPPORT BEARINGS

Nutator roller support bearings with large capacity tend to have large diameter rolling elements, and, therefore, for a given allowable OD, the maximum permissible support shaft diameter must be smaller. The smaller shaft diameter allows greater shaft deflection and also greater slopes. To reduce the deflection, either the roller length must be reduced, which is unacceptable due to stresses, or the shaft diameter must be increased. Increased shaft diameter requires smaller rolling elements and lower capacity. Thus, for a given load a tradeoff must be made between the life (capacity) of the available bearings and the corresponding shaft slopes.

If all the design criteria cannot be met, one solution is to increase the basic radius, thereby allowing the use of larger bearings and a larger shaft, while simultaneously lowering the loads. In addition to making the transmission larger and heavier, this technique may lead to loads which, although consistent with good bearing life, are so low that other problems are created. The contact forces may be insufficient to prevent roller skidding, or the stresses may be so low that the cam/nutator structural material is not efficiently utilized.

Alternatively, solid nutator rollers may be used and mounted with end bearings, if the added complexity is justified by smaller size. This configuration reduces the deflection and allows the use of larger roller support bearings. For very small nutator rollers this may be the only available means of support. For either type mounting, the load on the nutator roller is predominantly radial, with only small thrust loads due to the small roller taper; consequently, roller bearings are suitable for supporting the nutator rollers. Tapered roller bearings may be used, but cylindrical roller bearings and a thrust washer are probably adequate for most applications.

Another important factor is the DN of the nutator roller support bearings. The rotational speed of these bearings may become high, resulting in critical values of DN. This factor may not be significant for evaluating the relative merit of the two mounting methods, since the larger diameter of the solid roller support bearings may be offset by their slower speed.

Roller skidding may also be an important design limitation. The solid rollers and their accompanying larger bearings possess greater inertia resistance to rotation. Hence, the accelerations and normal loads on the nutator rollers may be such that the solid roller mounting is more susceptible to skidding.

Even though the solid roller configuration allows a smaller basic radius, the solid nutator rollers and larger bearings add weight. Although weight alone may be significant, a more significant possible effect is the greater unbalance moments generated and the resulting growth of the radial loads on the center support bearing. This may dictate the use of a larger center bearing and even greater weight. After complete evaluation, therefore, the solid roller mounting may not be as advantageous as it may have seemed initially.

NUTATOR SUPPORT BEARING

The nutator may be supported by either a center support bearing located on a central input shaft or by an outer support ring bearing located between the nutator OD and an input drum.

The load on the nutator center support bearing is due to the loads applied to the nutator rollers and the overturning moments created by the action of these loads. At speeds in excess of a few hundred rpm, single bearings (i.e., ball bearings) are not available to carry a large moment load. Hence, in order to react these overturning moments, it is necessary that the nutator center support bearing actually be

composed of two roller bearings positioned on either side of the nutator centerline of a spread distance w, where w is measured from the nutator centerline to the midpoint of the bearing width. See Figure 7-8. Thrust loads may be reacted by using tapered roller bearings; however, since the thrust is relatively small and maximum radial capacity is necessary, it is usually better to use two cylindrical roller bearings carrying only radial load, and an additional ball bearing located on the nutator centerline to carry the thrust load and to position the nutator axially.

The radial load on the center support bearings depends upon the moment applied from the forces on the nutator rollers and upon the spread distance between the two center roller bearings. The moment is practically independent of the basic transmission radius, because of the canceling effect of, for example, decreasing load magnitude with increasing moment arm. Therefore, the only significant means of controlling the center bearing life is by varying the bearing size and the bearing spread distance. Since the maximum center bearing diameter is limited by the unit's basic radius, the bearing life may be improved by increasing overall unit diameter. This technique is useful only to the point where the increase in bearing diameter causes the allowable DN to be exceeded.

The axial distance needed for the center bearing is determined by the spread distance w and the bearing width W. The axial distance available within the NMT is determined by the space swept by the nutator and by the space available in the center region of the cams. Mounting the cam support structure at approximatley 60 degrees to the mechanism centerline is required to provide added stiffness and better thrust load reaction. A cam structure mounted perpendicular to the axis (i.e., one resembling a flat circular plate) would have considerably less bending resistance.

A further limitation on the axial distance available is imposed by the diameter of the input shaft on which the bearings are mounted. Mounting as shown in Figure 7-8(a) is preferred since the basic diameter of the single piece shaft is not notched, and the bearing mounting pads can be made with large, smooth fillets. If shaft and bearing size constraints require a mounting such as Figure 7-8(b), the shaft must be split; and the configuration shown in Figure 7-8(c) may introduce stress concentration problems. In any case, the maximum possible shaft diameter must be adequate to carry the stress loads created at the rated NMT power.

If adequate space is not available within the NMT, the overall outside diameter and axial length may be stretched to provide the necessary additional space. This cannot be done, of course, where maximum external envelope limitations are

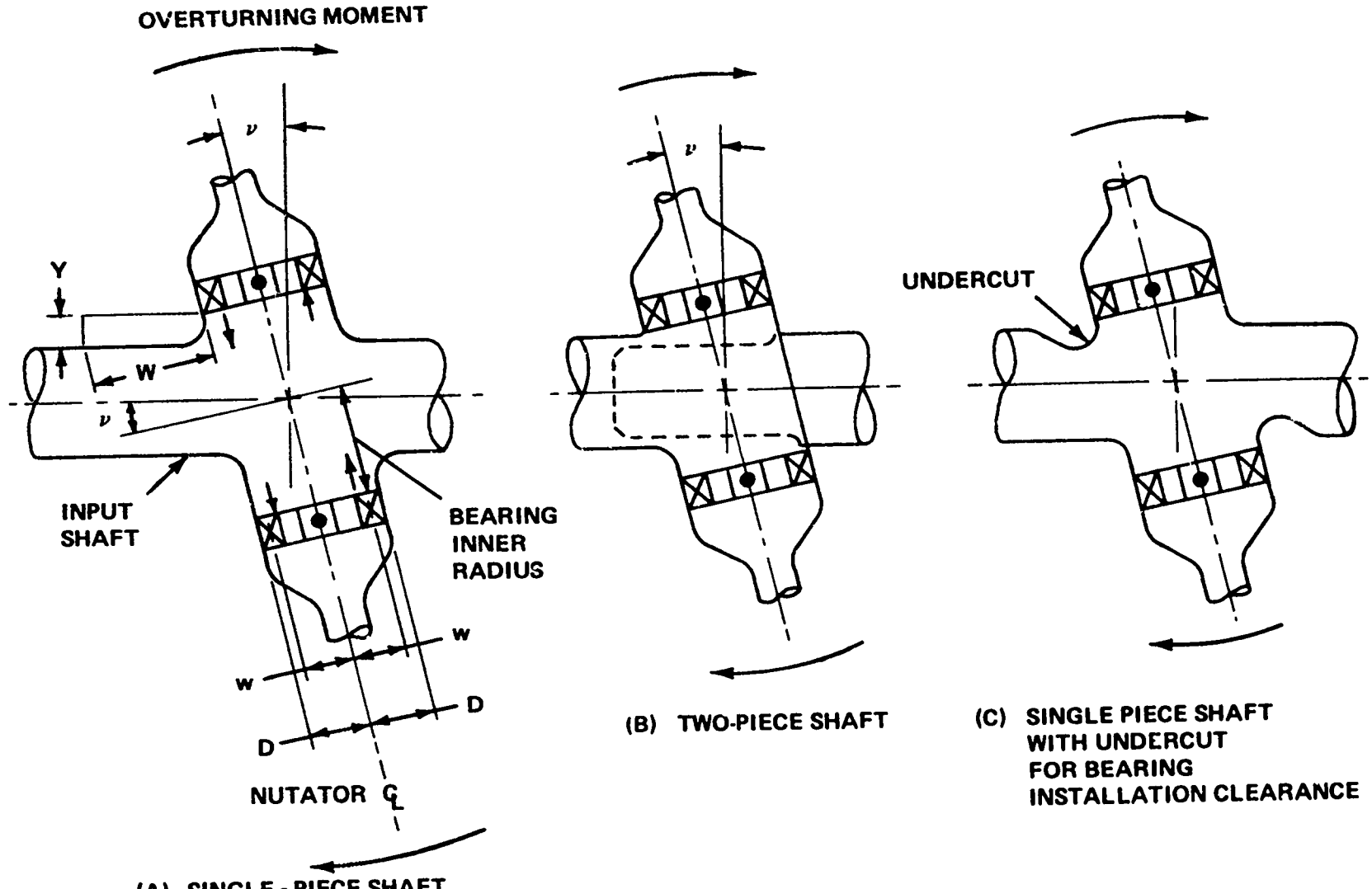

Figure 7-8. Nutator Center Support Bearing

specified by the design requirements. Obviously, a better, more efficient design will use only the axial space inherently available.

Summarizing, the center support bearing is sized by several factors interacting in a rather complex manner. The basic radius and/or DN establishes the maximum diametral bearing size. The applied loads and required bearing life, then, dictate the spread distance required and the bearing width, which, when combined with the nutation angle, specify the maximum size of the shaft diameter.

The outer ring support bearing configuration is generally larger in diameter. Nevertheless, this may be an acceptable tradeoff to gain such advantages as a relatively clear, open center region through which controls, instrumentation, etc. may be passed.

If the nutator is supported by an outer ring bearing, the overturning moments may be much more easily reacted. The reaction moment arm is greater than the applied force moment arm (Figure 7-9). Also, larger bearings may be used and the life improved. However, the DN for this bearing configuration is so large for all but the smaller size, and/or relatively low speed applications, that satisfactory bearings probably are not available for most cases.

The duration of tooth contact may be determined by examining the initial and final points of contact of a nutator roller as it travels along a cam tooth profile. If the contact points are specified in degrees of input rotation (ω_O), where $\omega_{NCA} = 0$ degrees is the start of contact and $\omega_{XCA} = 90$ degrees is the end of contact between a nutator roller and a theoretical cam tooth profile, then, ideally, the duration of contact would be throughout this 90-degree range. Long contact duration for each individual tooth results in a high overall mechanism contact ratio and better load distribution. However, practical design considerations reduce the duration below its maximum possible value of 90 degrees. For example, the cam tooth may be impractically thin at the theoretical tip point of 0 degrees. By cutting off the theoretical tip, the actual tooth tip thickness for manufacturing is increased, but the start of contact is correspondingly shifted to some point greater than 0 degrees.

At the other extreme of the range of contact, the tooth root is typically undercut with a fillet radius to insure positive clearance in this region. This also has the effect of terminating the roller/tooth contact prior to the theoretical maximum point of 90 degrees. Hence, a realistic contact duration is on the order of 70 degrees or from 10 to 80 degrees.

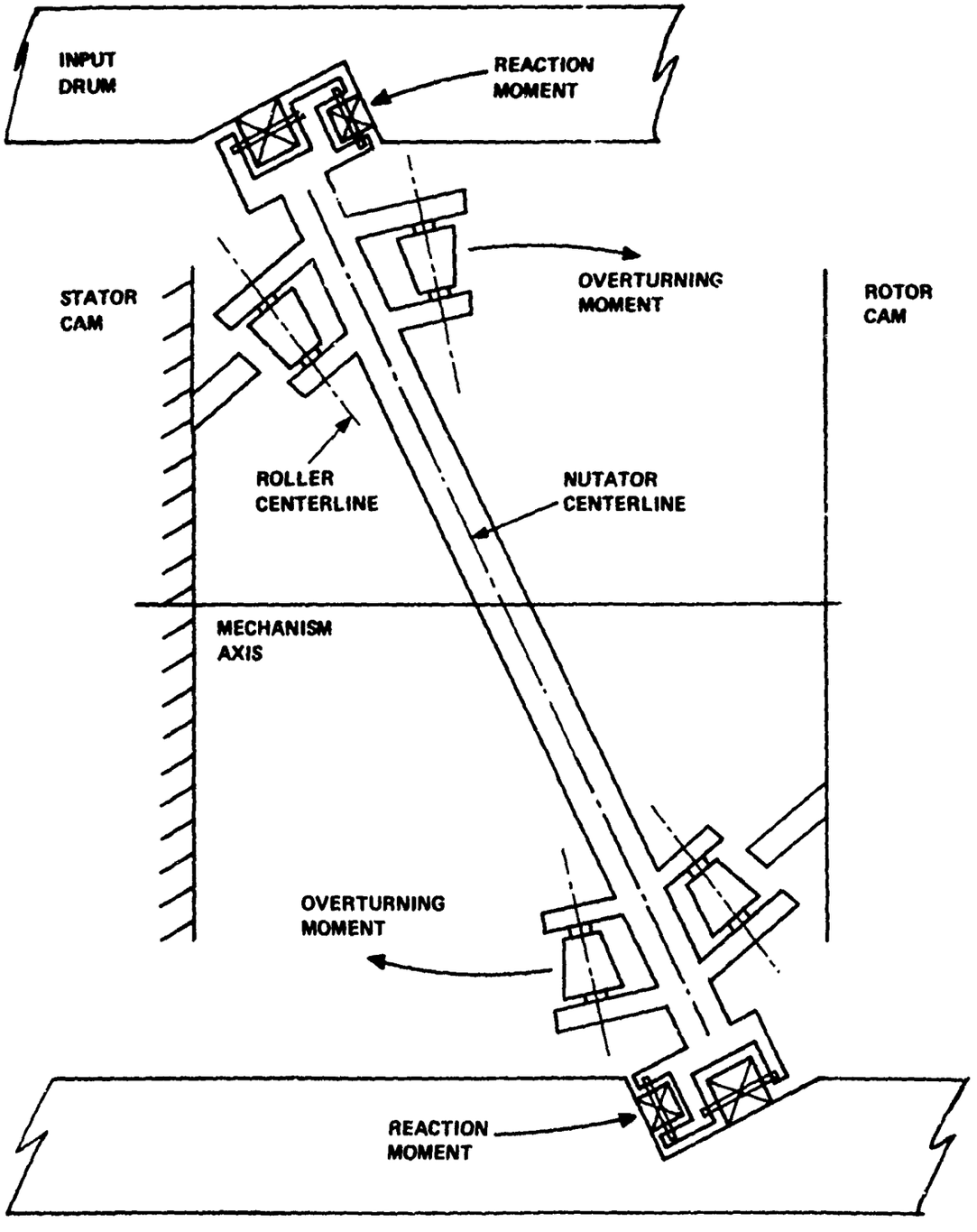

Figure 7-9. Nutator Outer Support Ring Bearing

Other reasons for varying the initial and/or final contact points may be to control nutator roller speed or to provide smoother meshing. Such factors must be weighed against the detrimental effect on contact ratio.

8. DESIGN CASE STUDIES

SPECIFICATION OF DESIGN CRITERIA

To evaluate the practical applicability of the nutating mechanical transmission, the designs of two sample configurations were studied in detail: Configuration A is a high power, long life machine typical of a marine power transmission unit; Configuration B represents an aircraft (helicopter) application, specifically patterned as a substitute unit for the forward rotor transmission of the CH-47 helicopter. Hence, these two examples represent NMT designs with widely varying design constraints and performance requirements. The specifications for each configuration are shown in Table 8-1.

TABLE 8-1. DESIGN SPECIFICATIONS

Parameter	Design Example	
	A	B
Rated Power (hp)	25,000	3600
Input Speed (rpm)	6,000	7000
Reduction Ratio	20:1	30:1
Minimum Bearing Life (B-10 hours)	12,000	2000

In addition to these specifications, which must be defined for any particular application, current engineering state-of-the-art dictates that the following general criteria be applied to any application (Table 8-2).

TABLE 8-2. GENERAL DESIGN CRITERIA

Maximum bending stress in cam teeth	45,000 psi
Maximum contact (Hertz) stress between nutator rollers and cam teeth	180,000 psi
Maximum slope across nutator roller support bearings	0.0005 in./in.
Maximum total roller length/mean diameter ratio (L_{CA}/d_{CA})	4.5
Maximum DN for cylindrical roller bearings	1.25×10^6 (desirable) 2.00×10^6 (current production max)

The bending and contact stress limitations are imposed because of the strength of available materials. Excessive values of bending stress will lead to fracture of the cam teeth near the root due to tensile fatigue. The surface fatigue caused by high contact stresses results in deterioration and pitting of the tooth/roller surface, which will ultimately lead to cracking and fracture of the element.

The slope of the nutator roller support shaft effects the life and speed limitations of the roller support bearings. Excessive shaft slope across the bearings causes misalignment of the inner and outer races and a consequent uneven load distribution along the bearing rollers.

The roller length/diameter ratio limitation is applied in order to minimize deflection, chatter, skidding, and misalignment due to skewing of the bearing rollers which may occur, particularly at high speeds, when the bearings become too long. Furthermore, longer rollers incur proportionately greater deflection causing the load to be concentrated near their ends. Current bearing technology imposes a maximum length/diameter ratio of 1.5 on the rolling elements of a cylindrical roller bearing,

$$\frac{\ell}{d} \leq 1.5 \tag{8.1}$$

where ℓ = length of rolling element
d = diameter of rolling element

It is useful for the design application to relate this ratio to the maximum allowable length of the nutator roller. If the nutator roller is supported by a double row of cylindrical rolling elements, the load is shared approximately equally between the rows. However, for a stack-up of three or more rows, the variations due to manufacturing tolerance are sufficient to cause unequal load sharing. This effect is documented by bearing manufacturers, and it is found that the capacity increases only as the 7/9 power for such a stack-up. For example, a three bearing stack provides only 2.35 times the load of a single bearing.

$$(3)^{7/9}\, C = 2.35C \tag{8.2}$$

Therefore, a maximum of two rows of rolling elements was assumed for support of the nutator rollers. Allowing an additional distance for cages, the total overall nutator roller length is approximately,

$$\ell_{CA} \leq 3(1.5d_{CA}) = 4.5d_{CA} \tag{8.3}$$

After determining the nutator roller support bearing OD and the necessary capacity, the rolling element diameter d_{CA} is available from bearing specifications. The nutator roller length may then be determined.

The DN factor is a measure of the bearing operating speed, and is defined as the product of the bearing mean diameter in millimeters and the relative bearing rotational speed in rpm. Bearings operating at a high DN are more sensitive to skidding and misalignment, and require special consideration to insure adequate lubrication. Ball bearings can generally be operated at a higher DN than cylindrical roller bearings, hence the latter imposes the critical design limitation.

The stresses and roller support shaft slope are calculated based on the maximum rated power which the unit may be required to transmit. The bearing life is calculated based on a cubic mean loading (whose derivation is discussed below), using the following relation which is based on the widely accepted AFBMA rating practice,

$$L = \left(\frac{C}{P_m}\right)^{10/3} \left(\frac{16667}{RPM_{Rel}}\right) \times MF \qquad (8.4)$$

where L = bearing life in hours (B-10)

C = bearing rated dynamic capacity (pounds)

P_m = cubic mean radial bearing load (pounds)

RPM_{Rel} = rotational speed of bearing outer race relative to inner race (rpm)

MF = material factor

This equation was empirically derived based on extensive testing accomplished many years ago. Materials used in current high-capacity bearings provide a linear increase in bearing life of approximately a factor of 5. This is accounted for by the material factor.

GENERAL DESIGN APPROACH AND TECHNIQUES

The double nutator split-power path concept was used for the high-speed/high-power applications considered here. Although this configuration is more complex, it provides many advantages. Since each nutator transmits only half the load, a large reduction in stress level and better bearing life are possible. Furthermore, the overall diameter is reduced.

Balancing and vibration, particularly critical at high speeds, are much less severe problems due to the inherent self-balancing characteristic of the double nutator. The balance weights necessary for a single nutator would be a nonfunctional addition to the overall transmission weight.

The specifications in Table 8-1 considerably limit the range within which parameters may be manipulated and design tradeoffs made. The required reduction ratio limits the number of practical tooth/roller combinations to a few specific values. Tooth width and roller diameter are determined by considering the number of teeth and rollers together with the overall unit diameter requirements. The roller length must be within the length-to-diameter ratio specified; the unit diameter also fixes the magnitude of the transmitted loads for a given power. Tooth and roller sizes, in conjunction with the loads, fix the tooth bending stress, tooth/roller contact stress, and roller loads.

In general, it is desirable to use a tooth/roller combination that allows a single set of nutator rollers to contact both the rotor and stator cams without experiencing reversal of the direction of roller rotation. This may be achieved by using a stator cam with two less teeth than the rotor cam ($N_S = N_R - 2$). However, high stress levels may require a larger tooth/roller size. The same reduction ratio may be maintained by using a stator cam with only one less tooth than the rotor cam ($N_S = N_R - 1$), but this combination requires two sets of nutator rollers, one set contacting the rotor cam and the other set contacting the stator cam to avoid roller reversal. Use of two sets of nutator rollers is achieved with a roller coning angle, and their use is necessary to prevent severe roller skidding induced by roller reversal. In addition to being more complex, heavier, and not as compact, the ($N_S = N_R - 1$) combination also has a reduced contact ratio; therefore, use of a single set of rollers is more desirable when feasible. If stress levels are unacceptable, several other techniques are available.

Although roller coning and nutation angle have some effect on load, the most dramatic effect is due to unit diameter. Increasing the basic spherical radius (R_{BCCA}) allows the use of larger rollers and thicker cam teeth, which, in turn, improves the stress levels and bearing life. Also, the larger radius results in lower transmitted loads for the same power, which further improves the stress and life. The roller size is particularly significant for the cam follower type mounting where the roller bearing must fit inside the roller and also provide sufficient space for a support shaft. A significant improvement in nutator roller bearing life may be obtained, if this is a limiting factor, by using a solid roller with a support bearing at each end. This permits the use of larger

bearings which have a ID approximately equal to the roller OD. Although the cam follower type roller is simpler, and its use is preferable where possible, the capacity is severely limited by the fact that the bearing OD must be smaller than the roller OD.

The bearing dimensions and rated capacities have been selected from catalogues of standardized bearings. Slight improvements in the design examples discussed below are probably possible if specialized bearings are designed. Consider, for example, the case where the capacity of a particular bearing is slightly too low. The capacity of the next larger standard size available may be much too large, and, in addition, the diameter may require an increase of several inches in the basic radius. Hence, the designer is forced to accept an NMT which is larger than is actually necessary to meet the design specifications, or a unit which may be life limited. The nutation angle must be kept small due to the high input speeds and consequent high angular velocities of the nutator rollers. For the same reasons, the nutator roller coning angle must be minimized consistent with the other design constraints. The resulting roller path and cam tooth profiles must be examined to avoid re-entrant or otherwise unacceptable paths. A summary of the general design approach is presented schematically in Figure 8-1.

BEARING CRITERIA

Each nutator roller is not always in contact with a cam tooth. In fact, each roller is never in contact with a cam tooth more than 50 percent of each cycle; and this contact time may be as short as 15 to 20 percent of each cycle. Hence, the computation of a realistic roller support bearing life must consider the overall load spectrum experienced by the bearing. The appropriate cubic mean loading spectrum (as defined in the load analysis section of this report) has been applied to both design examples.

As is the case with any mechanism which operates over varying conditions of load and speed, the maximum loads will not be used in the bearing life calculations. A cubic mean factor of 0.75 has been assumed for use in both design examples.

Because of the high speeds and relatively large sizes of both design examples studied, the DN values for an outer nutator support ring bearing are prohibitive; consequently, this type of support will not be analyzed here. The analysis will be restricted to consideration of center bearing concepts only.

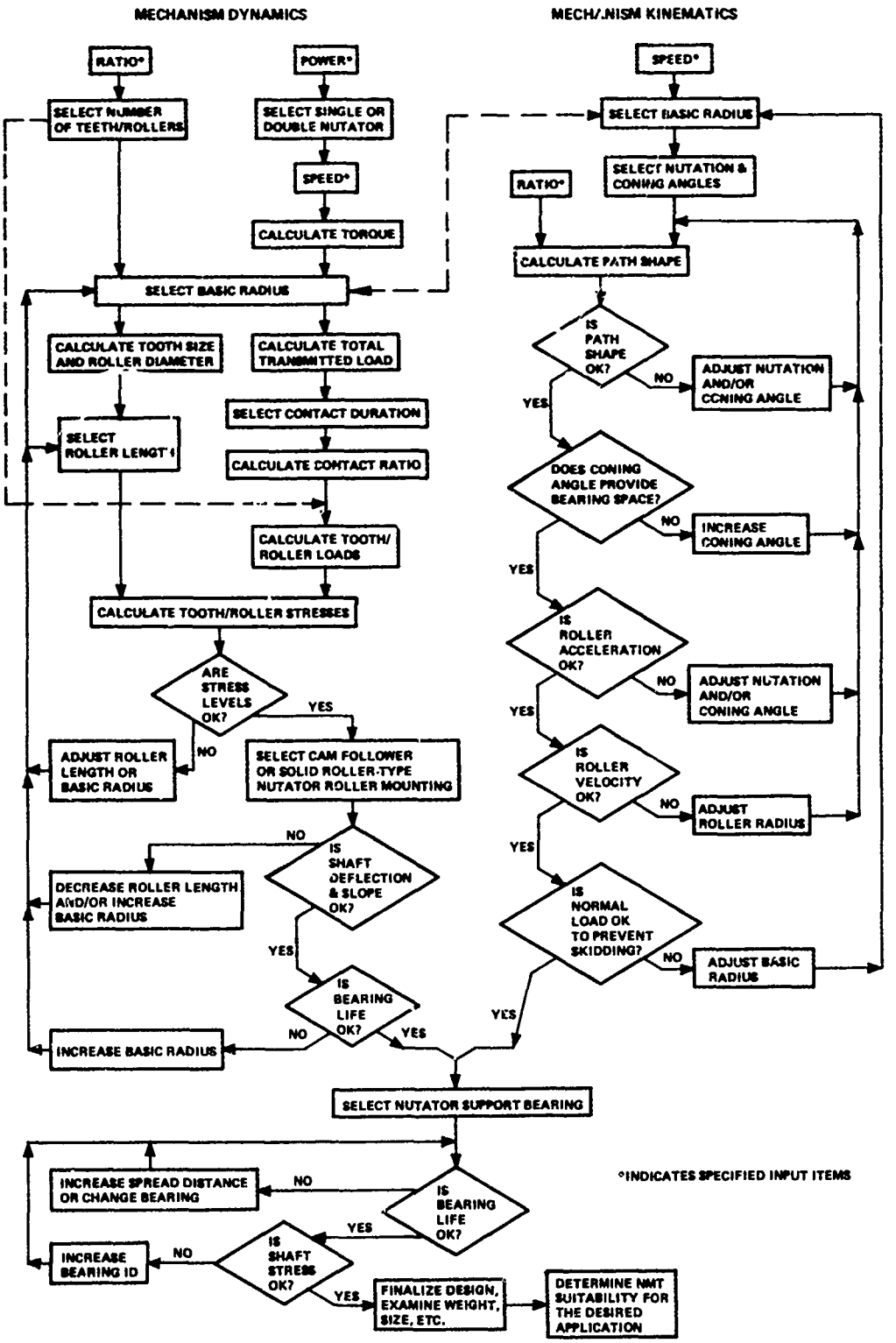

Figure 8-1. General Design Approach Flow Chart.

The center support bearing for the nutator ring is under continuous load since some of the nutator rollers are always in contact with the cam teeth. Furthermore, the variation of the magnitude of the load during a mesh cycle is assumed to be small. This assumption is justified by the large contact ratio which is characteristic of the NMT and the consequent good load sharing. Hence, no cubic mean load is considered for this relatively constant load spectrum. The factor of 0.75 due to the variation of power over the mission profile is still applied when calculating the bearing life.

The center support structure is composed of a radially relieved ball bearing located in the nutator plane to react thrust loads and two cylindrical roller bearings offset on either side of the nutator plane to react the radial loads and overturning moment. The net thrust load imposed on the ball bearing is due to F_{TNZR} and F_{TNZS}, but is small since these two forces are generally of the same order of magnitude but of opposite sence. Since ball bearings which yield satisfactory life under the imposed operating conditions are readily available, this is not a critical design area. Similarly, the radial forces F_{TNYR} and F_{TNYS} are generally of the same order of magnitude but opposite sense, so the resultant radial load applied to the cylindrical roller bearings due to the these forces is negligible relative to that caused by the overturning moment.

The critical center bearing loads are the radial loads applied to the roller bearings due to the net effect of F_{TNXR} and F_{TNXS} (the net driving forces), and predominantly, those necessary to react the overturning moment applied to the nutator ring by the action of F_{TNZR} and F_{TNZS}.

RELATIONSHIP BETWEEN NUTATOR CENTER SUPPORT BEARING AND SHAFT DIAMETER

After the power and speed of the nutator are given, the radial size of the nutator center support bearing may be determined. The upper bound is fixed by either the maximum allowable DN or basic radius (bearing max OD $\leq R_{BCCA}$), and the minimum shaft size for acceptable stress fixes the lower bound. Within these radial size limits, the designer may exercise some control over the bearing life by varying the effective radial load and/or bearing capacity. The load is a function of the bearing spread, and the capacity is a function of the type of bearing chosen. Hence, the limitations of the axial envelope will dictate the final bearing configuration; consequently, these limitations must be further considered. The bearing life can be improved by simply stretching the overall NMT length to increase the spread and decrease the effective loads; however, this is generally undesirab' .

An axial envelope, composed of two parts, is inherently available within the NMT. The first part is the space necessary for the nutator structure and rollers as they sweep through the nutation and coning angles (ν, σ) (see Figure 8-2). This requires an axial clearance (ds_{CA}) on both sides of the nutator centerline. Second, since it is generally desirable to mount the structural support of the cam at an angle of about 60 degrees to the NMT centerline for better stiffness and thrust reaction, additional space is available within the center regions of the cams (Figure 8-3). This axial clearance (dc_{CA}) is always available on the stator side of the nutator. The axial clearance required on the rotor side of the nutator may be less when using a double nutator configuration, since the back-to-back rotor cams cancel each other's thrust forces so that no net thrust is applied to the cam. Nevertheless, for the purpose of sizing the axial clearance (dc) will be assumed to be available on both sides of the nutator centerline.

The axial distance required for the sweep of the nutator (ds_{CA}) is defined by Equation (8.5) and is a function of the basic radius, roller length, coning and nutation angles, and structural mounting.

$$ds_{CA} = \left(R_{BCCA} + \frac{\ell_{CA}}{2} \sin\left(\sigma_{CA} + \nu\right)\right) + \left(r_{CA} + \frac{\ell_{CA}}{2} \tan\left(\gamma_{ROL/CA}\right) + SO_{CA}\right) \cos\left(\sigma_{CA} + \nu\right) \quad (8.5)$$

where r_{OCA} = outer roller radius ($r_{OCA} = r_{CA} + \frac{\ell_{CA}}{2} \tan\left(\gamma_{ROL/CA}\right)$)

SO_{CA} = structural overhang

$\gamma_{ROL/CA}$ = roller taper angle

The axial space available inside the cam is also a function of the mechanism geometry, but varies additionally with the diameter of the center support bearing chosen. The axial distance (dc_{CA}) available increases with decreasing bearing diameter, and is given by,

$$dc_{CA} = \left(h_{CA} - R_{BO} - fc_{CA}\right) \tan\left(30^{o}\right) \quad (8.6)$$

where $h_{CA} = R_{BCCA} \cos\left[\sigma_{CA} + \nu + \frac{3r_{CA}\ 180}{2R_{BCCA}\ \pi}\right]$

R_{BO} = center support bearing outer radius

fc_{CA} = clearance distance

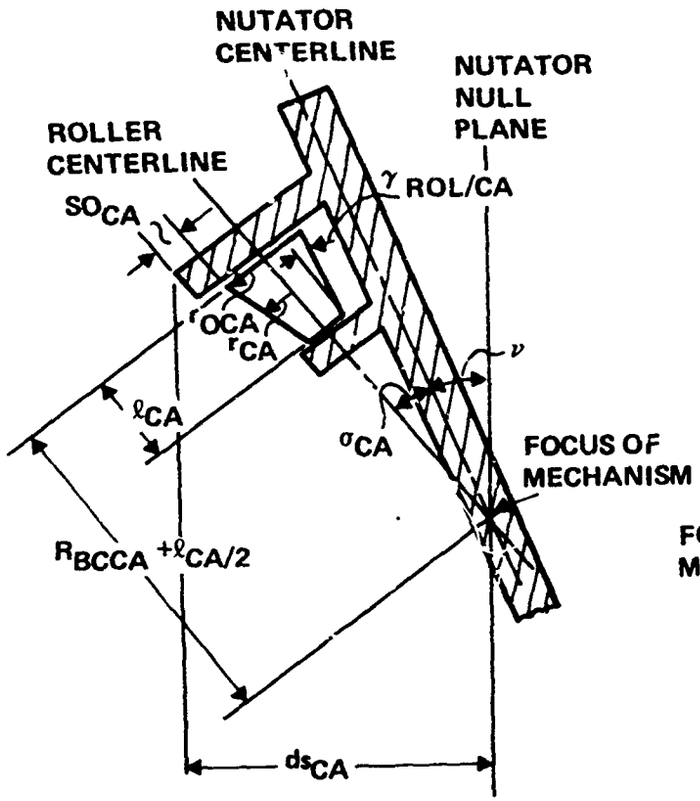

Figure 8-2. Axial Distance Required for Sweep of Nutator

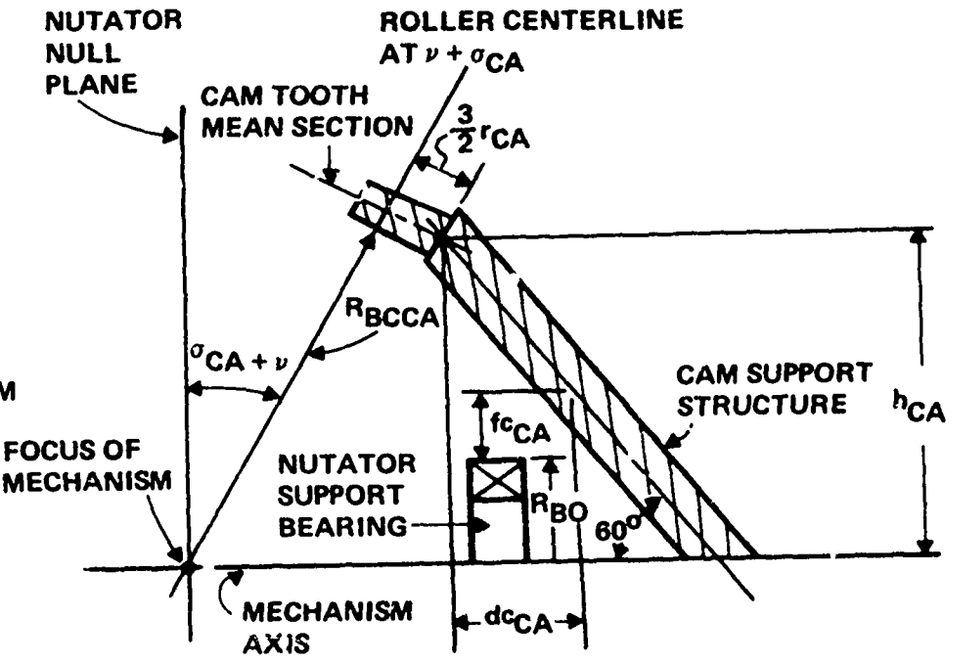

Figure 8-3. Axial Distance Available Within Cam Center

and the distance from the roller centerline at the angular position ($\nu + \sigma_{CA}$) to the cam tooth root has been estimated as 3/2 r_{CA}. Therefore, the total axial distance along the NMT centerline inherently available on either side of the nutator for spreading the center support bearings is,

$$D_{maxCA} = ds_{CA} + dc_{CA} \tag{8.7}$$

If any greater axial distance is required to further reduce the radial load due to the overturning moment, an overall increase of the NMT length is necessary. Equations (8.5) to (8.7) are general expressions applicable to any NMT configuration. (Since both design examples considered in this section use similar rotor and stator parameters (i.e., $\sigma_R = \sigma_S$, $r_R = r_S$, etc.), the CA subscript can henceforth be omitted.)

After a preliminary sizing of the center support bearing, a check of its compatability with the required shaft diameter must be performed. Referring to Figure 7-9(b), the maximum shaft diameter possible for a specified bearing ID, distance D normal to the nutator centerline, and nutation angle (ν) is,

$$D_{S\ MAX} = (\text{Bearing ID} - 2D \tan(\nu)) \cos(\nu) \tag{8.8}$$

Since the split shaft necessary for this configuration is generally undesirable because of the high shaft bending and torsion loads at the joint, the shaft diameter must be reduced to provide installation clearance. The requirement here is to allow sufficient clearance between the shaft OD and bearing ID to allow the bearing to be cocked relative to the shaft and aligned parallel to the bearing mounting pad. Reduction of the basic shaft diameter is the most desirable method of achieving the required clearance (Figure 7-9(a)). An alternative solution is to provide only localized undercuts in the maximum shaft diameter (Figure 7-9(c)). The analysis is the same for either method, although the shaft sizes and stress concentration factors differ.

The minimum shaft clearance required (Y) is a function of bearing width (W) and nutation angle,

$$Y = W \sin \nu \tag{8.9}$$

Consequently, the actual shaft diameter is restricted to values equal to or less than,

$$D_{S\ ACT} = D_{S\ MAX} - 2Y \tag{8.10}$$

This shaft diameter must be checked to ensure the stresses are within the allowables at the rated power.

Stress in Nutator Support Shaft

The combined stress equations for a hollow circular shaft subjected to both bending and torsion are well documented in standard texts. Therefore, these relationships will be only briefly summarized. The stress allowables are typical values used by the contractor. The bending (f_b) and torsional (f_{st}) stresses are,

$$f_b = \frac{MR_{so}}{I_S} \tag{8.11}$$

$$f_{st} = \frac{T_o R_{so}}{2I_S} \tag{8.12}$$

where M = overturning moment

T_o = output torque of mechanism

I_S = moment of inertia of shaft $\left[I_S = \frac{\pi}{4}\left(R_{so}^4 - R_{si}^4\right)\right]$

R_{so} = shaft outside radius

R_{si} = shaft inside radius

Since the purpose here is to insure that the allowable shaft diameter is sufficient to carry the imposed load Equation (8.11) and (8.12) become,

$$f_b = \frac{M\, D_{S\ ACT}}{2I_S} = \frac{2M\, D_{S\ ACT}}{\pi\left[\left(\frac{D_{S\ ACT}}{2}\right)^4 - R_{si}^4\right]} \tag{8.13}$$

Utilizing AISJ 9310 steel as the shaft material, the bending endurance limit is F_e = 25 ksi. From the ultimate torsional shear limit F_{su} = 95 ksi the allowable values for the torsional shear stress may be defined as,

$$F_{ast} = .577 \times F_e \left(1 - \frac{fst}{F_{su}}\right) \tag{8.15}$$

Thus, the ratio of actual to allowable stress may be defined for bending (R_b) and torsion (R_{st}) as,

$$R_b = \frac{K_b \times f_b}{F_e} \tag{8.16}$$

$$R_{st} = \frac{K_{st} \times f_{st}}{F_{ast}} \tag{8.17}$$

Where the stress concentration factors (K_b, K_{st}) are a function of shaft material and geometry, and it has been assumed that,

$$K_b = K_{st} = 1.05 \tag{8.18}$$

The final criteria for maintaining acceptable stress levels within the shaft is that,

$$\sqrt{R_b^2 + R_{st}^2} \leq 1 \tag{8.19}$$

Employing the design specifications and procedures outlined above, the following two design examples were evaluated.

DESIGN EXAMPLE A: MARINE PROPULSION UNIT

The specific design constraints which were applied to this example have been summarized in Tables 8-1 and 8-2; a brief general design philosophy follows. A marine propulsion or fixed-based unit, of which this configuration is representative, typically requires a minimum of several thousand operating hours before overhaul. Although size and weight are important, they are normally not as critical as, for example, in aircraft applications. Therefore, more latitude is permissable for conducting cost, size, and weight tradeoffs between various candidate designs; however weight is still one of the primary factors and must be treated accordingly. Because of the speed and power requirements of this transmission, a double nutator, split-power path configuration was selected to minimize size, vibration, and balancing problems. The size and ratio (20:1) constraints were such that an $N_S = N_R - 2$ tooth and roller combination yielded acceptable cam tooth and roller sizes. Therefore, since roller reversal was not a problem, only a single set of nutator rollers was required per nutator. The required number of rotor cam teeth, nutator rollers, and stator cam teeth were 40, 39, and 38, respectively. No roller coning angle was needed, since only a single set of nutator rollers was required, and a minimum practical nutation half-angle ν = 5 degrees was selected.

Based on extensive past experience with gear teeth, an allowance was made for tooth profile modification near the tip and root and the start and end points for the cam tooth/roller contact were selected at ω_{NCA} = 10 degrees and ω_{XCA} = 80 degrees. The resulting contact duration is 70 degrees and the contact ratio is 7.6.

Using those tentatively defined parameters, the tooth and roller loads were calculated for several basic radii (R_{BCCA}). The minimum basic radius at which the stress limitations are met is about 26 inches. The bending stress (36,500 psi) is considerably below the maximum allowable, but the contact stress (175,000 psi) is the critical factor. At this radius, the nutator support roller size envelope is about 2.05-inch diameter and series 304 nutator roller support bearings are available that allow a large enough support-shaft diameter to yield acceptable slopes (0.0004 in/in). However, the applied loads (cubic mean = 10,524 pounds) are too large for the allowable cam follower-type bearing size, resulting in an unacceptable bearing life of less than 25 hours.

By increasing the basic radius to 45 inches, the allowable roller diameter increases to 3.50 inches, while the load decreases by 42 percent (cubic mean = 6082 pounds). Using two Series 308 support bearings, each with a capacity of 17,100 pounds, this roller size-load relationship allows a bearing life of about 2700 hours.

In order to reach the design bearing life of 12,000 hours with the cam-follower roller mounting, it was necessary to increase the basic radius to 55 inches.

This final configuration allows a 4.35-inch diameter roller which may be supported by two 310-series cylindrical roller bearings. The bearing DN is 1.11×10^6. The maximum instantaneous load carried by a roller is 10,700 pounds which corresponds to a cubic mean load rating of 5000 pounds. Stresses and shaft slopes of course, continue to be below allowable limits (4400 psi bending stress, 60,900 psi contact stress, 0.0001 in/in slope). Since the basic radius is measured to the center of the nutator roller which is 2.2 inches long, making an allowance for the thickness of the transmission case and supporting structure, the actual outer radius of this configuration is about 63 inches. Therefore, the overall transmission diameter is slightly over 12 feet.

Even though the size is not a critical factor, this design which uses the cam-follower roller mounting is still not entirely satisfactory. The low stress levels do not allow complete use of the capacity of material. The added complexity of the solid nutator roller configuration with end-bearing support may not be justified in this case. A design tradeoff study would have to consider this in view of the relative importance of size, weight, and cost for a specific application. However, it is useful to examine what effect this mounting will have on transmission size and life.

At the same basic radius of 55 inches, the solid roller mounting allows the use of larger support bearings, providing

greatly increased nutator roller support bearing life. Using two Series 319 roller bearings which have an ID compatible with the 4.4 in roller OD, the life increases by more than an order of magnitude from the 12,000-hour design life achieved with the cam-follower mounting. The tooth and roller loads and stresses are unaffected, while the previously acceptable slope across the bearings is further reduced because of the greater stiffness of the solid roller. A reduction of the basic radius to 35 inches is possible, while still maintaining a life of 12,000 hours. Two Series 313 bearings, each with a capacity of 35,500 pounds, are compatible with the 2.8-inch maximum mean roller OD and length of 1.34 inches. The ℓ/d ratio from Equation (8.3) becomes

$$\ell/d = \frac{1.34 \text{ in.}}{22\text{mm}} \times \frac{25.4\text{mm}}{\text{in.}} = 1.5 \qquad (8.20)$$

which is well within the allowable value. Further diametral size reduction of the NMT is limited by the increase in loads and consequent reduction of bearing life. The bending stress (17,200 psi) and contact stress (120,000 psi) are higher and use of the material's capacity is better, although not total. The nutator roller shaft slope is quite small with a value of only 0.00004 in/in. The roller support bearing average DN is 7.3×10^5 ; however, near the start of contact. the instantaneous DN is about 1.4×10^6 . Making an allowance for the supporting structure, the resulting overall diameter of this NMT is about 7.3 feet. Axial sizing will subsequently be discussed.

The total cubic mean radial load on a nutator roller is 7800 pounds. It is, however, also necessary to examine the actual magnitudes of the instantaneous roller loads. Comparing the radial loads applied and the inertia of the roller and bearings which is related to the DN, the skidding tendency of the roller may be evaluated as it progresses along the tooth profile. The tangential force required to prevent skidding ranges from 1200 to 3150 pounds, which for an assumed friction coefficient of 0.01 corresponds to a required normal force range of 120,000 to 315,000 pounds. The instantaneous radial load applied to a nutator roller ranges from 5600 to 16,900. Therefore, the roller/tooth interface will probably experience a significant amount of skidding. A friction coefficient of about 0.2 is required to minimize this skidding.

Although the calculation based on cubic mean loading and the rated dynamic capacity has shown that the roller support bearings provide the required life, it is also necessary to insure that no instantaneous load applied to the bearings exceeds their rated static capacity. Such an overload would result in brinelling or fracture leading to early failure. The maximum instantaneous load applied to a nutator roller is about 16,900 pounds which results in a load of 8450 pounds per bearing. Since the rated static capacity for these Series 313

bearings is 24,800 pounds, the design is well within the allowable limits.

Another important limiting element in the design of an NMT is the nutator center support bearing which is composed of two radial cylindrical roller bearings and a ball thrust bearing. Since the radial load on each roller bearing is practically independent of radius (see Figure 8-4) for a fixed separation distance between the two roller bearings, it is a convenient design procedure to size the NMT based on an independent consideration of the nutator rollers and cam teeth as previously done. The center bearing analysis will then subsequently lead to axial sizing.

As the basic radius increases, the magnitude of the nutator roller and cam tooth loads decreases; however, the moment arm for these loads simultaneously increases. Therefore, the most significant control over the center support bearing life is simply to use a larger bearing, which is made possible as the radius increases. One other solution is to increase the spread distance w, but this is limited by the shaft diameter, nutation angle, and stress concentration induced at the bearing mounting pads which will be discussed later in this section. In order to meet the DN requirements, the maximum center support bearing mean diameter for this configuration is limited by

$$D_{BM} = \frac{DN}{25.4 \times RPM_{Rel}} = \frac{2.0 \times 10^6}{25.4 \times 5846} = 13.5 \text{ inches} \qquad (8.21)$$

The relative speed (RPM_{Rel}) experienced by the bearing is the difference between the input speed (6000 rpm for the inner race) and the speed of precession of the nutator (154 rpm for the outer race). This restriction on bearing diameter is quite a severe design limitation, since it imposes limits on the capacity of the bearings as well as on the maximum shaft diameter. A typical candidate cylindrical roller bearing is a Torrington 230-RN 93 which has a 9.055-inch ID, an 18.898-inch OD, a 7.25-inch width, and a capacity of 622,000 pounds. Applying Equation (8.4) and the methods outlined in the load analysis section, the desired operating life of 12,000 hours requires a spread distance, 2w, of 21.7 inches between the centers of the nutator center support bearings for the solid nutator roller configuration with a basic radius of 35 inches. Adding half of the bearing width, W/2, to the spread distance w, a total distance of D = 14.4 inches is necessary on each side of the nutator centerline for the center support bearings. Since the distance D is measured normal to the nutator centerline which is inclined at the nutation angle, υ = 5 degrees, the axial distance necessary along the centerline of the NMT is

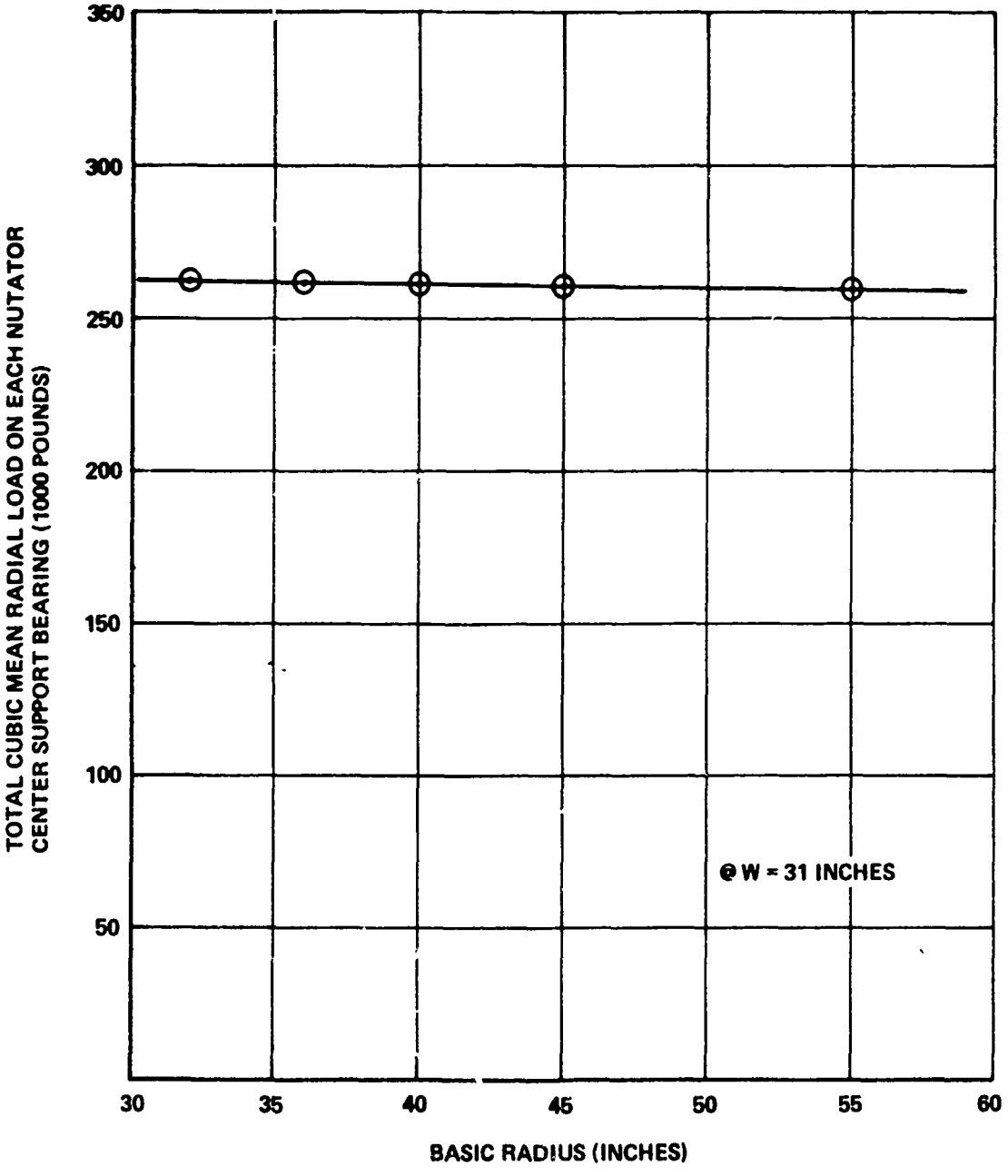

Figure 8-4. Nutator Center Support Bearing Radial Load Variation with Basic Radius

$$D_A = D \cos(\nu)$$

$$= 14.4 \cos(5^o) = 14.3 \text{ inches} \quad (8.22)$$

From Equations (8.8) through (8.10), the maximum axial distance available within the NMT is

$$d_s = (35.0 + .669) \sin(5^o) + (1.380 + .669 \tan(2.264) + .25) \cos(5^o) = 4.76 \text{ inches} \quad (8.23)$$

$$d_c = \left[35.0 \cos\left(5 + \frac{3x1.380x180}{2x35.0x\pi}\right) - 9.449 - 0.75\right] \tan(30°)$$

$$= 14.10 \text{ inches} \quad (8.24)$$

$$D_{max} = 4.76 + 14.10 = 18.86 \text{ inches} \quad (8.25)$$

is greater than the necessary axial distance D_A. Thus, the overall length need not be increased to provide any additional axial space. The total width per nutator is 28.8 inches. Since the tilt of each nutator through the angle ν is of opposite sense, an additional axial clearance

$$c = 2 R_{BO} \sin(\nu)$$

$$= 2 (9.449) \sin(5^o) = 1.65 \text{ inches} \quad (8.26)$$

must be provided between nutators to preclude interference of the bearings for each nutator at the bearing outer diameter. The resulting length is about 4.9 feet for the double nutator mechanism. By adding to this an allowance for supporting structure, the resulting total length is about 7.5 feet. Furthermore, from Equations (8.8) to (8.10) the shaft diameter, large spread distance, and large bearing width cause considerable shaft cutting for installation clearance. This unsatisfactory shaft condition greatly impairs stress reliability.

$$D_{S\ MAX} = \left[9.055 - 2 \times 14.4 \times \tan(5^o)\right] \cos(5^o) = 6.51 \text{ inches} \quad (8.27)$$

$$Y = 7.25 \sin(5^o) = .632 \text{ inches} \quad (8.28)$$

$$D_{S\ ACT} = 6.51 - 2 \times .632 = 5.25 \text{ inches} \quad (8.29)$$

Even for a solid shaft, the bending stress alone exceeds the allowable levels outlined in Equations (8.11) to (8.19).

$$f_b = \frac{2[(28,800 + 30,440)35]\ (5.25)}{\pi\ ((\frac{5.25}{2})^4 - 0)} = 145,950 \text{ psi} \quad (8.30)$$

$$R_b = \frac{1.05 \times 145,950}{25,000} = 6.13 \quad (8.31)$$

And, therefore, $\sqrt{R_b^2 + R_{st}^2} >> 1$

Roller bearings have been run successfully by bearing manufacturers under controlled laboratory conditions at a DN approaching 4.0×10^6. At this condition, the allowable mean bearing diameter goes to 27.0 inches. A Torrington 560RN30 bearing fits the criteria with a 22.047-inch ID, a 32.284-inch OD, a 7.677-inch width, and a dynamic capacity of 1,140,000 pounds. Applying the same procedure as before to calculate the required spread, w = 6.6 inches D = 10.5 inches, and the required axial distance

$$D_A = D \cos (\upsilon)$$

$$= 10.5 \cos (5^o) = 10.4 \text{ inches} \quad (8.32)$$

considering Equations (8.23) to (8.25), ds is unchanged and

$$dc = \left[35.0 \cos (5^o + \frac{3x1.380x180}{2x35.0 \times \pi}) - 16.142 - 0.75\right] \tan (30°)$$

$$= 10.24 \text{ inches} \quad (8.33)$$

$$D_{max} = 4.76 + 10.24 = 15.00 \text{ inches.} \quad (8.34)$$

Thus, the necessary axial distance, D_A, is available within the NMT. The resulting maximum radial load of about 202,000 pounds on the nutator center support bearing does not exceed the rated static capacity of 2,100,000 pounds. The total width per nutator is 21.0 inches and the minimum clearance required between nutators is

$$c = 2\ (16.142) \sin (5^o) = 2.81 \text{ inches} \quad (8.35)$$

The axial length of the double nutator mechanism is 44.8 inches which results in an overall NMT length of about 6.2 feet, including an allowance for structure.

From Equations (8.8) to (8.10), the corresponding shaft diameter is acceptable.

$$D_{S\ MAX} = \left[22.047 - 2 \times 10.5 \times \tan (5^{o})\right] \cos (5^{o})$$

$$= 20.13 \text{ inches} \qquad (8.36)$$

$$Y = 7.677 \sin (5^{o}) = 0.669 \text{ inches} \qquad (8.37)$$

$$D_{S\ ACT} = 20.13 - 2 \times 0.669 = 18.79 \text{ inches} \qquad (8.38)$$

Assuming a shaft wall thickness of 0.370 inch, the resulting combined stress levels for the largest possible shaft diameter are well within the allowables.

$$f_b = \frac{2\left[(28,800 + 30,440)\,35\right] 18.79}{\pi \left(\left(\frac{18.79}{2}\right)^4 - \left(\frac{18.05}{2}\right)^4\right)} = 21,443 \text{ psi} \qquad (8.39)$$

$$f_{st} = \frac{(131,300)(18.79)}{\pi \left(\left(\frac{18.79}{2}\right)^4 - \left(\frac{18.05}{2}\right)^4\right)} = 679 \text{ psi} \qquad (8.40)$$

$$F_{ast} = .577 \times 25,000 \left(1 - \frac{679}{95,000}\right) = 14,322 \text{ psi} \qquad (8.41)$$

$$R_b = \frac{1.05 \times 21,443}{25,000} = 0.901 \qquad (8.42)$$

$$R_{st} = \frac{1.05 \times 679}{14,322} = 0.050 \qquad (8.43)$$

$$\sqrt{R_b^2 + R_{st}^2} = \sqrt{0.812 + 0.0025} = 0.902 < 1 \qquad (8.44)$$

Therefore, latitude is available for the designer to optimize the shaft design. Although the bearings are critical to a successful NMT, with careful design and bearing development, a practical operating life can be obtained. An approximate scale layout of this design is presented in Figure 8-5.

The considerable mechanical complexity of the split nutator NMT is obvious. The need to anchor both stator cams to the stationary structure, for example, requires an inner shaft within the nutator support shaft and also leads to the offset input gearing.

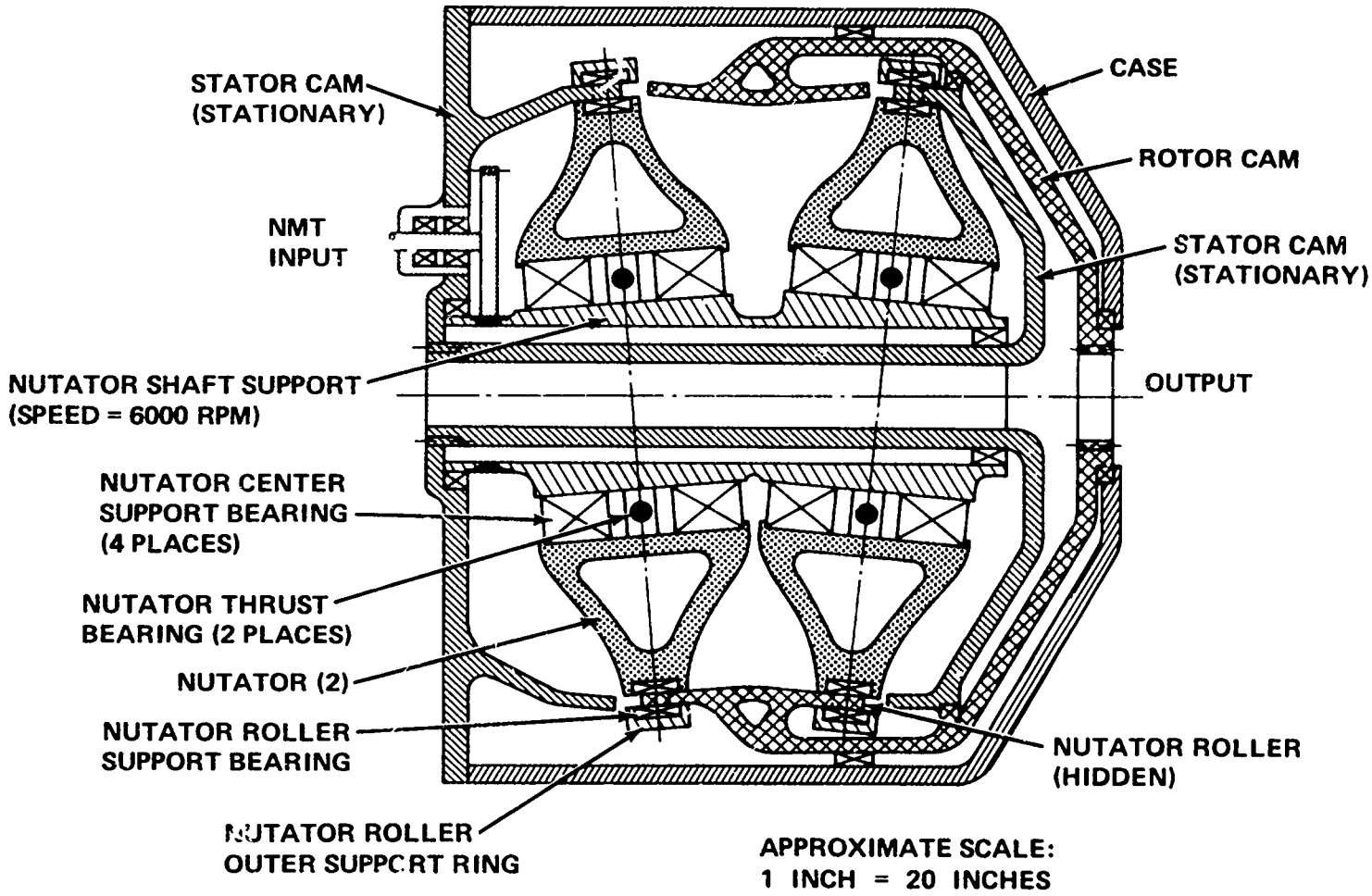

Figure 8-5. Design Example A

The bearings used to support the stator cams, rotor cam, and case are within current bearing technology and are assumed to be noncritical design items, since the loads and DN are well below those experienced by the nutator bearings.

A weight summary for the design example is presented in Table 8-3. The weight of each major component was calculated from the design layout (Figure 8-5). Miscellaneous hardware including nuts, bolts, washers, seals, etc. was assumed to account for 20 percent of the total NMT weight. This percentage is a typical value, based on existing aircraft transmissions and contractor experience. The resulting specific weight ratio of 2.4 lb/hp compares favorably with the 3-5 lb/hp values which are typical of conventional transmissions for applications of this type.

The weights presented do not include the lubricant, the lubrication system, cooling system, and associated hardware; therefore, caution must be exercised when comparing these figures to other transmission concepts.

A summary of the final design parameters is presented in Table 8-4.

DESIGN EXAMPLE B: AIRCRAFT APPLICATION (CH-47 HELICOPTER FORWARD TRANSMISSION)

The design specifications for this example are contained in Tables 8-1 and 8-2. The design philosophy here is quite different than for example A, since minimum weight and size are foremost, and operating life is typically on the order of a few thousand hours. Again the speed, power, and size requirements necessitate a split-power, double-nutator arrangement. Preliminary calculations for sizing the NMT indicated that the size and ratio constraints made the $N_S = N_R - 2$ tooth/roller combination impractical. The stresses were high due to the small teeth, and the rollers were too small to be compatible with a bearing that would yield any realistic life. Consequently, the $N_S = N_R - 1$ combination was used initially. After evaluating this configuration, the $N_S = N_R - 2$ will be more fully discussed and compared.

To obtain the required ratio (30:1), the number of rotor cam teeth, nutator rollers, and stator cam teeth selected were 30, 29, 29, respectively. Due to the roller reversal phenomenon associated with this combination, a roller coning angle σ of 5 degrees was used to allow clearance for two sets of rollers. One set contacts only the stator cam while the second set contacts only the rotor cam. The only condition applied for selection of the coning angle magnitude was that the roller

TABLE 8-3. WEIGHT SUMMARY OF NMT DESIGN EXAMPLE A (25,000 HP)

Item	Number	Unit Weight (lb)	Weight (lb)
Bearings			
a. Center support cylindrical	4	875.0	3,500.0
b. Thrust ball	2	50.0	100.0
c. Nutator roller support (2 per roller)	156	6.0	936.0
d. Miscellaneous (cam and shaft support)	5		1,546.0
Shaft (steel)	1	1,915.0	1,915.0
Nutator (aluminum)	2	2,758.0	5,516.0
Stator cam (steel)			
Outer plate	1	6,529.0	6,529.0
Inner shaft	1	3,616.0	3,616.0
Rotor cam (steel)	1	9,666.0	9,666.0
Case (steel)	1	12,745.0	12,745.0
Nutator rollers (steel)	78	6.8	530.0
Nutator support ring (steel)	2	634.0	1,268.0
NMT input pinion and bearings	1	165.0	165.0
Subtotal - major components			48,032.0
Misc. hardware (seals, bolts, nuts, washers, snap rings, retainer plates, etc.)	20% of total NMT weight		12,008.0
Total NMT Weight (lb)			60,040.0
Specific Weight* (lb/hp)			2.4

*Excluding weight of lubricant, lubrication system, cooling system, and associated hardware.

TABLE 8-4. SUMMARY OF NMT DESIGN EXAMPLE A

Type NMT	Dual Nutator - Split Power Path
Input configuration	Inline - Offset
Power	25,000 hp
Input speed	6,000 rpm
Reduction ratio	20:1
Bearing design life	12,000 B-10 hours
Number of teeth/rollers (rotor, nutator, stator)	40, 39, 38
Contact ratio	7.6
Nutation angle	5 degrees
Coning angle	0 degrees
Basic radius	35.0 inches
NMT diameter - max	7.3 feet
NMT length - max	6.2 feet
Nutator roller	
length	1.34 inches
ℓ/d	1.5
radius	1.4 inches
type	solid with end bearings
Bearings	
roller support	Series 313
nutator center support	560RN30 Torrington
Bearing DN	
Roller support (max)	1.4×10^6
Nutator center support	4.0×10^6
Bending stress	17.2 ksi
Contact stress	120.0 ksi
Nutator roller shaft slope	0.00004 in/in
Nutator support shaft	
diameter	18.8 inches
wall thickness	0.370 inches
Specific weight	2.4 lb/hp

centerline be tilted a sufficient distance from the nutator centerline to provide clearance between the two sets of rollers and allow for supporting structure.

A minimum practical nutation half-angle, ν = 5 degrees, was selected. Based on extensive past experience with gear teeth, the starting and ending points for the cam tooth/roller contact were selected as ω_{NCA} = 10 degrees and ω_{XCA} = 80 degrees, respectively. The resulting contact duration is 70 degrees and the contact ratio is 5.6

Using the tentative parameters defined at this point, the tooth/roller loads were calculated for several basic radii (R_{BCCA}). The design stress limits were met at a basic radius of 12 inches. Both the bending stress (44,700 psi) and the contact stress (177,800 psi) were critical as limit factors. Considering the cubic mean radial load (4400 pounds) and the available bearings (Series 200) compatible with the maximum roller diameter of 1.18 inches, the resulting bearing life was only a few hours and the corresponding shaft slope (0.0075 in/in) greatly exceeded the specified limitation.

By increasing the basic radius to 14 inches, the cubic mean radial load was reduced to 3750 pounds and the slope was reduced to a marginally acceptable limit (0.0006 in/in). However, the largest nutator roller support bearing (Series 1003) which fits within the 1.38 inch maximum diameter available provides a life of less than 25 hours. Although bearings with greater capacity(life) are available within the same OD limit, the radial space required for larger diameter rolling elements results in increased shaft deflection.

A design meeting all requirements except for a bearing life of 1000 hours was reached at a basic radius of 19.0 inches. In order to fulfill the design life of 2000 hours, a basic radius of 22 inches was required. At this configuration the maximum instantaneous load carried by a roller is 6700 pounds, which corresponds to a cubic mean loading of 2400 pounds. The maximum roller diameter is about 2.10 inches. Two series 304 cylindrical roller bearings, each with a capacity of about 6220 pounds, may be used to support a nutator roller. Bending stress (10,300 psi), contact stress (94,500 psi) and shaft slope (0.0004 in/in) continue, of course, to be within acceptable limits.

Allowing approximately 3 inches radial clearance for the nutator roller and its support structure, the overall transmission diameter is about 50 inches for the cam follower type nutator roller support. The CH-47 ring gear has a diameter of 21.5 inches, and the outer case diameter is about 22 inches.

Not only is this NMT design too large, but the stress levels are too low for efficient material utilization. An alternative design employs a solid nutator roller with end bearings. Previous calculation for the cam follower mounting indicated that the stress levels were acceptable at a basic radius of 12 inches. Since the tooth/roller sizes are not affected by the mounting method, the stress levels remain unchanged for the solid roller. The shaft slope and bearing life, which were limiting factors for the design employing cam follower mounting, are improved by using a solid roller. The slope is decreased to 0.0007 in/in since the solid roller is stiffer.

The two larger Series 306 bearings (bearing ID ≈ roller OD ≈ 1.180 inch) each have a capacity of 11,000 pounds and allow the design life of 2000 hours to be maintained. Thus, the solid roller mounting permits a reduction of the basic radius to 12.0 inches. The coning angle had to be increased to 10 degrees to provide adequate clearance for the 2.83-inch bearing outer diameter. Any further reduction in radius is prevented by both bending and contact stress levels and the deflection, which are 45,000 psi, 178,000 psi and 0.0007 in/in, respectively.

Since the shaft size of the solid roller configuration is already maximized (i.e., the shaft is the solid roller), the only remaining way to reduce the slope for a given load is to reduce the roller length (ℓ = 1.06 inch). However, since the corresponding stress level increase would not be acceptable, the slightly excess slope will be tolerated. The total ℓ/d ratio of 2.4 obtained from Equation (8.3) is also within allowable limits. The overall diameter of the solid roller case has, therefore, been reduced to about 30 inches, and the material has been stressed to acceptable values.

The tangential force required to prevent skidding of a nutator roller ranges from about 50 to 200 pounds, which for an assumed coefficient of friction of 0.01 corresponds to a required normal force range of 5000 to 20,000 pounds. Comparing these loads with the instantaneous radial loads applied to the roller which range from 1300 to 12,300 pounds, the roller/tooth interface will experience some skidding. This skidding may present a significant problem.

The maximum load per bearing of 6150 pounds does not exceed the rated static capacity of 7170 pounds for the Series 306 bearings used.

Although both NMT designs exceed the size of the CH-47 transmission, the diameter of the solid roller configuration compares reasonably well. With some bearing improvement, this comparison will become more favorable. A slight size or weight penalty for the NMT may be tolerated to gain the good fail-safe characteristics derived from the high contact ratio.

In order to meet the DN requirements, the maximum center support bearing mean diameter is limited by Equation (8.21) which becomes

$$D_{BM} = \frac{2.0 \times 10^6}{25.4 \times 7000} = 11.25 \text{ inches} \qquad (8.45)$$

The relative speed experienced by the center bearing in this example is simply the input speed since the nutator does not precess for the tooth/roller combination used. This restriction on the bearing diameter is a severe design limitation, since it imposes limits on the capacity of the bearing as well as on the maximum shaft diameter. A typical candidate cylindrical roller bearing is a Torrington 220 RN91 which has an 8.661-inch ID, 13.780-inch OD, 3.875-inch width, and a dynamic capacity of 278,000 pounds. Applying Equation (8.4), and the methods outlined in the load analysis section, the desired operating life of 2000 hours requires a spread distance w of 2.1 inches. The corresponding maximum radial load of about 110,000 pounds does not exceed the rated static capacity of 410,000 pounds.

Adding half the bearing width W/2 to this spread distance, the distance required along the nutator mounting pad is 4.1 inches. But since this does not allow sufficient space for the ball thrust bearing an additional 1.0 inch is necessary. Therefore, the required distance D = 5.1 inches and the total axial distance required is,

$$D_A = D \cos(\nu) = 5.1 \cos(5^\circ) = 5.1 \text{ inches} \qquad (8.46)$$

From Equations (8.5) to (8.7), for the 12-inch basic radius configuration,

$$d_s = (12 + .53) \sin(10^\circ + 5^\circ) + [.59 + .53 \tan(2.815^\circ) + .1] \cos(5^\circ)$$

$$= 3.95 \text{ inches} \qquad (8.47)$$

$$d_c = 12 \left[\cos\left(10^\circ + 5^\circ + \frac{3(.59)\ 180}{2\ (12\ \pi}\right) - 6.890 - 1.0\right] \tan(30^\circ)$$

$$= 3.44 \text{ inches} \qquad (8.48)$$

$$D_{max} = 3.95 + 3.44 = 7.39 \text{ inches} \qquad (8.49)$$

Sufficient axial distance is therefore available within the NMT. The total width per nutator is about 10.2 inches and the clearance between nutators is,

$$c = 2\ R_{BO} \sin(\nu) = 2(6.890) \sin(5^{o}) = 1.20 \text{ inches} \quad (8.50)$$

With allowance for the supporting structure, this results in an overall transmission length of about 27 inches. The airframe configuration of the CH-47 helicopter requires that the input shaft be approximately normal (approximatley 80 degrees) to the nutator shaft. Therefore, an additional axial length of about 6 inches is necessary to accommodate the input spiral bevel pinion and gear. Since this input pinion is an integral part of the CH-47 transmission, it must be included in the NMT for a valid comparison. The resulting overall NMT length of about 33 inches compares with a height of approximately 30 inches for the existing CH-47 transmission

Considering the allowable shaft diameter from Equations (8.8) to (8.10)

$$D_{S\ MAX} = \left[8.661 - 2\ (5.1) \tan(5^{o})\right] \cos(5^{o}) = 7.74 \text{ inches} \quad (8.51)$$

$$Y = (3.875) \sin(5^{o}) = 0.338 \text{ inch} \quad (8.52)$$

$$D_{S\ ACT} = 7.74 - 2\ (.338) = 7.06 \text{ inches} \quad (8.53)$$

Assuming a shaft wall thickness of 0.400 inch and applying Equations (8.13) to (8.19), the resulting combined stress levels for the largest possible shaft size are within allowable limits.

$$f_b = \frac{2\left[(18{,}150 + 7460)12\right](7.06)}{\pi\left(\left(\frac{7.06}{2}\right)^4 - \left(\frac{6.26}{2}\right)^4\right)} = 23{,}305 \quad (8.54)$$

$$f_{st} = \frac{(16{,}206)\ (7.06)}{\pi\left(\left(\frac{7.06}{2}\right)^4 - \left(\frac{6.26}{2}\right)^4\right)} = 614. \quad (8.55)$$

$$F_{ast} = .577 \times 25{,}000\ \left(1 - \frac{614.}{95{,}000}\right) = 14{,}332 \quad (8.56)$$

$$R_b = \frac{1.05 \times 23{,}305}{25{,}000} = 0.979 \quad (8.57)$$

$$R_{st} = \frac{1.05 \times 614.}{14,332} = 0.045 \quad (8.58)$$

$$\sqrt{R_b^2 + R_{st}^2} = \sqrt{0.958 + 0.002}$$

$$= 0.960 < 1 \quad (8.59)$$

An approximate scale layout of this design example is presented in Figure 8-6. The same general comments apply here as with the previous example. Although the bearings are critical to a successful NMT, with careful design and some bearing development, a practical operating life appears to be obtainable.

The considerable mechanical complexity of the split nutator NMT is obvious. The need to anchor both stator cams to the stationary structure, for example, requires an inner shaft within the nutator support shaft and also leads to the offset input gearing. The bearings used to support the stator cams, rotor cam, and case are within current bearing technology and are assumed to be noncritical design items since the loads and DN are well below those experienced by the nutator bearings.

A weight summary for this design example is presented in Table 8-5. The weight of each major component was calculated from the design layout (Figure 8-6). Miscellaneous hardware including nuts, bolts, washers, seals, spacers, retainers, etc. was assumed to account for 20 percent of the total NMT weight. This percentage is a typical value based on existing aircraft transmissions and contractor experience. The resulting specific weight ratio of 1.0 lb/hp is considerably greater than the 0.3 lb/hp weight ratio typical of current helicopter transmissions. It must be noted that the weights presented do not include the weight of lubricant, the lubrication system, cooling system, and associated hardware. Therefore, caution must be exercised when comparing these figures to other transmission concepts.

A summary of the final design parameters is presented in Table 8-6.

An investigation of the $N_S = N_R - 2$ tooth/roller combination follows. The ratio of 30:1 requires a 60, 59, 58 tooth/roller/tooth combination, no coning angle is necessary, and the nutation half-angle of 5 degrees has been maintained. A contact duration of 70 degrees provides a contact ratio of 11.5, thereby reducing the load carried per tooth.

Several problems become apparent when this configuration is compared with the previously discussed design which has a basic radius of 12 inches. Although contact stress is acceptable (176,000 psi), the bending stress is excessive (67,000 psi) due to the smaller cam teeth. The roller diameter is

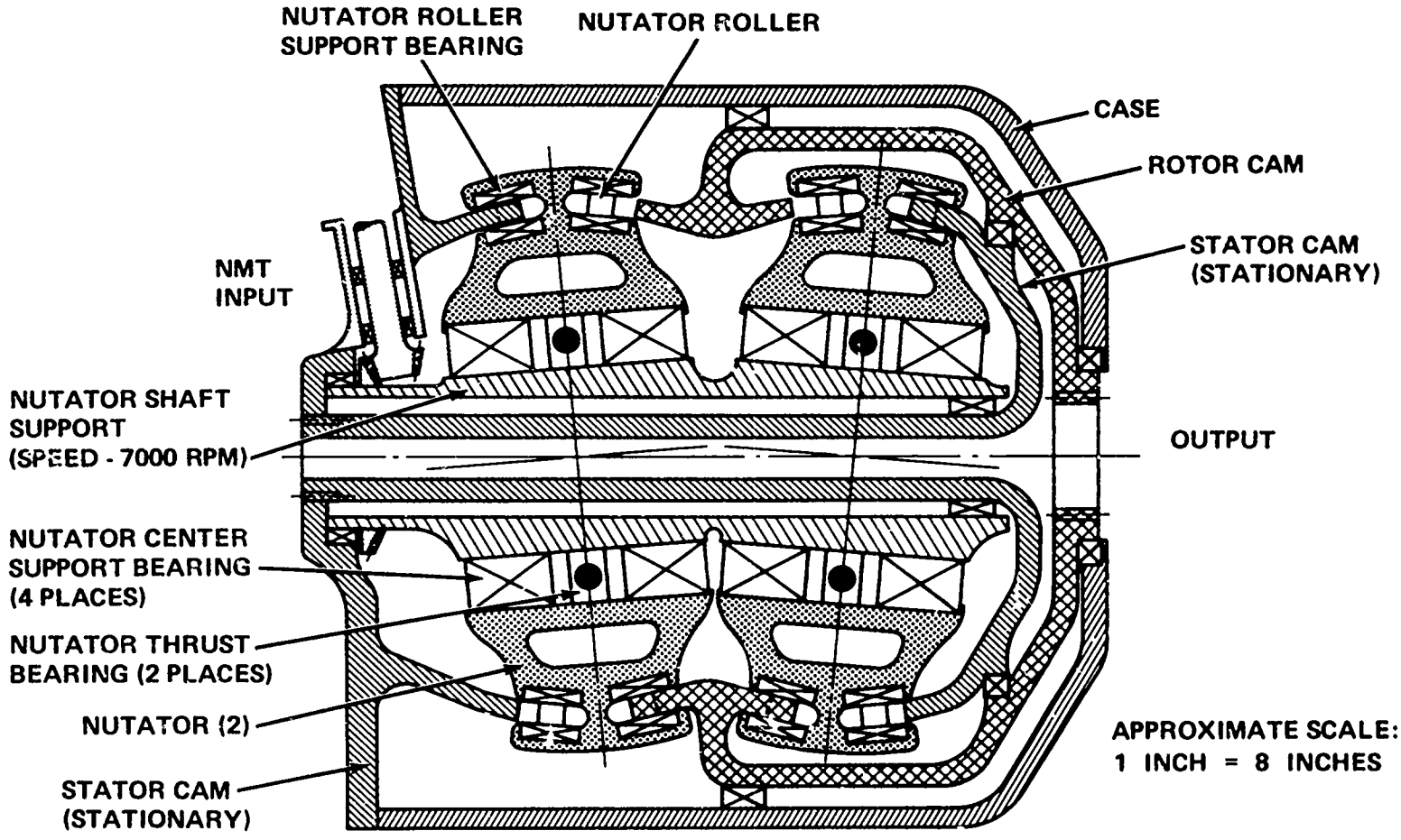

Figure 8-6. Design Example B

TABLE 8-5. WEIGHT SUMMARY OF NMT DESIGN EXAMPLE B (3600 HP)

Item	Number	Unit Weight (lb)	Weight (lb)
Bearings			
a. Center support cylindrical	4	83.0	333.0
b. Thrust ball	2	35.0	70.0
c. Nutator roller support (2 per roller)	232	1.0	232.0
d. Miscellaneous (cam and shaft support)	5		145.0
Shaft (steel)	1	225.0	225.0
Nutator (aluminum)	2	180.0	360.0
Stator cam (steel)			
Outer plate	1	375.0	375.0
Inner shaft	1	205.0	205.0
Rotor cam (steel)	1	605.0	605.0
Case (magnesium)	1	170.0	170.0
Nutator rollers (steel)	116	0.8	93.0
NMT input pinion and bearings	1	35.0	35.0
Subtotal - major components			2848.0
Misc. hardware (seals, bolts, nuts, washers, snap rings, retainer plates, etc.)	20% of total NMT weight		712.0
Total NMT Weight (lb)			3560.0
Specific Weight* (lb/hp)			1.0
CH-47 Forward Rotor Transmission Dry Weight (lb)			947.0

*Excluding weight of lubricant, lubrication system, cooling system, and associated hardware.

TABLE 8-6. SUMMARY OF NMT DESIGN EXAMPLE B

Type NMT	Dual Nutator - Split Power Path
Input configuration	Normal to mechanism axis
Power	3600 hp
Input speed	7000 rpm
Reduction ratio	30:1
Bearing design life	2000 B-10 hours
Number of teeth/rollers (rotor, nutator, stator)	30, 29, 29
Contact ratio	5.6
Nutation angle	5 degrees
Coning angle	10 degrees
Basic radius	12.0 inches
NMT diameter (max)	2.5 feet
NMT length (max)	2.8 feet
Nutator roller	
length	1.06 inches
ℓ/d	2.4
radius	0.59 inches
type	Solid with end bearings
Bearings	
Roller support	Series 306
Nutator center support	220 RN91 Torrington
Bearing DN	
Roller support (max)	6.8×10^5
Nutator center support	2.0×10^6
Bending stress	45.0 ksi
Contact stress	178.0 ksi
Nutator roller shaft slope	0.0007 in/in
Nutator support shaft	
diameter	7.1 inches
wall thickness	0.400 inch
Specific weight	1.0 lb/hp

impractically small (0.59 inch) for the cam follower mounting. Even for the solid roller mounting, which provides the minimum support shaft slope, the slope is excessive (0.0040 in/in). The only available way to reduce the slope is to reduce the roller length, but this is precluded by the already excessive stress levels; consequently, this tooth/roller combination will require a larger NMT diameter.

An acceptable design employing the 60, 59, 58 tooth/roller combination requires a basic radius of 16 inches. The bending (42,800 psi) and contact (155,900 psi) stresses are within allowable limits yet adequately utilize the capacity of the material. The slope (0.0006 in/in) is slightly above the specification, but is tolerable; the cubic mean radial load on a nutator roller is about 1900 pounds. A 0.7-inch long roller with a maximum radius of 0.800 inch may be supported by two Series 304 cylindrical roller bearings, each with a capacity of 6220 pounds. The life provided is in excess of 2000 hours. Although the average DN of such a bearing installation is about 6×10^5, it must be noted that instantaneous speeds in excess of 20,000 rpm are encountered. Since this is a potential source of considerable difficulty, it must be carefully weighed.

The center support bearing analysis is essentially the same as previously outlined since the overall load and speed of the NMT is unchanged.

Summarizing, the $N_S = N_R - 2$ combination provides a potentially feasible design; however, the overall size is larger than required for an $N_S = N_R - 1$ configuration. Consequently, for the aircraft application considered the latter combination is the more desirable alternative.

9. CONCLUSIONS

The following conclusions have been drawn from the analytical effort reported herein:

1. The feasibility of utilizing the nutating mechanical transmission concept has been demonstrated analytically.

2. In high speed, high load applications, the DN of the nutator support bearings and/or the nutator roller support bearings may exceed currently accepted state-of-the-art values, but may be within near term technology.

3. A split-power, double nutator, self balancing configuration appears to be the most practical design for high speed, high load applications.

4. Single nutator designs are inherently unbalanced and thus synchronous balance weights must be provided.

5. Although roller skidding is probable, design optimization may minimize its occurrence. However, it may be a limiting design factor in some cases.

6. Based on the aircraft design case study, the use of the nutating mechanical transmission in an aircraft application does not appear practical due to its weight to power ratio which is somewhat higher than that of current equivalent systems.

7. The weight to power ratio of the marine drive case study compares favorably with current equivalent systems and if the nutator support bearing DN and roller skidding problems can be resolved the Nutating Mechanical Transmission may be practical in this type of environment.

APPENDIX

DETAILED DERIVATION OF NUTATING MECHANICAL TRANSMISSION

MECHANISM SPEED RATIO AND COMPONENT SPEEDS

At this point, it will be advantageous to develop the equation for the reduction ratio of the mechanism. As in conventional gearing, the speed ratios between the various members of the nutating mechanical transmission are dependent upon the relative angular spacing of their teeth (i.e.: rotor and stator cam teeth and nutator rollers).

Considering the schematic diagram shown in Figure A1, we see that

$$\omega_{S/C} = \omega_{N/C} \left(N_{NS}/N_S \right) \tag{A1}$$

$$\omega_{R/C} = \omega_{N/C} \left(N_{NR}/N_R \right) \tag{A2}$$

Solving Equations (A1) and (A2) simultaneously yields

$$\omega_{R/C} \left(N_{NS}/N_S \right) - \omega_{S/C} \left(N_{NR}/N_R \right) = 0 \tag{A3}$$

But

$$\omega_{R/C} = \omega_R - \omega_C \tag{A4}$$

$$\omega_{S/C} = \omega_S - \omega_C \tag{A5}$$

Substituting Equations (A4) and (A5) into Equation (A3) yields

$$\omega_R \left(N_{NS}/N_S \right) - \omega_C \left[\left(N_{NS}/N_S \right) - \left(N_{NR}/N_R \right) \right] - \omega_S \left(N_{NR}/N_R \right) = 0 \tag{A6}$$

Solving for the rotor speed we have

$$\omega_R = \omega_C \left[1 - \frac{N_{NR}\, N_S}{N_R\, N_{NS}} \right] + \omega_S \left[\frac{N_{NR}\, N_S}{N_R\, N_{NS}} \right] \tag{A7}$$

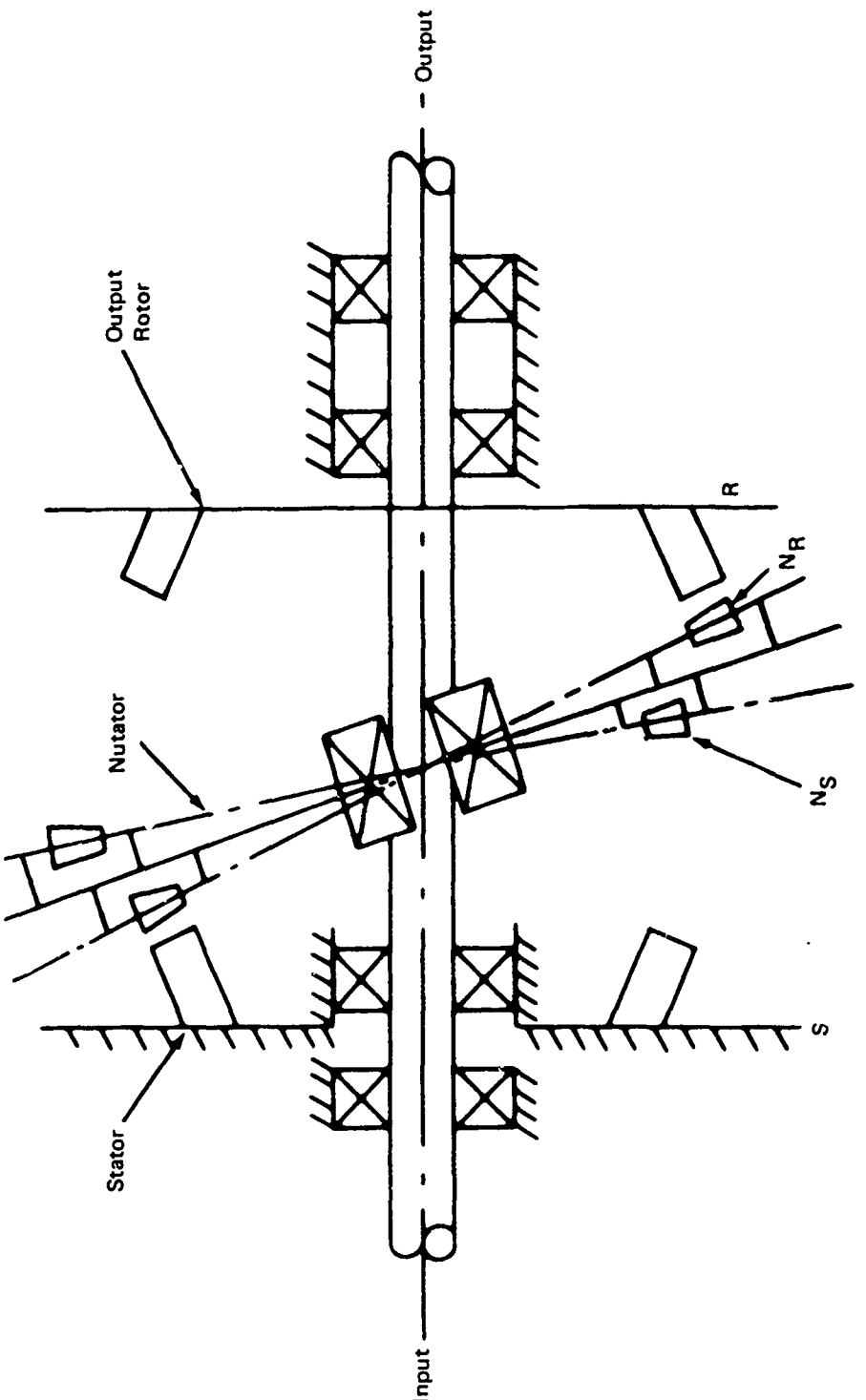

Figure A1. Nutating Mechanical Transmission.

Simplifying

$$\omega_R = \omega_C - \left[\frac{N_{NR}\, N_S}{N_R\, N_{NS}}\right](\omega_C - \omega_S) \tag{A8}$$

Some interesting observations may be made from Equation (A7).

If the stator is fixed, the reduction ratio of the mechanism is found by

$$M_{GF} = \frac{N_R\, N_{NS}}{N_R\, N_{NS} - N_{NR}\, N_S} : \left[\omega_{S/G} = 0\right] \tag{A9}$$

where

ω_R = rotor speed

ω_C = input speed

N_R = number of rotor teeth

N_{NR}= number of nutator rollers on the rotor side

N_{NS}= number of nutator rollers on the stator side

N_S = number of stator teeth

M_{GF}= fixed reduction ratio

If the stator is allowed to rotate at a controlled rate, we note that since

$$\frac{N_{NR}\, N_S}{N_R\, N_{NS}} = 1 - \frac{1}{M_{GF}} \tag{A10}$$

$$\omega_R = \omega_C/M_{GF} + \omega_S \left(\frac{M_{GF} - 1}{M_{GF}}\right) \tag{A11}$$

If the stator speed is expressed as a fraction, P, of the input speed, ω_C, then

$$\omega_R = \omega_C/M_{GF} + P\omega_C\left(\frac{M_{GF} - 1}{M_{GF}}\right) \tag{A12}$$

We may note that the rotor speed is zero if

$$0 = \omega_C \left(\frac{1}{M_{GF}}\right) + P\omega_C \left(\frac{M_{GF} - 1}{M_{GF}}\right) \tag{A13}$$

$$P = -\left(\frac{1}{M_{GF} - 1}\right) (\text{for } \omega_R = 0) \tag{A14}$$

Similarly, the variable reduction ratio may be expressed by

$$M_{GV} = \frac{M_{GF}}{1 + P\ (M_{GF} - 1)} \tag{A15}$$

In subsequent calculations, it will be necessary to use the relative angular velocities of the major components.

We will first derive the angular velocity of the nutator with respect to the rotor.

$$\omega_{R/G} = \omega_{R/N} + \omega_{N/G} \tag{A16}$$

$$\omega_{N/C} = \omega_{N/G} - \omega_{C/G} \tag{A17}$$

But from Equation (A1) we have

$$\omega_{N/C} = \omega_{S/C}\ (N_S/N_{NS}) \tag{A18}$$

So Equation (A17) becomes

$$\omega_{N/G} = \omega_{S/C}\ (N_S/N_{NS}) + \omega_{C/G} \tag{A19}$$

Substituting Equations (A19) and (A7) into equation (A16) yields

$$\omega_{C/G}\ \left[1 - \frac{N_{NR}\ N_S}{N_R N_{NS}}\right] + \omega_{S/G}\ \left[\frac{N_{NR}\ N_S}{N_R\ N_{NS}}\right] = \omega_{R/N}$$

$$+ \omega_{S/C}\ \left(\frac{N_S}{N_{NS}}\right) + \omega_{C/G} \tag{A20}$$

Simplifying

$$\omega_{S/G}\left(\frac{N_{NR}\,N_S}{N_R\,N_{NS}}\right) - \omega_{C/G}\left(\frac{N_{NR}\,N_S}{N_R\,N_{NS}}\right) = \omega_{R/N} + \omega_{S/C}\left(\frac{N_S}{N_{NS}}\right) \qquad \text{(A21)}$$

Noting that

$$\omega_{S/C} = -\omega_{C/S} = \omega_{S/G} - \omega_{C/G} \qquad \text{(A22)}$$

And substituting Equation (A22) into (A7) Equation (A21) gives

$$\omega_{S/G}\left(\frac{N_{NR}\,N_S}{N_R\,N_{NS}}\right) - \omega_{C/G}\left(\frac{N_{NR}\,N_S}{N_R\,N_{NS}}\right) = \omega_{R/N} - \omega_{C/G}\left(\frac{N_S}{N_{NS}}\right)$$

$$+\omega_{S/G}\left(\frac{N_S}{N_{NS}}\right) \qquad \text{(A23)}$$

Combining terms yields

$$\omega_{C/G}\left[\frac{N_S}{N_{NS}} - \frac{N_{NR}\,N_S}{N_R\,N_{NS}}\right] + \omega_{S/G}\left[\frac{N_{NR}\,N_S}{N_R\,N_{NS}} - \frac{N_S}{N_{NS}}\right] = \omega_{R/N} \qquad \text{(A24)}$$

Equation (A24) is the angular velocity of some point on the rotor with respect to some point on the nutator. The angular velocity of the nutator with respect to the rotor is the negative of this quantity, so

$$\omega_{N/R} = \omega_{C/G}\left(\frac{N_{NR}\,N_S - N_S\,N_R}{N_R\,N_{NS}}\right) + \omega_{S/G}\left(\frac{N_S\,N_R - N_S\,N_{NR}}{N_R\,N_{NS}}\right) \qquad \text{(A25)}$$

Simplifying Equation (A25) yields

$$\omega_{N/R} = \left(\frac{N_{NR}\,N_S - N_S\,N_R}{N_R\,N_{NS}}\right)\left(\omega_{C/G} - \omega_{S/G}\right) \qquad \text{(A26)}$$

Equation (A26) is valid for any tooth number combinations and for any member fixed; however, some interesting observations may be made by applying some restrictions:

$$\omega_{N/R} = \omega_{C/G}\left(\frac{N_{NR}\,N_S - N_S\,N_R}{N_R\,N_{NS}}\right) \quad (\omega_{S/G} = 0)$$

(Stator fixed) (A27)

Further, if the number of teeth on both sides of the nutator are the same,

$$\omega_{N/R} = \omega_{C/G}\left(\frac{N_S}{N_R} - \frac{N_S}{N_N}\right) \qquad \begin{matrix}(\omega_{S/G} = 0)\\ (N_{NS} = N_{NR} = N_N)\end{matrix} \tag{A28}$$

and finally, if the number of teeth on the stator and the nutator are identical,

$$\omega_{N/R} = \omega_{C/G}\left(\frac{N_N - N_R}{N_R}\right) \qquad \begin{matrix}(\omega_{S/G} = 0)\\ (N_{NS} = N_{NR} = N_N = N_S)\end{matrix} \tag{A29}$$

Similar reasoning may be used to derive the angular velocity of the nutator with respect to the stator.

Equation (A7) may be solved to yield the stator speed

$$\omega_{S/G} = \omega_{R/G}\left(\frac{N_R\, N_{NS}}{N_{NR} N_S}\right) - \omega_{C/G}\left(\frac{N_R\, N_{NS} - N_{NR}\, N_S}{N_{NR}\, N_S}\right) \tag{A30}$$

Noting that

$$\omega_{N/C} = \omega_{N/G} - \omega_{C/G} \tag{A31}$$

and from Equation (A2)

$$\omega_{N/C} = \omega_{R/C}\left(\frac{N_R}{N_{NR}}\right) \tag{A32}$$

also

$$\omega_{S/G} = \omega_{S/N} + \omega_{N/G} \tag{A33}$$

therefore,

$$\omega_{N/G} = \omega_{R/C}\left(\frac{N_R}{N_{NR}}\right) + \omega_{C/G} \tag{A34}$$

Substituting Equations (A34) and (A30) into Equation (A33) yields

$$\omega_{R/G}\left(\frac{N_R\, N_{NS}}{N_{NR}\, N_S}\right) - \omega_{C/G}\left(\frac{N_R\, N_{NS} - N_{NR}\, N_S}{N_{NR}\, N_S}\right) = \omega_{S/N} + \omega_{R/C}\left(\frac{N_R}{N_{NR}}\right) + \omega_{C/G} \tag{A35}$$

simplifing

$$\omega_{R/G}\left(\frac{N_R N_{NS}}{N_{NR} N_S}\right) - \omega_{C/G}\left(\frac{N_R N_{NS}}{N_{NR} N_S}\right) = \omega_{S/N} + \omega_{R/C}\left(\frac{N_R}{N_{NR}}\right) \quad \text{(A36)}$$

We note that

$$\omega_{R/C} = -\omega_{C/R} = \omega_{R/G} - \omega_{C/G} \quad \text{(A37)}$$

Substituting Equation (A37) into Equation (A36) gives

$$\omega_{R/G}\left(\frac{N_R N_{NS}}{N_{NR} N_S}\right) - \omega_{C/G}\left(\frac{N_R N_{NS}}{N_{NR} N_S}\right) = \omega_{S/N} - \omega_{C/G}\left(\frac{N_R}{N_{NR}}\right) + \omega_{R/G}\left(\frac{N_R}{N_{NR}}\right) \quad \text{(A38)}$$

Combining terms yields

$$\omega_{S/N} = \omega_{C/G}\left[\frac{N_R}{N_{NR}} - \frac{N_R N_{NS}}{N_{NR} N_S}\right] + \omega_{R/G}\left[\frac{N_R N_{NS}}{N_{NR} N_S} - \frac{N_R}{N_{NR}}\right] \quad \text{(A39)}$$

Equation (A38) may be written

$$\omega_{N/S} = \omega_{C/G}\left[\frac{N_R N_{NS} - N_R N_S}{N_{NR} N_S}\right] + \omega_{R/G}\left[\frac{N_R N_S - N_R N_{NS}}{N_{NR} N_S}\right] \quad \text{(A40)}$$

Simplifying yields

$$\omega_{N/S} = \left[\frac{N_{NS} N_R - N_R N_S}{N_S N_{NR}}\right]\left(\omega_{C/G} - \omega_{R/G}\right) \quad \text{(A41)}$$

Equations (A41) and (A25) are quite similar in form, which points out the basic similarity of the rotor and stator. Substituting Equation (A8) into Equation (A41) gives

$$\omega_{N/S} = \left[\frac{N_{NS} N_R - N_R N_S}{N_S N_{NR}}\right]\left[\omega_{C/G} - \omega_{C/G} + \left(\frac{N_{NR} N_S}{N_R N_{NS}}\right)(\omega_{C/G} - \omega_{S/G})\right] \quad \text{(A42)}$$

which simplifies to

$$\omega_{N/S} = \left[\frac{N_{NS} N_R - N_R N_S}{N_R N_{NS}} \right] (\omega_{C/G} - \omega_{S/G}) \quad \text{(A43)}$$

and ultimately

$$\omega_{N/S} = \left[\frac{N_{NS} - N_S}{N_{NS}} \right] (\omega_{C/G} - \omega_{S/G}) \quad \text{(A44)}$$

Equation (A44) is valid in the most general case. Some restrictions will prove interesting.

If the stator is fixed,

$$\omega_{N/S} = \left[\frac{N_{NS} - N_S}{N_{NS}} \right] \omega_{C/G} \; ; \; (\omega_{S/G} = 0) \quad \text{(A45)}$$

If the number of teeth on the stator and the stator side of the nutator are equal,

$$\omega_{N/S} = 0.0; \; (N_{NS} = N_S) \quad \text{(A46)}$$

If we now consider Equations (A26) and (A43) we may write a general expression for the angular velocity of the nutator with respect to either the rotor or stator:

$$\omega_{N/CA} = \left[\frac{N_{NCA} N'_{CA} - N_S N_R}{N_R N_{NS}} \right] [\omega_{C/G} - \omega_{S/G}] \quad \text{(A47)}$$

where N_{NCA} = number of rollers on cam side of nutator

N'_{CA} = number of teeth on the cam (rotor or stator) not under consideration (NOTE: If rotor is under consideration, $N'_{CA} = N_S$ and if stator is under consideration, $N'_{CA} = N_R$)

$\omega_{C/G}$ = Input speed

At this point it is convenient to derive the equations for the velocities of all the major components.

The angular velocity of the rotor with respect to the reference frame, in the most general case is given by Equation (A8)

$$\omega_R = \omega_C - \left[\frac{N_{NR}\, N_S}{N_R\, N_{NS}}\right]\left[\omega_C - \omega_S\right] \tag{A8}$$

where ω_C = input speed

ω_R = rotor speed

ω_S = stator speed

The angular velocity of the nutator with respect to the reference frame is found considering Equation (A19) by

$$\omega_{N/G} = \omega_{S/C}\,(N_S/N_{NS}) + \omega_{C/G} \tag{A19}$$

$$\omega_{S/C} = \omega_{S/G} - \omega_{C/G} \tag{A48}$$

Substituting Equation (A48) into Equation (A19) yields

$$\omega_{N/G} = (\omega_{S/G} - \omega_{C/G})\left(\frac{N_S}{N_{NS}}\right) + \omega_{C/G} \tag{A49}$$

But if we express the stator speed as a fraction P of the input speed,

$$\omega_{N/G} = \omega_{C/G}\left(\frac{(P-1)\, N_S}{N_{NS}} + 1\right) \tag{A50}$$

From Equation (A50) we can see that if the stator is stationary, that is if $\omega_{S/G} = 0$ and $P = 0$, the nutator speed is

$$\omega_{N/G} = \omega_{C/G}\left(\frac{N_{NS} - N_S}{N_{NS}}\right); \quad (\omega_{S/G} = 0) \tag{A51}$$

If the number of teeth on the stator and the stator side of the nutator are the same, Equation (A50) becomes

$$\omega_{N/G} = \omega_{C/G}\ [P]\ ;\ (N_{NS} = N_S) \tag{A52}$$

Obviously if the stator is also stationary, from equation (A52) we can see that the nutator does not rotate

$$\omega_{N/G} = 0 \qquad N_{NS} = N_S \ \&\ \omega_{S/G} = 0 \tag{A53}$$

In all cases, the nutator undergoes an oscillatory motion due to it's "Lemniscular" motion.

The angular velocity of the nutator with respect to the input shaft is required to calculate the life of the nutator support bearing. It is given by

$$\omega_{N/C} = \omega_{N/G} - \omega_{C/G} \tag{A54}$$

substituting Equation (A49) into Equation (A54) yields

$$\omega_{N/C} = (\omega_{S/G} - \omega_{C/G}) \left(\frac{N_S}{N_{NS}}\right) + \omega_{C/G} - \omega_{C/G} \tag{A55}$$

Simplifying

$$\omega_{N/C} = (\omega_{S/G} - \omega_{C/G}) \left(\frac{N_S}{N_{NS}}\right) \tag{A56}$$

Again expressing the stator speed as a fraction of the input

$$\omega_{N/C} = \omega_{C/G}\ (P-1) \left(\frac{N_S}{N_{NS}}\right) \tag{A57}$$

If the stator is stationary,

$$\omega_{N/C} = -\omega_{C/G} \left(\frac{N_S}{N_{NS}}\right)\ ;\ (\omega_{S/G} = 0) \tag{A58}$$

If the number of teeth on the stator and stator side of the nutator are the same,

$$\omega_{N/C} = \omega_{C/G}\,(P-1);\ (N_S = N_{NS}) \tag{A59}$$

finally if $\omega_{S/G} = 0$ and $N_S = N_{NS}$

$$\omega_{N/C} = -\omega_{C/G} \qquad (N_S = N_{NS})\ (\omega_{S/G} = 0) \tag{A60}$$

PATH OF POINT ON CENTERLINE OF NUTATOR ROLLER WITHIN CAM AS A FUNCTION OF INPUT ANGLE

Consider the schematic view of the nutator cam system shown in Figure A2. The XYZ coordinate system is attached to and rotates with the input shaft. Point 2 is the point of interest on the centerline of the nutator roller. Initially at $\omega_0 = 0$, points 3 and 1 are coincident. If we initially assume that there is no relative motion between the cams and the nutator, we may calculate the path of a point on the centerline of a nutator roller due solely to the nutation of the nutator with respect to the input.

The location of the point of interest 2 on the centerline of a nutator roller as a function of the input angle ω_0 is shown as a spherical projection in Figure A3. The coordinates of a point on the centerline of a nutator roller within a cam may be obtained by considering the rotation of the cam with respect to the nutator and super-imposing this motion upon that due to nutation. The net result is the total motion of a point on the centerline of a nutator roller within a cam (either rotor or stator).

The angle $\theta_{CA/N}$ shown in Figure A4 is that angle through which the cam rotates with respect to the nutator when the input rotates through an angle ω_0. $\theta_{CA/N}$ is the integral of the angular velocity of the cam with respect to the nutator.

Although the coordinates of the path of a point on the centerline of a nutator roller within a cam may be obtained directly, it will be of some interest to understand the contribution of the nutating action to this motion, thus the equations will be set up such that the net nutation path and the total path may be identified individually.

The nutating path of a point on the centerline of a nutator roller may be found by considering the spherical triangles formed when $\theta_{CA/N}$ is set equal to zero.

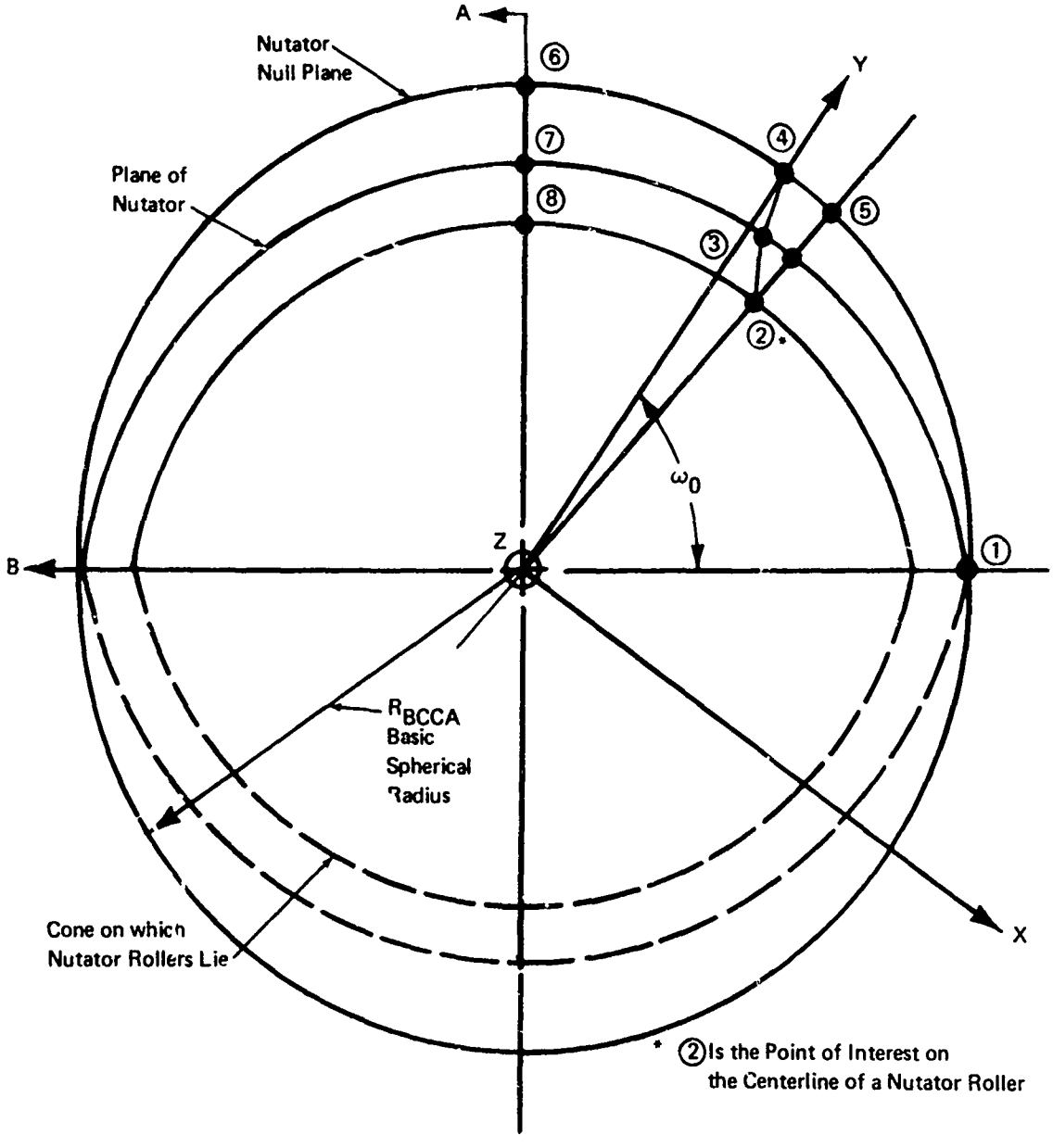

Figure A2. Basic Sphere.

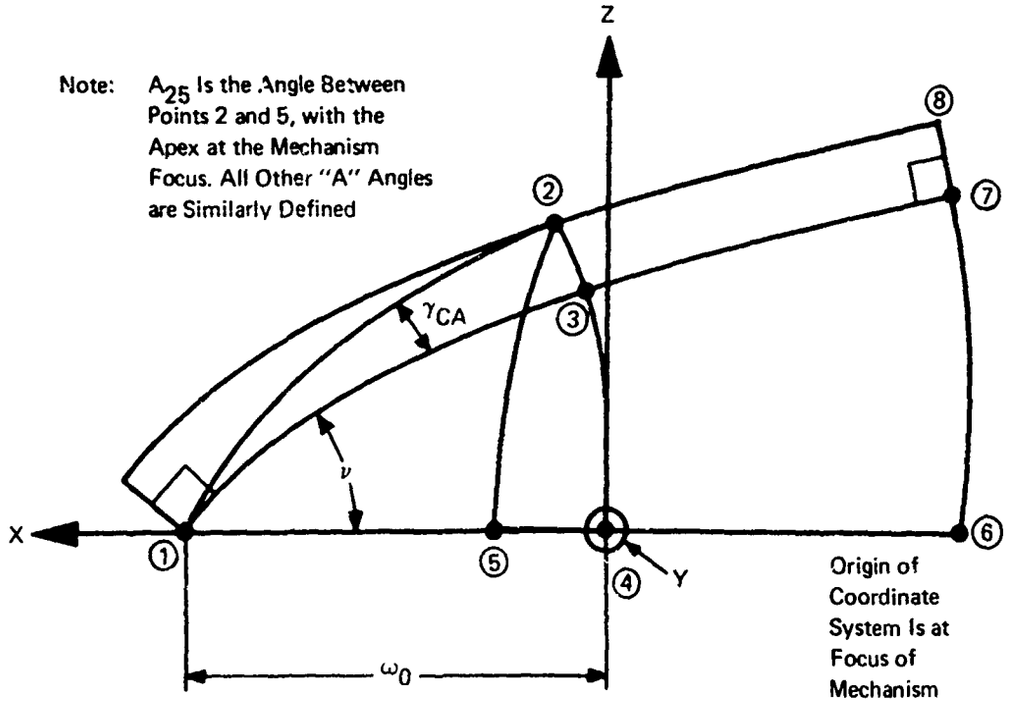

Figure A3. Spherical Projection of Instantaneous Nutator Position With No Relative Motion of Cam.

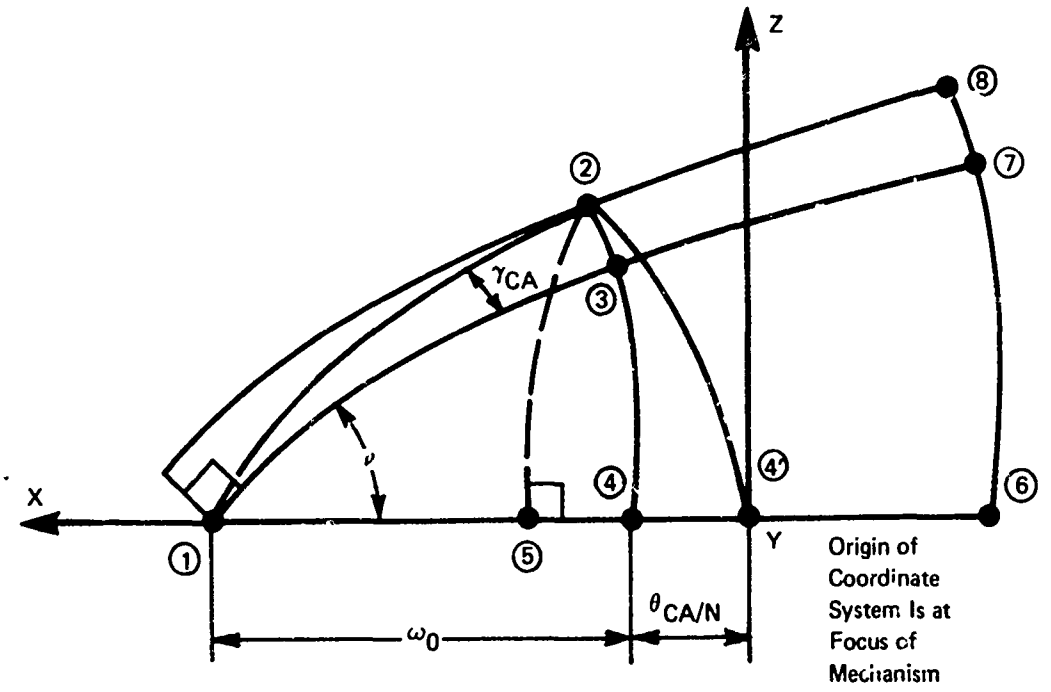

Figure A4. Spherical Projection of Instantaneous Nutator Position With Relative Motion of Cam.

Thus considering Figure A3 we follow the position of point 4 as it moves around the sphere:

$$A_{23CA} = \sigma_{CA} = \text{Roller Centerline Coning Angle} \quad \text{(A61)}$$

$$A_{14} = \omega_0 = A_{13} = \text{Input Angle} \quad \text{(A62)}$$

$$A_{12CA} = \text{Cos}^{-1} \left[\text{Cos } (A_{23CA}) \text{ Cos } (A_{13})\right] \quad \text{(A63)}$$

$$A_{12CA} = \text{Cos}^{-1} \left[\text{Cos } (\sigma_{CA}) \text{ Cos } (\omega_0)\right] \quad \text{(A64)}$$

$$\gamma_{CA} = \text{Sin}^{-1} \left[\text{Sin } (\sigma_{CA})/\text{Sin } (A_{12CA})\right] \quad \text{(A65)}$$

$$A_{25CA} = \text{Sin}^{-1} \left[\text{Sin } (\gamma_{CA} + \nu) \text{ Sin } (A_{12CA})\right] \quad \text{(A66)}$$

$$A_{15CA} = \text{Sin}^{-1} \left[\text{Tan } (A_{25CA})/\text{Tan } (\gamma_{CA} + \nu)\right] \quad \text{(A67)}$$

$$A_{54CA} = A_{14} - A_{15CA} = \omega_0 - A_{15CA} \quad \text{(A68)}$$

$$Z_{PCA} = R_{BCCA} \text{ Sin } (A_{25CA}) \quad \text{(A69)}$$

$$X_{PCA} = R_{BCCA} \text{ Cos } (A_{25CA}) \text{ Sin } (A_{54CA}) \quad \text{(A70)}$$

$$Y_{PCA} = R_{BCCA} \text{ Cos } (A_{25CA}) \text{ Cos } (A_{54CA}) \quad \text{(A71)}$$

where

R_{BCCA} = Basic Spherical Radius

X_{PCA}, Y_{PCA}, and Z_{PCA} = Coordinates of nutating path of a point on the centerline of a nutator roller

The actual path of a point on the centerline of a roller within a cam may be determined by observing from the nutator the motion of the cam with respect to it. In general, the cam will turn, with respect to the nutator, through some angle, $\theta_{CA/N}$, while the input turns through the angle ω_0.

The angle $\theta_{CA/N}$ is the integral of the angular velocity of the cam with respect to the nutator. A later section, dealing with the gross mechanism kinematics, defines the angular velocity of the nutator with respect to the cam. By taking the negative integral of this parameter, the parameter may be derived as

$$\theta_{CA/N} = \left[\frac{N_S N_R - N_{NCA} N'_{CA}}{N_R N_{NS}}\right] (\omega_0 - \theta_S) \quad \text{(A72)}$$

where $\theta_{CA/N}$ = Angular rotation of cam with respect to nutator

θ_S = Angular rotation of stator (Generally = 0.0)

N_S = Number of teeth on stator

N_R = Number of teeth on rotor

N_{NS} = Number of rollers on stator side of nutator

N_{NCA} = Number of rollers on cam side of nutator

N'_{CA} = Number of teeth on cam <u>not</u> under consideration.

The coordinates of the path of a point on the centerline of a nutator roller within a cam are (considering Figure A4) given by

$$A'_{54CA} = A_{14} - A_{15CA} + A'_{44CA} \quad \text{(A73)}$$

$$A'_{54CA} = \omega_0 - A_{15CA} + \theta_{CA/N} \quad \text{(A74)}$$

Care must be exercised in determining the proper sign for $\theta_{CA/N}$

$$X_{PCA/CA} = R_{BCCA} \text{ Cos } (A_{25CA}) \text{ Sin } (A'_{54CA}) \quad \text{(A75)}$$

$$Y_{PCA/CA} = R_{BCCA} \text{ Cos } (A_{25CA}) \text{ Cos } (A'_{54CA}) \quad \text{(A76)}$$

$$Z_{PCA/CA} = Z_{PCA} \quad \text{(A77)}$$

COORDINATES OF CAM TOOTH PROFILES

At this point it is of great interest to develop the equations required to define the coordinates of the required profiles on the rotor and stator teeth. Having defined equations for the X, Y, and Z coordinates of the path of a point on the centerline of a nutator roller (i.e., the "pitch path") we may now proceed to find the equation of the tangent line at any point along this path. The corresponding point of contact on the tooth profile may then be found by deriving an equation for a line through the pitch path point which is mutually perpendicular to the tangent line and to the roller axis. Finally the actual coordinate points may be calculated by proceeding along this line from the pitch path point of interest a distance equal to the roller radius (see Figure A5).

Since the coordinates of the pitch path are expressed in parametric form as

$$X_{PCA/CA} = f_1\ (\omega_0) \tag{A78}$$

$$Y_{PCA/CA} = f_2\ (\omega_0) \tag{A79}$$

$$Z_{PCA/CA} = f_3\ (\omega_0) \tag{A80}$$

The direction cosines of a line tangent to the path of a point on the centerline of a nutator roller may be defined by differentiating equations (A78), (A79), and (A80) with respect to the parameter ω_0.

$$\frac{d\ X_{PCA/CA}}{d\ \omega_0} = \alpha'_{PCA/CA} \tag{A81}$$

$$\alpha'_{PCA/CA} = R_{BCCA}\left[\cos(A_{25CA})\frac{d\ \sin(A'_{54CA})}{d\ \omega_0} + \sin(A'_{54CA})\frac{d\ \cos(A_{25CA})}{d\ \omega_0}\right] \tag{A82}$$

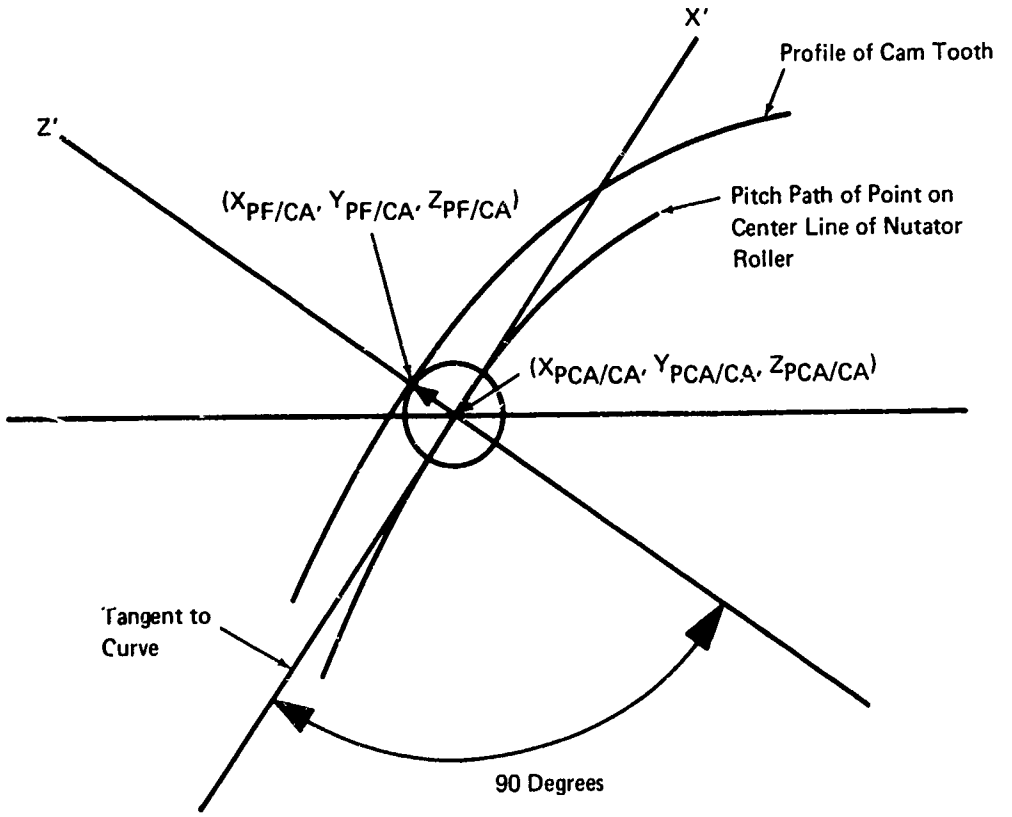

Figure A5. View in Plane of Roller Diameter, Perpendicular to Axis of Roller.

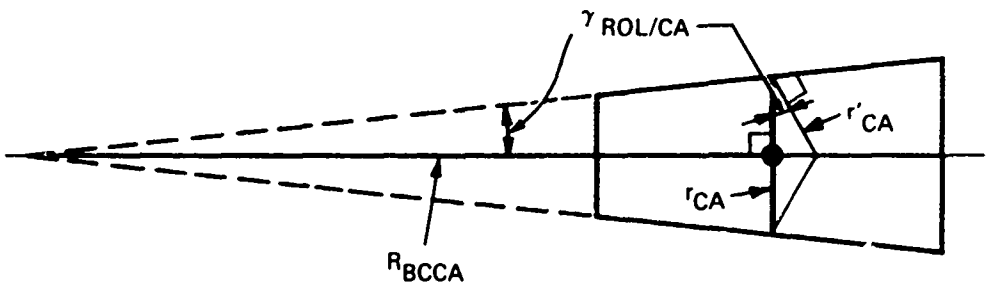

Figure A6. Derivation of the Radius of Curvature of the Roller.

$$\frac{d\ Y_{PCA/CA}}{d\omega_0} = \beta'_{PCA/CA} = R_{BCCA}\left[\text{Cos}(A_{25CA})\ \frac{d\ \text{Cos}\ (A'_{54CA})}{d\omega_0}\right. \tag{A83}$$

$$\left. + \text{Cos}\ (A'_{54CA})\ \frac{d\ \text{Cos}\ (A_{25CA})}{d\omega_0}\right]$$

$$\frac{d\ Z_{PCA/CA}}{d\omega_0} = \gamma'_{PCA/CA} = R_{BCCA}\frac{d\ \text{Sin}\ (A_{25CA})}{d\omega_0} \tag{A84}$$

$$\frac{d\ A_{25CA}}{d\omega_0} = \text{Sin}\ (\gamma_{CA} + \nu)\ \frac{d\ \text{Sin}\ (A_{12CA})}{d\omega_0} \tag{A85}$$

$$+ \text{Sin}\ (A_{12CA})\ \frac{d\ \text{Sin}\ (\gamma_{CA} + \nu)}{d\omega_0}$$

$$\frac{d\ \text{Sin}\ (A_{12CA})}{d\omega_0} = \text{Cos}\ (A_{12CA})\frac{dA_{12CA}}{d\omega_0} \tag{A86}$$

$$\frac{d\ A_{12CA}}{d\omega_0} = \frac{\text{Cos}\ (\sigma_{CA})\ \text{Sin}\ (\omega_0)}{\sqrt{1 - \text{Cos}^2\ (\sigma_{CA})\ \text{Cos}^2\ (\omega_0)}} \tag{A87}$$

$$\frac{d\ \text{Sin}\ (\gamma_{CA} + \nu)}{d\omega_0} = \text{Cos}\ (\gamma_{CA} + \nu)\ \frac{d\gamma_{CA}}{d\omega_0} \tag{A88}$$

$$\frac{d\gamma_{CA}}{d\omega_0} = \frac{-\ \text{Sin}(\sigma_{CA})\ \text{Cos}\ (A_{12CA})\ \frac{d\ A_{12CA}}{d\omega_0}}{\text{Sin}^2\ (A_{12CA})\sqrt{1-\text{Sin}^2(\sigma_{CA})/\text{Sin}^2(A_{12CA})}} \tag{A89}$$

$$\frac{d\ \text{Cos}\ (A_{25CA})}{d\omega_0} = -\ \text{Sin}\ (A_{25CA})\ \frac{d\ A_{25CA}}{d\omega_0} \tag{A90}$$

$$\frac{d\,A_{25CA}}{d\,\omega_0} = \frac{\sin(\gamma_{CA}+\nu)\,\frac{d\,\sin(A_{12CA})}{d\,\omega_0} + \sin(A_{12CA})\frac{d\,\sin(\gamma_{CA}+\nu)}{d\,\omega_0}}{\sqrt{1 - \sin^2(\gamma_{CA}+\nu)\,\sin^2(A_{12CA})}} \quad \text{(A91)}$$

$$\frac{d\,\sin(A_{12CA})}{d\,\omega_0} = \cos(A_{12CA})\,\frac{d\,A_{12CA}}{d\,\omega_0} \quad \text{(A92)}$$

$$\frac{d\,\cos(A'_{54CA})}{d\,\omega_0} = -\sin(A'_{54CA})\,\frac{d\,A'_{54CA}}{d\,\omega_0} \quad \text{(A93)}$$

$$\frac{d\,A'_{54CA}}{d\,\omega_0} = 1. - \frac{d\,A_{15CA}}{d\,\omega_0} + \frac{d\,\theta_{CA/N}}{d\,\omega_0} \quad \text{(A94)}$$

$$\frac{d\,\theta_{CA/N}}{d\,\omega_0} = \left[\frac{N_S N_R - N_{NCA} N'_{CA}}{N_R\,N_{NS}}\right]\left(1. - \frac{d\,\theta_S}{d\,\omega_0}\right) \quad \text{(A95)}$$

If $\theta_S = 0$,

$$\frac{d\,\theta_{CA/N}}{d\,\omega_0} = \left[\frac{N_S N_R - N_{NCA} N'_{CA}}{N_R\,N_{NS}}\right] \quad \text{(A96)}$$

$$\frac{d\,\tan(A_{25CA})}{d\,\omega_0} = \frac{\frac{d\,A_{25CA}}{d\,\omega_0}}{\cos^2(A_{25CA})} \quad \text{(A97)}$$

$$\frac{d\,\tan(\gamma_{CA}+\nu)}{d\,\omega_0} = \frac{\frac{d\,\gamma_{CA}}{d\,\omega_0}}{\cos^2(\gamma_{CA}+\nu)} \quad \text{(A98)}$$

$$\frac{d\,A_{15CA}}{d\,\omega_0} = \frac{\left[\left(\frac{\mathrm{Tan}(\gamma_{CA}+\nu)}{\mathrm{Cos}^2\,(A_{25CA})}\right)\left(\frac{d\,A_{25CA}}{d\,\omega_0}\right) - \left(\frac{\mathrm{Tan}(A_{25CA})}{\mathrm{Cos}^2\,(\gamma_{CA}+\nu)}\right)\left(\frac{d\,\gamma_{CA}}{d\,\omega_0}\right)\right]}{\mathrm{Tan}^2\,(\gamma_{CA}+\nu)\sqrt{1-\mathrm{Tan}^2(A_{25CA})/\mathrm{Tan}^2(\gamma_{CA}+\nu)}} \quad \text{(A99)}$$

$$\frac{d\,\mathrm{Sin}\,(A'_{54CA})}{d\,\omega_0} = \mathrm{Cos}\,(A'_{54CA})\,\frac{d\,A'_{54CA}}{d\,\omega_0} \quad \text{(A100)}$$

The equation of the tangent line may now be written as

$$\frac{X_{TCA}-(X_{PCA/CA})_i}{(\alpha'_{PCA/CA})_i} = \frac{Y_{TCA}-(Y_{PCA/CA})_i}{(\beta'_{PCA/CA})_i} = \frac{Z_{TCA}-(Z_{PCA/CA})_i}{(\gamma'_{PCA/CA})_i} \quad \text{(A101)}$$

where

$$(\alpha'_{PCA/CA})_i,\ (\beta'_{PCA/CA})_i,\ (\gamma'_{PCA/CA})_i$$

are the derivatives of the coordinates of the path evaluated at the point of interest (direction numbers of the line)

$$(X_{PCA/CA})_i,\ (Y_{PCA/CA})_i,\ (Z_{PCA/CA})_i$$

are the coordinates of the path evaluated at the point of interest.

The direction cosines of the tangent line are

$$\mathrm{Cos}(\alpha_{PCA/CA}) = \frac{\alpha'_{PCA/CA}}{\sqrt{\alpha'^2_{PCA/CA} + \beta'^2_{PCA/CA} + \gamma'^2_{PCA/CA}}} \quad \text{(A102)}$$

$$\mathrm{Cos}(\beta_{PCA/CA}) = \frac{\beta'_{PCA/CA}}{\sqrt{\alpha'^2_{PCA/CA} + \beta'^2_{PCA/CA} + \gamma'^2_{PCA/CA}}} \quad \text{(A103)}$$

$$\mathrm{Cos}(\gamma_{PCA/CA}) = \frac{\gamma'_{PCA/CA}}{\sqrt{\alpha'^2_{PCA/CA} + \beta'^2_{PCA/CA} + \gamma'^2_{PCA/CA}}} \quad \text{(A104)}$$

For a straight line, we know that the direction cosines may be found by

$$\mathrm{Cos}\,(\alpha) = \frac{X_2-X_1}{d} \quad \text{(A105)}$$

$$\text{Cos } (\beta) = \frac{Y_2 - Y_1}{d} \tag{A106}$$

$$\text{Cos } (\gamma) = \frac{Z_2 - Z_1}{d} \tag{A107}$$

Where Cos (α), Cos (β), Cos (γ) are the direction cosines X_1, X_2, Y_1, Y_2, Z_1, Z_2 are the coordinates of points 1 and 2 on the line and d is the distance between points 1 and 2 along the line.

Thus the direction cosines of a line from the mechanism focus to a point on the centerline of a nutator roller are given by

$$\text{Cos } (\alpha_{CLCA}) = \frac{X_{PCA/CA}}{R_{BCCA}} \tag{A108}$$

$$\text{Cos } (\beta_{CLCA}) = \frac{Y_{PCA/CA}}{R_{BCCA}} \tag{A109}$$

$$\text{Cos } (\gamma_{CLCA}) = \frac{Z_{PCA/CA}}{R_{BCCA}} \tag{A110}$$

This line is, of course, the radius vector R_{BCCA}. The radius vector fro the origin to a point on the roller axis, the radius vector of a cylindrical roller from this point on the roller axis, and the tangent line to the pitch path at this point are all mutually perpendicular. In addition, the sum of the squares of the direction cosines for any line is unity and the angle between any two lines may be expressed as a function of the products of their direction cosines, that is

$$\text{Cos}^2 (\alpha) + \text{Cos}^2 (\beta) + \text{Cos}^2 (\gamma) = 1 \tag{A111}$$

and

$$\text{Cos } (\theta) = \text{Cos } (\alpha_1) \text{ Cos } (\alpha_2) + \text{Cos } (\beta_1) \text{ Cos } (\beta_2) + \text{Cos } (\gamma_1) \text{ Cos } (\gamma_2) \tag{A112}$$

where α_1, β_1, γ_1 and α_2, β_2, γ_2 are the direction cosines of two intersecting lines

θ = angle between the two lines measured in the plane defined by the lines

The direction cosines of a line between a point on the pitch path and the tooth profile may be found by solving three simultaneous equations in three unknowns.

If we define $\text{Cos}(\alpha_{PFCA})$, $\text{Cos}(\beta_{PFCA})$, and $\text{Cos}(\gamma_{PFCA})$ as the direction cosines of a line from a point on the pitch path to a corresponding point on the tooth profile, we may write the following equations:

$$\text{Cos}^2(\alpha_{PFCA}) + \text{Cos}^2(\beta_{PFCA}) + \text{Cos}^2(\gamma_{PFCA}) = 1 \qquad \text{(A113)}$$

$$\begin{aligned}\text{Cos}\ (\theta_{PF/PPCA}) = {} & \text{Cos}\ (\alpha_{PCA/CA})\ \text{Cos}\ (\alpha_{PFCA}) \\ & + \text{Cos}\ (\beta_{PFCA})\ \text{Cos}\ (\beta_{PCA/CA}) \\ & + \text{Cos}\ (\gamma_{PFCA})\ \text{Cos}\ (\gamma_{PCA/CA}) = 0\end{aligned} \qquad \text{(A114)}$$

where $\theta_{PF/PPCA}$ = angle between the line defined by a point on the pitch path and the corresponding point on the tooth profile and the tangent line to the pitch path at the point of interest. This is a right angle.

$$\begin{aligned}\text{Cos}\ (\theta_{PF/RVCA}) = {} & \text{Cos}\ (\alpha_{PFCA})\ \text{Cos}\ (\alpha_{CLCA}) \\ & + \text{Cos}\ (\beta_{PFCA})\ \text{Cos}\ (\beta_{CLCA}) + \text{Cos}\ (\gamma_{PFCA})\ \text{Cos}\ (\gamma_{CLCA})\end{aligned} \qquad \text{(A115)}$$

where $\theta_{PF/RVCA}$ = angle between the line defined by a point on the pitch path and the corresponding point on the tooth profile, and the radius vector from the mechanism focus to the point on the pitch path. This is also a right angle for an untapered cylindrical roller.

$\theta_{PF/RVCA}$ is a function of the roller radius and the basic spherical radius.

Since the rollers actually are tapered, $\theta_{PF/RVCA}$ must be modified to account for the effective roller curvature radius seen by the cam teeth.

From Figure A6 we have

$$\gamma_{ROL/CA} = \text{Tan}^{-1}\ (r_{CA}/R_{BCCA}) \qquad \text{(A116)}$$

$$r'_{CA} = r_{CA}/\text{Cos}\ (\gamma_{ROL/CA}) \qquad \text{(A117)}$$

$$\theta_{PF/RVCA} = 90 - \gamma_{ROL/CA} \qquad \text{(A118)}$$

where r'_{CA} = roller curvature radius

Equations (A113), (A114), and (A115) may be written in the following form

$$X^2 + Y^2 + Z^2 = 1 \tag{A119}$$

$$AX + BY + CZ = 0 \tag{A120}$$

$$DX + EY + FZ = K \tag{A121}$$

where $X = \cos(\alpha_{PFCA})$

$Y = \cos(\beta_{PFCA})$

$Z = \cos(\gamma_{PFCA})$

$A = \cos(\alpha_{PCA/CA})$

$B = \cos(\beta_{PCA/CA})$

$C = \cos(\gamma_{PCA/CA})$

$D = \cos(\alpha_{CLCA})$

$E = \cos(\beta_{CLCA})$

$F = \cos(\gamma_{CLCA})$

$K = \cos(\theta_{PF/RVCA})$

Equation (A121) may be solved for X and the result substituted into Equation (A120).

$$X = \frac{K - EY - FZ}{D} \tag{A122}$$

$$\frac{AK}{D} - \frac{AE}{D} Y - \frac{AF}{D} Z + BY + CZ = 0 \tag{A123}$$

Equation (A123) may now be solved for Y and the result substituted into Equation (A122).

$$Y = \left[\frac{AF - CD}{DB - EA}\right] Z - \left[\frac{AK}{DB - EA}\right] \tag{A124}$$

$$X = \frac{K}{D} - \left[\frac{E}{D}\left[\frac{AF - CD}{DB - EA}\right] + \frac{F}{D}\right] Z + \left[\frac{EAK}{D\,(DB - EA)}\right] \tag{A125}$$

If we now define the following auxiliary variables,

$$A_O = \frac{AF - CD}{DB - EA} \tag{A126}$$

$$B_O = \frac{AK}{DB - EA} \tag{A127}$$

$$C_O = \frac{K}{D} + \frac{EAK}{D\,(DB - EA)} \tag{A128}$$

$$D_O = \frac{E}{D}\left[\frac{AF - CD}{DB - EA}\right] + \frac{F}{D} \tag{A129}$$

we may write

$$Y^2 = A_O{}^2\, Z^2 - 2\, A_O B_O\, Z + B_O{}^2 \tag{A130}$$

$$X^2 = C_O{}^2 - 2\, C_O D_O\, Z + D_O{}^2\, Z^2 \tag{A131}$$

and finally substitution into Equation (A119) will yield

$$Z^2(A_O{}^2 + D_O{}^2 + 1) - Z\,2(A_O B_O + C_O D_O) + B_O{}^2 + C_O{}^2 - 1 = 0 \tag{A132}$$

which is a quadratic in Z so

$$Z = \frac{2(A_O B_O + C_O D_O) \pm \sqrt{(2(A_O B_O + C_O D_O))^2 - 4(A_O{}^2 + D_O{}^2 + 1)(B_O{}^2 + C_O{}^2 - 1)}}{2(A_O{}^2 + D_O{}^2 + 1)} \tag{A133}$$

(repeating)

$$Z = \cos\,(\gamma_{PFCA}) \tag{A134}$$

Thus one of the direction cosines has been identified. The two remaining may be found by substituting the results of Equation (A133) into Equations (A124) and (A125).

Keeping in mind the geometric relationships among the pitch path, rollers, and tooth forms, the following equations for the tooth form coordinates may be written.

$$X_{PF/CA} = -r'_{CA}\left|\cos\,(\alpha_{PFCA})\right| + X_{PCA/CA} \tag{A135}$$

$$Y_{PF/CA} = -r'_{CA}\cos\,(\beta_{PFCA}) + Y_{PCA/CA} \tag{A136}$$

$$Z_{PF/CA} = r'_{CA} \cos(\gamma_{PFCA}) + Z_{PCA/CA} \quad \text{(A137)}$$

CONTACT RATIO AND ROLLER SIZE/TOOTH THICKNESS RELATIONSHIP

From the results of the previous section, it is obvious that in general it is not desirable to utilize the entire cam tooth profile. The effect of this reduced profile contact area may best be understood by calculating the contact ratio for each side of the mechanism (i.e., rotor and stator).

The contact ratio is defined as the ratio of the active angle of contact to the nutator roller angular pitch. It may be considered to be the average number of rollers carrying the total load. Its integer component specifies the minimum number of rollers in contact at any time during the meshing cycle. If the entrance and exit points of cam tooth profile contact are specified in terms of input angle, as shown in Figure A7, the following equations may be developed to define the contact ratio.

$$C_{TCA} = \omega_{XCA} - \omega_{NCA} \quad \text{(A138)}$$

The angular pitch of the nutator rollers is

$$C_{PCA} = \frac{360}{N_{NCA}} \quad \text{(A139)}$$

Therefore the contact ratio may be defined as

$$L_{ACA} = C_{TCA}/C_{PCA} \quad \text{(A140)}$$

The minimum number of teeth in contact at any time is given by the integer component of L_{ACA} and may be expressed as IL_{ACA}.

Another relationship which must be defined prior to evaluating the loads and stresses within the mechanism is that between the cam tooth thickness and the nutator roller diameter.

Figure A8 shows, in an exaggerated schematic manner, the relationship between roller size and cam thickness.

Because the rollers may be coned away from the plane of the nutator, the radius perpendicular to the mechanism axis may not be equal to the basic spherical radius, thus

$$R'_{BCCA} = R_{BCCA} \cos(\sigma_{CA}) \quad \text{(A141)}$$

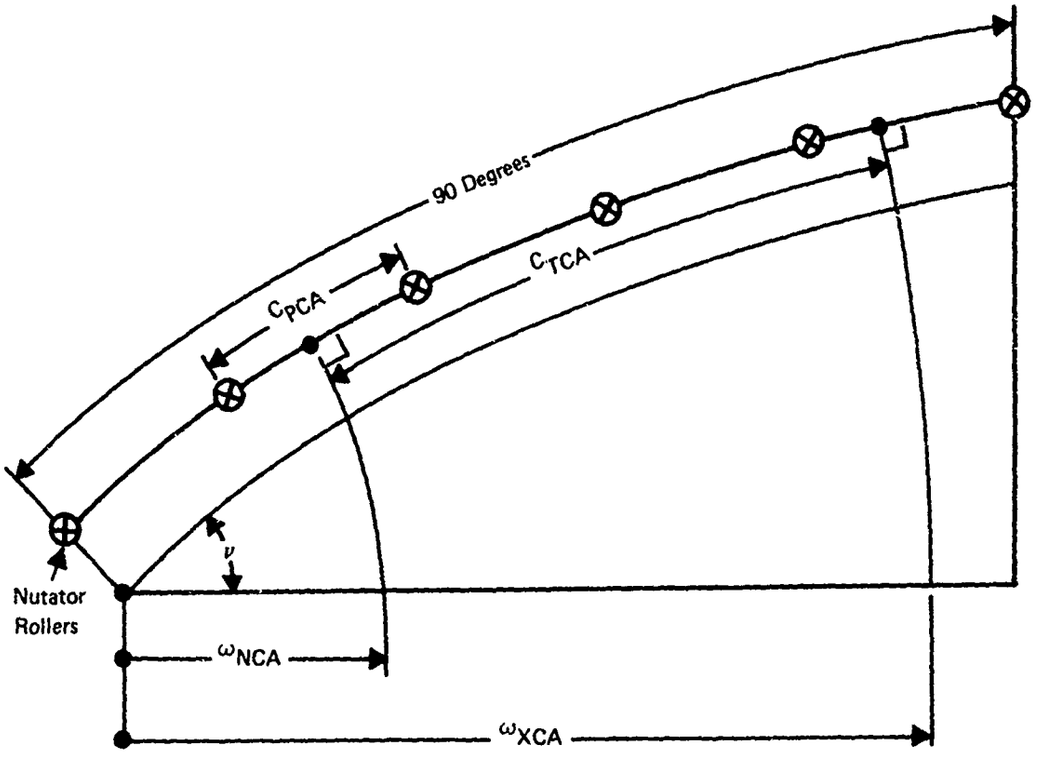

Figure A7. Parameters of Contact Ratio.

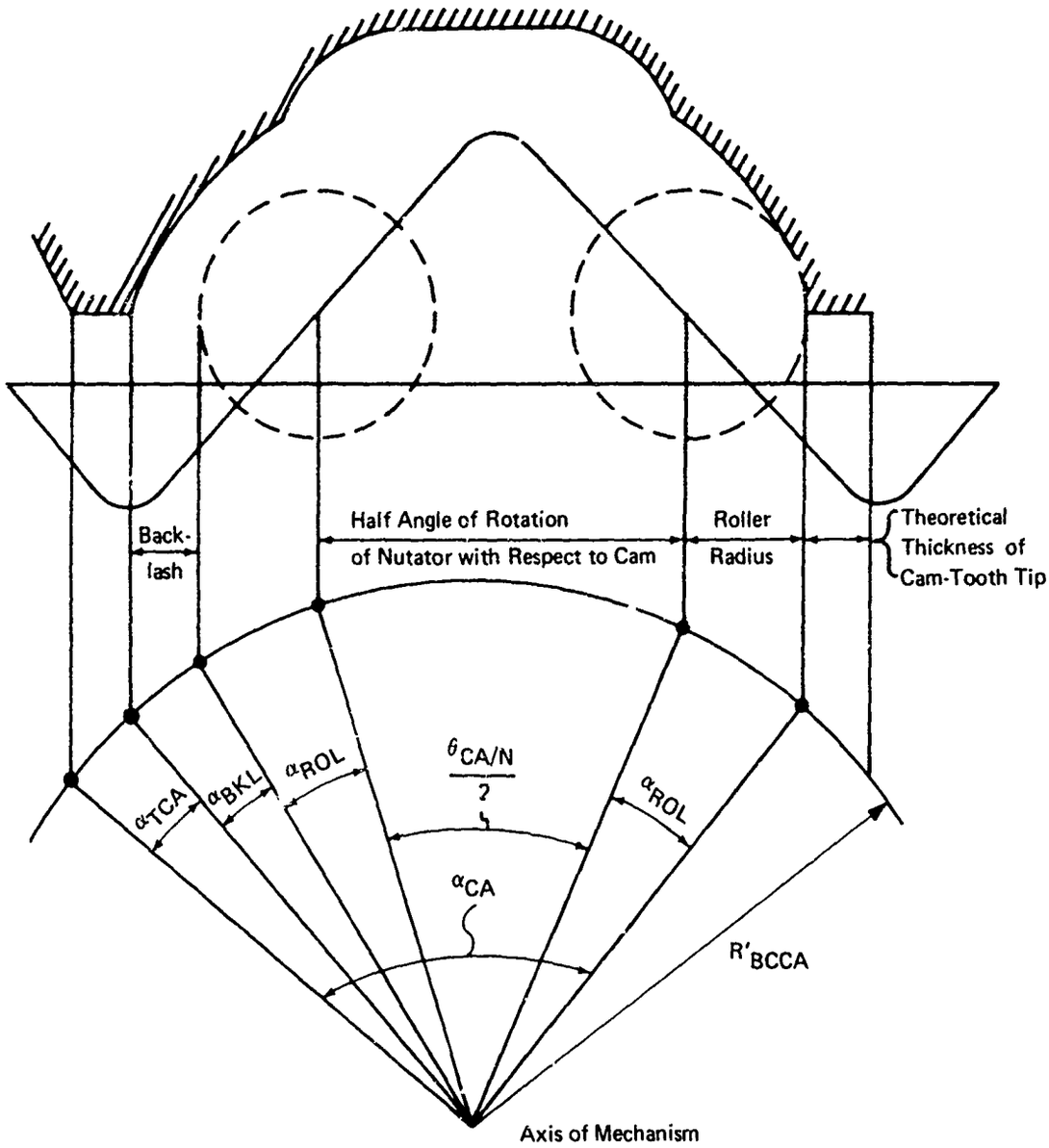

Figure A8. Relation of Cam-Tooth Thickness to Roller Size.

The angle α_{CA} is the angular pitch of the cam teeth

$$\alpha_{CA} = 360/N_{CA} \tag{A142}$$

If backlash is expressed in terms of arc distance, as is the practice in gearing, the angular backlash is

$$\alpha_{BKL} = \frac{BKL_{CA}}{R'_{BCCA}} \tag{A143}$$

noting, of course, the proper degrees-radians conversion.

Similarly, if the cam tooth tip thickness is expressed as an arc measurement,

$$\alpha_{TCA} = \frac{T_{TCA}}{R'_{BCCA}} \tag{A144}$$

The included roller half angle α_{ROL} may be defined as

$$\alpha_{ROL} = \sin^{-1}\left[\frac{r_{CA}}{R'_{BCCA}}\right] = \sin^{-1}\left[\frac{r_{CA}}{R_{BCCA}\cos(\sigma_{CA})}\right] \tag{A145}$$

Having defined all the requisite parameters, the equations defining the maximum roller size for a given tooth thickness or the maximum tooth thickness for a given roller size may be written.

$$T_{TCA} = R_{BCCA}\cos(\sigma_{CA})\left[\alpha_{CA}-\alpha_{BKL}-2\alpha_{ROL} - \frac{\theta_{CA/N}}{2}\right] \tag{A146}$$

$$\alpha_{ROL} = \left[\alpha_{CA}-\alpha_{BKL}-\alpha_{TCA} - \frac{\theta_{CA/N}}{2}\right] \tag{A147}$$

$$r_{CA} = R_{BCCA}\cos(\sigma_{CA})\sin(\alpha_{ROL}) \tag{A148}$$

The quantity $\theta_{CA/N}$ is the angular rotation of the nutator with respect to the cam, and is dependent only on the relative element numbers. As $\theta_{CA/N}$ becomes larger, the maximum roller size and/or the maximum cam tooth thickness decrease.

ANGULAR VELOCITY OF ROLLER ABOUT ITS OWN CENTERLINE

The angular velocity of a nutator roller about its own centerline may be determined by taking the first derivative of the path equations to yield the linear velocities. The angular velocities may then be found by the familiar relationships between angular and linear velocities, thus

$$V_{XPCA/CA} = \frac{d\ X_{PCA/CA}}{dt} \tag{A149}$$

$$V_{YPCA/CA} = \frac{d\ Y_{PCA/CA}}{dt} \tag{A150}$$

$$V_{ZPCA/CA} = \frac{d\ Z_{PCA/CA}}{dt} \tag{A151}$$

$$\frac{d\ X_{PCA/CA}}{dt} = R_{BCCA}\left[\text{Cos}\ (A_{25CA})\ \frac{d\ \text{Sin}\ (A'_{54CA})}{dt} + \text{Sin}\ (A'_{54CA})\ \frac{d\ (\text{Cos}\ A_{25CA})}{dt}\right] \tag{A152}$$

$$\frac{d\ Y_{PCA/CA}}{dt} = R_{BCCA}\left[\text{Cos}\ (A_{25CA})\ \frac{d\ \text{Cos}\ (A'_{54CA})}{dt} + \text{Cos}\ (A'_{54CA})\ \frac{d\ \text{Cos}\ (A_{25CA})}{dt}\right] \tag{A153}$$

$$\frac{d\ Z_{PCA/CA}}{dt} = R_{BCCA}\ \frac{d\ \text{Sin}\ (A_{25CA})}{dt} \tag{A154}$$

$$\frac{d\ \text{Sin}\ (A_{25CA})}{dt} = \text{Sin}\ (\gamma_{CA} + \nu)\ \frac{d\ \text{Sin}\ (A_{12CA})}{dt} + \text{Sin}\ (A_{12CA})\ \frac{d\ \text{Sin}\ (\gamma_{CA} + \nu)}{dt}$$

$$= \text{Cos}\ (A_{25CA})\ \frac{d\ A_{25CA}}{dt} \tag{A155}$$

$$\frac{d\ \text{Sin}(A_{12CA})}{dt} = \text{Cos}\ (A_{12CA})\ \frac{d\ A_{12CA}}{dt} \tag{A156}$$

$$\frac{d\ A_{12CA}}{dt} = -\frac{\text{Cos}\ (\sigma_{CA})\ \dfrac{d\ \text{Cos}\ (\omega_o)}{dt}}{\sqrt{1 - \text{Cos}^2\ (\sigma_{CA})\ \text{Cos}^2\ (\omega_o)}} \qquad \text{(A157)}$$

$$\frac{d\ A_{12CA}}{dt} = \frac{\text{Cos}\ (\sigma_{CA})\ \text{Sin}\ (\omega_o)\ \omega_c}{\sqrt{1 - \text{Cos}^2\ (\sigma_{CA})\ \text{Cos}^2\ (\omega_o)}} \qquad \text{(A158)}$$

$$\frac{d\ \text{Sin}\ (\gamma_{CA} + \nu)}{dt} = \text{Cos}\ (\gamma_{CA} + \nu)\ \frac{d\ \gamma_{CA}}{dt} \qquad \text{(A159)}$$

$$\frac{d\ \gamma_{CA}}{dt} = \frac{-\ \text{Sin}\ (\sigma_{CA})\ \text{Csc}\ (A_{12CA})\ \text{Cot}\ (A_{12CA})\ \dfrac{d\ A_{12CA}}{dt}}{\sqrt{1 - \text{Sin}^2\ (\sigma_{CA})/\text{Sin}^2\ (A_{12CA})}} \qquad \text{(A160)}$$

$$\frac{d\ \gamma_{CA}}{dt} = \frac{-\ \text{Cos}\ (A_{12CA})\ \text{Sin}\ (\sigma_{CA})\ \dfrac{d\ A_{12CA}}{dt}}{\text{Sin}^2\ (A_{12CA})\sqrt{1 - \text{Sin}^2\ (\sigma_{CA})/\text{Sin}^2(A_{12CA})}} \qquad \text{(A161)}$$

$$\frac{d\ \text{Cos}\ (A_{25CA})}{dt} = -\ \text{Sin}\ (A_{25CA})\ \frac{d\ A_{25CA}}{dt} \qquad \text{(A162)}$$

$$\frac{d\ A_{25CA}}{dt} = \frac{\text{Sin}(\gamma_{CA} + \nu)\dfrac{d\ \text{Sin}(A_{12CA})}{dt} + \text{Sin}\ (A_{12CA})\dfrac{d\ \text{Sin}(\gamma_{CA} + \nu)}{dt}}{\sqrt{1 - \text{Sin}^2\ (\gamma_{CA} + \nu)\ \text{Sin}^2\ (A_{12CA})}} \qquad \text{(A163)}$$

$$\frac{d\ \text{Sin}\ (A_{12CA})}{dt} = \text{Cos}\ (A_{12CA})\ \frac{d\ A_{12CA}}{dt} \qquad \text{(A164)}$$

$$\frac{d \cos (A'_{54CA})}{dt} = - \sin (A'_{54CA}) \frac{d A'_{54CA}}{dt} \quad \text{(A165)}$$

$$\frac{d A'_{54CA}}{dt} = \frac{d\omega_o}{dt} - \frac{d A_{15CA}}{dt} + \frac{d \theta_{CA/N}}{dt} \quad \text{(A166)}$$

$$\frac{d \theta_{CA/N}}{dt} = \left[\frac{N_S N_R - N_{NCA} N_{CA}'}{N_R N_{NS}}\right] \left[\frac{d \omega_o}{dt} - \frac{d \theta_S}{dt}\right] \quad \text{(A167)}$$

$$\frac{d A_{15CA}}{dt} = \frac{\tan (\gamma_{CA} + \nu) \frac{d \tan A_{25CA}}{dt} - \tan (A_{25CA}) \frac{d \tan (\gamma_{CA}+\nu)}{dt}}{\tan^2 (\gamma_{CA} + \nu) \sqrt{1 - \tan^2 (A_{25CA})/\tan^2 (\gamma_{CA} + \nu)}} \quad \text{(A168)}$$

$$\frac{d \tan (A_{25CA})}{dt} = \frac{\frac{d A_{25CA}}{dt}}{\cos^2 (A_{25CA})} \quad \text{(A169)}$$

$$\frac{d \tan (\gamma_{CA} + \nu)}{dt} = \frac{\frac{d \gamma_{CA}}{dt}}{\cos^2 (\gamma_{CA} + \nu)} \quad \text{(A170)}$$

$$\frac{d A_{15CA}}{dt} = \frac{\frac{\tan (\gamma_{CA} + \nu)}{\cos^2 (A_{25CA})} \frac{d A_{25CA}}{dt} - \frac{\tan (A_{25CA}) \frac{d \gamma_{CA}}{dt}}{\cos^2 (\gamma_{CA} + \nu)}}{\tan^2 (\gamma_{CA} + \nu) \sqrt{1 - \tan^2 (A_{25CA})/\tan^2 (\gamma_{CA} + \nu)}} \quad \text{(A171)}$$

$$\frac{d \sin A'_{54CA}}{dt} = \cos (A'_{54CA}) \frac{d A'_{54CA}}{dt} \quad \text{(A172)}$$

The vector sum of the X Y Z components of the velocity acts tangent to the path;

$$V_{PCA/CA} = \sqrt{V^2_{XPCA/CA} + V^2_{YPCA/CA} + V^2_{ZPCA/CA}} \quad \text{(A173)}$$

thus

$$\omega_{RCA/CL} = \frac{V_{PCA/CA}}{r_{CA}} \tag{A174}$$

where

$\omega_{RCA/CL}$ = angular velocity of roller about its own centerline

r_{CA} = radius of roller at R_{BCCA}

ACCELERATION OF ROLLER ABOUT ITS OWN CENTERLINE

Since the roller angular velocity may undergo considerable change during one input cycle, a knowledge of its angular acceleration is required so that the tendency of the roller to skid may be predicted.

The angular acceleration of the roller about its own centerline may be obtained by differentiating the expression for the roller velocity about its own centerline. Therefore,

$$\alpha_{RCA/CL} = \frac{d\,\omega_{RCA/CL}}{dt} \tag{A175}$$

$$\alpha_{RCA/CL} =$$

$$\frac{2V_{XPCA/CA}\frac{dV_{XPCA/CA}}{dt} + 2V_{YPCA/CA}\frac{dV_{YPCA/CA}}{dt} + 2V_{ZPCA/CA}\frac{dV_{ZPCA/CA}}{dt}}{2r_{CA}\sqrt{V^2_{XPCA/CA} + V^2_{YPCA/CA} + V^2_{ZPCA/CA}}} \tag{A176}$$

$$\frac{dV_{XPCA/CA}}{dt} = \frac{d^2X_{PCA/CA}}{dt^2} \tag{A177}$$

$$\frac{dV_{YPCA/CA}}{dt} = \frac{d^2Y_{PCA/CA}}{dt^2} \tag{A178}$$

$$\frac{dV_{ZPCA/CA}}{dt} = \frac{d^2Z_{PCA/CA}}{dt^2} \tag{A179}$$

$$\frac{d^2 X_{PCA/CA}}{dt^2} = R_{BCCA} \left[\cos (A_{25CA}) \frac{d^2 \sin (A'_{54CA})}{dt^2} \right.$$

$$- \frac{d \sin (A'_{54CA})}{dt} \sin (A_{25CA}) \frac{d(A_{25CA})}{dt}$$

$$+ \sin (A'_{54CA}) \frac{d^2 \cos (A_{25CA})}{dt^2} + \frac{d \cos (A_{25CA})}{dt}$$

$$\left. \cos (A'_{54CA}) \frac{dA'_{54CA}}{dt} \right] \qquad \text{(A180)}$$

$$\frac{d^2 Y_{PCA/CA}}{dt^2} = R_{BCCA} \left[\cos (A_{25CA}) \frac{d^2 \cos (A'_{54CA})}{dt^2} \right.$$

$$- \frac{d \cos (A'_{54CA})}{dt} \sin (A_{25CA}) \frac{d A_{25CA}}{dt}$$

$$+ \frac{d^2 \cos (A_{25CA})}{dt^2} \cos (A'_{54CA}) - \frac{d \cos (A'_{54CA})}{dt}$$

$$\left. \sin (A'_{54CA}) \frac{d A'_{54CA}}{dt} \right] \qquad \text{(A181)}$$

$$\frac{d^2 Z_{PCA/CA}}{dt^2} = R_{BCCA} \frac{d^2 \sin (A_{25CA})}{dt^2} \qquad \text{(A182)}$$

$$\frac{d^2 \sin (A_{25CA})}{dt^2} = \sin (\gamma_{CA} + \nu) \frac{d^2 \sin (A_{12CA})}{dt^2}$$

$$+ \frac{d \sin (A_{12CA})}{dt} \cos (\gamma_{CA} + \nu) \frac{d\gamma_{CA}}{dt} + \sin (A_{12CA}) \frac{d^2 \sin (\gamma_{CA} + \nu)}{dt^2}$$

$$+ \frac{d \sin (\gamma_{CA} + \nu)}{dt} \cos (A_{12CA}) \frac{d A_{12CA}}{dt} \qquad \text{(A183)}$$

$$\frac{d^2 \sin (A_{12CA})}{dt^2} = \cos (A_{12CA}) \frac{d^2 A_{12CA}}{dt^2} - \sin (A_{12CA}) \left(\frac{d A_{12CA}}{dt}\right)^2 \quad \text{(A184)}$$

$$\frac{d^2 A_{12CA}}{dt^2} =$$

$$\cos (\sigma_{CA}) \left[\frac{\sqrt{1 - \cos^2 (\sigma_{CA}) \cos^2 (\omega_0)} \left(\cos(\omega_0) \omega_c^2 + \alpha_c \sin(\omega_0)\right) - \sin (\omega_0) \omega_c \frac{d\sqrt{1 - \cos^2 (\sigma_{CA}) \cos^2 (\omega_0)}}{dt}}{\left(1 - \cos^2 (\sigma_{CA}) \cos^2 (\omega_0)\right)} \right] \quad \text{(A185)}$$

$$\frac{d^2 A_{12CA}}{dt^2} =$$

$$\cos (\sigma_{CA}) \left[\frac{\sqrt{1-\cos^2 (\sigma_{CA}) \cos^2 (\omega_0)} \left(\cos (\omega_0) \omega_c^2 + \alpha_c \sin (\omega_0)\right) - \frac{\sin^2 (\omega_0) \cos^2 (\sigma_{CA}) \cos (\omega_0) \omega_c^2}{\sqrt{1-\cos^2 (\sigma_{CA}) \cos^2 (\omega_0)}}}{1 - \cos^2 (\sigma_{CA}) \cos^2 (\omega_0)} \right] \quad \text{(A186)}$$

$$\frac{d^2 \sin (\gamma_{CA} + \nu)}{dt^2} = \frac{d^2 \gamma_{CA}}{dt} \cos (\gamma_{CA} + \nu) - \sin (\gamma_{CA} + \nu) \left(\frac{d\gamma_{CA}}{dt}\right)^2 \quad \text{(A187)}$$

$$\frac{d^2 \cos (A'_{54CA})}{dt^2} = - \left(\sin(A'_{54CA}) \frac{d^2 A'_{54CA}}{dt^2} + \cos A'_{54CA} \left(\frac{d A'_{54CA}}{dt} \right)^2 \right) \tag{A188}$$

$$\frac{d^2 A'_{54CA}}{dt^2} = \frac{d^2 \omega_0}{dt^2} - \frac{d^2 A_{15CA}}{dt^2} + \frac{d^2 \theta_{CA/N}}{dt^2} \tag{A189}$$

$$\frac{d^2 \theta_{CA/N}}{dt^2} = \left[\frac{N_S N_R - N_{CA} N'_{CA}}{N_R N_{NS}} \right] \left(\frac{d^2 \omega_0}{dt^2} - \frac{d \theta_s^2}{dt^2} \right) \tag{A190}$$

The mathematics from this point becomes rather lengthy; therefore we will define the following auxiliary variables to simplify the nomenclature.

$$A_{CA} = \frac{\text{Tan } (\gamma_{CA} + \nu)}{\text{Cos}^2 \ (A_{25CA})} \frac{d A_{25CA}}{dt} \tag{A191}$$

$$B_{CA} = \frac{\text{Tan } (A_{25CA})}{\text{Cos}^2 \ (\gamma_{CA} + \nu)} \frac{d\gamma_{CA}}{dt} \tag{A192}$$

$$C_{CA} = \sqrt{1 - \text{Tan}^2 (A_{25CA}) / \text{Tan}^2 (\gamma_{CA} + \nu)} \tag{A193}$$

$$D_{CA} = \text{Tan}^2 (\gamma_{CA} + \nu) \ C_{CA} \tag{A194}$$

$$\frac{dA_{CA}}{dt} = \frac{\text{Tan } (\gamma_{CA} + \nu)}{\text{Cos}^2 \ (A_{25CA})} \frac{d^2 A_{25CA}}{dt^2} + \frac{dA_{25CA}}{dt} \left[\frac{\text{Cos}^2 (A_{25CA}) \dfrac{\dfrac{d \gamma_{CA}}{dt}}{\text{Cos}^2 \ (\gamma_{CA} + \nu)} + \text{Tan } (\gamma_{CA} + \nu) \, 2 \cos(A_{25CA}) \sin(A_{25CA}) \dfrac{dA_{25CA}}{dt}}{\text{Cos}^4 (A_{25CA})} \right] \tag{A195}$$

$$\frac{d B_{CA}}{dt} = \frac{\text{Tan } (A_{25CA})}{\text{Cos}^2 (\gamma_{CA} + \nu)} \frac{d^2 \gamma_{CA}}{dt} +$$

$$\frac{d\gamma_{CA}}{dt}\left[\frac{\text{Cos}^2(\gamma_{CA}+\nu)\dfrac{d\ A_{25CA}}{dt}}{\text{Cos}^2\ (A_{25CA})} + \text{Tan}(A_{25CA})2\text{Cos}(\gamma_{CA}+\nu)\text{Sin}(\gamma_{CA}+\nu)\frac{d\gamma_{CA}}{dt}}{\text{Cos}^4\ (\gamma_{CA}+\nu)}\right] \quad \text{(A196)}$$

$$\frac{d\ C_{CA}}{dt} = -\left[\frac{\text{Tan } (A_{25CA})}{\text{Tan}^3\ (\gamma_{CA}+\nu)}\right]\left[\frac{\text{Tan } (\gamma_{CA}+\nu)}{\text{Cos}^2\ (A_{25CA})}\left(\frac{d\ A_{25CA}}{dt}\right) - \frac{\text{Tan } (A_{25CA})}{\text{Cos}^2\ (\gamma_{CA}+\nu)}\left(\frac{d\gamma_{CA}}{dt}\right)\right]$$
$$\sqrt{1 - \left[\text{Tan } (A_{25CA})/\text{Tan } (\gamma_{CA}+\nu)\right]^2} \quad \text{(A197)}$$

$$\frac{d\ D_{CA}}{dt} = \frac{d\ C_{CA}}{dt}\text{Tan}^2\ (\gamma_{CA}+\nu) + \frac{2\ C_{CA}\dfrac{d\gamma_{CA}}{dt}\text{Tan } (\gamma_{CA}+\nu)}{\text{Cos}^2\ (\gamma_{CA}+\nu)} \quad \text{(A198)}$$

Now the first derivative of A_{15CA} Equation (A197) may be expressed as

$$\frac{d\ A_{15CA}}{dt} = \frac{A_{CA} - B_{CA}}{D_{CA}} \quad \text{(A199)}$$

and

$$\frac{d^2\ A_{15CA}}{dt^2} = \frac{D_{CA}\left(\dfrac{d\ A_{CA}}{dt} - \dfrac{d\ B_{CA}}{dt}\right) - (A_{CA} - B_{CA})\dfrac{d\ D_{CA}}{dt}}{D_{CA}^2} \quad \text{(A200)}$$

Let

$$E_{CA} = - \cos (A_{12CA}) \sin (\sigma_{CA}) \frac{d A_{12CA}}{dt} \tag{A201}$$

$$FF_{CA} = \sqrt{1 - \sin^2(\sigma_{CA})/\sin^2 (A_{12CA})} \sin^2(A_{12CA}) \tag{A202}$$

$$\frac{d\gamma_{CA}}{dt} = \frac{E_{CA}}{FF_{CA}} \tag{A203}$$

$$\frac{d^2 \gamma_{CA}}{dt^2} = \frac{FF_{CA} \frac{d E_{CA}}{dt} - E_{CA} \frac{d FF_{CA}}{dt}}{FF^2_{CA}} \tag{A204}$$

$$\frac{d E_{CA}}{dt} = - \sin (\sigma_{CA}) \left[\frac{d^2 A_{12CA}}{dt} \cos(A_{12CA}) - \sin (A_{12CA}) \left(\frac{d A_{12CA}}{dt} \right)^2 \right] \tag{A205}$$

$$\frac{d FF_{CA}}{dt} = \cos(A_{12CA}) \frac{d A_{12CA}}{dt} \left[2 \sin(A_{12CA}) \sqrt{1 - \left(\frac{\sin(\sigma_{CA})}{\sin (A_{12CA})} \right)^2} + \frac{\sin^2(\sigma_{CA})}{\sin(A_{12CA}) \sqrt{1 - \left(\sin (\sigma_{CA}) / \sin (A_{12CA}) \right)^2}} \right] \tag{A206}$$

$$\frac{d^2 \cos (A_{25CA})}{dt^2} = - \left[\sin(A_{25CA}) \frac{d^2 A_{25CA}}{dt^2} + \cos (A_{25CA}) \left(\frac{d A_{25CA}}{dt} \right)^2 \right] \tag{A207}$$

Let

$$G_{CA} = \sin (\gamma_{CA} + \nu) \frac{d \sin A_{12CA}}{dt} \tag{A208}$$

$$H_{CA} = \sin (A_{12CA}) \frac{d \sin (\gamma_{CA} + \nu)}{dt} \tag{A209}$$

$$I_{CA} = \sqrt{1 - \sin^2 (\gamma_{CA} + \nu) \sin^2 (A_{12CA})} \tag{A210}$$

$$\frac{d\,A_{25CA}}{dt} = \frac{GG_{CA} + H_{CA}}{I_{CA}} \tag{A211}$$

$$\frac{d^2 A_{25CA}}{dt^2} = \frac{I_{CA}\left[\frac{dGG_{CA}}{dt} + \frac{dH_{CA}}{dt}\right] - (GG_{CA} + H_{CA})\frac{dI_{CA}}{dt}}{I_{CA}^2} \tag{A212}$$

$$\frac{dGG_{CA}}{dt} = \text{Sin}\,(\gamma_{CA} + \nu)\,\frac{d^2\,\text{Sin}\,(A_{12CA})}{dt^2} + \text{Cos}\,(\gamma_{CA} + \nu)\,\frac{d\,\gamma_{CA}}{dt}\,\frac{d\,\text{Sin}\,A_{12CA}}{dt} \tag{A213}$$

$$\frac{dH_{CA}}{dt} = \text{Sin}\,(A_{12CA})\,\frac{d^2\,\text{Sin}\,(\gamma_{CA} + \nu)}{dt^2} + \text{Cos}\,(A_{12CA})\,\frac{d\,A_{12CA}}{dt}\,\frac{d\,\text{Sin}\,(\gamma_{CA} + \nu)}{dt} \tag{A214}$$

$$\frac{dI_{CA}}{dt} =$$

$$-\left[\text{Sin}^2(\gamma_{CA}+\nu)\,\text{Sin}(A_{12CA})\,\text{Cos}(A_{12CA})\frac{dA_{12CA}}{dt} + \text{Sin}^2(A_{12CA})\,\text{Sin}(\gamma_{CA}+\nu)\,\text{Cos}(\gamma_{CA}+\nu)\frac{d\gamma_{CA}}{dt}\right]$$

$$\Big/\sqrt{1-\text{Sin}^2(\gamma_{CA}+\nu)\,\text{Sin}^2\,(A_{12CA})} \tag{A215}$$

$$\frac{d^2\,\text{Sin}\,(A'_{54CA})}{dt^2} = \text{Cos}(A'_{54CA})\,\frac{d^2\,A'_{54CA}}{dt^2} - \text{Sin}(A'_{54CA})\left(\frac{d\,A'_{54CA}}{dt}\right)^2 \tag{A216}$$

FRICTION TORQUE REQUIRED TO PREVENT ROLLER SKIDDING

Knowing the angular acceleration of the roller, we may now calculate the torque required to prevent skidding.

$$T_{FRCA} = J_{RCA}\, \alpha_{RCA/CL} \tag{A217}$$

where J_{RCA} = roller polar moment of inertia about its central axis

T_{FRCA} = required friction torque

In general, the roller may have a cylindrical hole along its central axis. Considering the roller shown in Figure A9 we find that

$$r_{ICA} = \frac{r_{CA}}{R_{BCCA}} \left(R_{BCCA} - \frac{\ell_{CA}}{2}\right) \tag{A218}$$

$$r_{OCA} = \frac{r_{CA}}{R_{BCCA}} \left(R_{BCCA} + \frac{\ell_{CA}}{2}\right) \tag{A219}$$

The polar moment of inertia may thus be written (considering the frustrum of a cone minus the cylindrical hole) as

$$J_{RCA} = \frac{3}{10}\, M_F\, \frac{(r_{OCA}^5 - r_{ICA}^5)}{(r_{OCA}^3 - r_{ICA}^3)} - \frac{1}{2}\, M_C\, r_{IN}^2 \tag{A220}$$

where M_F = mass of solid frustrum of a cone

M_C = mass of cylinder

The mass of a frustrum of a cone may be expressed as

$$M_F = \frac{\gamma_{ROL} V_F}{g} \tag{A221}$$

Similarly, for the cylindrical hole,

$$M_C = \frac{\gamma_{ROL} V_C}{g} \tag{A222}$$

where g = acceleration of gravity

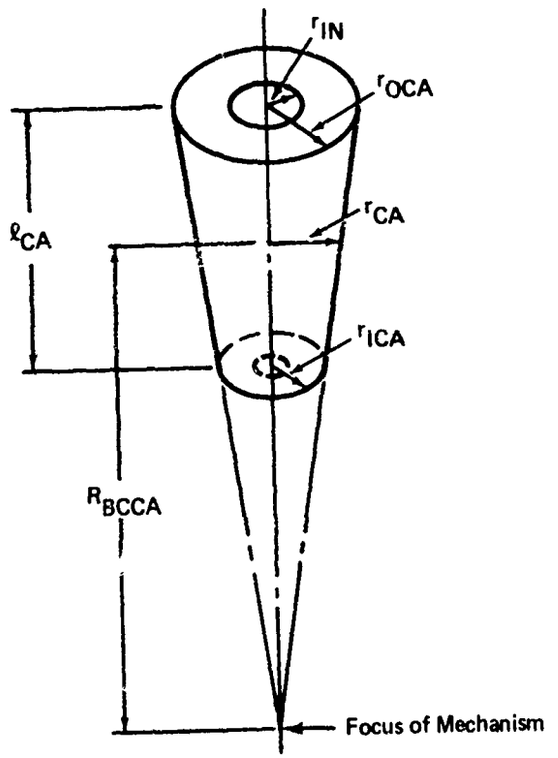

Figure A9. Derivation of Nutator Roller Inertia.

Finally, the volumes V_F and V_C may be expressed as

$$V_C = \pi r_{IN}^2 \ell_{CA} \tag{A223}$$

and

$$V_F = \frac{1}{3}\left(\pi r_{OC}^2 + \pi r_{IC}^2 + \sqrt{(\pi r_{OC}^2)\ (\pi r_{IC}^2)}\right)\ell_{CA} \tag{A224}$$

$$V_F = \frac{\pi \ell_{CA}}{3}\left(r_{OC}^2 + r_{IC}^2 + \sqrt{r_{OC}^2\ r_{IC}^2}\right) \tag{A225}$$

A small approximation at this point may yield some very useful information concerning the skidding tendencies of the nutator rollers. If we consider the rollers' mean sections we may make the assumption that the total roller load acts at this point. That is

$$F_{FRCA} = T_{FRCA}/r_{CA} \tag{A226}$$

where F_{FRCA} = friction force required to prevent roller skidding

thus

$$F_{N_{FRCA}} = F_{FRCA}/f \tag{A227}$$

where f = coefficient of friction between the roller and the cam surface

$F_{N_{FRCA}}$ = normal roller load required to keep the roller from skidding

The foregoing analysis contains several implicit assumptions which may not be immediately obvious. Primary among these is the neglect of any extension on the ends of a roller which may be required to mount the roller in its bearings. The second assumption is that the bearings supporting the roller have no effect on the skidding tendency of the rollers. In addition, the skidding tendency of the support rollers themselves has been ignored.

The first two assumptions may be reduced in their impact by varying the roller material density to approximate the actual case. The third assumption requires a detailed knowledge of the internal geometry of the support bearings, which is beyond the scope of the current investigation.

NUTATOR UNBALANCE MOMENTS

Since the nutator is mounted at some angle (the nutation half-angle) to the axis of nutation, the mechanism is inherently unbalanced. In order to provide for smooth vibration-free operation, it will be necessary to provide some type of balancing mechanism.

Prior to investigating any methods available for balancing the mechanism, it will be necessary to define the magnitudes and directions of the moments generated by the nutator unbalance. At first it would seem a simple matter to take the first derivative of the nutator velocity matrix and multiply it by the inertia matrix, however both matrices are functions of time, which complicates the analysis somewhat.

The moments due to the nutator unbalance may be found by

$$M_{XN} = \frac{d}{dt} \left(I_{XN}\omega_{XN} - J_{XYN}\omega_{YN} - J_{XZN}\omega_{ZN}\right) \tag{A228}$$

$$M_{YN} = \frac{d}{dt} \left(I_{YN}\omega_{YN} - J_{YZN}\omega_{ZN} - J_{YXN}\omega_{XN}\right) \tag{A229}$$

$$M_{ZN} = \frac{d}{dt} \left(I_{ZN}\omega_{ZN} - J_{ZX}\omega_{XN} - J_{ZY}\omega_{YN}\right) \tag{A230}$$

The reference system for the above equations is an X Y Z coordinate system fixed in the stator with the origin at the mechanism focus. The stator is generally fixed to the frame so that the moments will be with respect to the ground. It should be noted that, not only are the angular velocities functions of ω_o and thus time, the I's and J's are also functions of time. The equations defining the angular velocities of the nutator and the inertia matrix must now be developed.

From Figure A10, we may write

$$A_{13} = \omega_o \tag{A231}$$

$$\tau_{CA} = 90 - \text{Cos}^{-1}\left[\text{Cos}\ (\omega_o)\ \text{Sin}\ (\nu)\right] \tag{A232}$$

$$A_{35}' = \text{Tan}^{-1}\left[\text{Sin}\ (\omega_o)\ \text{Tan}\ (\nu)\right] \tag{A233}$$

where τ_{CA} = rotation of the $X_A\ Y_B\ Z_B$ system about the Y axis in the XZ plane

A_{35}' = rotation of the $X_A\ Y_A\ Z_A$ system about the X_A axis in the Y_A, Z_A plane

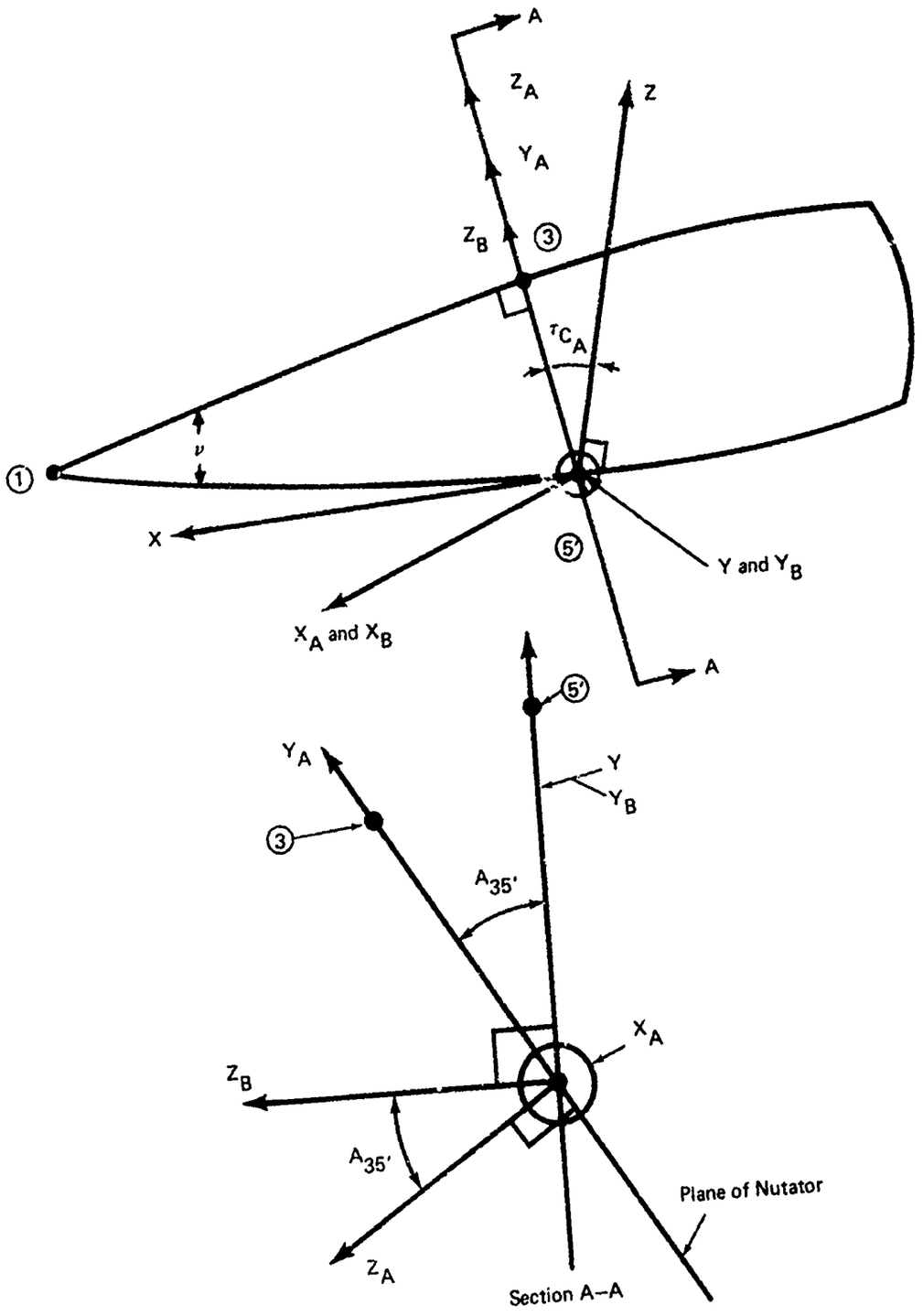

Figure A10. Relationship of Coordinate System Fixed in Nutator, Cam, and Ground.

If the moment of inertia matrix $[I_N]$ of the nutator is known in the $X_A\ Y_A\ Z_A$ system (as it will be) then it may be found as a function of time in the X Y Z system by operating on this matrix with the two matrices representing the direction cosines of the two axis rotations.

If $[\gamma_A]$ represents the direction cosines of the X Y Z system with respect to the $X_A\ Y_B\ Z_B$ system after the rotation A_{35}' about X, and $[\gamma_B]$ represents the direction cosines of the X Y Z system with respect to the $X_A\ Y_B\ Z_B$ system after the rotation τ_{CA} about Y, we may write

$$[I]_{XYZ} = [\gamma_B]\ [\gamma_A]\ [I_N]\ [\gamma_A]'\ [\gamma_B]' \tag{A234}$$

where $[\gamma_A]'$ and $[\gamma_B]'$ are the respective transposes of matrices $[\gamma_A]$ and $[\gamma_B]$

Then from Figure A10 we may write

$$[\gamma_A] = \begin{bmatrix} 0 & 0 & 1 \\ 0 & \text{Cos}\ (A_{35}') & \text{Sin}\ (A_{35}') \\ 0 & -\text{Sin}\ (A_{35}') & \text{Cos}\ (A_{35}') \end{bmatrix} \tag{A235}$$

Thus,

$$[\gamma_A]' = \begin{bmatrix} 0 & 0 & 0 \\ 0 & \text{Cos}\ (A_{35}') & -\text{Sin}\ (A_{35}') \\ 1 & \text{Sin}\ (A_{35}') & \text{Cos}\ (A_{35}') \end{bmatrix} \tag{A236}$$

By similar inspection of Figure A10 we find

$$[\gamma_B] = \begin{bmatrix} \text{Cos}\ (\tau_{CA}) & 0 & -\text{Sin}\ (\tau_{CA}) \\ 0 & 1 & 0 \\ \text{Sin}\ (\tau_{CA}) & 0 & \text{Cos}\ (\tau_{CA}) \end{bmatrix} \tag{A237}$$

$$[\gamma_B]' = \begin{bmatrix} \text{Cos } (\tau_{CA}) & 0 & \text{Sin } (\tau_{CA}) \\ 0 & 1 & 0 \\ -\text{Sin } (\tau_{CA}) & 0 & \text{Cos } (\tau_{CA}) \end{bmatrix} \quad \text{(A238)}$$

The inertia matrix of the nutator with respect to an axis system with Z along the nutator (not mechanism) axis and the origin at the mechanism focus is given by,

$$[I_N] = \begin{bmatrix} I_{XA} & -J_{XYA} & -J_{XZA} \\ -J_{YXA} & I_{YA} & -J_{YZA} \\ -J_{ZXA} & -J_{ZYA} & I_{ZA} \end{bmatrix} \quad \text{(A239)}$$

The inertia matrix $[I_N]$ must be calculated based on the specific geometry of the nutating ring assembly. Since the actual methodology depends on the configuration of this assembly, it is not practical to define a system of equations here. The general methods are, however, well documented in many texts.

If we let

$$[\gamma]_C = [\gamma_B]\ [\gamma_A] \quad \text{(A240)}$$

and

$$[\gamma]_D = [\gamma_A]'[\gamma_B]' \quad \text{(A241)}$$

Thus Equation (A234) may be rewritten as

$$[I]_{XYZ} = [\gamma]_C\ [I_N]\ [\gamma]_D \quad \text{(A242)}$$

$[\gamma]_C$ and $[\gamma]_D$ are expressed as

$$[\gamma]_C = \begin{bmatrix} 0 & \text{Sin } (\tau_{CA}) \text{ Sin } (A_{35}') & \text{Cos } (\tau_{CA}) - \text{Sin } (\tau_{CA}) \text{ Cos } (A_{35}') \\ 0 & \text{Cos } (A_{35}') & \text{Sin}(A_{35}') \\ 0 & -\text{Cos } (\tau_{CA}) \text{ Sin } (A_{35}') & \text{Sin}(\tau_{CA}) + \text{Cos}(\tau_{CA}) \text{Cos}(A_{35}') \end{bmatrix} \quad \text{(A243)}$$

$$[\gamma]_D = \begin{bmatrix} 0 & 0 & 0 \\ \text{Sin}(A_{35}')\ \text{Sin}\ (\tau_{CA}) & \text{Cos}(A_{35}') & -\text{Cos}(\tau_{CA})\text{Sin}(A_{35}') \\ \text{Cos}(\tau_{CA})-\text{Sin}(\tau_{CA})\text{Cos}(A_{35}') & \text{Sin}(A_{35}') & \text{Sin}(\tau_{CA}) + \\ & & \text{Cos}(\tau_{CA})\ \text{Cos}(A_{35}') \end{bmatrix} \quad \text{(A244)}$$

It should be noted that

$$[\gamma]_D = [\gamma]_C' \quad \text{(A245)}$$

By noting that the X Y axis will always be an axis of symmetry, some simplification may be made to the basic inertia matrix.

$$[I_N] = \begin{bmatrix} I_{XA} & 0 & -J_{XZA} \\ 0 & I_{YA} & -J_{YZA} \\ -J_{ZXA} & -J_{ZYA} & I_{ZA} \end{bmatrix} \quad \text{(A246)}$$

The nutator will always be symmetrical in the X Y plane but may not be symmetrical in the X Z or Y Z planes due to nutator coning. A further simplification may be made by noting that

$$J_{YZA} = -J_{ZXA} \quad \text{(A247)}$$

$$J_{YZA} = -J_{ZYA} \quad \text{(A248)}$$

$$[I_N] = \begin{bmatrix} I_{XA} & 0 & -J_{NA} \\ 0 & I_{YA} & -J_{NA} \\ J_{NA} & J_{NA} & I_{ZA} \end{bmatrix} \quad \text{(A249)}$$

$$[\gamma]_C = \begin{bmatrix} 0 & \gamma_{C12} & \gamma_{C13} \\ 0 & \gamma_{C22} & \gamma_{C23} \\ 0 & \gamma_{C32} & \gamma_{C33} \end{bmatrix} I_N = \begin{bmatrix} I_{XN} & 0 & -J_{NA} \\ 0 & I_{YN} & -J_{NA} \\ J_{NA} & J_{NA} & I_{XN} \end{bmatrix} \quad \text{(A250)}$$

$$[\gamma]_C\ [I]_N = [\gamma_E] = \begin{bmatrix} J_{NA}\gamma_{C13} & I_{YA}\gamma_{C12}+J_{NA}\gamma_{C13} & I_{ZA}\gamma_{C13}-J_{NA}\gamma_{C12} \\ J_{NA}\gamma_{C23} & I_{YA}\gamma_{C22}+J_{NA}\gamma_{C23} & I_{ZA}\gamma_{C23}-J_{NA}\gamma_{C22} \\ J_{NA}\gamma_{C33} & I_{YA}\gamma_{C32}+J_{NA}\gamma_{C33} & I_{ZA}\gamma_{C33}-J_{NA}\gamma_{C32} \end{bmatrix} \quad \text{(A251)}$$

$$[\gamma]_D = \begin{bmatrix} 0 & 0 & 0 \\ \gamma_{D21} & \gamma_{D22} & \gamma_{D23} \\ \gamma_{D31} & \gamma_{D32} & \gamma_{D33} \end{bmatrix} \quad \text{(A252)}$$

$$[\gamma]_E = \begin{bmatrix} \gamma_{E11} & \gamma_{E12} & \gamma_{E13} \\ \gamma_{E21} & \gamma_{E22} & \gamma_{E23} \\ \gamma_{E31} & \gamma_{E32} & \gamma_{E33} \end{bmatrix} \quad \text{(A253)}$$

$$[\gamma]_C [I]_N [\gamma]_D =$$

$$\begin{bmatrix} \gamma_{D21}\gamma_{E12}+\gamma_{D31}\gamma_{E13} & \gamma_{D22}\gamma_{E12}+\gamma_{D32}\gamma_{E13} & \gamma_{D23}\gamma_{E12}+\gamma_{D33}\gamma_{E13} \\ \gamma_{D21}\gamma_{E22}+\gamma_{D31}\gamma_{E23} & \gamma_{D22}\gamma_{E22}+\gamma_{D32}\gamma_{E23} & \gamma_{D23}\gamma_{E22}+\gamma_{D33}\gamma_{E23} \\ \gamma_{D21}\gamma_{E32}+\gamma_{D31}\gamma_{E33} & \gamma_{D22}\gamma_{E32}+\gamma_{D32}\gamma_{E33} & \gamma_{D23}\gamma_{E32}+\gamma_{D33}\gamma_{E33} \end{bmatrix} \quad \text{(A254)}$$

$$[\gamma]_C[I]_N[X]_D = \begin{bmatrix} I_{XN} & -J_{XYN} & -J_{XZN} \\ -J_{YXN} & I_{YN} & -J_{YZN} \\ -J_{ZYN} & -J_{ZYN} & I_{ZN} \end{bmatrix} \quad \text{(A255)}$$

The angular velocity of the nutator with respect to the stator may be shown to be

$$\omega_{XN/S} = V_{ZPN/S}/Y_{PN/S} - V_{YPN/S}/Z_{PN/S} \quad \text{(A256)}$$

$$\omega_{YN/S} = V_{XPN/S}/Z_{PN/S} - V_{ZPN/S}/X_{PN/S} \quad \text{(A257)}$$

$$\omega_{ZN/S} = V_{YPN/S}/X_{PN/S} - V_{XPN/S}/Y_{PN/S} \quad \text{(A258)}$$

The derivatives of these parameters with respect to time will also be required.

$$\frac{d\omega_{XN/S}}{dt} = \frac{Y_{ZPN/S}\ \frac{dV_{ZPN/S}}{dt} - V_{ZPN/S}\ \frac{dY_{PN/s}}{dt}}{Y_{PNS}^{2}}$$

$$- \frac{Z_{PN/S}\ \frac{dV_{YPN/S}}{dt} - V_{YPN/S}\ \frac{dZ_{PNS}}{dt}}{Z_{PN/S}^{2}} \qquad \text{(A259)}$$

$$\frac{d\omega_{YN/S}}{dt} = \frac{Z_{PN/S}\ \frac{dV_{XPN/S}}{dt} - V_{XPN/S}\ \frac{dZ_{PN/S}}{dt}}{Z_{PN/S}^{2}}$$

$$- \frac{X_{PN/S}\ \frac{dV_{ZPN/S}}{dt} - V_{ZPN/S}\ \frac{dX_{PN/S}}{dt}}{X_{PNS}^{2}} \qquad \text{(A260)}$$

$$\frac{d\omega_{ZN/S}}{dt} = \frac{X_{PN/S}\ \frac{dV_{YPN/S}}{dt} - V_{YPN/S}\ \frac{dX_{PN/S}}{dt}}{X_{PN/S}^{2}}$$

$$- \frac{Y_{PN/S}\ \frac{dV_{XPN/S}}{dt} - V_{XPN/S}\ \frac{dY_{PN/S}}{dt}}{Y_{PN/S}^{2}} \qquad \text{(A261)}$$

The linear velocities, X,Y,Z coordinates, and the derivatives of these parameters have been calculated in other sections of this analysis and will not be repeated here.

Equations (A228), (A229), and (A230) may now be expanded to yield

$$M_{XN} = \frac{dI_{XN}}{dt}\,\omega_{XN} + I_{XN}\ \frac{d\omega_{XN}}{dt} - \left(J_{XYN}\ \frac{d\omega_{YN}}{dt} + \frac{dJ_{XYN}}{dt}\,\omega_{YN}\right)$$

$$- \left(J_{XZN}\ \frac{d\omega_{ZN}}{dt} + \frac{dJ_{XZN}}{dt}\,\omega_{ZN}\right) \qquad \text{(A262)}$$

$$M_{YN} = \frac{dI_{YN}}{dt}\,\omega_{YN} + I_{YN}\,\frac{d\omega_{YN}}{dt} - \left(J_{YZN}\,\frac{d\omega_{ZN}}{dt} + \frac{dV_{YXN}}{dt}\,\omega_{ZN}\right)$$

$$- \left(J_{YXN}\,\frac{d\omega_{XN}}{dt} + \frac{dJ_{YXN}}{dt}\,\omega_{XN}\right) \qquad \text{(A263)}$$

$$M_{ZN} = \frac{dI_{ZN}}{dt}\,\omega_{ZN} + I_{ZN}\,\frac{d\omega_{ZN}}{dt} - \left(J_{XN}\,\frac{d\omega_{XN}}{dt} + \frac{dJ_{ZX}}{dt}\,\omega_{XN}\right)$$

$$- \left(J_{ZY}\,\frac{d\omega_{YN}}{dt} + \frac{dJ_{ZY}}{dt}\,\omega_{YN}\right) \qquad \text{(A264)}$$

Since $J_{XYN} = - J_{YXN}$

$J_{XZN} = - J_{ZXN}$

$J_{YZN} = - J_{ZYN}$

There are actually only six unknown quantities in Equations (A262), (A263), and (A264).

$$\frac{dI_{XN}}{dt} = \frac{d\gamma_{D21}}{dt}\,\gamma_{E12} + \gamma_{D21}\,\frac{d\gamma_{E12}}{dt}$$

$$+ \frac{d\gamma_{D31}}{dt}\,\gamma_{E13} + \gamma_{D31}\,\frac{d\gamma_{E13}}{dt} \qquad \text{(A265)}$$

$$\frac{dJ_{XYN}}{dt} = -\left[\frac{d\gamma_{D22}}{dt}\,\gamma_{E12} + \gamma_{D22}\,\frac{d\gamma_{E12}}{dt}\right.$$

$$\left. + \frac{d\gamma_{D32}}{dt}\,\gamma_{E13} + \gamma_{D32}\,\frac{d\gamma_{E13}}{dt}\right] \qquad \text{(A266)}$$

$$\frac{dJ_{XZN}}{dt} = -\left[\frac{d\gamma_{D23}}{dt}\,\gamma_{E12} + \gamma_{D23}\,\frac{d\gamma_{E12}}{dt}\right.$$

$$\left. + \frac{d\gamma_{D33}}{dt}\,\gamma_{E13} + \frac{d\gamma_{E13}}{dt}\,\gamma_{D33}\right] \qquad \text{(A267)}$$

$$\frac{dI_{YN}}{dt} = \frac{d\gamma_{D22}}{dt}\gamma_{E22} + \gamma_{D22}\frac{d\gamma_{E22}}{dt} + \frac{d\gamma_{D32}}{dt}\gamma_{E23} + \gamma_{D32}\frac{d\gamma_{E23}}{dt} \quad \text{(A268)}$$

$$\frac{dJ_{YZN}}{dt} = -\left[\frac{d\gamma_{D23}}{dt}\gamma_{E22} + \gamma_{D23}\frac{d\gamma_{E22}}{dt} + \frac{d\gamma_{D33}}{dt}\gamma_{E23} + \gamma_{D33}\frac{d\gamma_{E23}}{dt}\right] \quad \text{(A269)}$$

$$\frac{dI_{ZN}}{dt} = \frac{d\gamma_{D23}}{dt}\gamma_{E32} + \gamma_{D23}\frac{d\gamma_{E32}}{dt} + \frac{d\gamma_{D33}}{dt}\gamma_{E33} + \gamma_{D33}\frac{d\gamma_{E33}}{dt} \quad \text{(A270)}$$

$$\frac{d\gamma_{D21}}{dt} = \frac{d\text{Sin}(A_{35}')}{dt}\text{Sin}(\tau_{CA}) + \text{Sin}(A_{35}')\frac{d\text{Sin}(\tau_{CA})}{dt} \quad \text{(A271)}$$

$$\frac{d\gamma_{D22}}{dt} = \frac{d\text{Cos}(A_{35}')}{dt} \quad \text{(A272)}$$

$$\frac{d\gamma_{D23}}{dt} = -\left[\frac{d\text{Cos}(\tau_{CA})}{dt}\text{Sin}(A_{35}') + \text{Cos}(\tau_{CA})\frac{d\text{Sin}(A_{35}')}{dt}\right] \quad \text{(A273)}$$

$$\frac{d\gamma_{D31}}{dt} = \frac{d\text{Cos}(\tau_{CA})}{dt} - \frac{d\text{Sin}(\tau_{CA})}{dt}\text{Cos}(A_{35}') - \text{Sin}(\tau_{CA})\frac{d\text{Cos}(A_{35}')}{dt} \quad \text{(A274)}$$

$$\frac{d\gamma_{D32}}{dt} = \frac{d\text{Sin}(A_{35}')}{dt} \quad \text{(A275)}$$

$$\frac{d\gamma_{D33}}{dt} = \frac{d\text{Sin}(\tau_{CA})}{dt} + \frac{d\text{Cos}(\tau_{CA})}{dt}\text{Cos}(A_{35}') + \text{Cos}(\tau_{CA})\frac{d\text{Cos}(A_{35}')}{dt} \quad \text{(A276)}$$

$$\frac{d\gamma_{E12}}{dt} = I_{YA}\left[\frac{d\mathrm{Sin}(\tau_{CA})}{dt}\mathrm{Sin}(A_{35}')+\mathrm{Sin}(\tau_{CA})\frac{d\mathrm{Sin}(A_{35}')}{dt}\right] \qquad (A277)$$

$$+ J_{NA}\left[\frac{d\mathrm{Cos}(\tau_{CA})}{dt} - \frac{d\mathrm{Sin}(\tau_{CA})}{dt}\mathrm{Cos}(A_{35}') - \mathrm{Sin}(\tau_{CA})\frac{d\mathrm{Cos}(A_{35}')}{dt}\right]$$

$$\frac{d\gamma_{E13}}{dt} = I_{ZA}\left[\frac{d\mathrm{Cos}(\tau_{CA})}{dt} - \frac{d\mathrm{Sin}(\tau_{CA})}{dt}\mathrm{Cos}(A_{35}') - \mathrm{Sin}(\tau_{CA})\frac{d\mathrm{Cos}(A_{35}')}{dt}\right]$$

$$- J_{NA}\left[\frac{d\mathrm{Sin}(\tau_{CA})}{dt}\mathrm{Sin}(A_{35}')+\mathrm{Sin}(\tau_{CA})\frac{d\mathrm{Sin}(A_{35}')}{dt}\right] \qquad (A278)$$

$$\frac{d\gamma_{E22}}{dt} = I_{YA}\frac{d\mathrm{Cos}(A_{35}')}{dt} + J_{NA}\frac{d\mathrm{Sin}(A_{35}')}{dt} \qquad (A279)$$

$$\frac{d\gamma_{E23}}{dt} = I_{ZA}\frac{d\mathrm{Sin}(A_{35}')}{dt} - J_{NA}\frac{d\mathrm{Cos}(A_{35}')}{dt} \qquad (A280)$$

$$\frac{d\gamma_{E32}}{dt} = -I_{YA}\left[\frac{d\mathrm{Cos}(\tau_{CA})}{dt}\mathrm{Sin}(A_{35}')+\mathrm{Cos}(\tau_{CA})\frac{d\mathrm{Sin}(A_{35}')}{dt}\right] \qquad (A281)$$

$$+ J_{NA}\left[\frac{d\mathrm{Sin}(\tau_{CA})}{dt}+\frac{d\mathrm{Cos}(\tau_{CA})}{dt} + \mathrm{Cos}(A_{35}')+\mathrm{Cos}(\tau_{CA})\frac{d\mathrm{Cos}(A_{35}')}{dt}\right]$$

$$\frac{d\gamma_{E33}}{dt} = I_{ZA}\left[\frac{d\mathrm{Sin}(\tau_{CA})}{dt}+\frac{d\mathrm{Cos}(\tau_{CA})}{dt}\mathrm{Cos}(A_{35}')+\mathrm{Cos}(\tau_{CA})\frac{d\mathrm{Cos}(A_{35}')}{dt}\right]$$

$$- J_{NA}\left[\frac{d\mathrm{Cos}(\tau_{CA})}{dt}\mathrm{Sin}(A_{35}')+\mathrm{Cos}(\tau_{CA})\frac{d\mathrm{Sin}(A_{35}')}{dt}\right] \qquad (A282)$$

$$\frac{d\mathrm{Sin}(\tau_{CA})}{dt} = \mathrm{Cos}(\tau_{CA})\frac{d(\tau_{CA})}{dt} \qquad (A283)$$

$$\frac{d\mathrm{Cos}(\tau_{CA})}{dt} = -\mathrm{Sin}(\tau_{CA})\frac{d(\tau_{CA})}{dt} \qquad (A284)$$

$$\frac{d\mathrm{Sin}(A_{35}')}{dt} = \mathrm{Cos}(A_{35}')\frac{dA_{35}'}{dt} \qquad (A285)$$

$$\frac{dCos(A_{35}')}{dt} = -Sin(A_{35}') \frac{dA_{35}'}{dt} \tag{A286}$$

$$\frac{d_{\gamma CA}}{dt} = \frac{-Sin\ \gamma Sin(\omega_o)\ \omega_C}{\sqrt{1 - Cos^2\ (\omega_o)\ Sin^2\ (\gamma)}} \tag{A287}$$

$$\frac{d\ A_{35}'}{dt} = \frac{Tan(\gamma)\ Cos(\omega_o)\ \omega_C}{1 + Sin^2\ (\omega_o)\ Tan^2\ (\gamma)} \tag{A288}$$

NUTATOR BALANCING

Perhaps the most obvious method available for balancing the mechanism is to utilize a split power arrangement in which two nutating ring assemblies are driven simultaneously from a single input shaft, as shown in Figure A11. If the nutation half angles of each nutator are exactly opposed, the unbalance forces generated by each will be cancelled by the other. The disadvantages of this method are seemingly obvious -- double components are required resulting in increased cost, complexity, and weight. However, in the case of a high power unit, a split power arrangement may be quite desirable from a load capacity standpoint.

Another method which may be utilized to balance the nutators dynamic loads is shown schematically in Figure A12. Two equal weights represented by the concentrated masses M_C acting at equal radii R_m from the mechanism axis and at equal distances L_m from the mechanism focus (along the mechanism axis) may be utilized to generate unbalance moments which tend to cancel the nutator moments.

If we consider the same X Y Z coordinate system utilized in the calculation of the nutator unbalance moments, the moments generated by the masses M_C may then be calculated.

The inertia force produced by a mass M_C rotating at an angular velocity ω_C at a radius R_m from the rotational axis is given by

$$F_{mc} = M_C R_m \omega_C^2 \tag{A289}$$

The moment generated by these forces about the origin of the coordinate system is

$$M_{mc} = 2F_{mc}\ L_m \tag{A290}$$

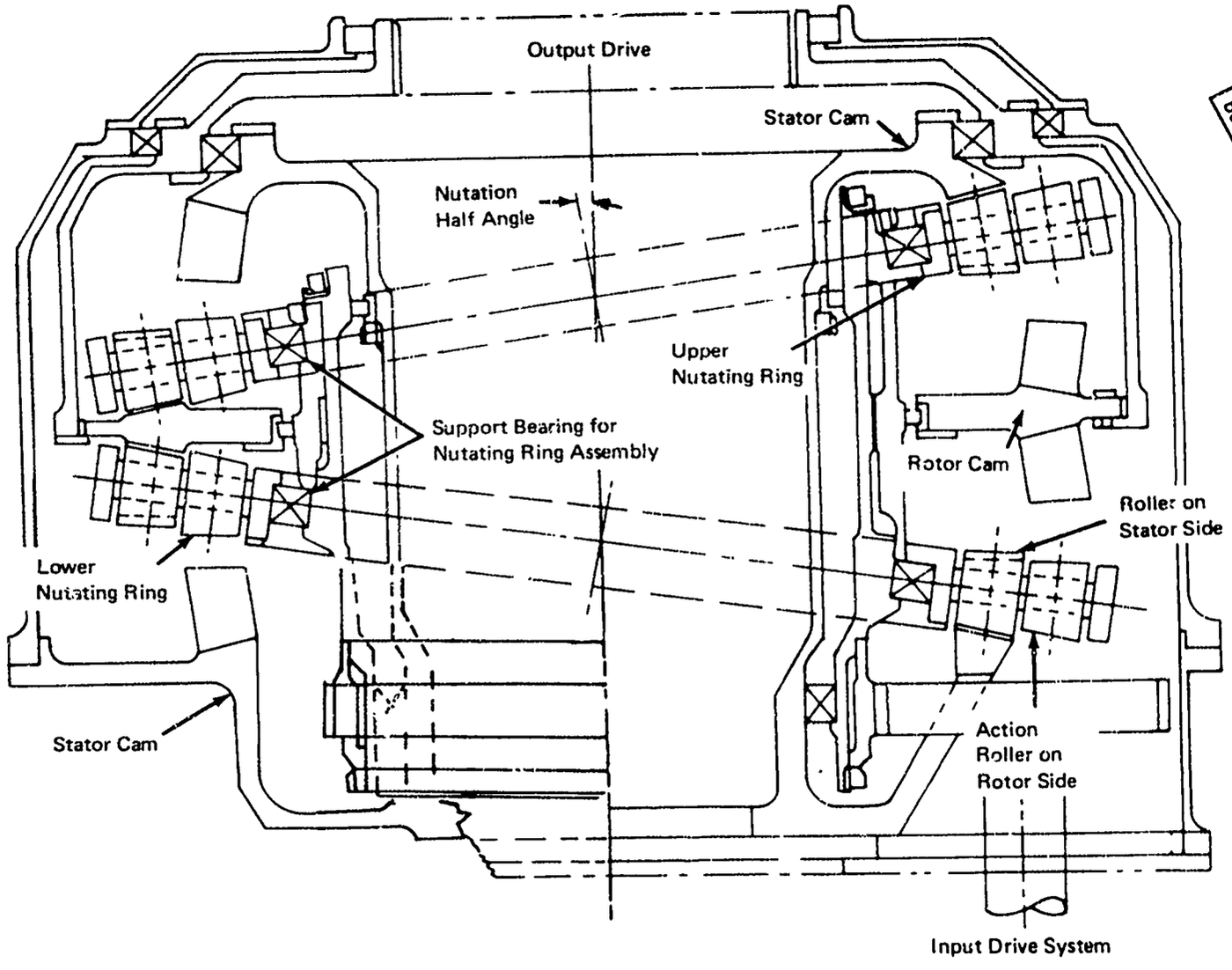

Figure All. Split-Power Concept.

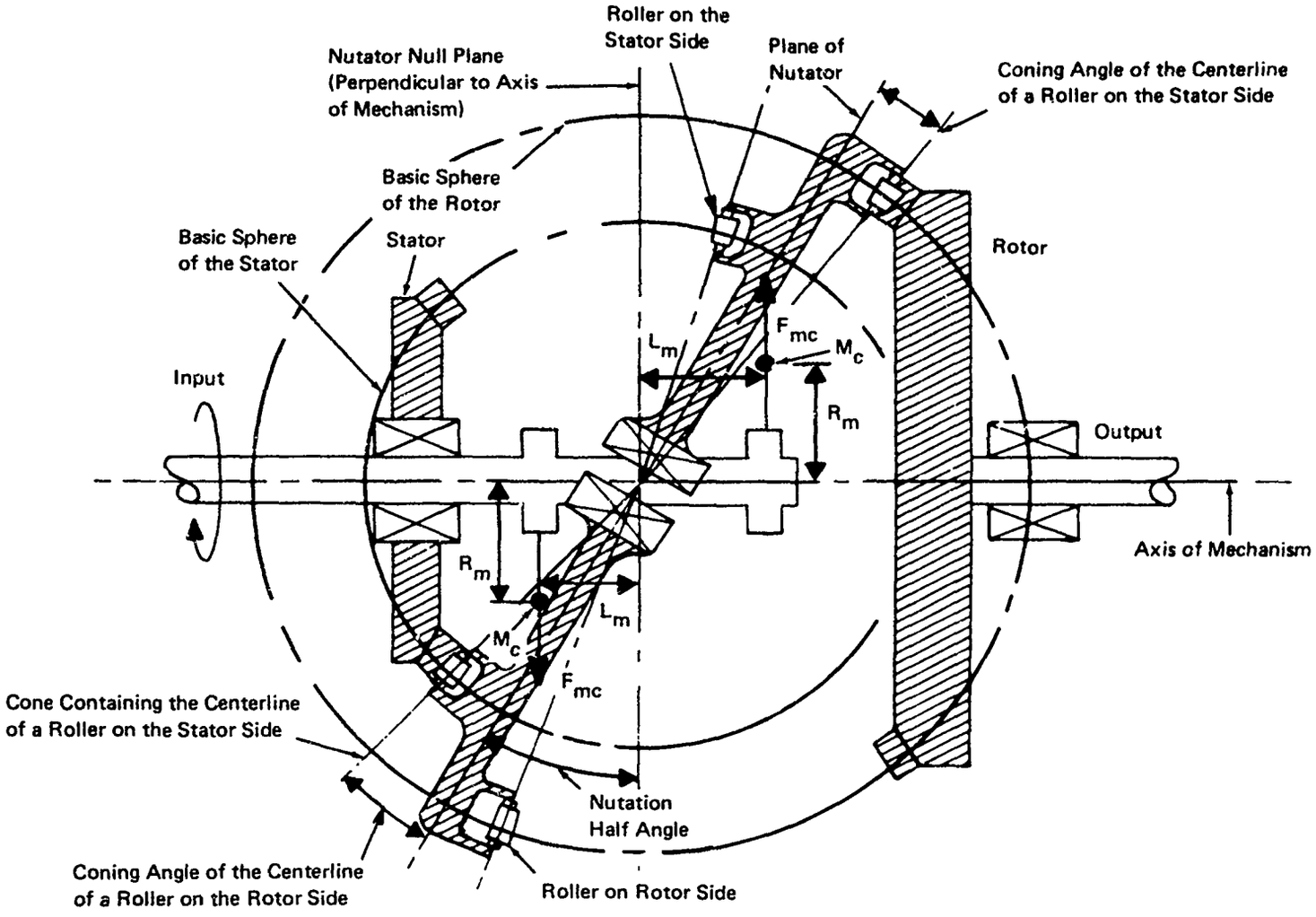

Figure A12. Nutator Balancing Mechanism.

The X Y Z components of this moment are

$$M_{mcZ} = 0.0 \tag{A291}$$

$$M_{mcX} = M_{mc} \text{ Cos } (\omega_o) \tag{A292}$$

$$M_{mcY} = M_{MC} \text{ Sin } (\omega_o) \tag{A293}$$

Since the directions of the moments generated by the nutator and the weights are opposite, their X and Y components will cancel to some extent. By the proper choice of M_c, R_m, and L_m this cancellation effect may be maximized.

Obviously, the mechanism will not be balanced by utilizing ideal point masses. The actual mechanism will consist of a pair of wedge shaped masses which fit in the space between the nutator and the cams as shown in Figure A13. The radius R_m and the length L_m are then measured to the center of mass of the weights.

LOAD DISTRIBUTION DEVELOPMENT

The manner in which the load will be shared among the tooth/roller contact points depends to a great extent on the relative compliance of each contact. The nutating ring assembly is relatively rigid, and the rollers themselves must of necessity be designed so that their deflection under load is slight. The cam teeth, relative to the size of the cam rollers and especially with respect to equivalent gear teeth, are quite large; thus their deflections will also be rather small. In addition, a method for the accurate evaluation of the flexural deflection of a flexibly mounted projection such as a gear tooth or a cam tooth is not available at this time. Considering these facts, and the inaccuracies which will be apparent in any approximate load sharing solution, the development of an intuative model for the load sharing spectrum will provide data of sufficient accuracy to rate the mechanism within about 10 percent of true capacity. Considering the standardized approximations used in the analysis of other similar systems (such as the tip loading assumption for helical gears and the uniform load distribution assumed for multiplanet epicyclic systems) the results should be directly comparable.

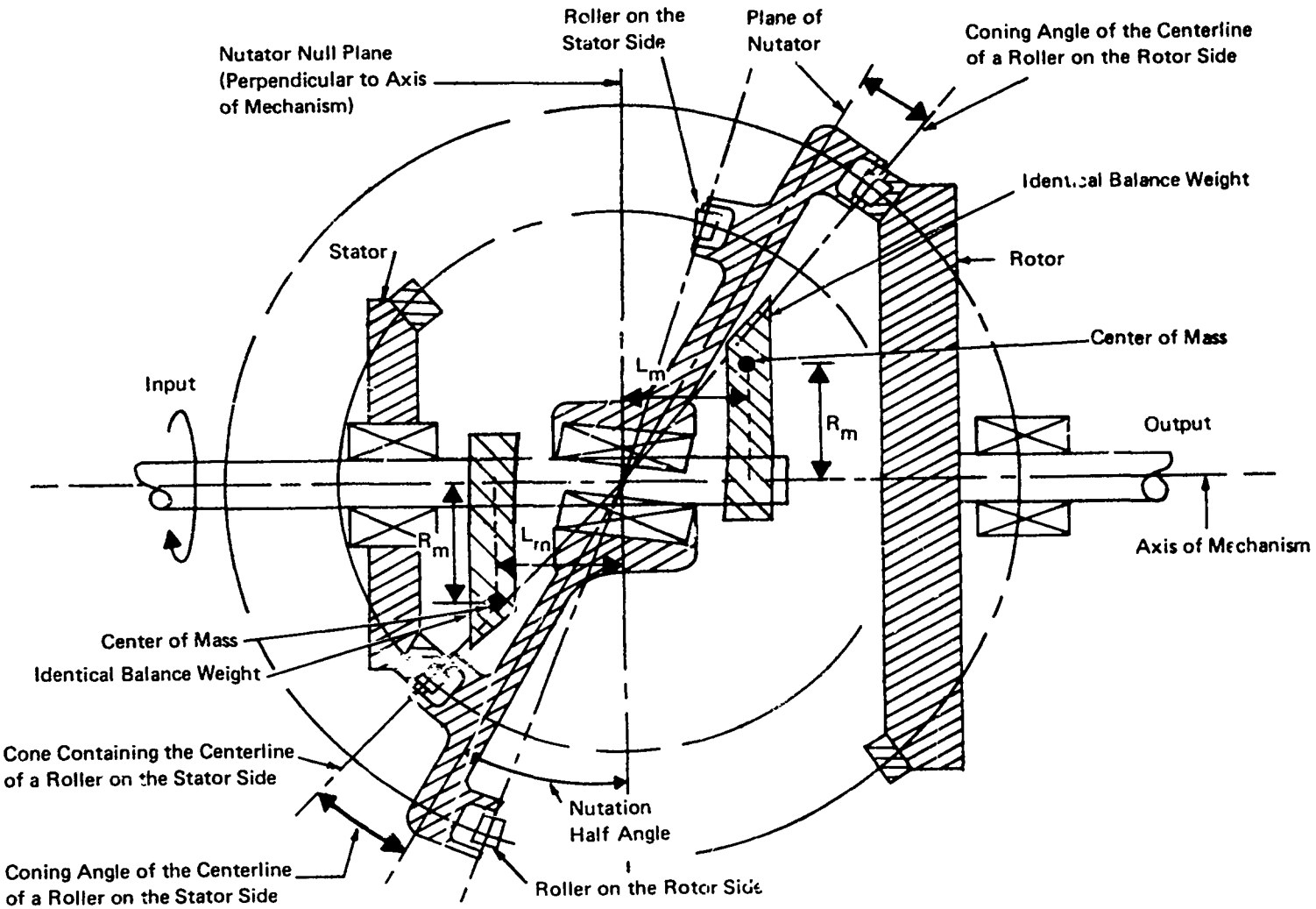

Figure A13. Typical Arrangement of Balancing Weights.

When properly designed, the rollers should begin contact with the cam tooth at very near zero load, however, the load should build to a maximum quite rapidly. Considering the relative stiffnesses of the mating parts, this is most likely the actual case; thus each roller in contact will share a substantial portion of the load over most of its engagement cycle. The distribution shown in Figure A14 certainly meets this criteria and, for lack of experimental substantiation to the contrary, will be utilized in this analysis.

The factor K' is determined by the size of the arc of contact.

$$K' = \frac{180}{\left(\omega_{XCA} - \omega_{NCA}\right)} \tag{A294}$$

The quantity ω'_{oi} is a function of the point at which active contact commences and the input angle ω_o.

$$\omega_{oi}' = \omega_{oi} - \omega_{NCA} \; ; \; \omega_{NCA} \leq \omega_{oi} \leq \omega_{XCA} \tag{A295}$$

The load distribution may thus be written as

$$F_{XCAi} = F_{MAXCA} \, \mathrm{Sin} \left(K' \, \omega_{oi}' \right) \tag{A296}$$

Since both F_{XCAi} and F_{MAXCA} are unknowns, additional equations must be defined.

$$T_{CA} = \sum_{i=1}^{IL_{ACA}} R_{CAi} \, F_{XCAi} = \sum_{i=1}^{IL_{ACA}} F_{MAXCA} \, \mathrm{Sin}(K' \, \omega_{oi}') \, R_{CAi} \tag{A297}$$

Since F_{MAXCA} is a constant, it may be removed from the summation sign to yield.

$$F_{MAXCA} = \frac{T_{CA}}{\sum_{i=1}^{IL_{ACA}} \left(R_{CAi} \, \mathrm{Sin}(K' \omega_{oi}') \right)} \tag{A298}$$

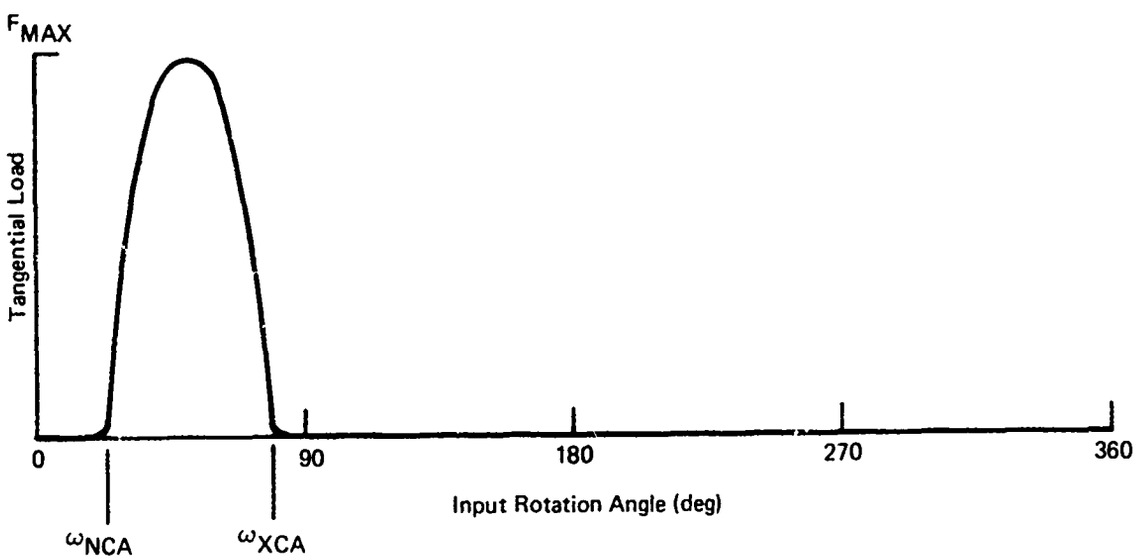

Figure A14. Load Distribution as a Function of Input Angle.

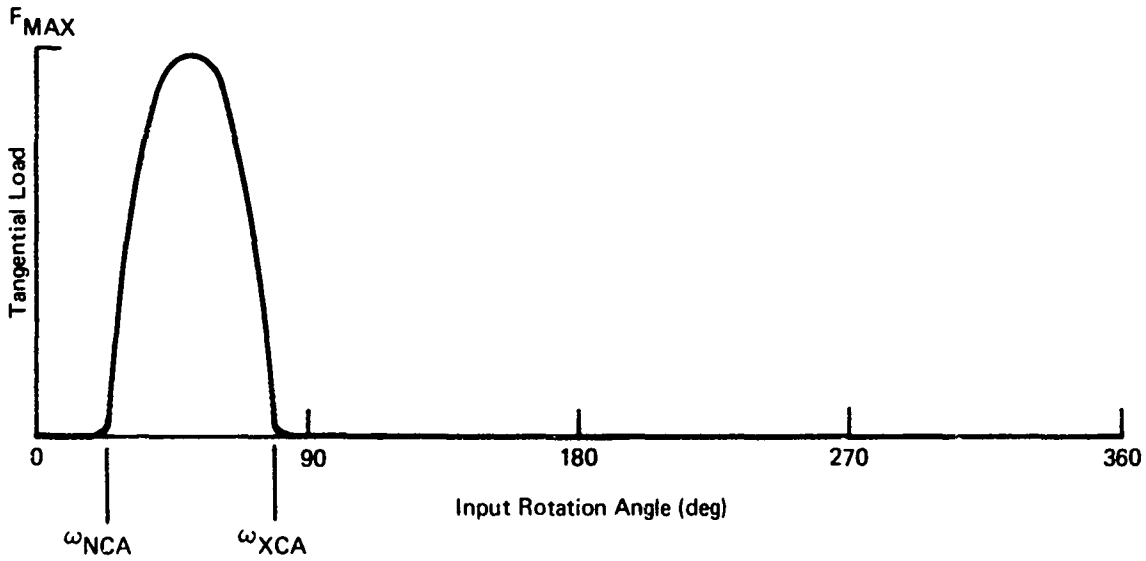

Figure A14. Load Distribution as a Function of Input Angle.

where T_{CA} = total torque on the cam

IL_{ACA} = minimum number of cams in contact

R_{CAi} = radius to the load point perpendicular to the shaft centerline

Once F_{MAXCA} has been defined, it may be substituted into Equation (A296) to calculate the individual cam loads.

Component Load Analysis

If we consider a single cam tooth at any point of contact, it will be acted on by a single normal load distribution. In order to simplify the analysis this distribution may be represented by a single normal force, which is the vector sum of the distribution, acting at the basic spherical radius. The basic spherical radius must then pass through the mean roller section. This simulation has been used with much success in the analysis of tapered roller bearings. This normal force may be utilized directly in the calculation of the contact stress at the roller - cam tooth interface. However, most other calculations will require a knowledge of the X Y Z components of the normal load. Utilizing the same coordinate system and conventions as was used in deriving the cam tooth form coordinates, these components may be easily derived.

The normal load acts along the adjusted roller radius, and as such, the direction cosines of this line may be utilized to define the desired force components as

$$F_{XCAi} = F_{NCAi} \text{ Cos } (\alpha_{PFCA}) \quad \text{(A299)}$$

$$F_{YCAi} = F_{NCAi} \text{ Cos } (\beta_{PFCA}) \quad \text{(A300)}$$

$$F_{ZCAi} = F_{NCAi} \text{ Cos } (\gamma_{PFCA}) \quad \text{(A301)}$$

where F_{NCAi} = normal load on the i^{th} cam tooth

F_{XCAi}, F_{YCAi}, F_{ZCAi} = the X-, Y-, and Z- components of the normal load on the i^{th} cam tooth respectively

Cos (α_{PFCA}), Cos (β_{PFCA}), Cos (γ_{PFCA}) = the direction cosines of a line joining a point on the pitch path and the cam tooth surface (i.e., the direction cosines of the normal tooth load vector)

A little thought at this point will reveal the significance of each load component. The driving force is the X- component, since it acts in a direction perpendicular to a radius vector and serves to generate torque. The Z- component results in a net thrust and overturning moment on the cam. The Y- component results in a net radial load on the cam.

The vector sum of these loads over all the cam teeth in contact is the load which must be reacted by the cam support bearings.

It will be convenient for the purposes of bearing life analysis to express the loads on the cam in terms of net components along the X_o, Y_o, and Z_o directions.

Figure A15 shows schematically the load distribution applied to a single cam. Referring to the contact ratio analysis, the minimum number of cam teeth in contact is IL_{ACA}. Thus the net loads on the cam may be written as

$$F_{TXCA} = \sum_{i=1}^{IL_{ACA}} F_{XCAi} \text{Sin}(i\alpha_{CA}); \ \omega_{NCA} \leq i\ \alpha_{CA} \leq \omega_{XCA} \qquad \text{(A302)}$$

$$F_{TYCA} = \sum_{i=1}^{IL_{ACA}} F_{YCAi} \text{Cos}(i\alpha_{CA}); \ \omega_{NCA} \leq i\ \alpha_{CA} \leq \omega_{XCA} \qquad \text{(A303)}$$

$$F_{TZCA} = \sum_{i=1}^{IL_{ACA}} F_{ZCAi} \qquad \text{(A304)}$$

The thrust forces also result in overturning moments about the X_o and Y_o axes.

$$M_{TXCA} = \sum_{i=1}^{IL_{ACA}} F_{ZCAi} Y_{PCA/CAi} \text{ Sin } (i\alpha_{CA}); \quad \omega_{NCA} \leq i\ \alpha_{CA} \leq \omega_{XCA} \qquad \text{(A305)}$$

$$M_{TYCA} = \sum_{i=1}^{IL_{ACA}} F_{ZCAi} Y_{PCA/CAi} \text{ Cos } (i\alpha_{CA}); \quad \omega_{NCA} \leq i\ \alpha_{CA} \leq \omega_{XCA} \qquad \text{(A306)}$$

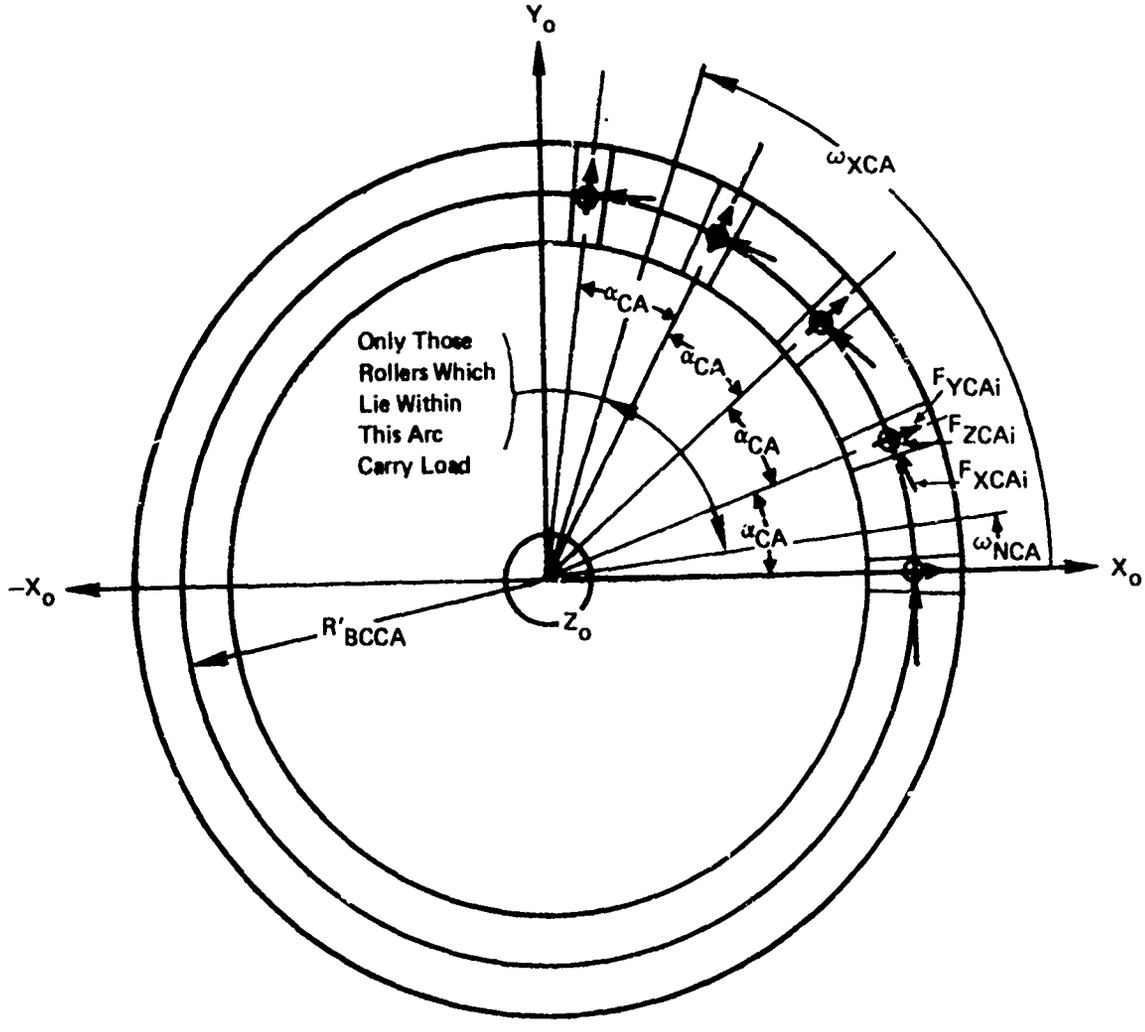

Figure A15. Cam Loading Shown Along Axis of Mechanism.

Although it is obvious that the instantaneous individual roller loads vary as a function of time, the net resultant load on the cams does not vary appreciably. The foregoing equations represent the worst case loading, that is the minimum number of teeth sharing the load. Since this is, in general, the manner in which geared systems are analyzed, it will be applied to the NMT. Equations (A302) through (A306) therefore completely define the loads on both the rotor and stator cams.

The net forces on the nutator may be derived by considering Figure A16, adjusting the net loads on each cam by the nutation half-angle ν thus

$$F_{TNXCA} = F_{TXCA} \text{ Cos } (\nu) - F_{TZCA} \text{ Sin } (\nu) \qquad \text{(A307)}$$

$$F_{TNZCA} = F_{TXCA} \text{ Sin } (\nu) + F_{TZCA} \text{ Cos } (\nu) \qquad \text{(A308)}$$

$$F_{TNYCA} = F_{TYCA} \qquad \text{(A309)}$$

Similarly the moment equations may be written

$$M_{TNXCA} = M_{TXCA} \text{ Cos } (\nu) - M_{TYCA} \text{ Sin } (\nu) \qquad \text{(A310)}$$

$$M_{TNYCA} = M_{TXCA} \text{ Sin } (\nu) + M_{TYCA} \text{ Cos } (\nu) \qquad \text{(A311)}$$

Equations (A307) through (A311) therefore define the net loading on the nutator.

The net torque on each cam must be equal to the output torque of the mechanism.

$$T_o = \sum_{i=1}^{IL_{ACA}} (F_{XCAi} \, Y_{PCA/CAi}) \qquad \text{(A312)}$$

Equation (A312) will be utilized in a later analysis to develop the roller load spectrum.

Due to the tapered shape of the nutator rollers, the normal load on the roller surface will be reacted by the roller support bearings as a combination of radial and thrust loads as shown in Figure A17.

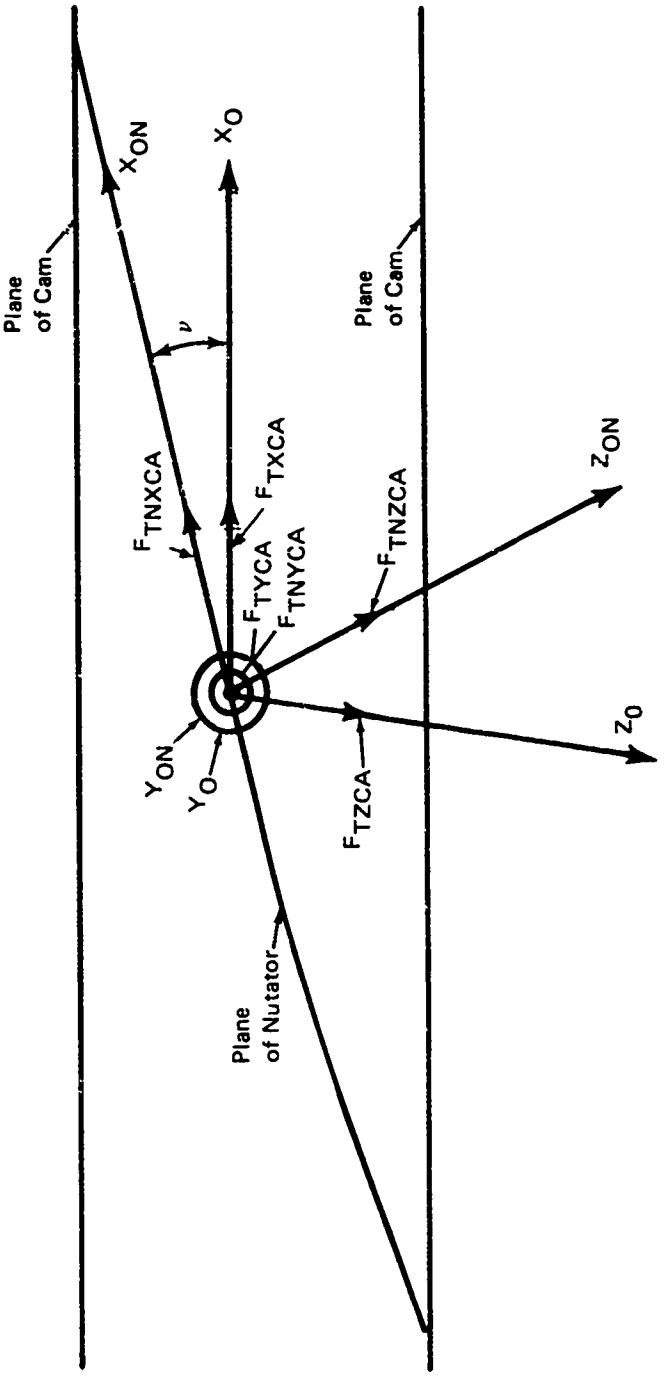

Figure A16. Net Loading of Nutator.

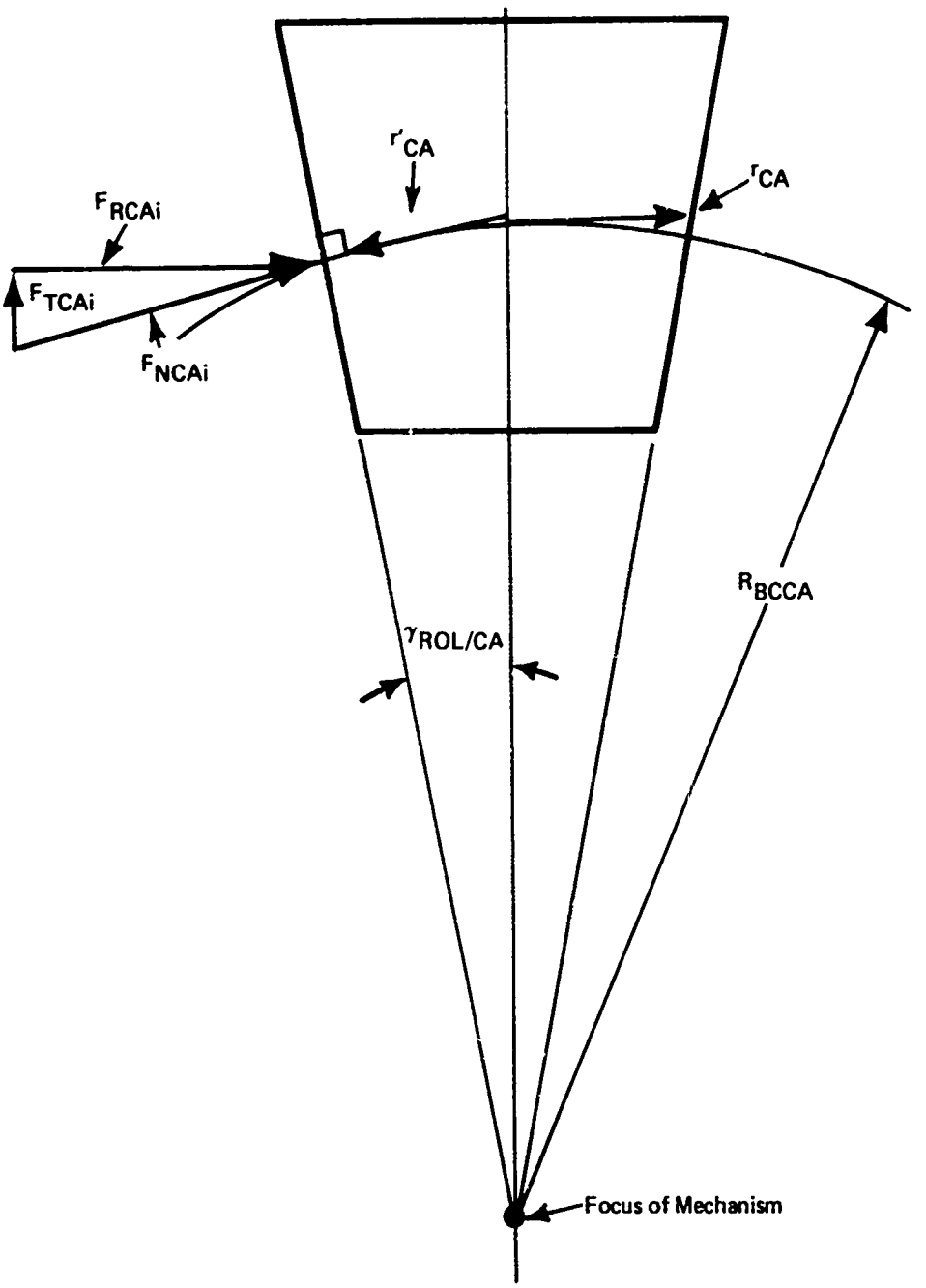

Figure A17. Loading of a Nutator Roller.

The angle $\gamma_{ROL/CA}$ is defined in the cam tooth form development section, thus the radial and thrust components may be written as

$$F_{RCAi} = F_{NCAi} \text{ Cos } (\gamma_{ROL/CA}) \quad \text{(A313)}$$

$$F_{TCAi} = F_{NCAi} \text{ Sin } (\gamma_{ROL/CA}) \quad \text{(A314)}$$

COMPONENT STRESS ANALYSIS

Unless the nutator rollers and/or the cam teeth are crowned significantly, the nutator roller-cam tooth interface will be in a state of line contact. The stress equations for such a contact are well documented in many texts and will, therefore, only be restated in this section rather than derived. The contact bandwidth may be shown to be

$$b_{CA_i} = \left[\frac{4 F_{NCA_i} \rho_{CA_i} r'_{CA} (\zeta_{CA} + \zeta_{RCA})}{\ell'_{CA} (\rho_{CA_i} + r'_{CA})} \right]^{1/2} \quad \text{(A315)}$$

where

F_{NCA_i} = normal load on a roller at the i^{th} contact point

ρ_{CA_i} = cam tooth profile curvature radius at the i^{th} point

ℓ'_{CA} = length of the roller contact

r'_{CA} = curvature radius of the nutator roller

$$\zeta_{CA} = \frac{1-\mu_{CA}^2}{E_{CA}} \quad \text{(A316)}$$

$$\zeta_{RCA} = \frac{1-\mu_{RCA}^2}{E_{RCA}} \quad \text{(A317)}$$

where

μ_{CA}, μ_{RCA} = Poission's ratio for the cam tooth and the roller, respectively

E_{CA}, E_{RCA} = the elastic modulii of the cam tooth and the roller respectively

The maximum compressive stress may then be expressed as a function of the unit tooth loading and the contact bandwidth as

$$S_{CCA_i} = \frac{-2\left|F_{NCA_i}\right|}{\pi \ell'_{CA} b_{CA_i}} \tag{A318}$$

It is commonly accepted in the analysis of rolling element bearings that fatigue damage is a function of, among other parameters, the maximum range of subsurface shear stress which occurs during the loading cycle. This stress and its depth are given by

$$S_{SCA_i} = 0.242 \frac{2\left|F_{NCA_i}\right|}{\pi \ell'_{CA} b_{CA_i}} \tag{A319}$$

$$Z_{SCA_i} = 0.4\, b_{CA_i} \tag{A320}$$

The next parameter of interest is the bending stress of the cam teeth. Again, we will make use of the mean section simulation utilized earlier. In general, the mean section of a cam tooth will appear as shown in Figure A18. The undercut is shown so that positive clearance may be assured.

The bending stress at the fillet of a cam tooth may be found, considering the section shown in Figure A18, by utilizing a formula developed by Heywood and later modified by Kelley and Pederson. Utilizing the nomenclature defined by the figure,

$$S_{TCA_i} = \frac{\left|F_{NCA_i}\right|}{\ell'_{CA}} \left[1 + .26 \frac{\ell'_{CA}}{R_{FCA}}\right] \left[\frac{1.5a_{CA_i}}{e_{CA_i}^2} + \frac{\cos(\beta_{CA_i})}{2e_{CA_i}} + \frac{0.45}{(d_{CA_i}\, \ell'_{CA})^{1/2}}\right] \tag{A321}$$

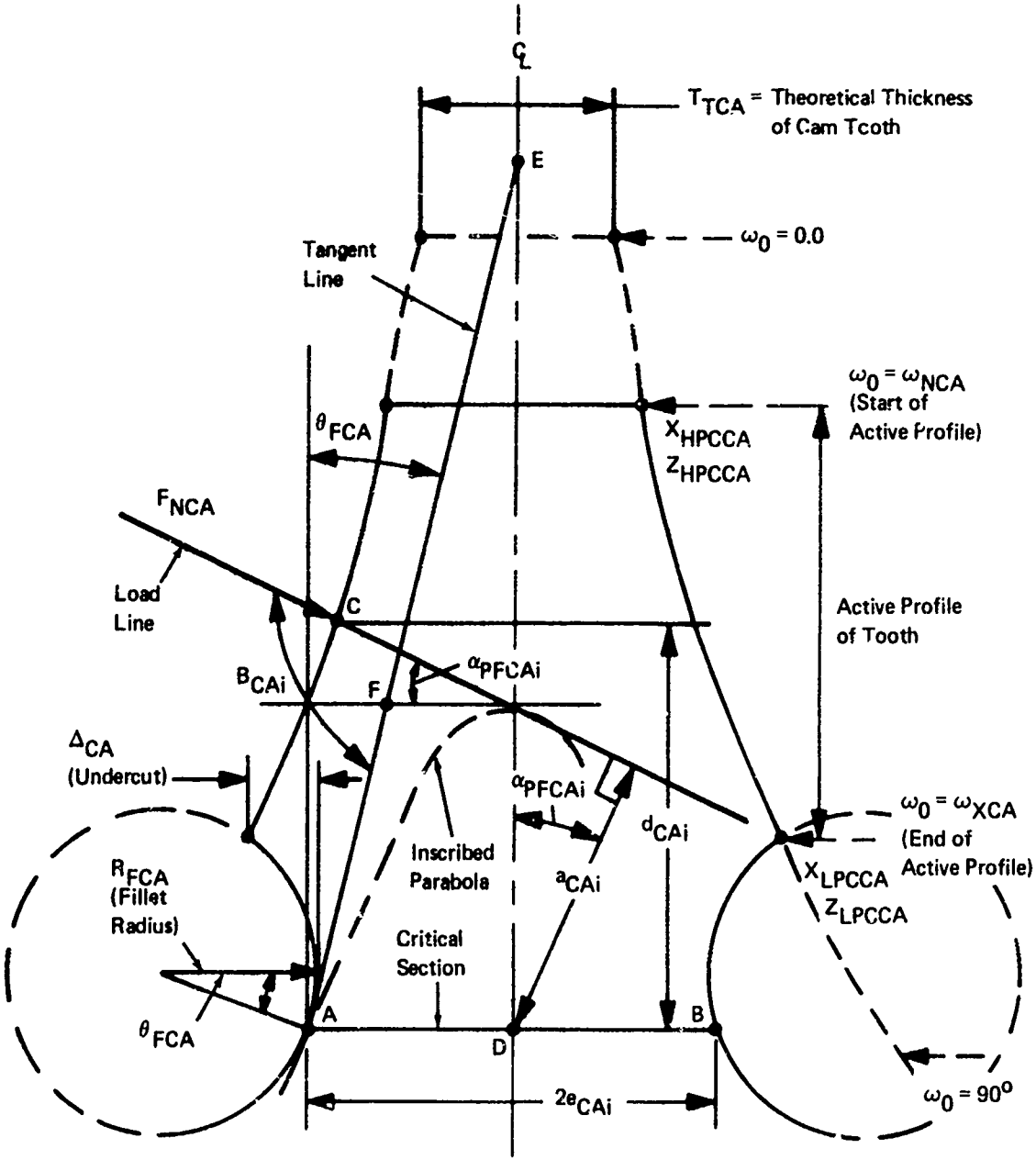

Figure A18. Mean Section of Cam Tooth.

where

R_{FCA} = cam fillet radius

β_{CA_i} = angle between fillet tangent line and load line

e_{CA_i} = tooth thickness at critical section

a_{CA_i} = distance from point D to load line

d_{CA_i} = distance between point of load application and critical section

The critical section, which occurs at the tangency point of the inscribed parabola, may be found by trial (i.e., choosing values for the dependent parameters until the distances between points AF and FE are equal).

In order to calculate the root tensile stress, it will first be necessary to derive expressions for the geometric terms in equation (A321). The first item to be considered is the placement and size of the fillet. It must be large enough to allow the nutator roller to clear at the proper point in the cycle, yet small enough to prevent a sharp groove at the base of the tooth due to the intersection of two oversized fillets. An undercut may or may not be provided depending on the exact tooth shape and the desired lowest point of contact. If we denote the X and Z coordinates of the lowest point of contact as $X_{LP_{CCA}}$ and $Z_{LP_{CCA}}$ and the end of the theoretical cam tooth as X_{90} and Z_{90}, the following equations may be written:

$$\beta_{CA_i} = -\theta_{FCA} + \alpha_{PFCA_i} + 90. \tag{A322}$$

$$e_{CA_i} = r_{CA} + X_{LP_{CCA}} - \Delta_{CA} + R_{FCA}\,(1-\cos\theta_{FCA}) + \frac{T_{TCA}}{2} \tag{A323}$$

$$d_{CA_i} = -Z_{PF/CA_i} + Z_{LP_{CCA}} + R_{FCA}\,\sin\left(\cos^{-1}\left(\frac{R_{FCA}-\Delta_{CA}}{R_{FCA}}\right)\right) + R_{FCA}\,\sin(\theta_{FCA}) \tag{A324}$$

$$a_{CA_i} = \left[d_{CA_i} - \left(r_{CA} + \frac{T_{TCA}}{2} + X_{PF/CA_i} \right) \text{Tan} \left(\alpha_{PFCA_i} \right) \right] \text{Cos} \left(\alpha_{PFCA_i} \right) \tag{A325}$$

The distances AF and FE may now be defined

$$AF = \frac{\left[d_{CA_i} - \left(r_{CA} + \frac{T_{TCA}}{2} + X_{PF/CA_i} \right) \text{Tan} \left(\alpha_{PFCA_i} \right) \right]}{\text{Cos} \left(\theta_{FCA} \right)} \tag{A326}$$

$$FE = \frac{\left[e_{CA_i} - \left(r_{CA} + \frac{T_{TCA}}{2} + X_{PF/CA_i} \right) \text{Tan} \left(\alpha_{PFCA_i} \right) \text{Tan} \left(\theta_{FCA} \right) \right]}{\text{Sin} \left(\theta_{FCA} \right)} \tag{A327}$$

If the angle θ_{FCA} is originally chosen as zero, equations (A326) and (A327) may be evaluated by taking successive increments on θ_{FCA} until AF is equal to FE within some preset tolerance.

The final stress component of interest is the bending stress in a nutator roller or its support shaft, depending on its configuration. The slope across the roller is also of considerable interest since, as this slope increases, the capacity of the support bearing decreases rapidly. Two methods of supporting the nutator roller are available as shown in Figures A19 and A20. Each configuration has both advantages and disadvantages, neither of which will be discussed at this point.

From the point of view of analysis, the configuration shown in Figure A19 presents the easier problem. It is basically a uniform beam fixed at both ends, a classic beam problem whose solution exists in many texts. Because of this the equations for stress and deflection will be stated in terms of the design parameters, with the derivation omitted. Since the roller included angle is generally quite small, the thrust load on the rollers will be very small when compared to the radial roller load (less than 3 to 5 percent in most cases) and the

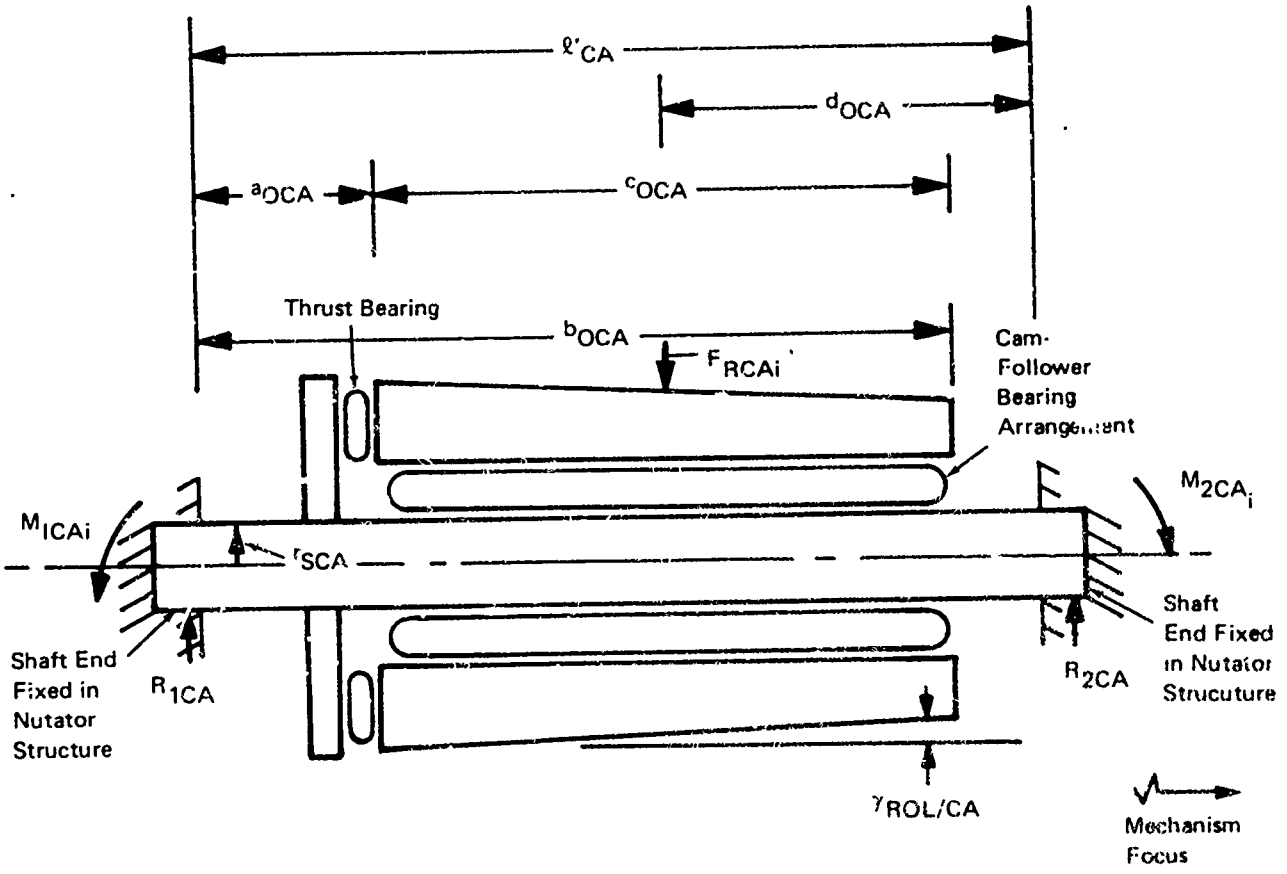

Figure A19. Cam-Follower Shell Roller.

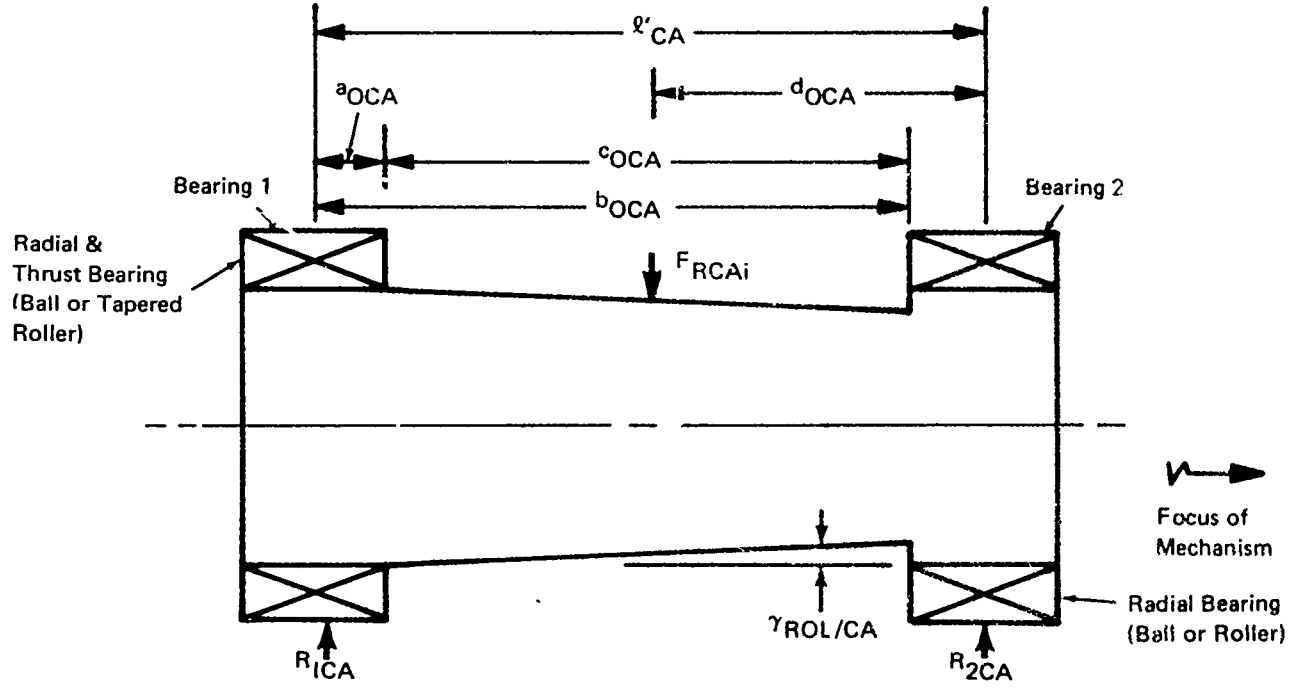

Figure A20. Solid Roller With End Bearing Support.

beam will be considered to be acted on only by the radial load. This being the case, the following equations may be written:

$$M_{1CA_i} = -\frac{1}{24}\frac{F_{RCA_i}}{\ell_{CA}}\left[24\frac{d_{OCA}^3}{\ell_{CA}} - \frac{6\,b_{OCA}c_{OCA}^2}{\ell_{CA}} + \frac{3c_{OCA}^2}{\ell_{CA}} - 4c_{OCA}^2 - 24d_{OCA}^2\right] \quad \text{(A328)}$$

$$M_{2CA_i} = \frac{1}{24}\frac{F_{RCA_i}}{\ell_{CA}}\left[24\frac{d_{OCA}^3}{\ell_{CA}} - \frac{6\,b_{OCA}\,c_{OCA}^2}{\ell_{CA}} + \frac{3c_{OCA}^3}{\ell_{CA}} + 2c_{OCA}^2 - 48d_{OCA}^2 + 24d_{OCA}\,\ell_{CA}\right] \quad \text{(A329)}$$

M_{1CA_i}, M_{2CA_i}, R_{1CA_i} and R_{2CA_i} are the reaction moments and forces which must be exerted by the nutator structure to restrain the roller.

$$R_{1CA_i} = \frac{1}{4}\frac{F_{RCA_i}}{\ell_{CA}^2}\left(12d_{OCA}^2 - \frac{8d_{OCA}^3}{\ell_{CA}} + \frac{2b_{OCA}c_{OCA}^2}{\ell_{CA}} - \frac{c_{OCA}^3}{\ell_{CA}} - c_{OCA}^2\right) \quad \text{(A330)}$$

$$R_{2CA_i} = F_{RCA_i} - R_{1CA_i} \quad \text{(A331)}$$

$$M_{OCA_i} = -M_{1CA_i} + R_{1CA_i}\,a_{OCA} + \frac{R_{1CA_i}^2\,C_{OCA}}{2F_{RCA_i}} \quad \text{(A332)}$$

$$S_{bCA_i} = \frac{4M_{OCA_i}}{\pi r_{SCA}^3} \quad \text{(A333)}$$

MO_{CA_i} is the maximum moment exerted on the loaded portion of roller shaft. S_{bCA_i} is the stress at the section to which M_{OCA_i} is applied.

The deflection at the point at which M_{OCA_i} is applied is:

$$Y_{SCA_i} = \frac{2}{3\pi E_{RCA} r_{SCA}^4}\left[R_{1CA_i}\left(a_{OCA} + \frac{R_{1CA_i} C_{OCA}}{F_{RCA_i}}\right)^3 - 3M_{1CA_i}\left(a_{OCA} + \frac{R_{1CA_i} C_{OCA}}{F_{RCA_i}}\right)^2 - \frac{1}{4}\left(\frac{C_{OCA}}{F_{RCA_i}}\right)^3 R_{1CA_i}^4\right] \quad \text{(A334)}$$

Depending on the exact configuration of the end restraints, this deflection may not be the maximum; however, it will be quite close. If a more accurate value is required, examination of section a short distance on either side will quickly reveal the maximum.

If the roller is supported as shown in Figure A20, a somewhat different set of equations apply.

Although the roller has a taper, it is so slight that the maximum stress will still occur very near the center of the roller.

$$R_{1CA_i} = F_{RCA_i}\frac{d_{OCA}}{\ell_{CA}} \quad \text{(A335)}$$

$$R_{2CA_i} = \frac{F_{RCA_i}}{\ell_{CA}}\left(a_{OCA} + \frac{C_{OCA}}{2}\right) \quad \text{(A336)}$$

$$M_{OCA_i} = \frac{F_{RCA_i} d_{OCA}}{\ell_{CA}}\left(a_{OCA} + \frac{C_{OCA} d_{OCA}}{2\ell_{CA}}\right) \quad \text{(A337)}$$

$$S_{bCA_i} = \frac{4M_{OCA_i}}{\pi r_{CA}^3} \quad \text{(A338)}$$

The deflection of the roller at the section at which M_{OCA_i} is applied is

$$Y_{SCA_i} = \frac{1}{12E_{RCA}\pi r_{CA}^4}\left[8R_{1CA_i}\left(a_{OCA} + \frac{C_{OCA}d_{OCA}}{\ell_{CA}}\right)^3 - \ell_{CA}^2\left(a_{OCA} + \frac{C_{OCA}d_{OCA}}{\ell_{CA}}\right)\right] + F_{RCA_i}\left(a_{OCA} + \frac{C_{OCA}d_{OCA}}{\ell_{CA}}\right)\left[\frac{8d_{OCA}^3}{\ell_{CA}} - \frac{2b_{OCA}C_{OCA}^2}{\ell_{CA}} + \frac{C_{OCA}^3}{\ell_{CA}} + 2C_{OCA}^2\right] - 2F_{RCA_i}\left(C_{OCA}^3 d_{OCA}^4\right) \quad \text{(A339)}$$

Of particular interest is the slope of the roller across its support bearings. If this slope is too high, severe maldistribution of load may occur within the bearing greatly shortening its life.

$$\theta_{1CA_i} = \frac{1}{12E_{RCA}\pi r_{CA}^4}\left[-8R_{1CA_i}\ell_{CA}^2 + F_{RCA_i}\left(\frac{8d_{OCA}^3}{\ell_{CA}} - \frac{2b_{OCA}C_{OCA}^2}{\ell_{CA}} + \frac{C_{OCA}^3}{\ell_{CA}} + 2C_{OCA}^2\right)\right] \quad \text{(A340)}$$

at bearing 1.

$$\theta_{2CA_i} = \frac{1}{12E_{RCA}\pi r_{CA}^4}\left[16R_{1CA_i}\ell_{CA}^2 - F_{RCA_i}\left(24d_{OCA}^2 - \frac{8d_{OCA}^3}{\ell_{CA}} + \frac{2b_{OCA}C_{OCA}^2}{\ell_{CA}} - \frac{C_{OCA}^3}{\ell_{CA}}\right)\right] \quad \text{(A341)}$$

at bearing 2.